



**HAL**  
open science

# Rôle de l'hémostase dans l'inflammation induite par les virus influenza A

Fatma Berri

► **To cite this version:**

Fatma Berri. Rôle de l'hémostase dans l'inflammation induite par les virus influenza A. Immunologie. Université Claude Bernard - Lyon I, 2014. Français. NNT : 2014LYO10351 . tel-01128271

**HAL Id: tel-01128271**

**<https://theses.hal.science/tel-01128271>**

Submitted on 9 Mar 2015

**HAL** is a multi-disciplinary open access archive for the deposit and dissemination of scientific research documents, whether they are published or not. The documents may come from teaching and research institutions in France or abroad, or from public or private research centers.

L'archive ouverte pluridisciplinaire **HAL**, est destinée au dépôt et à la diffusion de documents scientifiques de niveau recherche, publiés ou non, émanant des établissements d'enseignement et de recherche français ou étrangers, des laboratoires publics ou privés.

**UNIVERSITE CLAUDE BERNARD - LYON 1**  
Ecole doctorale BMIC : Biologie Moléculaire Intégrative et Cellulaire

**Doctorat**

Pour l'obtention du grade de Docteur en Sciences de l'Université  
Lyon 1  
N° : 351-2014

Présentée est soutenue publiquement le 17 Décembre 2014  
Par

**Fatma BERRI**

**Rôle de l'hémostase dans l'inflammation induite par  
les virus influenza A**

Thèse dirigée par le Dr. Béatrice RITEAU

Laboratoire EA4610, Unité VirPath  
Faculté de Médecine de Laennec, Lyon, France

Jury

Professeur Bruno LINA	Président
Docteur Nathalie ROUAS-FREISS	Rapporteur
Docteur Mustapha SI-TAHAR	Rapporteur
Docteur Martine JANDROT-PERRUS	Examineur
Docteur Jean-Claude BORDET	Examineur
Docteur Béatrice RITEAU	Directeur de Thèse

## UNIVERSITE CLAUDE BERNARD - LYON 1

Président de l'Université	M. François-Noël GILLY
Vice-président du Conseil d'Administration	M. le Professeur Hamda BEN HADID
Vice-président du Conseil des Etudes et de la Vie Universitaire	M. le Professeur Philippe LALLE
Vice-président du Conseil Scientifique	M. le Professeur Germain GILLET
Directeur Général des Services	M. Alain HELLEU

### *COMPOSANTES SANTE*

Faculté de Médecine Lyon Est – Claude Bernard	Directeur : M. le Professeur J. ETIENNE
Faculté de Médecine et de Maïeutique Lyon Sud – Charles Mérieux	Directeur : Mme la Professeure C. BURILLON
Faculté d'Odontologie	Directeur : M. le Professeur D. BOURGEOIS
Institut des Sciences Pharmaceutiques et Biologiques	Directeur : Mme la Professeure C. VINCIGUERRA
Institut des Sciences et Techniques de la Réadaptation	Directeur : M. le Professeur Y. MATILLON
Département de formation et Centre de Recherche en Biologie Humaine	Directeur : Mme. la Professeure A-M. SCHOTT

### *COMPOSANTES ET DEPARTEMENTS DE SCIENCES ET TECHNOLOGIE*

Faculté des Sciences et Technologies	Directeur : M. F. DE MARCHI
Département Biologie	Directeur : M. le Professeur F. FLEURY
Département Chimie Biochimie	Directeur : Mme Caroline FELIX
Département GEP	Directeur : M. Hassan HAMMOURI
Département Informatique	Directeur : M. le Professeur S. AKKOUCHE
Département Mathématiques	Directeur : M. le Professeur Georges TOMANOV
Département Mécanique	Directeur : M. le Professeur H. BEN HADID
Département Physique	Directeur : M. Jean-Claude PLENET
UFR Sciences et Techniques des Activités Physiques et Sportives	Directeur : M. Y. VANPOULLE
Observatoire des Sciences de l'Univers de Lyon	Directeur : M. B. GUIDERDONI
Polytech Lyon	Directeur : M. P. FOURNIER
Ecole Supérieure de Chimie Physique Electronique	Directeur : M. G. PIGNAULT
Institut Universitaire de Technologie de Lyon 1	Directeur : M. le Professeur C. VITON
Ecole Supérieure du Professorat et de l'Education	Directeur : M. le Professeur A. MOUGNIOTTE
Institut de Science Financière et d'Assurances	Directeur : M. N. LEBOISNE

## *Remerciements*

Pour commencer, je tiens à remercier Madame le **Docteur Nathalie ROUAS-FREISS** et Monsieur le **Docteur Mustapha SI-TAHAR** qui m'ont fait l'honneur d'accepter de juger ce travail et d'accomplir la lourde tâche d'en être les rapporteurs. Mes remerciements vont également à Madame le **Docteur Martine JANDROT-PERRUS** et Monsieur le **Docteur Jean-Claude BORDET**, qui ont eu la gentillesse de faire partie de ce jury. Veuillez trouver en ces lignes toute ma reconnaissance et mon respect.

Un grand merci à Monsieur le **Professeur Bruno LINA**, qui m'a accueillie dans son laboratoire depuis 2011. Ainsi qu'à toutes les personnes de l'unité avec qui j'ai eu l'occasion de travailler et de côtoyer durant toute cette thèse.

Les mots sont juste insuffisants pour assez remercier ma directrice de thèse, **Docteur Béatrice RITEAU**, avec qui j'ai eu l'honneur et le plaisir de travailler. Je tiens à lui exprimer toute ma gratitude. J'ai beaucoup appris, merci. J'ai vraiment apprécié les moments passés au sein de l'équipe, et j'en garderai que de bons souvenirs !

Je tiens également à remercier tous ceux qui ont contribué à l'élaboration de ce travail de près ou de loin, merci à : Mr Ba Vuong Lê avec qui j'ai partagé le bureau et la paillasse durant ma thèse, Ghina HAFFAR, Marie Laure Faucoult, Marie DELENE, Marjorie Comte et Julie Frouard, à l'équipe du CECIL : Chantal THEVENON, Elisabeth, et toute l'équipe de l'animalerie ALEC et du PBES pour leur gentillesse et aide.

Je passe ensuite une dédicace spéciale à tous mes amis et les gens que j'ai eu le plaisir de côtoyer pendant ces quatre années à Lyon, à savoir : Tata, Djahida, Billal, Thomas, Wassim, Djamel Saidj, Nathalie, Josette, Ramousse, Guillaume Leberre et sa femme Carolina, merci pour vos encouragements.

Et pour finir, une pensée toute particulière à toute ma famille qui ne cesse de m'encourager et de toujours être là pour moi. Un grand merci également à la famille Leberre en particulier Maryvonne pour leur accueil et aide !

*A mes parents et mon frère*

## Résumé

La grippe est une maladie respiratoire aiguë, due à une infection par des virus influenza et qui représente un problème important de santé publique. Une meilleure compréhension des interactions entre le virus influenza et son hôte nous permettra de mieux comprendre la physiopathologie de l'infection grippale, et donc, à terme, de mieux se protéger contre la maladie. La morbidité et la mortalité, causées par les infections grippales sévères, sont associées à une dérégulation de la réponse immunitaire, au niveau pulmonaire. Cette inflammation délétère serait à l'origine de dommages collatéraux du poumon, entraînant une diminution de la capacité respiratoire du patient. Bien que les mécanismes impliqués ne soient pas totalement élucidés, de récents travaux mettent en évidence un rôle central des cellules endothéliales dans la dérégulation de la réponse de l'hôte face à l'infection grippale. Lors d'une agression de l'endothélium, le processus physiologique de l'hémostase (activation plaquettaire, coagulation et fibrinolyse) s'active afin de permettre la cicatrisation de la plaie et de maintenir l'intégrité des vaisseaux sanguins. Dans de nombreuses maladies inflammatoires, la seule dérégulation de l'hémostase est directement liée à une réponse inflammatoire délétère. Lors de ma thèse, nous avons émis l'hypothèse que l'hémostase pouvait être à l'origine de la dérégulation inflammatoire durant les infections grippales. Nos données montrent le rôle de deux facteurs fortement impliqués dans l'hémostase : le récepteur activé par la thrombine, PAR-1 (*Protease Activated Receptor 1*) ainsi que le plasminogène, dans l'inflammation délétère des poumons et dans la pathogénicité des virus influenza. Outre le rôle de l'hémostase, nous avons également pu mettre en évidence que le virus influenza incorpore des protéines cellulaires dans l'enveloppe virale, lui permettant d'échapper au système immunitaire, ce qui pourrait aussi contribuer à la dérégulation de la réponse de l'hôte. L'ensemble des résultats obtenus ont permis de mieux comprendre les mécanismes à l'origine d'une réponse immunitaire dérégulée dans les infections grippales et de proposer de nouvelles cibles thérapeutiques pour lutter contre la maladie.

# Table des matières

Liste des tableaux et figures .....	6
Liste d'abréviations .....	7
<b>Chapitre 1: INTRODUCTION</b> .....	10
<b>A. Généralités sur les virus influenza</b> .....	11
1. Le virus influenza de type A.....	13
2. Le cycle viral des virus influenza A .....	15
3. Moyens de prévention des infections grippales.....	18
<b>B. La réponse de l'hôte aux infections par le virus influenza</b> .....	19
<b>I. Reconnaissance du virus et réponse inflammatoire</b> .....	19
1. Reconnaissance des virus influenza par les TLRs .....	20
2. Reconnaissance des virus influenza par RIG-1.....	21
3. Reconnaissance des virus influenza par NLRP3.....	22
<b>II. Dérégulation de l'inflammation</b> .....	24
1. Inflammation excessive durant les gripes sévère.....	24
2. Intensité versus durée inflammatoire .....	25
<b>III. L'hémostase et l'inflammation</b> .....	27
1. L'hémostase primaire.....	28
2. La Coagulation.....	30
3. La fibrinolyse .....	33
<b>IV. Les récepteurs activés par la thrombine et le plasminogène, des molécules au cœur de l'hémostase et de l'inflammation</b> .....	35
1 - Les récepteurs activés par la thrombine.....	35
2. Le plasminogène.....	39
<b>C. Hémostase et virus influenza</b> .....	41

1 - Etudes cliniques .....	41
2 - Activation des cellules endothéliales par les virus Influenza A.....	42
3 - Activation de l'hémostase par les virus influenza .....	43
<b>Objectif de la thèse</b> .....	45
<b><i>Chapitre 2: RESULTATS</i></b> .....	46
<b>Manuscrit n°1:</b> PAR1 contributes to influenza A virus pathogenicity in mice. ....	47
<b>Manuscrit n°2:</b> Plasminogen Controls Inflammation and Pathogenesis of Influenza Virus Infection via Fibrinolysis. ....	49
<b>Manuscrit n°3:</b> Annexin V Incorporated into Influenza Virus Particles Inhibits Gamma Interferon Signaling and Promotes Viral replication. ....	51
<b><i>Chapitre 3 : Discussions &amp; Conclusions</i></b> .....	53
<b>Perspectives</b> .....	61
<b>Annexes</b> .....	63
<b>Références</b> .....	68

## Liste des tableaux et figures

**Tableau 1** : Gènes et protéines du virus influenza A

**Figure 1** : Présentation schématique des virus influenza A

**Figure 2** : Cycle viral des virus influenza A

**Figure 3** : Reconnaissance des virus influenza par les PRRs

**Figure 4** : Dérégulation de l'hémostase

**Figure 5** : Présentation schématique des étapes du processus de l'hémostase

**Figure 6** : Présentation schématique de l'activation plaquettaire

**Figure 7** : Cascade enzymatique de la coagulation *in vivo*

**Figure 8** : Activation des PARs par les protéases de coagulation

**Figure 9** : Activation des PARs par la thrombine et réponse cellulaire

**Figure 10** : Les PARs sur les plaquettes humaines et de souris

**Figure 11** : Rôle anti-et pro-inflammation de PAR1

**Figure 12** : Représentation schématique du modèle proposé de l'interaction entre PLG et PAR1 dans la pathogénicité des virus influenza A

## Liste d'abréviations

**A5:** Annexine 5

**ADP :** Adénosine Diphosphate

**ARNc:** ARN complémentaire

**ARNdb:** ARN double brin

**ARNsb:** ARN simple brin

**ARNv** ARN viraux

**ASC:** Apoptotic-Associated Speck-like Protein containing a caspase recruitment domain

**AT:** Antithrombine

**ATP:** Adénosine TriPhosphate

**CARDIF:** CARD Adapter Inducing interferon- $\beta$

**EPCR :** Endothelial Protein C Receptor

**FT:** Facteur Tissulaire

**GDP:** Guanosine DiPhosphate

**GTP:** Guanosine TriPhosphate

**HA :** Hémagglutinine

**ICAM :** InterCellular Adhesion Molecule

**IFN:** Interferon

**IL:** Interleukine

**IP-10:** INF- $\gamma$  inducible protein 10

**IPS-1:** Interferon- $\beta$  Promoter Stimulator-1

**IRF 3/7:** Interferon Response Factor 3/7

**LBS:** Lysine Binding Site

**M1:** Matrice 1

**M2:** Matrice 2

**MAP-Kinase:** Mitogen Activated Proteins-Kinase

**MAVS:** Mitochondrial Antiviral Signaling

**MCP-1:** Monocyte Chemoattractant Protein-1

**MIP-1:** Macrophage Inflammatory Protein-1

**NA:** Neuraminidase

**NEP:** Nuclear Export Protein

**NF- $\kappa$ B:** Nuclear Factor  $\kappa$ B

**NLR:** Nod-Like Receptor

**NO:** Monoxyde d'azote

**NP:** Nucléoprotéine

**PA:** Polymerase Acidic Protein

**PAF:** Platelet Activating Factor

**PAI:** Plasminogen Activator Inhibitor

**PAMP:** Pathogen Associated Molecular Pattern

**PAR:** Protease Activated Receptor

**PB1:** Polymerase Basic Protein 1

**PB2:** Polymerase Basic Protein 2

**PC:** Protéine C

**PCa:** Protéine C active

**PDF :** Produits de dégradation de la fibrine

**PG:** Prostaglandine

**PLG:** Plasminogène

**PRR:** Pattern Recognition Receptor

**PYCARD:** Apoptosis-associated speck-like protein containing a CARD

**RANTES:** Regulated on Activation Normal T cell Expression and Secreted

**RIG-1:** Retinoic acid Inducible Gene-1

**RLR:** RIG like receptor

**RNP:** RiboNucléoProtéine

**S1P1:** Sphingosin-1 Phosphate 1

**TAT:** Thrombine anti-thrombine

**TFPI:** Tissue Factor Pathway Inhibitor

**TLR:** Toll-Like Receptor

**TNF:** Tumor Necrosis Factor

**t-PA:** tissue-Plasminogen Activator

**TRIF:** Tool/IL-1R domain containing adaptor inducing IFN- $\beta$

**TXA2:** Thromboxane A2

**u-PA :** Urokinase-Plasminigen activator

**VIA :** Virus Influenza de type A

**VIB:** Virus Influenza de type B

**VISA:** Virus Induced Signaling Adaptor

**vWF:** Von Willebrand Factor

## Chapitre 1: INTRODUCTION

## A. Généralités sur les virus influenza

Les virus influenza font partie de la famille des *Orthomyxoviridea*, qui comporte cinq genres de virus à ARN : les togo virus, isavirus, et les virus influenza de type A (VIA), B (VIB) et C. Les VIA ainsi que les VIB sont à l'origine des épidémies saisonnières de grippe annuelles. En revanche, les virus influenza de type C infectent l'homme mais n'entraînent ni épidémies, ni pandémies. La grippe est une infection aiguë des voies respiratoires. Elle se caractérise par une forte fièvre, une toux, des céphalées ainsi que des douleurs musculaires et articulaires. Les personnes infectées guérissent, en général, après une ou deux semaines, sans traitement médical. Néanmoins, des complications peuvent survenir, telles que des pneumonies ou des encéphalites, entraînant dans les cas les plus graves, le décès du patient (Kunisaki & Janoff 2009, Ruuskanen et al 2011).

Parmi les virus influenza, les VIA sont les virus les plus pathogènes chez l'homme. Les VIA sont divisés en sous-types selon l'expression de deux protéines de surface, la HA (Hémagglutinine) et la NA (Neuraminidase). Leur taille varie entre 80 et 120 nm de diamètre. A ce jour, 18 HA et 11 NA différentes ont été décrites (Garcia-Sastre 2012, Tong et al 2013). Selon l'Organisation Mondiale de la Santé, les VIA sont responsables, chaque année, de 3 à 5 millions de cas graves d'infections dans le monde, entraînant 250 000 à 500 000 décès ((WHO) 2014). En plus des gripes saisonnières, les VIA sont également à l'origine de pandémies. L'oiseau sauvage est le réservoir naturel de ces virus (Webster & Hulse 2004). Cependant, chaque adaptation d'un sous-type aviaire ou animal à l'espèce humaine peut entraîner des pandémies, avec des conséquences importantes en pertes humaines et économiques. Ceci fut le cas lors : (i) de la grippe espagnole ou pandémie de 1918, qui fut provoquée par un virus aviaire de sous-type H1N1, dont l'origine est encore mal connue (Anhlan et al 2011, Reid et al 2004) (Johnson & Mueller 2002, Yewdell & Garcia-Sastre 2002); (ii) de la pandémie asiatique ou pandémie de 1957, causée par le virus de sous-type H2N2, dont l'origine est aviaire ; (iii) de la

pandémie de Hong Kong ou pandémie de 1968, causée par le virus de sous-type H3N2, qui est un virus hybride abritant des gènes de virus d'origine humaine et aviaire (Tscherne & Garcia-Sastre 2011); et (iv) de la pandémie de 2009, appelée « grippe porcine », causée par un VIA de sous-type H1N1 et ayant réassorti plusieurs gènes de virus d'origine porcine, aviaire et humaine (Garten et al 2009) (Dawood et al 2012).

La nomenclature des virus influenza est en fonction du type de virus (A, B ou C), de l'espèce chez laquelle il a été isolé, de la localisation géographique, du numéro d'isolat, de l'année d'isolation ; et dans le cas des virus influenza de type A, des sous-types des glycoprotéines de surface, HA et NA. Ainsi, par exemple, le virus H5N1 isolé chez le poulet à Hong Kong en 1997, possède la nomenclature suivante: Influenza A/Chicken/Hong Kong/220/97 (H5N1) (Palese 2001).

## 1. Le virus influenza de type A

Les VIA sont des virus enveloppés, de forme sphérique ou filamenteuse. Ce sont des virus à ARN simple brin de polarité négative. Leur génome est constitué de huit segments d'ARN, codant pour une ou plusieurs protéines virales ayant des fonctions bien précises. En particulier, onze protéines ont été identifiées et leur fonction bien étudiées (Tscherne & Garcia-Sastre 2011) (**Tableau 1**).

**Tableau 1:** Gènes et protéines du virus Influenza A

N° Segment	Protéines	Fonctions
1	PB2	Réplication virale
2	PB1	Réplication virale
	PB1-F2	Pathogénicité des virus
3	PA	Réplication virale
4	HA	Attachement à la surface de la cellule, Déterminant antigénique
5	NP	Protéine de la nucléocapside
6	NA	Libération des nouveaux virions, Déterminant antigénique
7	M1	Stabilité de la particule virale
	M2	Canal à protons, libération des RNPv dans le cytoplasme
8	NS1	Inhibition de la production de cytokines antivirales (IFN)
	NEP	Transport des RNPv du noyau vers la membrane plasmique

En plus de ces 11 protéines, des protéines virales supplémentaires ont plus récemment été découvertes. Ainsi, la protéine PA-X est issue d'un deuxième cadre de lecture du segment 3 (Jagger et al 2012). PA-X réprime l'expression des gènes de l'inflammation et de l'apoptose et

diminue la virulence du virus influenza chez la souris. Des formes tronquées de la protéine PA (PA-N155 et PA-N182) ont également été découvertes. Ces protéines n'auraient pas d'activité polymérase mais auraient un rôle dans la capacité répliquative des VIA (Muramoto et al 2013). Par ailleurs, le segment 2 code également pour PB1-N40 qui est une forme tronquée de PB1 et qui joue un rôle dans l'expression relative de PB1 et PB1-F2, modulant ainsi la répliquative du virus (Wise et al 2009). La protéine M42, quant à elle, est issue du segment 7 et peut remplacer la fonction de la protéine M2, en son absence (Wise et al 2012). Pour terminer, la protéine NS3, issue du segment 8, pourrait jouer un rôle dans l'adaptation des VIA à la souris (Mohammed Selman 2012).

A l'intérieur des virions (**Figure 1**), les huit segments d'ARN sont entourés par des protéines virales NP (*NucléoProtéines*) et d'un complexe polymérase, composé de PB1 (*Polymerase basic protein 1*), PB2 (*Polymerase basic protein2*) et PA (*Polymerase acidic protein*), formant ainsi le complexe RNP (*RiboNucléoProtéique*) (Noda et al 2006). Les RNPs sont entourés par la protéine de matrice M1 (*matrice 1*) qui constitue la couche interne du virus. L'enveloppe virale, quant à elle, est une bicouche lipidique, provenant de la cellule infectée, dans laquelle sont ancrées trois protéines virales transmembranaires, HA, NA et M2. Les protéines HA et NA sont exprimées de manière majoritaire, en comparaison à la protéine M2 ; la protéine HA étant la plus abondante avec un ratio de 1:4 par rapport à la NA (Bouvier & Palese 2008). Des protéines NEP (*Nuclear Export Protein*) sont également retrouvées à l'intérieur de la particule virale. (Tscherne & Garcia-Sastre 2011)

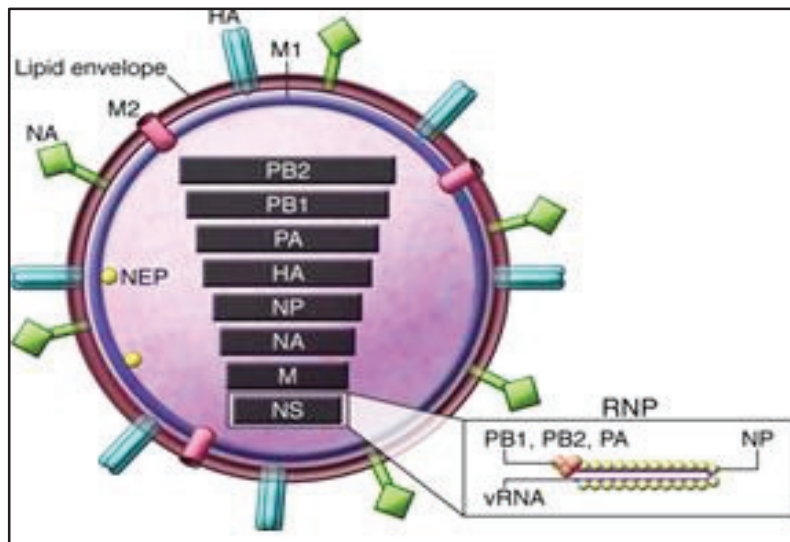


**Figure 1 : Représentation schématique des virus influenza A.**

Le virus influenza de type A est un virus qui comprend une enveloppe, d'origine cellulaire, dans laquelle s'insère trois protéines virales, HA, NA, et M2. La protéine M1 tapisse l'intérieur de la particule virale. Le génome viral est composé de huit segments d'ARN, recouverts de protéine NP formant les RNP. Chaque RNP est associé au complexe polymérase, composé des protéines PB1, PB2 et PA. Des protéines NEP sont également présentes à l'intérieur de la particule virale. (Figure extraite de Tscherne D.M., et al, 2011).

## 2. Le cycle viral des virus influenza A

La première étape du cycle viral du VIA est l'attachement du virus à la cellule qui s'effectue via la reconnaissance de la protéine virale HA aux acides sialiques présents à la surface de la cellule (**Figure 2**). Les acides sialiques peuvent être liés aux chaînes glucidiques par deux liaisons, une liaison alpha 2,3 ou une liaison alpha 2,6. Les virus aviaires reconnaissent préférentiellement l'acide sialique alpha 2,3 galactose alors que les virus humains reconnaissent préférentiellement l'acide sialique alpha 2,6 galactose (Matrosovich et al 2004, Skehel & Wiley 2000).

Suite à l'attachement, le virus est internalisé par endocytose, au sein d'une vésicule ou endosome (Skehel & Wiley 2000). A l'intérieur de l'endosome, dont le PH est acide, l'homo-tétramère M2 forme un canal à protons et permet l'acidification de l'intérieur de la particule virale, ce qui induit la dissociation des RNP viraux (RNPv) de la protéine M1 (Cady et al 2009). Le PH acide de l'endosome permet également à la HA, lorsqu'elle est préalablement clivée par des protéases de l'hôte, d'exposer son peptide de fusion, permettant la fusion de la membrane de l'endosome et de l'enveloppe virale. Les RNPv sont ainsi libérés dans le cytoplasme et importés dans le noyau pour la transcription et la réplication (Neumann et al 1997). Les ARN viraux (ARNv), néo-synthétisés à l'intérieur du noyau, sont produits à partir des ARN complémentaires de polarité positive (ARNc). Dans le noyau, la polymérase permet la transcription des ARNv en ARNm qui migrent par la suite dans le cytoplasme pour être traduit en protéines virales. Les protéines PB1, PB2, PA et NP, retournent ensuite dans le noyau pour s'associer avec les ARNv et former le complexe RNPv. M1 et NEP retournent également dans le noyau pour se lier au RNPv et permettre leur transport dans le cytoplasme au niveau du site d'assemblage (O'Neill et al 1998, Shimizu et al 2011). Les protéines HA, NA et M2, quant à elles, sont transportées vers la membrane plasmique. Les virions nouvellement synthétisés bourgeonnent par la suite dans des régions membranaires spécifiques, riches en glycosphingolipides et cholestérol, que sont les radeaux lipidiques (Nayak et al 2004). Contrairement à la protéine M2, les protéines HA et NA sont enrichies dans les radeaux lipidiques, ce qui pourrait expliquer la moindre présence de M2 dans l'enveloppe virale. Lors de leur libération, les virus néo-synthétisés se ré-attachent à la cellule hôte et s'auto-agrègent, de part la forte affinité de la HA pour les acides sialiques, présents sur les virus et sur les cellules de l'hôte. C'est la NA, qui par son activité de sialidase, permet la libération des nouveaux virions, par le clivage des liaisons entre les acides sialiques et les résidus galactose.

De manière intéressante, en plus des protéines virales HA, NA et M2, des protéines cellulaires sont également incorporées dans l'enveloppe virale, lors du bourgeonnement. Ainsi, 36 protéines cellulaires ont été décrites dans les VIA (Shaw et al 2008). Les protéines de la famille des annexines sont fortement représentées, notamment les annexines A1, A2, A4, A5 et A6. Cependant, le rôle de ces protéines a peu été étudié, à l'exception du rôle de l'annexine 2. En effet, notre équipe a précédemment démontré que l'annexin-2, incorporée dans les particules virales permet la transformation du PLG (Plasminogène) en plasmine, capable de cliver la HA et favorise ainsi la réplication virale (LeBouder et al 2008).

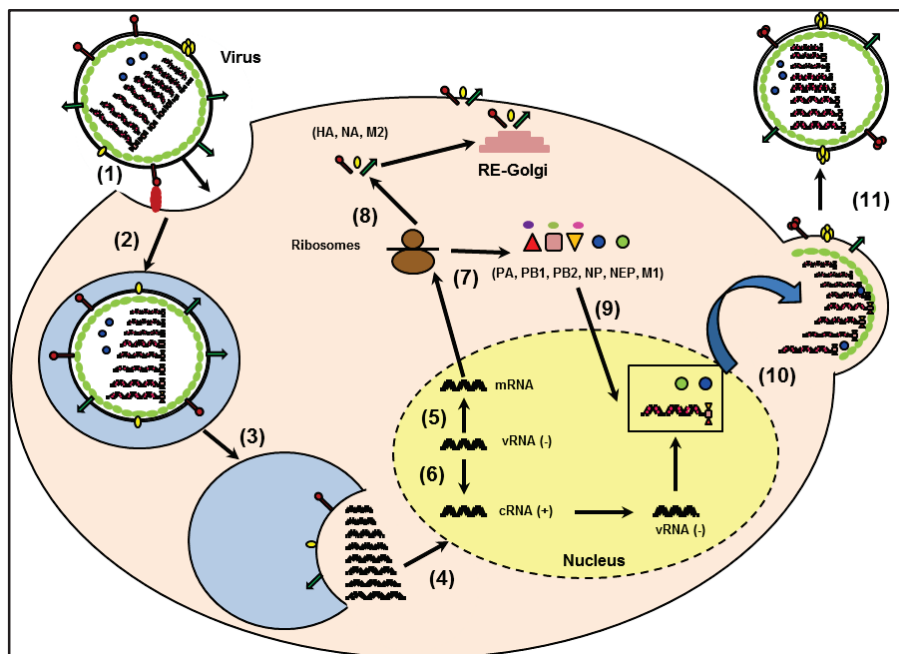


**Figure 2 : Cycle viral des virus influenza A.**

1) Attachement du virus sur la cellule. 2) Entrée du virus dans la cellule hôte par endocytose. 3) Fusion des membranes virale et de l'endosome et libération des RNPv dans le cytoplasme. 4) Transport des RNPv vers le noyau. 5) Transcription des ARNm viraux. 6) Réplication des ARNv. 7) Transport des ARNm viraux vers le cytoplasme et traduction en protéines virales. 8) Maturation des protéines HA, NA et M2 dans l'appareil de Golgi et leur insertion dans la membrane cellulaire. 9) Retour des protéines PA, PB1, PB2, NP, NEP et M1 dans le noyau pour la formation des nouveaux RNPv. 10) Translocation des RNPv néo-synthétisés vers le site d'assemblage, grâce à leur association aux protéines virale M1 et NEP. 11) Libération des nouveaux virions, grâce à l'activité sialidase de la NA. (Figure extraite de Berri F. et al, 2014).

### **3. Moyens de prévention des infections grippales**

A l'heure actuelle, la meilleure façon de se protéger contre la grippe, reste la vaccination. Cependant, le vaccin doit être ajusté chaque année en fonction des souches circulantes et n'aurait aucune efficacité contre de nouvelles souches de VIA qui pourraient émerger du réservoir animal ou contre des virus aviaires hautement pathogènes chez l'homme, tels que le H5N1. Le délai de production de vaccins étant de 6 mois minimum, ceci s'avérerait être un problème de santé public majeur en cas de pandémie qui nécessiterait une prise en charge rapide. Ainsi, le développement de vaccins universels contre la grippe constitue un réel défi pour la recherche actuelle.

Outre la vaccination (préventive), il est possible de traiter les patients infectés par des antiviraux spécifiques (curatifs). Ces derniers, dirigés contre des protéines virales, visent à diminuer le pouvoir répliquatif du virus, réduisant ainsi l'intensité des symptômes, la durée de la maladie et le risque de contamination. Il existe deux classes d'antiviraux: les inhibiteurs de la NA que sont le zanamivir (Relenza®) et l'oseltamivir (Tamiflu®), et les inhibiteurs de la protéine M2 (rimantadine et amantadine). Ces derniers ne sont actifs que sur les virus de type A et la plupart des virus circulant sont devenus résistants aux inhibiteurs de la M2. La NA, quant à elle, est une protéine qui présente un fort taux de mutation, ce qui explique l'apparition de virus résistants aux inhibiteurs de la NA (Escuret et al 2008). Au-delà des phénomènes de résistance, une limitation des antiviraux, actuellement sur le marché, est la nécessité d'une administration précoce pour être efficace, notamment dans les 48h suivant l'infection. Un second défi à relever pour lutter contre la grippe est donc de trouver de nouvelles cibles thérapeutiques qui limiteraient l'émergence de virus résistants, et qui auraient un effet à large spectre, tout en ayant un effet protecteur à des temps plus tardifs d'administration après l'infection.

## **B. La réponse de l'hôte aux infections par le virus influenza**

### **I. Reconnaissance du virus et réponse inflammatoire**

Une des caractéristiques principales du système immunitaire est sa capacité à reconnaître et à détruire le virus et les cellules infectées par le virus, d'où l'importance considérable du système immunitaire dans les défenses antigrippales. Les trois étapes critiques de la défense immunitaire sont (i) la reconnaissance du pathogène, (ii) l'induction de la réponse immunitaire et son amplification et (iii) la résolution inflammatoire. En effet, l'hôte doit tout d'abord reconnaître l'élément étranger, puis les défenses immunitaires sont activées, et lorsque le pathogène est éliminé, l'inflammation doit retourner à l'état basal. La réponse immunitaire consiste en une réponse immunitaire innée, non spécifique du pathogène et en une réponse adaptative, spécifique du pathogène. Nous allons ici développer la reconnaissance du virus influenza et l'induction de l'inflammation, étape initiale de la réponse immunitaire.

Lors d'une infection des cellules épithéliales, mais aussi monocytes, macrophages et cellules dendritiques par le VIA, des récepteurs cellulaires très conservés de l'immunité innée, appelés en anglais PRRs (*Pattern Recognition Receptors*), reconnaissent le pathogène et sont activés. Ces récepteurs reconnaissent des motifs associés aux pathogènes, en anglais *PAMP* (*Pathogen Associated Molecular Pattern*) (Medzhitov 2001). Ces PAMP ont quatre caractéristiques: (i) ils sont absents de la cellule de l'hôte, (ii) ils sont communs à de nombreuses espèces de micro-organismes, ce qui permet de reconnaître la grande diversité des microbes par un nombre restreint de récepteurs, (iii) ils sont essentiels à la survie du pathogène et (iv) ils sont soit présents au niveau des pathogènes soit produits durant l'infection (Medzhitov 2001) (Tsai et al 2014).

Les virus influenza sont reconnus par trois PRRs différents : (i) les TLRs (*Toll-Like Receptor*); (ii) les RIG-1 (*Retinoic acide Inducible Gene-1*) et (iii) les NLRs (*Nod-Like Receptor*) (Wu et al 2011).

## 1. Reconnaissance des virus influenza par les TLRs

Les TLRs sont les premiers récepteurs de la famille des PRRs à détecter les virus influenza. Selon leur localisation, les TLRs sont divisés en deux groupes. Les TLRs 1, 2, 4, 5, 6, 10 et 11 sont exprimés à la surface de la cellule et reconnaissent des structures de la surface des pathogènes. Le rôle de ce premier groupe de récepteurs dans la reconnaissance des virus influenza n'est pas encore bien documenté, à l'exception de TLR4, dont le rôle est très controversé. En effet, alors que l'équipe de Vogel suggère que TLR4 est délétère durant les infections grippales (Shirey et al 2013), Abdul-Careem et ses collègues ainsi que Shinya et ses collègues montrent, au contraire, que TLR4 est protecteur (Abdul-Careem et al 2011) (Shirey et al 2013). Le deuxième groupe de récepteurs TLR, quant à lui, comprend les TLR 3, 7, 8, et 9. Ces récepteurs sont exprimés au niveau de la membrane de l'endosome et reconnaissent des acides nucléiques. La localisation de ces TLR, au niveau de l'endosome, facilite la reconnaissance des virus influenza qui entrent dans la cellule par endocytose. Les TLR 7/8 reconnaissent des ARNs (ARN simple brins) et sont, de part le génome ARNs des virus influenza, les récepteurs privilégiés de ces virus (Heil et al 2004). Ainsi, la réplication du virus n'est pas nécessaire, et l'entrée seule est suffisante pour l'activation de ces récepteurs (Wang et al 2008). La signalisation induite par l'activation des TLR-7/8, après infection par le VIA, induit des facteurs de transcription qui stimulent l'expression de gènes codant des cytokines et des chimiokines, via le signal adaptateur MYD88 (**Figure 3**). Les facteurs de transcription activés par les TLR-7/8 sont NF- $\kappa$ B (*nuclear factor  $\kappa$ B*) et IRF-3/7 (*Interferon Response Factor-3/7*)

(Honda et al 2005, Sasai et al 2010). Après translocation dans le noyau, la co-activation de la transcription des gènes par les IRFs et NF- $\kappa$ B induit la production d'interférons (IFN), cytokines à propriétés antivirales. En revanche, l'activation de la transcription des gènes par NF- $\kappa$ B seul induit la production de cytokines et chimiokines pro-inflammatoires. TLR3, quant à lui, reconnaît des ARNdb (ARN double brins) (Alexopoulou et al 2001). Bien que le virus influenza ne génère pas d'ARNdb au niveau de l'endosome, TLR3 joue un rôle délétère durant les infections grippales (Le Goffic et al 2006). Un récent rapport a confirmé ce rôle délétère de TLR3 dans la pathogénicité des VIA, bien qu'un rôle protecteur puisse également être observé d'une manière souche dépendante (Leung et al 2014). Le mécanisme d'activation de TLR3 serait une reconnaissance par celui-ci d'une structure ARN, encore non identifiée, qui serait présente dans la cellule infectée phagocytée (Schulz et al 2005). Via la molécule adaptatrice TRIF (*Tool/IL-1R domaine-containing adaptor inducing IFN-beta*), les signaux subséquents à l'activation de TLR3 sont ensuite identiques à ceux générés par l'activation de TLR7/8.

## **2. Reconnaissance des virus influenza par RIG-1**

Outre les TLRs, la reconnaissance par RIG-I d'une infection par le VIA, est très importante (Kato et al 2005). A l'intérieur du cytoplasme des cellules infectées, RIG-I reconnaît des groupements triphosphate en 5' de l'ARN viral (Pichlmair et al 2006, Rehwinkel et al 2010). Après activation du récepteur, le domaine hélicase de RIG-I lie une molécule d'ATP (*Adénosine triphosphate*), lui permettant de changer de conformation et de lier la protéine adaptatrice MAVS (*mitochondrial antiviral signaling*) (Luo D 2011). La protéine MAVS est aussi connue sous le nom de VISA (*virus-induced signaling adapter*), IPS-1 (*interferon-beta promoter stimulator 1*) et CARDIF (*CARD adapter inducing interferon beta*). L'activation de ce signal, induit l'activation de IRF-3 et NF- $\kappa$ B, ce qui permet la production de cytokines pro-inflammatoires et des IFNs de type I (Le Goffic et al 2007, Opitz B 2007).

### 3. Reconnaissance des virus influenza par NLRP3

En plus des TLRs et RIG-I, le VIA est aussi reconnu par un complexe protéique cytoplasmique, appelé inflammasome, dont l'activation aboutit à la production de cytokines IL-1 $\beta$  et IL-18 (IL, pour *interleukine*). Le complexe inflammasome est formé d'un récepteur NLRP3, d'une molécule ASC (*apoptotic-associated speck-like protein containing a caspase recruitment domain*), aussi connue sous le nom de PYCARD (*apoptosis-associated speck-like protein containing a CARD*) et d'une caspase inactive, la pro-caspase 1. La formation du complexe inflammasome conduit à son activation et induit l'auto-clivage de la pro-caspase 1 en sa forme active qui, à son tour, clive les cytokines pro-IL-1 $\beta$  et pro-IL-18 en IL-1 $\beta$  et IL-18 qui peuvent être secrétées (Pang IK 2011). Ainsi, la sécrétion des cytokines IL-1 $\beta$  et IL-18 via l'inflammasome, nécessite l'activation de deux signaux. Le signal 1 induit la synthèse de pro-IL-1 $\beta$  et pro-IL-18, via l'activation des TLRs; et le signal 2 permet la formation du complexe inflammasome « NLRP3/ASC/caspase-1 » pour la maturation des cytokines. Ichinohe et ses collaborateurs ont démontré que l'activation de NLRP3 et de l'inflammasome s'effectue grâce au flux de protons, médié par la protéine virale M2 (Ichinohe et al 2010). Il est à noter que ce mécanisme de production d'IL-1 $\beta$  et d'IL-18 s'effectue au niveau des macrophages et des cellules dendritiques. L'activation de l'inflammasome n'est pas nécessaire dans des monocytes infectés car ces derniers expriment de manière constitutive la caspase-1 activée. Ainsi, dans ces cellules, seul le signal 1 est nécessaire pour la libération de l'IL-1 $\beta$  et de l'IL-18 (Netea et al 2010).

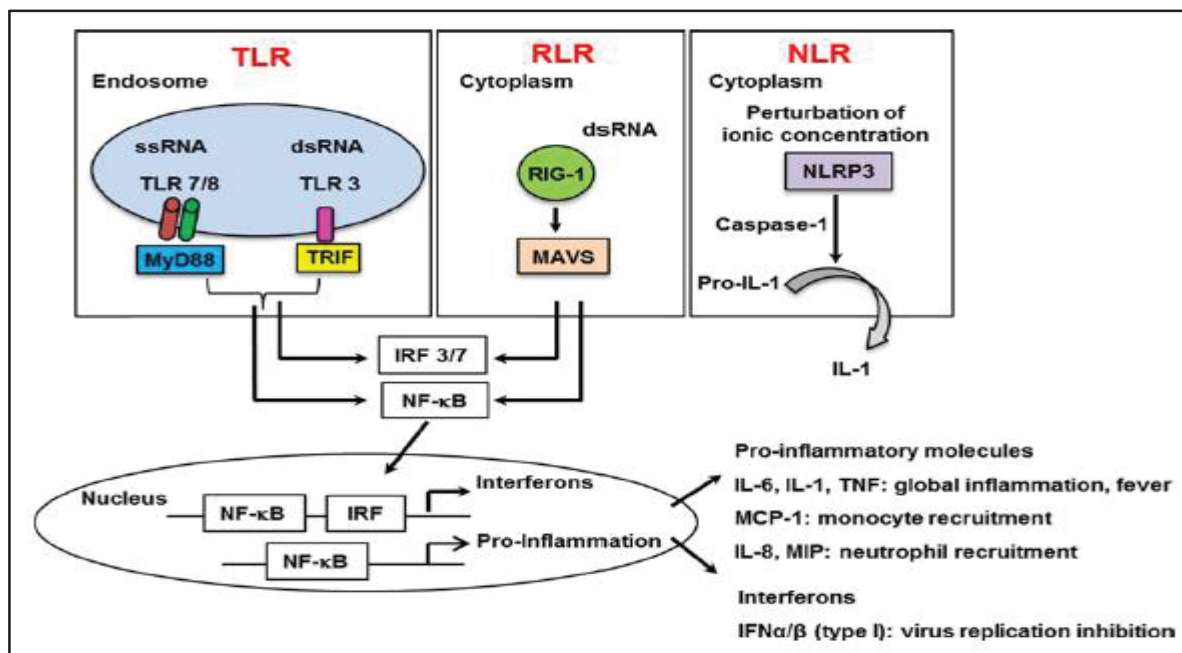


**Figure 3 : Reconnaissance du virus influenza par les PRRs.**

Les virus influenza sont reconnus comme étranger par des récepteurs de l'immunité innée que sont, les TLR, RLR et NLR. Les TLR7/8 et TLR3 reconnaissent des ARN, au niveau de l'endosome. RIG-I reconnaît le groupement 5'triphosphate du génome viral dans le cytoplasme. La perturbation ionique, via la protéine M2, induit l'activation de NLRP3. L'activation des PRRs induit la production des cytokines pro-inflammatoires et des interférons. (Figure extraite de Berri F. et al, 2014).

En conclusion, l'activation des PRRs déclenche une inflammation qui se traduit, par la production (i) de cytokines telles que IL-6, TNF (*Tumor Necrosis Factor*), IL-8, IL-1 $\beta$  et IFN et (ii) de chimiokines (aussi dénommés chémokines) telles que MIP-1 (*Macrophage Inflammatory Protein 1*), MCP-1 (*Monocyte Chemoattractant Protein 1*). De manière générale, les cytokines permettent l'amplification de l'inflammation, les IFN inhibent la réplication virale et les chimiokines permettent le recrutement des cellules immunitaires telles que les neutrophiles, les macrophages, les cellules tueuses naturelles et les cellules dendritiques au niveau du site inflammatoire (Wu et al 2011). L'ensemble de cette réponse innée permet de limiter la réplication virale, d'éliminer les cellules infectées et de protéger ainsi l'organisme.

## **II. Dérégulation de l'inflammation**

### **1. Inflammation excessive durant les gripes sévère**

Comme nous l'avons vu, suite à l'infection par les VIAs, une réponse immunitaire se déclenche dans le but d'éliminer le virus. Cependant, dans les cas pathologiques, la réponse immunitaire est dérégulée et excessive (Kuiken et al 2012). In fine, la réponse de l'hôte est délétère pour l'organisme. Cette réaction disproportionnée de l'hôte est connue sous le nom d'orage cytokinique ou « cytokine storm » en anglais. Ainsi, au cours de la grippe, certains aspects du processus physiopathologique observé, correspondrait à l'induction d'un orage cytokinique dans le poumon (Cheung et al 2002, de Jong et al 2006, La Gruta et al 2007). Cette inflammation dérégulée entrainerait des dommages collatéraux des poumons, qui serait responsable de la défaillance des fonctions pulmonaires, limitant les capacités respiratoires du patient, et entraînant son décès, dans les cas les plus graves. A ce jour, les causes exactes du non-contrôle de la réponse de l'hôte aux infections grippales sévères sont mal connues. Une meilleure compréhension des mécanismes moléculaires impliqués dans la pathogénicité des VIA permettrait de proposer de nouvelles stratégies thérapeutiques. En effet, une voie de recherche alternative pour enrayer efficacement ces formes graves consisterait à réguler l'inflammation afin d'en contrôler les effets délétères. Cette stratégie qui cible l'hôte et non le virus aurait le double avantage d'être indépendante de la souche virale et de limiter la pression de sélection virale, pouvant conduire à l'émergence de virus résistants aux traitements.

## 2. Intensité versus durée inflammatoire

Étant donné que le virus est reconnu comme étranger par les PRRs, l'amplification de l'inflammation est, de ce fait, dépendante de la capacité répliquative du virus. Cela détermine l'intensité de l'inflammation. Lorsque la réponse immunitaire, qui suit cette inflammation initiale, est efficace, le virus est éliminé et s'enclenche alors, de manière active, une phase de résolution de l'inflammation. Cette phase détermine en partie la durée inflammatoire (McCracken & Allen 2014). La plupart des études, ayant pour objectif de mieux comprendre les mécanismes qui engendrent l'inflammation excessive des poumons lors des infections grippales, se sont focalisées sur les phases d'activation et d'amplification de l'inflammation. Cependant, plusieurs études ont démontré qu'à charge virale identique, les VIAs pouvaient induire une maladie sévère ou bénigne (Garcia et al 2010, Teijaro et al 2011). Ainsi, le pouvoir pathogène du virus ne serait pas uniquement lié à son pouvoir répliquatif (Reperant et al 2012). Outre l'apoptose des cellules et la production de résolvines, lipoxines et de molécules anti-inflammatoires, la résolution de l'inflammation est également influencée par l'endothélium vasculaire (Kadl & Leitinger 2005). Récemment, il a été démontré que les cellules endothéliales orchestraient l'avalanche cytokinique durant les infections par les VIAs (Teijaro et al 2011). Ainsi, il est possible que l'hypercytokinémie ne soit pas due à une intensité inflammatoire anormalement élevée mais à un défaut de sa résolution. Les deux phénomènes pouvant être associés. Ceci augmenterait de manière anormale la durée de l'inflammation. L'endothélium vasculaire est une couche unicellulaire qui tapisse les vaisseaux sanguins, en contact direct avec le sang. Lorsque les cellules endothéliales sont activées, l'hémostase, qui est un mécanisme de défense de l'organisme, s'enclenche afin de réparer la lésion. L'inflammation et l'hémostase sont des processus intimement liés. Dans de nombreuses pathologies inflammatoires, telles que le sepsis par exemple, la seule dérégulation de l'hémostase est directement responsable d'une inflammation dérégulée (Engelmann & Massberg 2013) (**Figure 4**).

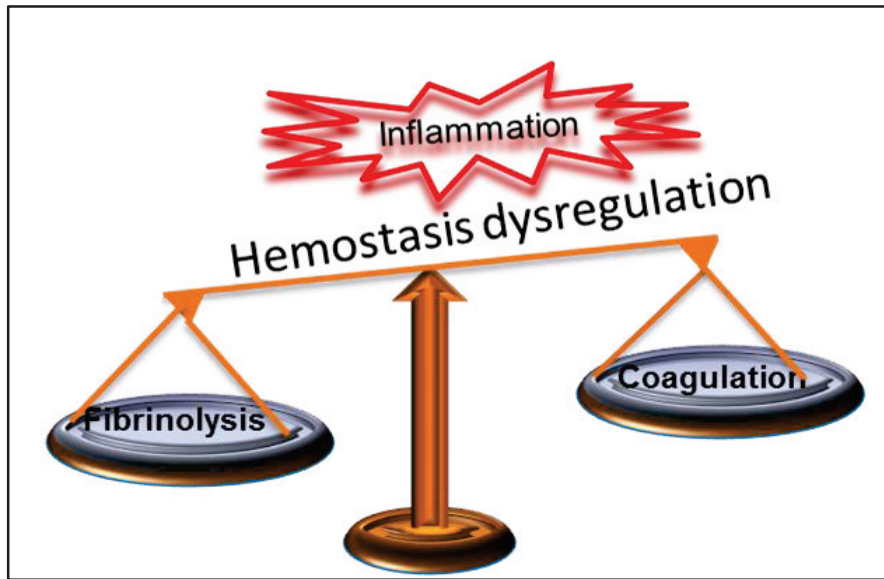


**Figure 4 : Dérégulation de l'hémostase et inflammation.**

La dérégulation de la balance hémostatique est directement associée à une inflammation excessive et incontrôlée dans de nombreuses maladies inflammatoires.

### III. L'hémostase et l'inflammation

L'hémostase est un processus physiologique qui permet le maintien de l'intégrité des vaisseaux sanguins, lors d'une agression vasculaire. L'hémostase peut également être activée en vue de réparer des lésions au niveau des cellules épithéliales. A l'état physiologique, l'endothélium, qui tapisse le vaisseau sanguin, a des propriétés antiplaquettaires, et anticoagulantes, en sécrétant des molécules telles que la PG (*prostaglandine*), le NO (*monoxyde d'azote*), la prostacyclin et l'ectoADPase (CD39) (Jones et al 2012). Lors d'une agression de l'endothélium, par une infection directe des cellules endothéliales ou sous l'effet d'un environnement inflammatoire, les cellules endothéliales expriment des facteurs pro-coagulants à leur surface et en particulier le FT (*Facteur Tissulaire*), une protéine clé de la cascade de la coagulation. Par ailleurs, les cellules endothéliales libèrent des molécules d'activation et d'adhésion des plaquettes et des leucocytes, telles que des ICAM (*Intracellular Adhesion molecule*), PAF (*Platelet Activating Factor*), le facteur de Willerbrand (vWF), l'ADP (*Adénosine DiPhosphate*) et la thrombine. Ceci déclenche l'activation du processus de l'hémostase qui conduit à la formation d'un caillot constitué, de plaquettes agrégées et de fibrine. On distingue trois étapes lors de l'hémostase qui sont activées simultanément: (i) l'hémostase primaire ou agrégation plaquettaire, (ii) la coagulation ou production de thrombine et formation de fibrine et (iii) la fibrinolyse, ou dissolution de la fibrine et donc du caillot (Figure 5).

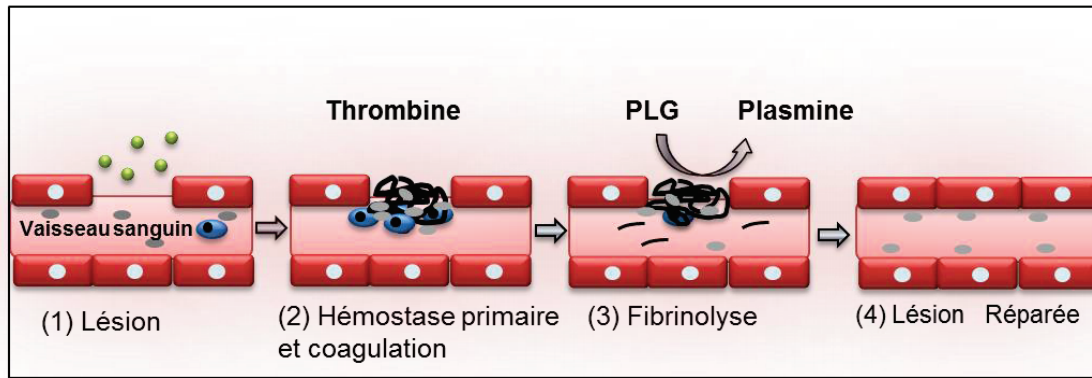


**Figure 5: Représentation schématique des étapes du processus de l'hémostase.**

1) Lésion vasculaire. 2) Formation du clou plaquettaire et transformation du fibrinogène en réseau de fibrine (coagulation). Ces deux processus sont médiés essentiellement par la thrombine 3) Fibrinolyse ou dégradation enzymatique de la fibrine par la plasmine. 4) Réparation de la lésion et rétablissement du flux sanguin.

## 1. L'hémostase primaire

L'hémostase primaire est la première étape de réaction à l'agression de l'endothélium. Elle débute par une étape de contraction vasculaire ou vasoconstriction, mécanisme reflexe qui réduit le flux sanguin et permet la formation d'un thrombus blanc, qui est un agrégat de plaquettes, cellules sanguines anucléés d'environ 4µm (Morrell et al 2014). A l'état physiologique, les plaquettes circulent dans le sang sous forme inactives. Elles portent à leur surface des récepteurs, dont les plus importants sont : la glycoprotéine GPIb, le complexe glycoprotéique GPIIb/IIIa (ou intégrine  $\alpha$ IIb $\beta$ 3) et des récepteurs activés par des protéases (notamment la thrombine) ou en anglais PAR (*Protease-activated-receptor*) (sfh 2011).

Le déclenchement de l'activation des plaquettes est dû à la fixation du vWF au collagène du sous-endothélium. Le vWF est une molécule multimérique de très haut poids moléculaire, synthétisé par la cellule endothéliale et le mégacaryocyte, qui établit un pont entre les glycoprotéines Ib plaquettaires et le sous-endothélium. Ainsi, une première couche monocellulaire de plaquettes se constitue. L'adhésion provoque l'activation des plaquettes par la thrombine via les PARs et cette activation est amplifiée par le collagène, l'ADP et le TXA2

(*thromboxane A2*) (**Figure 6**). Ceci se traduit par : 1) Un changement de forme des plaquettes. De discoïde, elles deviennent sphériques, émettent des pseudopodes et se contractent. Ceci permet la centralisation des granules, étape indispensable à la dégranulation. 2) Les plaquettes activées libèrent le contenu de leurs granules denses, réserve d'ATP, d'ADP et de sérotonine, ce qui amplifie l'activation initiale des plaquettes. Elles libèrent également le contenu de leurs granules alpha qui contiennent entre autre la p-sélectine et des protéines diverses telles que des protéines de la coagulation et de la fibrinolyse ainsi que des cytokines (Mitsuhashi et al 2001). 3). L'activation plaquettaire provoque également le changement de conformation des glycoprotéines  $\alpha_{IIb}\beta_{III}$  à leur surface, permettant la fixation du fibrinogène, en présence de calcium, et leur agrégation. L'interaction des plaquettes, entre elle, est donc médiée par le fibrinogène, ce qui crée un thrombus initial, lequel sera consolidé ensuite par la coagulation et la formation du réseau de fibrine.

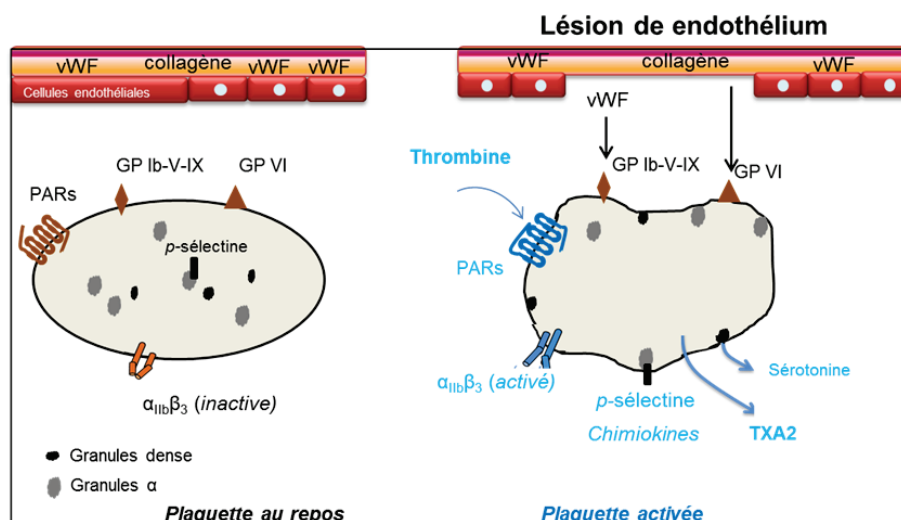


**Figure 6 : Présentation schématique de l'activation plaquettaire.**

L'agression de l'endothélium induit l'activation du processus de l'hémostase afin de réparer la lésion. L'activation de l'hémostase primaire et la formation du premier clou plaquettaire comprend, (i) l'adhésion des plaquettes au facteur de vWF et au sous-endothélium via GPIb-V-IX, (ii) l'activation des plaquettes, ce qui se traduit par un changement de conformation plaquettaire, l'activation de l'intégrine  $\alpha_{IIb}\beta_{III}$  permettant l'agrégation des plaquettes et l'adhésion des leucocytes, (iii) La libération du contenu de leur granules.

L'activation des plaquettes jouent un rôle important dans de nombreux processus inflammatoires. Les plaquettes activées, comme nous l'avons mentionné, libèrent le contenu de leurs granules denses, contenant des cytokines et chémokines telles que RANTES (*Regulated on Activation, Normal T cell Expressed and Secreted*), IL-1( $\alpha$ - $\beta$ ), MCP-1 ou PAF (Guanfang Shi 2011). Des molécules telles que l'ADP, la sérotonine et le TXA<sub>2</sub>, qui sont libérées par les plaquettes jouent, quant à elles, un rôle important dans le recrutement des leucocytes (Gawaz et al 2005). Par ailleurs, l'adhésion primaire des neutrophiles et des plaquettes au sous-endothélium favorise le recrutement secondaire de nouvelles cellules immunitaires (Zarbock et al 2007). De manière intéressante, la stimulation des cellules endothéliales par l'IL-1 et le TNF, induit l'expression du FT (Hawrylowicz et al 1991). Ainsi, en boucle d'auto-amplification, l'inflammation amplifie l'activation de l'hémostase (Darbousset et al 2012).

## **2. La Coagulation**

La coagulation est une cascade d'activation enzymatique, déclenchée par la mise en contact du sang circulant avec le FT et qui a pour objectif de consolider le clou plaquettaire initial en liant les plaquettes entre elles avec un réseau de fibrine. Le FT est une glycoprotéine membranaire associée aux phospholipides. Certaines cellules, en contact permanent avec le flux sanguin, n'expriment le FT que lorsqu'elles sont activées, ce qui est le cas des monocytes et des cellules endothéliales. Il existe deux types de FT : le FT lié aux cellules et le FT soluble. Le rôle biologique du FT soluble est moins connu que celui du FT cellulaire. Cependant, des études ont montré que le FT soluble joue aussi un rôle important dans l'inflammation et l'hémostase (Busso et al 2008). Lorsque le FT se trouve en contact du sang, il fixe et active le facteur VII (FVII) en FVII activé (FVIIa). L'activation du complexe FT/FVIIa induit une cascade

d'activation de facteurs de la coagulation, aboutissant à la formation de la thrombine (**Figure 7**). Cette cascade est la voie extrinsèque de la coagulation. Au-delà de cette voie classique, une seconde voie, la voie intrinsèque de la coagulation amplifie la production de thrombine. Cette dernière est une sérine protéase qui a pour fonction principale de transformer le fibrinogène soluble en réseau de fibrine insoluble. Ainsi, le thrombus initialement formé lors de l'hémostase primaire est consolidé par le réseau de fibrine.

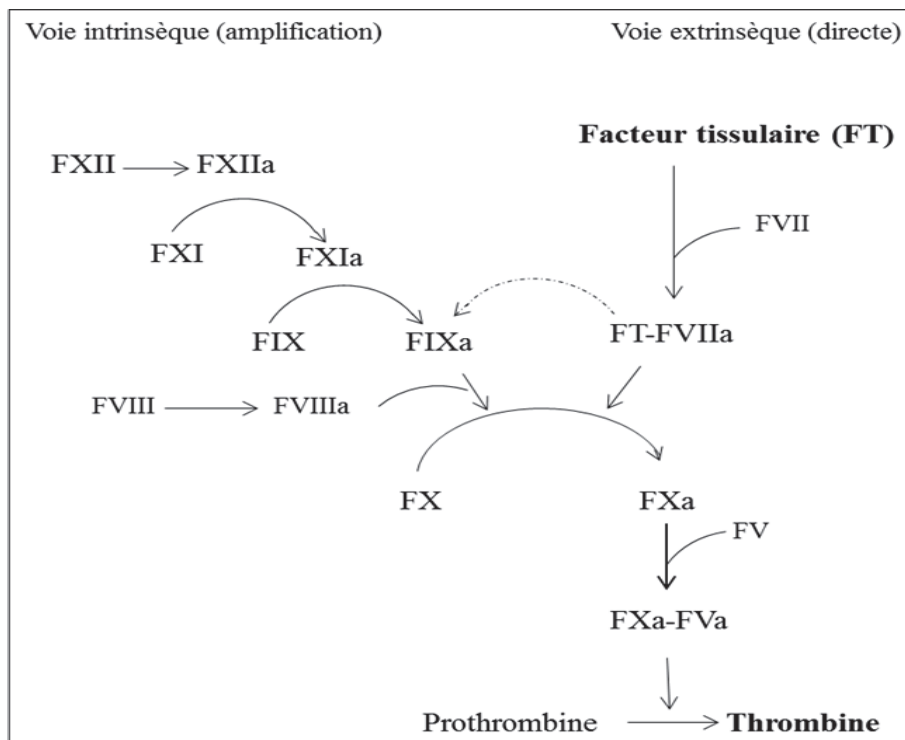


**Figure 7 : Cascade enzymatique de la coagulation.**

L'élément déclenchant la coagulation est l'expression du FT à la surface des cellules. La génération de thrombine provient, tout d'abord, d'une voie directe (voie extrinsèque), initiée par le complexe FT/FVIIa, puis d'une voie d'amplification (voie intrinsèque). La fixation du FT au FVII, circulant, favorise l'activation du FVII en FVII activé (FVIIa). Le complexe FT/FVIIa agit de façon préférentielle sur le FX pour le transformer en FXa. Ce dernier en présence de son cofacteur FV activé (FVa), forme le complexe prothrombinase qui active la prothrombine en thrombine. Les premières traces de thrombine ainsi générée par la voie directe vont activer la voie intrinsèque permettant ainsi la génération de la thrombine. (Figure extraite de SFH, 2011).

Afin d'empêcher une activation excessive et potentiellement dangereuse de la coagulation, telle que les thromboses veineuses, le système de coagulation est régulé par des inhibiteurs dont

les plus connus sont : (i) l'AT (*antithrombine*) qui se fixe directement sur la thrombine et inhibe son action. L'activité de l'AT est augmentée par la molécule d'héparane sulfate présente à la surface de l'endothélium ou par les héparines, utilisées comme médicament; (ii) l'inhibiteur de la voie du facteur tissulaire ou en anglais TFPI (*Tissue Factor Pathway Inhibitor*) qui est un inhibiteur naturel de la phase initiale de la coagulation. Le TFPI forme un complexe quaternaire avec le FT/FVIIa et FXa, limitant ainsi la génération du FXa et donc de la thrombine; (iii) le système de protéine C/protéine S : la protéine C (PC) est une proenzyme, qui se fixe à la surface des cellules endothéliales sur son récepteur EPCR (*Endothelial Protein C Receptor*). La PC est activée en PC active (PCa) par la thrombine préalablement fixée à la thrombomoduline, protéine récepteur, elle aussi exprimée à la surface des cellules endothéliales. La PCa, en présence de son cofacteur protéine S, est un inhibiteur puissant de la génération de thrombine. Lorsque le caillot est formé, la fibrinolyse physiologique sera ensuite activée afin de restituer la fluidité sanguine.

La coagulation est un processus intimement liée à l'inflammation. Dès le clivage du fibrinogène en fibrine et la formation du clou plaquettaire, des leucocytes sont directement recrutés au niveau du site de lésion et adhèrent aux plaquettes (sfh 2011). Une dérégulation de la coagulation aboutit à des cas pro-thrombotiques sévères, généralement associés à une inflammation délétère (Gando et al 1999). La dérégulation du lien entre la coagulation et l'inflammation contribue à des cas graves d'infections, tels que la coagulation intravasculaire disséminée, généralement associée aux sepsis bactériens (Dellinger 2003). L'injection directe du FT soluble chez la souris induit un état inflammatoire (Busso et al 2008). Par ailleurs, les produits de la cascade de la coagulation tels que la thrombine et la fibrine sont pro-inflammatoires (Jensen et al 2007, Kaplanski et al 1998). La fibrine induit l'expression de la molécule d'adhésion (ICAM-1) à la surface des cellules endothéliales, ce qui augmente

l'adhésion des neutrophiles (Qi et al 1997). Quant à la thrombine, elle induit sur les cellules endothéliales, l'expression des molécules d'adhésion (Sugama et al 1992), de la sécrétion de PAF (Shuman et al 1979) et la production de cytokines telles que Il-6, Il-8 ou MCP-1 (Bachli et al 2003, Kaplanski et al 1997). Le rôle de la thrombine pourrait être dépendant de l'activation des PARs (Coughlin 1999). En particulier, la thrombine via ces récepteurs provoque l'augmentation du niveau d'expression des gènes des cytokines pro-inflammatoires tels que le TNF- $\alpha$ , l'IL-6 ou l'IL-1 $\beta$  (Asokanathan et al 2002, Lin et al 2006). Ainsi, les PARs, en activant les plaquettes, en régulant la coagulation et activant la libération de cytokines, sont à l'interface entre l'hémostase et l'inflammation.

### **3. La fibrinolyse**

La fibrinolyse est un processus physiologique qui permet d'éliminer progressivement le caillot de fibrine. En effet, le caillot ne doit jouer qu'un rôle temporaire. Lorsque la fonction tissulaire est restaurée, le caillot doit disparaître. La destruction des polymères de fibrine, s'effectue essentiellement par la plasmine qui provient d'un précurseur plasmatique inactif, le PLG. Une fois le PLG activé en plasmine, cette dernière a pour rôle principal de dégrader la fibrine en produits de dégradation de tailles variables, identifiés comme PDF (*Produits de Dégradation de la Fibrine*). Les PDF les plus connus sont les D-Dimer qui sont des marqueurs spécifiques de la fibrinolyse, alors que d'autres PDF peuvent également provenir du clivage du fibrinogène. Les PDF et D-Dimer sont quantifiables dans le plasma, leur taux est ainsi un reflet de l'activité de la plasmine et de l'activation de la fibrinolyse.

La fibrinolyse est tempérée par des inhibiteurs naturels qui contrôlent son activation. Ces inhibiteurs sont de deux types : (i) les inhibiteurs directs de la plasmine, principalement l' $\alpha$ 2-antiplasmine plasmatique, mais aussi l' $\alpha$ 2-macroglobuline. (ii) les inhibiteurs indirects de la production de la plasmine et notamment les PAI (*Plasminogen Activator Inhibitor*). Ces

derniers inhibent en amont les activateurs de la transformation du PLG en plasmine : le t-PA (*Tissue-Plasminogen Activator*) et l'u-PA (*Urokinase-Plasminogen Activator*).

La fibrinolyse joue un rôle important sur l'état inflammatoire. La plasmine contribue de manière considérable à l'amplification de l'inflammation via les PDF qui ont une forte activité chimio-attractante (Jennewein et al 2011, Leavell et al 1996). Cet aspect pro-inflammatoire sera développé dans le chapitre consacré au plasminogène.

## IV. Les récepteurs activés par la thrombine et le plasminogène, des molécules au cœur de l'hémostase et de l'inflammation

### 1 - Les récepteurs activés par la thrombine

Au-delà de cliver le fibrinogène en fibrine, lors de la coagulation, la thrombine agit également via des récepteurs cellulaires à sept domaines transmembranaires, couplés à des protéines G, que sont les récepteurs activés par les protéases ou PAR (Vu et al 1991). Ces récepteurs comprennent 4 membres : PAR-1 à PAR-4. A l'exception de PAR-2, PAR-1, PAR-3 et PAR-4 sont activés par la thrombine. Les deux récepteurs principaux de la thrombine sont toutefois PAR1 et PAR4. Outre la thrombine, d'autres protéases, générées lors de la coagulation, activent aussi ces mêmes récepteurs (**Figure 8**). L'effet principal de l'activation de ces derniers est une modulation de l'inflammation. Les PARs sont donc à l'interface entre l'hémostase et l'inflammation.

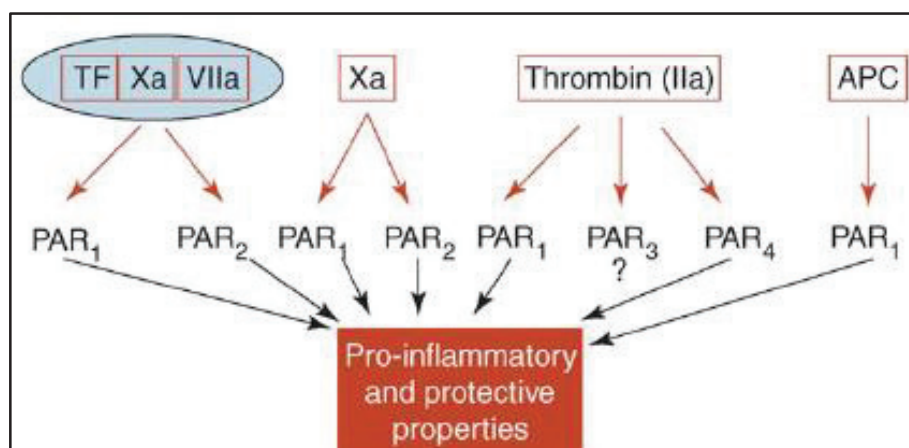


**Figure 8 : Activation des PARs par les protéases de coagulation.**

La cascade de la coagulation aboutit à l'activation de plusieurs protéases, telles que le facteur Xa, le facteur VIIa et la thrombine. Ces protéases clivent et activent des PARs conduisant, entre autre à la modulation de l'inflammation. (Figure extraite de Cirino G. et al, 2006).

Le clivage de l'extrémité N-terminale extracellulaire du récepteur par la thrombine, génère une nouvelle extrémité N-terminale qui démasque le ligand du PAR. Cette nouvelle extrémité se fixe alors sur son site de liaison sur le récepteur, permettant l'activation de ce dernier. L'activation du récepteur permet l'activation des petites protéines G, formées des sous-unités  $\alpha$ ,  $\beta$  et  $\gamma$  ( $G\alpha$ ,  $G\beta$  et  $G\gamma$ , respectivement). La catalyse d'échange de GDP (*Guanosine* diphosphate) en GTP (*Guanosine* triphosphate) au niveau de la sous-unité alpha de la protéine G entraîne sa dissociation du complexe  $\beta\gamma$ . Ainsi, la forme activée de la sous-unité  $\alpha$  et le complexe  $\beta\gamma$  stimulent des voies de signalisation, dont celles de la phospholipase C (IP3/diacyl Glycerol) et MAP Kinase (Arora et al 2007) (van Biesen et al 1995). Ces voies de signalisation sont impliquées dans la modulation de l'inflammation et de l'hémostase (Coughlin 2000, Coughlin 2005, Vu et al 1991) (**Figure 9**). Une des caractéristiques de ces récepteurs est leur désensibilisation (absence de réponse à un second stimulus), ces récepteurs étant rapidement internalisés et dégradés, une fois activés (Cirino & Vergnolle 2006).

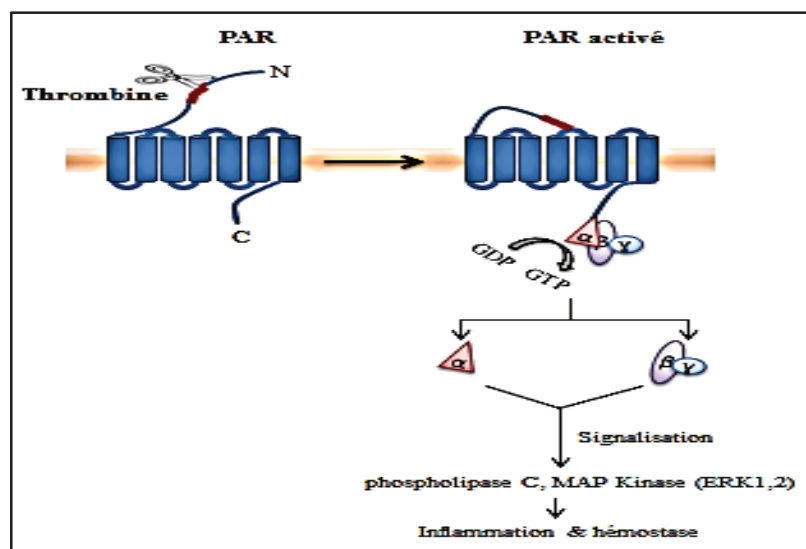


**Figure 9 : Activation de PARs par la thrombine et réponse cellulaire.**  
 La thrombine se lie et clive le récepteur PAR au niveau de l'extrémité N-terminale du récepteur. La nouvelle extrémité N-terminale ainsi générée joue le rôle de ligand et se lie au récepteur pour l'activer. Cette activation induit l'activation de différents messagers intracellulaires, via la signalisation des petites protéines G. Au final cette activation aboutit à la modulation de l'hémostase et de l'inflammation.

Les PARs sont exprimés de manière ubiquitaire (Hollenberg 2003) et ils jouent un rôle important dans différents processus physiologique, notamment au niveau de l'activation plaquettaire. L'activation de l'hémostase primaire, par la thrombine, fait intervenir en moins deux PARs, de manière différentielle chez l'homme et la souris (**Figure 10**). Chez l'homme, les plaquettes humaines sont activées par PAR1 et PAR4, PAR1 présentant une affinité plus grande pour la thrombine que PAR4. La différence d'activation de ces récepteurs par la thrombine est de l'ordre d'un facteur 100. Les plaquettes de souris, quant à elles, expriment PAR3 et PAR4, mais seul PAR4 est impliqué directement dans l'activation des plaquettes. En effet, la présence unique de PAR3 est insuffisante pour l'activation des plaquettes, bien que PAR3 joue un rôle de cofacteur pour PAR4 (Coughlin 2005).

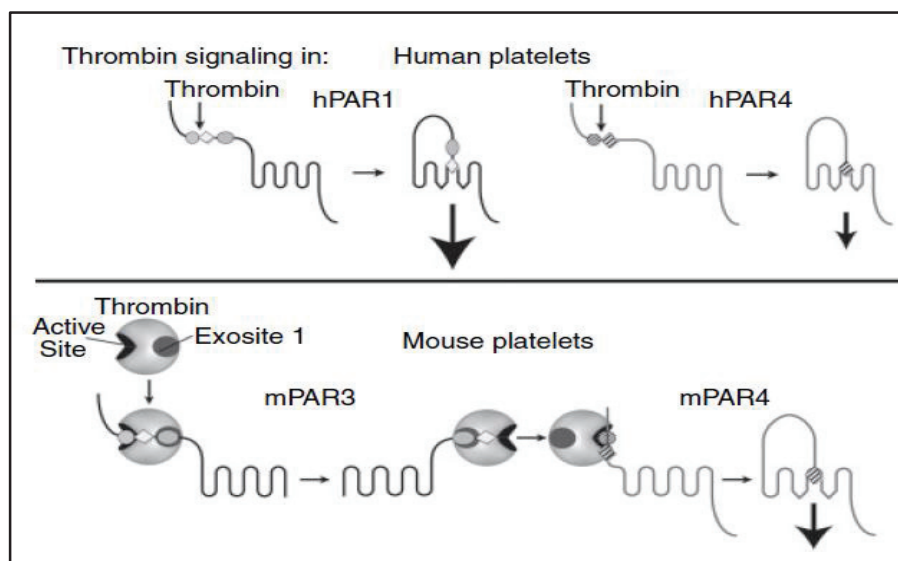


**Figure 10 : Activation différentielle des PARs sur les plaquettes humaines et murines.**

PAR1 et PAR4 sont exprimés sur les plaquettes humaines (panel du haut). PAR1 et PAR4 sont tous deux directement activés par la thrombine. En revanche, chez la souris les plaquettes expriment PAR3 et PAR4 (panel du bas). PAR3 n'est pas activé par la thrombine, cependant, il joue un rôle de cofacteur d'activation pour PAR4. (Figure extraite de Coughlin S.R., 2005).

Le rôle des PARs, en réponse à la thrombine provient également de leur activation sur les cellules épithéliales et/ou endothéliales. Bien que PAR1 puisse avoir un rôle ambivalent, il a

plutôt été décrit comme un récepteur pro-inflammatoire, notamment via la production de cytokines et chimiokines, de l'expression des molécules d'adhésions et de l'augmentation de la perméabilité cellulaire (Coughlin 2000, Vu et al 1991). L'effet pro- ou anti-inflammatoire de PAR1 serait en fonction du taux de thrombine (Weiler 2010). A de faibles concentrations de thrombine, PAR1 serait activé par le complexe APC/EPCR et aurait des effets anti-inflammatoires, via l'activation du récepteur S1P1 (*sphingosin 1 phosphate 1*). L'activation de ce dernier permettrait aussi le maintien de l'intégrité des vaisseaux sanguins (Feistritz C 2005). En présence de fortes concentrations de thrombine, PAR1 serait directement activé par la thrombine et aurait plutôt un effet pro-inflammatoire via l'activation de S1P3 (Niessen et al 2008) (Niessen et al 2009)(Figure 11). Ces effets ambigus de PAR1 sont toutefois mal compris.

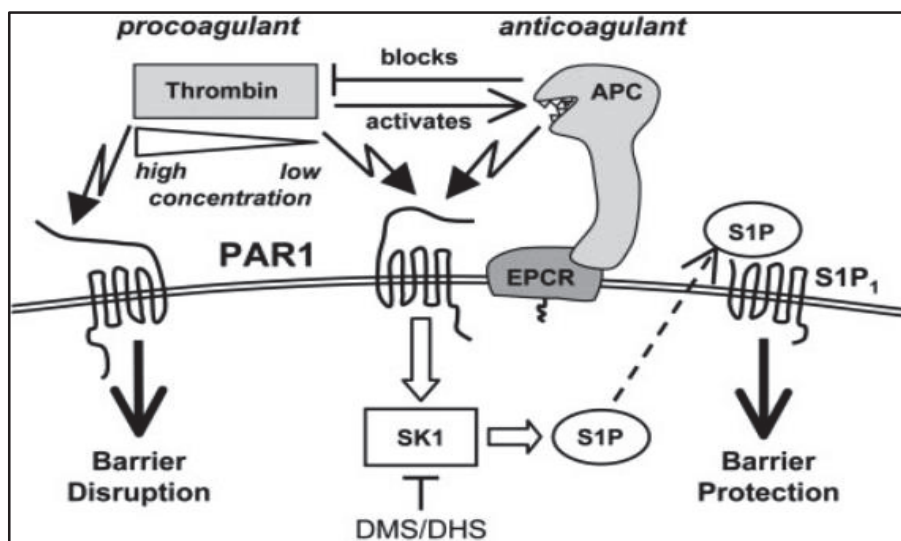


**Figure 11 : Rôle pro et anti-inflammatoire de PAR1.**

A de faible concentration de thrombine, PAR1 est clivé par l'APC, ce qui induit une co-activation de l'activation de la voie de signalisation S1P1 et dont les effets seraient protecteurs. En revanche, à forte concentration de thrombine, PAR1 est directement clivé par la thrombine, et aurait un effet pro-coagulant et pro-inflammatoire via S1P3 (Niessen et al 2008). Les mécanismes exacts d'activation de PAR1 à faible et forte concentrations de thrombine sont encore mal élucidés. (Figure extraite de Feistritz C. et al, 2005).

## 2. Le plasminogène

Le PLG est une glycoprotéine monocaténaire, principalement synthétisée par les hépatocytes. Ses propriétés sont essentiellement conditionnées par sa structure. Son extrémité N-terminale se compose de cinq structures en boucle qui possèdent des sites de haute affinité pour la lysine, nommés LBS (*Lysine Binding Site*). Ces sites sont des sites de fixation à la fibrine, aux produits de dégradation de la fibrine, à l' $\alpha$ 2-antiplasmine et à des protéines matricielles ou cellulaires capables d'exposer des groupements lysines. Le PLG et son activateur le t-PA possèdent une grande affinité pour la fibrine. En se fixant sur celle-ci, le PLG est clivé en plasmine au niveau de la liaison peptidique Arg<sup>561</sup>\_Val<sup>562</sup> permettant ainsi le démasquage du site protéolytique. Un second activateur du PLG est l'uPA qui active préférentiellement le PLG à la surface des cellules (Collen 1980, Forsgren et al 1987). Le PLG peut se fixer sur des protéines cellulaires telles que l'annexine 2, ou des récepteurs tels que le PLG-R<sub>KT</sub> (Andronicos et al 2010). La liaison du PLG/plasmine sur son récepteur induit l'activation de différentes voies de signalisation, dont NF- $\kappa$ B, impliquées dans l'expression des gènes de l'inflammation mais également de l'hémostase tel que cela a été démontré pour le FT (Syrovets et al 2012). De plus, la plasmine est également capable d'activer le récepteur PAR-4 permettant ainsi d'induire l'agrégation plaquettaire (Arora et al 2007). D'une manière intéressante, à des concentrations élevées, la plasmine est également capable d'activer PAR-1 et d'induire l'apoptose des cellules endothéliales. La plasmine est également impliquée dans la dégradation de la matrice extracellulaire ce qui induit l'augmentation de la perméabilité des cellules.

Le rôle essentiel de la plasmine est d'activer la fibrinolyse. Le système PLG/plasmine contribue également d'une manière considérable à l'amplification de l'inflammation. Tout d'abord, le PLG et la plasmine augmente l'infiltration des cellules immunitaires la production de cytokines lors d'une lésion tissulaire (Gong et al 2008, Syrovets et al 1997, Wygrecka et al

2009). Ainsi, des souris déficientes en PLG sont protégées d'une inflammation excessive et des lésions subséquentes dans différentes maladies inflammatoires (Leavell et al 1996, Moons et al 1998, O'Connell et al 2010, Ploplis et al 1998). Par ailleurs, via une activation de la fibrinolyse, les PDF générés augmentent le recrutement des leucocytes, notamment les neutrophiles, et stimule la libération de cytokines et chimiokines (Jennewein et al 2011, Lu et al 2011). En conclusion le système PLG/plasmine en activant la fibrinolyse et en modulant l'inflammation est à l'interface entre l'hémostase et l'inflammation.

## **C. Hémostase et virus influenza**

### **1 - Etudes cliniques**

Au niveau clinique, de nombreuses anomalies de l'hémostase ainsi que des complications cardio-vasculaires ont été observées chez des patients atteints de gripes sévères (Tran et al 2004, Warren-Gash et al 2012, Warren-Gash et al 2009). Aussi, de nombreux cas de thrombopénies ont été rapportés (Choe et al 2013, Cunha 2013, Gao et al 2013) ainsi que des dérégulations de la fibrinolyse (Soepandi et al 2010, Wang et al 2011). Bien que effectué sur de faibles groupes, il semblerait qu'une augmentation de l'activation plaquettaire corrèle avec une sévérité de la maladie (Rondina et al 2012). En revanche, la coagulation intravasculaire disséminée a rarement été observée (Krummel-McCracken 2011, Ohrui et al 2000). De manière intéressante, parmi les biomarqueurs de sévérité des cas d'infections grippales, outre les cytokines, des études viennent de suggérer que des marqueurs de la coagulation pourraient être utilisés (Davey et al 2013). A l'inverse, des patients présentant des troubles de l'hémostase ont une susceptibilité accrue de faire des infections grippales sévères (Rupa-Matysek et al 2014). L'ensemble de ces désordres de l'hémostase, étant exacerbés par les surinfections bactériennes (Nguyen et al 2012), des études expérimentales sont donc nécessaires afin de déterminer le rôle précis de l'hémostase durant les infections grippales.

## **2 - Activation des cellules endothéliales par les virus Influenza A**

*In vitro*, les cellules endothéliales pulmonaires sont sensibles aux infections par les virus de la grippe (Armstrong et al 2012, Zeng et al 2012). Un endothéliotropisme a également été observé dans des embryons de poulets et de chats (Feldmann et al 2000, Reperant et al 2012). Aussi, chez la souris, les cellules endothéliales semblent être sensibles aux virus de la grippe (Armstrong et al 2012). En revanche, pour la première fois en 2011, au niveau expérimental, l'implication de l'endothélium dans l'orage cytokinique, induit par les virus influenza A, a été proposé (Teijaro et al 2011) (Short et al 2014). L'endothélium étant la couche tapissant l'intérieur des vaisseaux sanguins, un premier pas vers le rôle de l'hémostase dans les infections grippales peut être ainsi envisagé. Cependant, cette étude n'a pas lié le rôle de l'endothélium à une dérégulation de l'hémostase mais à un recrutement dérégulé des leucocytes au niveau du site infectieux. Dans cette étude, il a en effet été démontré que les S1P1 jouaient un rôle central dans la régulation de l'orage cytokinique (Teijaro et al 2011).

### **3 - Activation de l'hémostase par les virus influenza**

A l'heure actuelle, au niveau expérimental, l'implication de l'hémostase dans les infections grippale est peu documentée mais attire beaucoup d'attention. En 2006, Keller et ses collaborateurs ont démontré, pour la première fois, une activation de la coagulation et de la fibrinolyse dans un modèle de souris infectées par le VIA. De manière intéressante, l'augmentation de la production de thrombine, l'inhibition du système de la protéine C et l'augmentation des marqueurs de l'activation de la fibrinolyse, PAI-1 et D-Dimer corrélaient avec une augmentation de l'inflammation (Keller 2006). Plus récemment, l'activation de l'hémostase a été confirmée chez le furet. Ainsi, après une infection par le VIA, il a été observé une augmentation du complexe TAT dans le plasma (marqueur de la génération de thrombine et donc de l'activation de la coagulation), ainsi qu'une déposition de fibrine dans les tissus d'animaux infectés, en comparaison avec des animaux non infectés (Goeijenbier et al 2014). Aussi, très récemment et pour la première fois, le mécanisme d'activation des plaquettes par le virus influenza a été élucidé (Boilard E 2014). Dans cette étude, chez la souris et chez l'homme, il a été démontré que le virus influenza activait les plaquettes via le FcγRIIA et la génération de thrombine. Par ailleurs, une étude préalable avait montré chez la souris que PAF jouait un rôle dans le recrutement des neutrophiles et dans les lésions pulmonaires induites par le VIA (Garcia et al 2010). Le rôle de la PC dans les infections grippales a aussi été évalué. Le traitement de souris, infectées par le VIA, avec de la PCa recombinante, inhibe la coagulopathie induite par l'infection. Cependant, ce traitement n'a eu aucun effet protecteur sur l'inflammation et la mortalité des souris (Schouten et al 2010). LaRosa et ses collaborateurs ont tempéré les résultats négatifs sur la protection grippale en proposant que les doses de protéines recombinantes, les temps et mode d'administration du traitement pourraient en être la cause (LaRosa 2010). De manière contradictoire, une étude, menée par les mêmes auteurs, a montré que le traitement des souris avec un anticorps anti-PCa, inhibe la coagulopathie et

l'inflammation et favorise le recrutement des neutrophiles au niveau du site d'infection, ceci corrélait avec une augmentation de mortalité (Schouten et al 2011).

## **Objectif de la thèse**

Bien que des études aient montrées l'activation du processus de l'hémostase durant les infections grippales, le rôle de l'hémostase dans la pathogénicité des VIAs et son lien dans la dérégulation inflammatoire au cours des gripes sévères reste à être évalué. Dans le cadre des travaux, réalisés au cours ma thèse, je me suis intéressée au rôle de l'hémostase durant les infections grippales : en particulier, nous avons étudié le rôle du récepteur à la thrombine, PAR-1 et du plaminogène dans la pathogénocité des VIAs. J'ai également contribué à des résultats en cours sur le rôle de la coagulation et de l'activation des plaquettes. En utilisant des approches génétiques et pharmacologiques, *in vitro* et *in vivo*, nos résultats ont montré que l'hémostase joue un rôle important dans l'inflammation délétère des poumons durant les infections grippales sévères. Lors d'un travail en parallèle, je me suis également intéressée à l'échappement des VIAs au système immunitaire, via l'incorporation de la protéine cellulaire Annexin 5 dans les particules virales.

## Chapitre 2: RESULTATS

# **Manuscrit n°1: PAR1 contributes to influenza A virus pathogenicity in mice.**

Khaled Khoufache\*, Fatma Berri\*, Wolfgang Nacken, Annette B.Vogel, Marie Delenne, Eric Camerer, Shaun R.Coughlin, Peter Carmeliet, Bruno Lina, Guus F.Rimmelzwaan, Oliver Planz, Stephan Ludwig, and Béatrice Riteau.

**J Clin. Invest. 2013. Doi: 10.1172/JCI61667**

\* co-premier auteurs

## **Résumé**

La thrombine est une protéase clé de la coagulation et de l'hémostase primaire. Chez la souris, au cours de l'infection grippale, la thrombine est retrouvée en grande quantité au niveau des sites infectieux (Keller 2006). Au-delà de cliver le fibrinogène en fibrine dans le cadre de la coagulation, la thrombine agit également sur les cellules via l'activation du récepteur PAR-1. Ce dernier est par ailleurs surexprimé à la surface des cellules au cours d'une infection grippale (Lan et al 2004). Ainsi, PAR1 est susceptible d'être activé lors des infections grippales. Dans cette étude, nous nous sommes intéressés au rôle de PAR1 dans la pathogénicité des virus influenza A.

Afin d'étudier le rôle de PAR1 dans l'infection grippale, l'approche générale que nous avons utilisée est l'infection *in vivo* chez la souris, en utilisant soit des souris déficientes en PAR1, soit une stimulation ou une inhibition pharmacologique de PAR1. Nos résultats ont montré que l'administration intranasale d'agonistes spécifiques de PAR1 augmentait la mortalité induite par le VIA chez la souris, en comparaison avec des souris stimulées avec un peptide contrôle. De manière intéressante, les agonistes de PAR1 n'ont eu aucun rôle sur

l'inflammation induite par le VIA chez des souris déficientes en PLG. Ainsi, le rôle délétère de PAR1 dans la pathogénicité des VIA est, du moins en parti, PLG-dépendent. L'administration d'agoniste de PAR1 chez la souris a également augmenté l'inflammation des poumons induite par le VIA. Nous avons donc conclu que PAR1 jouait un rôle délétère dans l'inflammation induite par le virus de la grippe. Ces résultats ont été confirmés en utilisant des souris déficientes en PAR1, qui ont été protégées de la mortalité induite par le VIA, en comparaison avec des souris sauvages. Puisque la dérégulation de l'inflammation pourrait être responsable de certaines formes de grippe sévère, nous avons ensuite testé l'effet de l'administration d'antagonistes de PAR1 (molécule SCH79797) chez la souris infectée. Nos résultats ont montré que l'administration intranasale de SCH79797 protégeait les souris de la mortalité induite par le VIA, de manière indépendante de la souche grippale (H1N1, H3N2 et H5N1 hautement pathogène) et que cette protection était corrélée à une inhibition de l'inflammation pulmonaire. L'ensemble de ces résultats suggèrent que PAR1 joue un rôle dans la pathogénicité des VIA et qu'il pourrait être une nouvelle cible thérapeutique contre la grippe.



# PAR1 contributes to influenza A virus pathogenicity in mice

Khaled Khoufache,<sup>1,2</sup> Fatma Berri,<sup>1</sup> Wolfgang Nacken,<sup>3</sup> Annette B. Vogel,<sup>4,5</sup> Marie Delenne,<sup>1</sup> Eric Camerer,<sup>6,7</sup> Shaun R. Coughlin,<sup>8</sup> Peter Carmeliet,<sup>9,10</sup> Bruno Lina,<sup>1</sup> Guus F. Rimmelzwaan,<sup>11</sup> Oliver Planz,<sup>4</sup> Stephan Ludwig,<sup>3</sup> and Béatrice Riteau<sup>1,2</sup>

<sup>1</sup>Virologie et Pathologie Humaine, EA 4610, Université Lyon1, Faculté de Médecine RTH Laennec, Lyon, France. <sup>2</sup>INRA Tours, Nouzilly, France.

<sup>3</sup>Institute of Molecular Virology, ZMBE, Westfälische-Wilhelms-University, Münster, Germany. <sup>4</sup>Friedrich-Loeffler-Institute, Institute of Immunology, University Hospital, Tuebingen, Germany. <sup>5</sup>Institute of Immunology, Friedrich-Loeffler-Institut, Greifswald-Insel Riems, Germany. <sup>6</sup>INSERM U970, Paris Cardiovascular Centre, Paris, France. <sup>7</sup>Université Paris-Descartes, Paris, France. <sup>8</sup>Cardiovascular Research Institute, UCSF, San Francisco, California, USA. <sup>9</sup>Laboratory of Angiogenesis and Neurovascular link, Vesalius Research Center, VIB, Leuven, Belgium.

<sup>10</sup>Laboratory of Angiogenesis and Neurovascular link, Vesalius Research Center, KU Leuven, Leuven, Belgium.

<sup>11</sup>Department of Virology, Erasmus Medical Center, Rotterdam, the Netherlands.

**Influenza causes substantial morbidity and mortality, and highly pathogenic and drug-resistant strains are likely to emerge in the future. Protease-activated receptor 1 (PAR1) is a thrombin-activated receptor that contributes to inflammatory responses at mucosal surfaces. The role of PAR1 in pathogenesis of virus infections is unknown. Here, we demonstrate that PAR1 contributed to the deleterious inflammatory response after influenza virus infection in mice. Activating PAR1 by administering the agonist TFLLR-NH<sub>2</sub> decreased survival and increased lung inflammation after influenza infection. Importantly, both administration of a PAR1 antagonist and PAR1 deficiency protected mice from infection with influenza A viruses (IAVs). Treatment with the PAR1 agonist did not alter survival of mice deficient in plasminogen (PLG), which suggests that PLG permits and/or interacts with a PAR1 function in this model. PAR1 antagonists are in human trials for other indications. Our findings suggest that PAR1 antagonism might be explored as a treatment for influenza, including that caused by highly pathogenic H5N1 and oseltamivir-resistant H1N1 viruses.**

## Introduction

Influenza is an ineradicable contagious disease that occurs in seasonal epidemics and sporadic pandemic outbreaks that pose significant morbidity and mortality for humans and animals (1–3). The continuous sporadic infections of humans with highly pathogenic avian influenza viruses of the H5N1 subtype and the recent pandemic caused by swine-origin H1N1 viruses highlight the permanent threat caused by these viruses (4–6). The pathogenesis of influenza A virus (IAV) infection is not fully understood, but involves both viral traits and the host immune response (3). Full understanding of the host response may aid in the development of intervention strategies that target these host factors.

Both innate and adaptive components of the immune system are activated shortly after virus infection, which provides an efficient line of defense against IAV (7). However, excessive inflammation may also result in lung damage that limits respiratory capacity and may account for IAV pathogenesis in humans (1, 8, 9). Recruitment of inflammatory cells to inflamed sites is controlled by a number of cellular components, including proteases (10). These proteases not only cleave extracellular substrates, but also mediate signal transduction in part via protease-activated receptors (PARs) (11–14). PAR1, which links local protease activity to cellular responses involved in thrombosis, inflammation, and cytoprotection (15, 16), shows increased expression in the airways of IAV-infected mice (17). The role of PAR1 in the context of IAV infection

has not been studied. We report evidence that PAR1 signaling contributed to the deleterious inflammation that followed influenza virus infection in mice in a manner dependent on plasminogen (PLG). While administration of a PAR1 agonist to mice increased severity of IAV infection, PAR1 deficiency protected mice from fatal outcome. Administration of the PAR1 antagonist SCH79797 (18) to mice decreased inflammation and improved survival after infection with multiple IAV strains, including a highly pathogenic avian H5N1 strain and 2009 pandemic H1N1 virus. Importantly, administration of SCH79797 improved survival in mice even when administered 48 or 72 hours after inoculation. PAR1 antagonists are currently in clinical trials for potential use as antithrombotic drugs (19–22). Because an intervention strategy aimed at a host cellular protein would be effective against virus strains that develop resistance to existing antiviral drugs, PAR1 antagonists might be explored for the treatment of IAV in additional preclinical models and, if appropriate, in humans.

## Results

**PAR1 contributes to the pathogenesis of IAV infection.** To investigate the role of PAR1 in the pathogenesis of IAV infection, WT mice were inoculated with 50 or 500 PFU of H1N1 strain A/PR/8/34 (referred to herein as H1N1) and either left untreated or stimulated with 50 μM of the PAR1 agonist TFLLR-NH<sub>2</sub> (referred to herein as PAR1-activating peptide; PAR1-AP). Mice treated with PAR1-AP displayed enhanced weight loss and higher mortality rates after infection compared with untreated control mice, differences that were statistically significant at both doses (Figure 1A). In contrast, treatment of uninfected mice with PAR1-AP did not affect survival or body weight of mice (Figure 1B), which indicates that the effect of PAR1-AP on survival and weight loss requires IAV infection.

**Authorship note:** Khaled Khoufache and Fatma Berri contributed equally to this work.

**Conflict of interest:** Khaled Khoufache and Béatrice Riteau have a patent concerning the use of PAR1 antagonist against influenza.

**Citation for this article:** *J Clin Invest*. doi:10.1172/JCI16667.

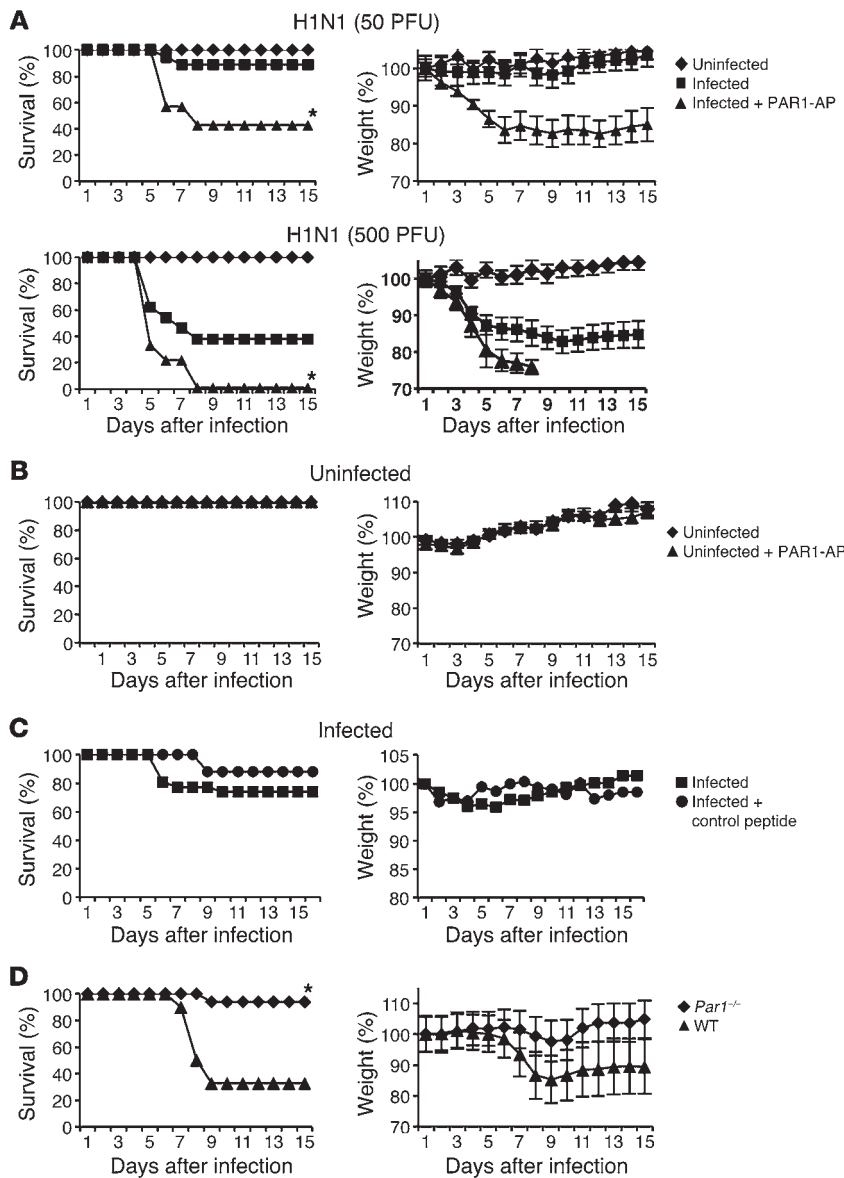


**Figure 1**

Effect of PAR1 activation and PAR1 deficiency on IAV pathogenicity. (A) Time course of IAV-induced pathogenesis and death in mice in response to PAR1 stimulation. Mice were inoculated intranasally with H1N1 (50 PFU,  $n = 22$  per group; 500 PFU,  $n = 18$  per group) and treated with either vehicle or 50  $\mu$ M PAR1-AP. (B) Time course of uninfected mice treated or not with 50  $\mu$ M PAR1-AP ( $n = 13$  per group). (C) Mice were infected with 50 PFU H1N1 and treated with control peptide or vehicle ( $n = 10$  per group). Results are average percent survival or weight loss from 3 independent experiments. (D) Survival and weight loss of *Par1*<sup>-/-</sup> mice and WT littermates after infection with 100 PFU H1N1 ( $n = 12$  per group). Results are average percent survival or weight loss from 2 experiments.  $P < 0.05$ , PAR1-AP vs. untreated or *Par1*<sup>-/-</sup> vs. WT, Kaplan-Meier test.

Moreover, treatment with a control peptide did not impair survival or increase weight loss in IAV-infected mice (Figure 1C), militating against nonspecific effects of peptide administration. Thus, PAR1 activation led to increased pathogenicity of IAV infection.

To further explore the role of PAR1 in IAV pathogenesis, we investigated the consequence of PAR1 deficiency. *Par1*<sup>-/-</sup> mice were intercrossed to generate WT and *Par1*<sup>-/-</sup> mice, which were infected with 100 PFU H1N1, and weight loss and survival rates were monitored. Compared with WT littermates, *Par1*<sup>-/-</sup> mice were more resistant to IAV infection (Figure 1D). Thus, PAR1 contributed to death and weight loss caused by IAV infection.

*PAR1-AP increases cytokine release and neutrophil recruitment in the lungs of infected mice.* Because PAR1 can trigger cytokine production in endothelial and other cell types (14), we next investigated the effects of PAR1-AP in the inflammatory response induced by IAV infection. Mice infected with 50 PFU H1N1 were treated or not with 50  $\mu$ M PAR1-AP, and bronchoalveolar lavages (BALs) were collected to assess the presence of cytokines and polymorpho-

nuclear neutrophils (PMNs) in the lungs at different time points after inoculation. IAV infection resulted in increased levels of all cytokines tested (RANTES, IL-6, and KC) in a time course-dependent manner, and PAR1-AP treatment augmented this response (Figure 2A). Similar results were obtained when the effect of PAR1 was compared with that of a control peptide (Supplemental Figure 1; supplemental material available online with this article; doi:10.1172/JCI61667DS1), confirming PAR1-AP specificity. PAR1-AP treatment also increased the occurrence of BAL PMNs 24 and 48 hours after infection, but had little effect in uninfected mice (Figure 2B). By 72 hours after infection, the PMN content of BAL in PAR1-AP-treated and control mice was not different. These results suggest that PAR1 activation can increase IAV-induced production of cytokines and increase early recruitment of neutrophils in the lungs of infected mice.

*Virus replication in the lungs.* We then investigated whether the effect of PAR1 activation on the outcome of IAV infection in mice correlates with an increase of virus production in the lungs. To this end,

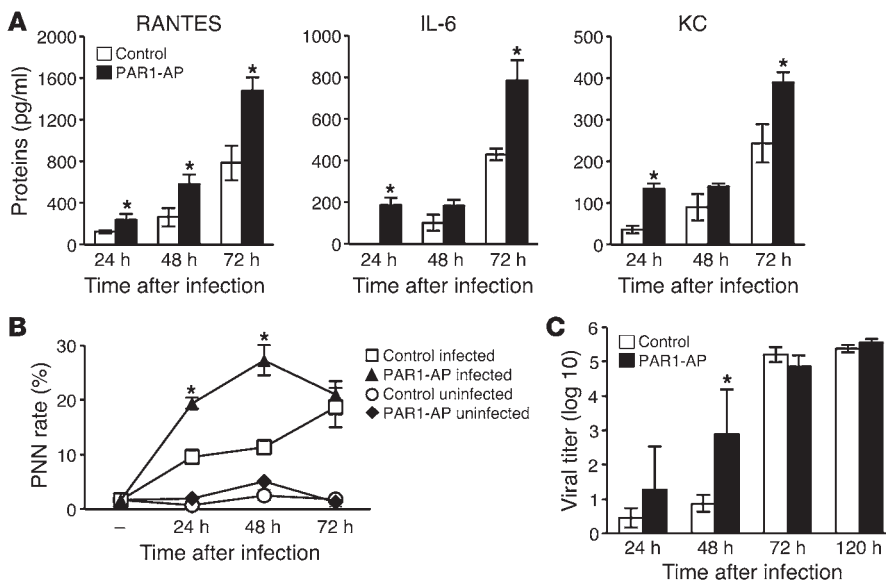


**Figure 2**

PAR1-AP increases inflammation and virus replication during 50 PFU H1N1 infection in mice. (A) Cytokines in the BAL of infected mice treated or not with PAR1-AP were measured by ELISA 24, 48, and 72 hours after inoculation. Data are mean  $\pm$  SD from 5–11 individual animals per group from 3 experiments. (B) Relative PMN numbers in BAL from infected mice treated or not with PAR1-AP. PMN percentage was determined by May-Grünwald-Giemsa staining 24, 48, or 72 hours after inoculation. Results are mean  $\pm$  SD from 4–5 individual mice per group from 2 individual experiments. Noninfected mice were used as control ( $n = 2–4$  per group). (C) H1N1 virus titers in the lungs at the indicated times after infection of mice treated or not with 50  $\mu$ M PAR1-AP. Data are average  $\pm$  SD from 3–5 individual animals per group. \* $P < 0.05$ , treated vs. untreated, Mann-Whitney test.

infectious virus titers were determined in lungs collected from mice treated with PAR1-AP (50  $\mu$ M) or control peptide at different time points after inoculation. At 24 and 48 hours after inoculation, virtually no virus replication was detected ( $10^1$  was the detection limit of the assay), but lung virus titers significantly increased after PAR1-AP treatment (Figure 2C). No significant differences were observed 3 and 5 days after infection. These data suggest that PAR1 activation promotes an early increase in virus production in mouse lungs.

*The effect of PAR1 activation on virus production, weight loss, and survival after IAV infection is PLG dependent.* To decipher the mechanism by which PAR1 accelerated virus production in vivo, we performed in vitro experiments to assess the effect of PAR1 activation on virus replication in alveolar epithelial A549 cells. PAR1-AP triggered ERK phosphorylation in these cells, with a maximal effect at about 40  $\mu$ M (Figure 3A); this concentration was used in all subsequent in vitro experiments. Because proteolytic cleavage of HA is essential for IAV infectivity, and PLG promotes IAV replication through HA cleavage (23, 24), we examined the effect of adding PLG – alone or in combination with PAR1-AP – on virus production. As expected, viral production was barely detectable in untreated A549 cultures, but was markedly increased by the addition of PLG (Figure 3B). Importantly, addition of PAR1-AP augmented this effect 8 and 24 hours after infection. The effect of PAR1-AP was not seen when trypsin was used as an alternative protease for IAV replication (data not shown), and PAR1 signaling did not affect virus entry into cells (Supplemental Figure 2). However, inclusion of PAR1-AP appeared to increase PLG-dependent cleavage of HA. Thus, we next infected A549 cells (MOI 0.5) in the presence or absence of PLG, with or without PAR1-AP, and evaluated HA cleavage by Western blot analysis 16 hours after infection. In the absence of PLG, similar amounts of uncleaved HA (HA<sub>0</sub>) accumulated in infected cells, and PAR1-AP was without effect (Figure 3C). In the presence of PLG, in addition to HA<sub>0</sub>, a 25-kDa band corresponding to HA<sub>2</sub> was observed. Importantly, in PAR1-AP-treated cultures, the intensity of HA<sub>2</sub> increased and HA<sub>0</sub> decreased relative to that in control cultures. Thus, viral HA was cleaved in a PLG-dependent manner that was enhanced by PAR1-AP and correlated with increased viral production.

PLG is an important mediator of lung inflammation (25, 26) and is known to influence IAV virulence (27, 28). Importantly, PLG binding to cells and activation may be controlled by PAR1 signaling (29, 30). In combination with the findings outlined above, these observations prompted us to investigate whether the effect of PAR1 signaling on the pathogenicity of IAV infection also depends on PLG in vivo. We therefore inoculated *Plg*<sup>-/-</sup> mice with 50 PFU H1N1 with or without PAR1-AP treatment. In contrast to WT mice, treatment of *Plg*<sup>-/-</sup> mice with PAR1-AP did not increase mortality rates, weight loss, or virus titers in lungs after IAV infection (Figure 3, D and E).

Histopathological examination showed that treatment with PAR1-AP increased cellular infiltrates in lungs from infected WT mice, but not *Plg*<sup>-/-</sup> mice (Supplemental Figure 3). These results suggest that PAR1 activation increased early virus production, inflammation, and pathogenicity of IAV infection in a PLG-dependent fashion. Notably, when this low 50-PFU dose was used, virtually no virus replication was detected in the lungs of WT or *Plg*<sup>-/-</sup> mice at the indicated time points after inoculation (Figure 3E). Additionally, leukocyte infiltration in IAV-infected WT or *Plg*<sup>-/-</sup> mice was barely detectable (Supplemental Figure 3). However, when a higher virus dose was used for inoculation, leukocyte infiltration and lung virus titers of *Plg*<sup>-/-</sup> mice were substantially lower than those of WT mice (F. Berri, unpublished observations), which suggests that PLG promotes IAV replication and inflammation. While the finding that PAR1-AP increased PLG-dependent cleavage of HA in vitro suggests that PAR1 signaling might promote viral replication by enhancing PLG/plasmin function, our data do not exclude a PAR1-independent permissive role for PLG or PLG-independent roles for PAR1 activation in IAV infection and pathogenesis.

*PAR1 antagonist protects against H1N1 and H3N2 infection.* We next investigated whether pharmacological inhibition of PAR1 signaling alters the course of IAV infection. The pharmacology of PARs is not well developed, and inhibitors capable of blocking PAR1 function in mouse models have not been well characterized with respect to off-target effects. Nonetheless, SCH79797 has been used to probe PAR1 function in rodent models (31–33); thus, encouraged by the protection against IAV seen in *Par1*<sup>-/-</sup> mice, we examined the effects of this compound on the course of IAV infection.

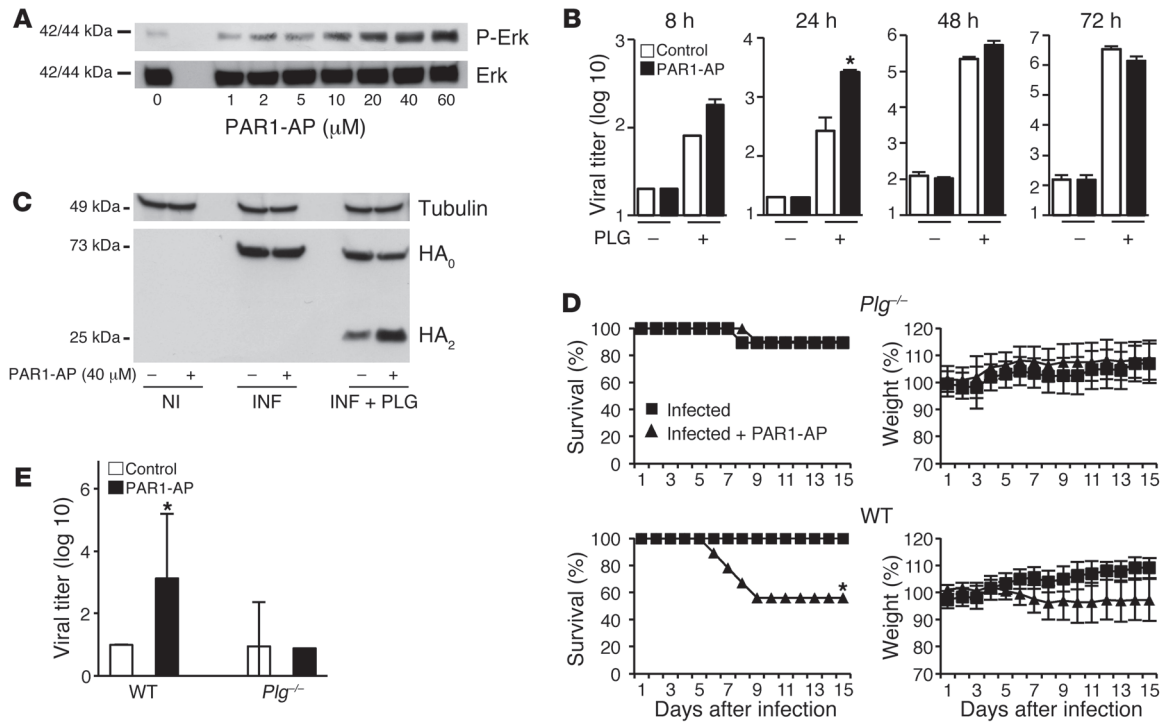


**Figure 3**

Effect of PLG and PLG deficiency on IAV production and PAR1-AP effects. (A) ERK phosphorylation after stimulation of A549 cells with the indicated PAR1-AP concentrations. Anti-phospho-Erk and anti-Erk antibodies were used. (B) Infectious virus titers in the supernatant of infected cells after stimulation with 40 μM PAR1-AP or control peptide in the presence or absence of PLG. (C) Noninfected (NI) or infected (INF) cells were stimulated with 40 μM PAR1-AP or control peptide in the presence or absence of PLG. After cell lysis, proteins were analyzed by Western blot for HA cleavage. (D) Time course of IAV-induced pathogenesis in *Plg*<sup>-/-</sup> and WT littermates after treatment or not with PAR1-AP (*n* = 9–10 mice per group from 2 experiments). (E) Virus titers 48 hours after infection (50 PFU) in lungs of WT or *Plg*<sup>-/-</sup> mice stimulated or not with 50 μM PAR1-AP. Data are average ± SD from 5 individual animals per group from 2 experiments. \**P* < 0.05, treated vs. untreated, Kaplan-Meier test (D), Mann Whitney test (B and E).

SCH79797 inhibited PAR1-AP-induced ERK activation in mouse NIH3T3 cells (Figure 4A), which suggests that it is capable of blocking signaling by the mouse homolog of PAR1. SCH79797 treatment prevented decreased survival and increased weight loss associated with administration of PAR1-AP to IAV-infected mice (Figure 4B). More strikingly, when mice were infected with lethal doses of H1N1 (500 and 5,000 PFU), SCH79797 treatment protected mice from weight loss and death: 47% and 16% survival, respectively, was observed in untreated control mice, whereas 84%–94% of SCH79797-treated mice survived the infections (Figure 4C). Moreover, when SCH79797 was administered beginning 2 or 3 days after infection, mice were also significantly protected from H1N1 and from H3N2 strain A/Hong-Kong/68 (referred to herein as H3N2; Figure 4, D and E). Treatment of uninfected mice with SCH79797 did not affect their survival rates or body weight (Supplemental Figure 4), which suggests that PAR1 antagonists do not cause side effects. Thus, SCH79797 treatment protected mice from IAV infection, consistent with the notion that PAR1 contributes to IAV pathogenesis in this model.

*Inflammation and virus replication are attenuated by SCH79797.* Since PAR1 activation promoted inflammation in the lungs during IAV infection, we determined whether blockade of PAR1 signaling would result in reduced IAV-induced inflammation in vivo. Mice were infected with 500 PFU H1N1 and treated or not with SCH79797, and BAL was collected at different times after inocu-

lation. SCH79797 treatment significantly reduced the levels of RANTES, IL-6, and KC in BAL 24, 48, and 72 hours after inoculation, as measured by ELISA (Figure 5A). 5 days after inoculation, cytokine levels were still high in the BAL from untreated mice, but barely detectable in the BAL from SCH79797-treated mice (Supplemental Figure 5). SCH79797 treatment also significantly decreased PMN frequency in the BAL of infected mice: 24 and 48 hours after inoculation, PMNs were hardly detectable in the BAL of SCH79797-treated mice, whereas they represented 10% of cells in BAL from untreated mice (Figure 5B). Accordingly, histopathological examination revealed a reduction of cell infiltration in the lungs of infected mice treated with SCH79797 (Supplemental Figure 6).

Finally, a reduction in lung virus titers was observed 24 and 48 hours after 500 PFU H1N1 inoculation compared with untreated controls (Figure 5C). At day 3 after inoculation, lung virus titers were similar in SCH79797-treated and untreated mice (approximately 10<sup>4</sup> PFU/ml), which suggests that SCH79797 delayed, but did not prevent, virus production. Lung virus titers dropped to less than 10<sup>2</sup> PFU/ml at days 5 and 7 in both SCH79797-treated and control mice (Figure 5C). The observation that SCH79797 suppressed markers of inflammation, but not viral titers, at day 3 suggests that inhibition of PAR1 signaling may inhibit inflammation and early virus replication by at least partially independent mechanisms.

*SCH79797 protects against highly pathogenic H1N1v and H5N1 infection.* To test whether inhibition of PAR1 signaling by SCH79797

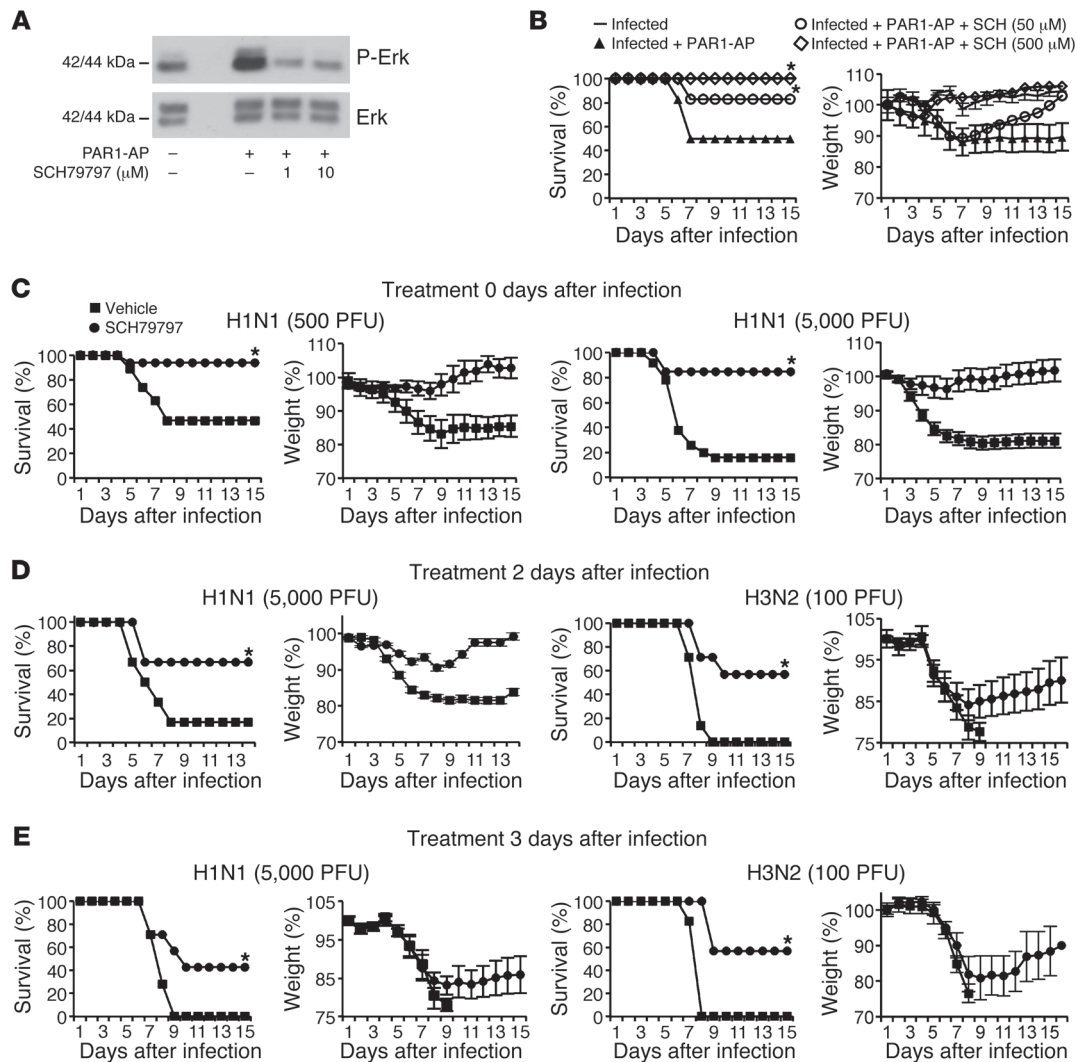


**Figure 4** PAR1 antagonist protects mice against infection with H1N1 and H3N2. (A) Treatment of NIH3T3 cells with SCH79797 blocked ERK activation by 10 μM PAR1-AP. (B) SCH79797 treatment prevented PAR1-AP-induced mouse mortality in a dose-dependent manner. (C) IAV-induced pathogenesis in infected mice treated or not with SCH79797. Mice were inoculated with 500 PFU ( $n = 17-19$  per group) or 5,000 PFU ( $n = 14$  per group) H1N1 and treated or not with 50 μM SCH79797 on days 0–2 after infection. (D) SCH79797 treatment on days 2–4 after infection with 5,000 PFU H1N1 ( $n = 12$  per group) or 100 PFU H3N2 ( $n = 7$  per group). (E) SCH79797 treatment on days 3–5 after infection with 5,000 PFU H1N1 ( $n = 7$  per group) or 100 PFU H3N2 ( $n = 7$  per group). \* $P < 0.05$ , treated vs. control, Kaplan-Meier test.

also affects infection with other IAV strains, mice were infected with a highly pathogenic H5N1 strain or a pandemic H1N1v strain that had acquired oseltamivir resistance during treatment of a severe infection (see Methods and ref. 34), then treated or not with SCH79797. After lethal infection with 5,000 PFU H5N1 and 500 PFU H1N1v, 60% and 100% of untreated control mice died, respectively, whereas almost full protection was observed in SCH79797-treated animals of both inoculation groups ( $P < 0.05$ ; Figure 6, A and B). In addition to mortality and body weight, the onset of clinical signs was also inhibited when H5N1-infected mice were treated with SCH79797 compared with untreated mice (data not shown). Mouse mortality was monitored until day 21 after inoculation, and sustained survival was observed after SCH79797 treatment (data not shown), which indicated that SCH79797 protection was durable. Thus, inhibition of PAR1 sig-

naling protected mice against infection with various IAVs, including highly pathogenic strains.

**Discussion**

Our present findings support an important role for PAR1 in mouse models of IAV infection. Studies with PAR1-AP indicated that PAR1 activation increased inflammation, early virus production, weight loss, and mortality after infection (Figures 1 and 2), and studies using *Par1*<sup>-/-</sup> mice indicated that PAR1 contributed to the pathogenesis of IAV infection (Figure 1). The observation that SCH79797, a drug that inhibits PAR1 signaling, decreased inflammation, early virus production, weight loss, and mortality after infection was in accord with the PAR1-AP and *Par1*<sup>-/-</sup> results. Moreover, the observation that SCH79797 decreased mortality after infection with multiple IAV strains (H1N1, H3N2, and

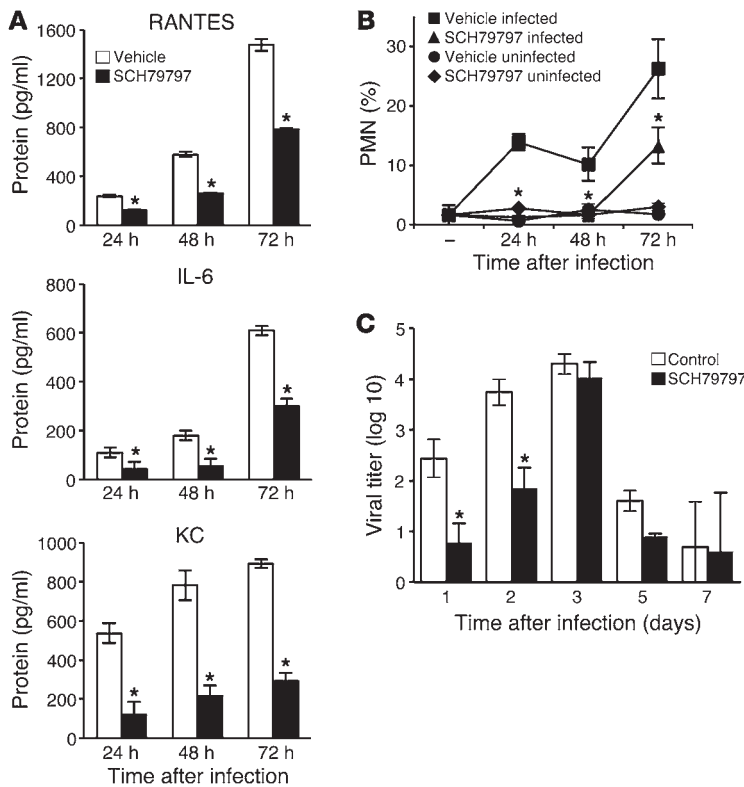


**Figure 5**

PAR1 antagonist inhibits lung inflammation and virus replication. (A) Cytokines in the BAL of infected mice treated or not with SCH79797 were measured by ELISA 24, 48, and 72 hours after inoculation. Data are average ± SD from 7–11 individual animals per group, representative of 3 experiments. (B) Relative PMN frequency in BAL from infected mice treated or not with SCH79797. PMN percentage was determined by May-Grünwald-Giemsa staining 24, 48, and 72 hours after inoculation. Data are average ± SD from 3–5 individual mice per group. Noninfected mice were used as control ( $n = 3–5$  per group). Results are representative of 2 individual experiments. (C) Virus titers in lungs of infected mice at the indicated times after infection with 500 PFU H1N1 and treatment with SCH79797. Data are average ± SD from 3–5 individual animals per group. \* $P < 0.05$ , treated vs. control, Mann-Whitney test.

H5N1), and was effective even when dosing was initiated at day 3 after inoculation, suggests that PAR1 inhibition should be explored in additional preclinical studies and, if appropriate, in humans as a possible treatment for influenza.

To our knowledge, a role for PAR1 in the response to, and the pathogenesis of, virus infections has not been previously described. PAR1 activation in endothelial cells, fibroblasts, and other cell types triggers various responses, many of which are proinflammatory (e.g., chemokine and cytokine production, adhesion molecule display, prostaglandin production, and permeability increases; refs. 14, 15). In accord with our observations, intratracheal delivery of PAR1 agonist was not sufficient to trigger inflammation in the lungs of otherwise normal mice (35), but did exacerbate ventilation injury-induced pulmonary edema (36). Additionally, *Par1*<sup>-/-</sup> mice are protected from ventilation injury-induced and bleomycin-induced lung injury (36–38). Like our results, these observations suggest that PAR1 signaling contributes to inflammatory responses to injury in the lung, the major target in our IAV infection model.

PAR1 activation did not exacerbate the effects of IAV infection in *Plg*<sup>-/-</sup> mice (Figure 3). It is possible that PLG is simply playing a permissive role for the effect of PAR1 activation in IAV infection; that is, PLG supports infection and injury, and PAR1 activation exacerbates their effects. Interestingly, however, PAR1-AP did promote PLG-dependent HA cleavage in lung epithelial cultures, suggestive of a possible interaction of PAR1 signaling with the ability of IAV to become infectious and hence replicate. These findings are consistent with the prior observation that PLG contributes to the pathogenesis of IAV infection (27, 28). Additionally, PAR1 signaling may promote PLG activation to plasmin (29, 30), thereby providing a possible link to increased HA cleavage and IAV

production. It is also possible that PAR1 activation contributes to proinflammatory functions of PLG (25, 39–41), by promoting its conversion to plasmin or by other mechanisms.

Additional considerations suggest that PAR1 activation's abilities to promote early virus replication and to enhance a harmful inflammatory response in the respiratory tract are, at least in part, independent of each other. When PAR1-AP was delivered 3 days after infection, despite similar virus replication in the lungs, treatment still had a deleterious effect (data not shown). Additionally, based on critical residues in HA involved for cleavage by plasmin, it is unlikely that the replication of highly pathogenic H5N1 and 2009 pandemic H1N1 are modulated by plasmin (42), yet SCH79797 treatment still decreased mortality.

As noted above, we found that in IAV-infected A549 cells, activation of PAR1 increased PLG-dependent HA cleavage, an essential step for virus infectivity. Indeed, only the cleaved form of HA permits pH-dependent fusion of the viral envelope within the endosomal membranes and subsequent release of the genome into the cytosol and virus replication. In vivo, PAR1 also promoted virus replication shortly after infection. However, at 48 hours after infection, no difference in lung virus titers was observed between PAR1-AP-stimulated and unstimulated mice, which suggests that HA cleavage could be compensated by other proteases that are either recruited or activated by infection in the lungs.

Therefore, we propose a model (Figure 7) in which PAR1 promotes activation of PLG into plasmin. Subsequently, plasmin acts on virus replication through HA cleavage, enhancement of which likely enhances inflammation via pathogen-associated molecular patterns. Simultaneously, plasmin also acts as a proinflammatory mediator that accounts for the deleterious lung inflammation. Additionally, PAR1 triggers a variety of proinflammatory responses

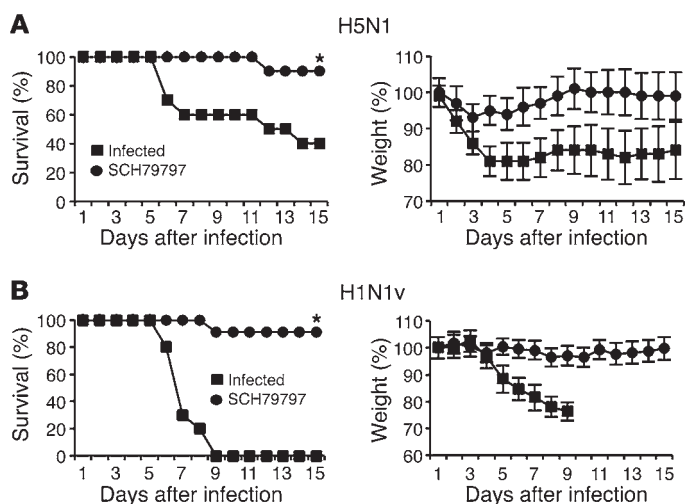


**Figure 6** PAR1 antagonist protects mice from lethal infection with H5N1 or H1N1v. Mice were inoculated intranasally with (A) 5,000 PFU H5N1 ( $n = 10$  per group) or (B) 500 PFU H1N1v ( $n = 10$ –11 per group) and treated or not with 50  $\mu$ M SCH79797. Results are expressed as percent survival or weight loss from 2 experiments. \* $P < 0.05$ , treated vs. control, Kaplan-Meier test.

es, independent of PLG and virus, that may exacerbate inflammation and injury. Because PAR1 couples coagulation to inflammation (14, 15) and coagulation to fibrinolysis (30), further studies are needed to investigate the overall impact of hemostasis dysregulation in PAR1-mediated inflammation during IAV infection.

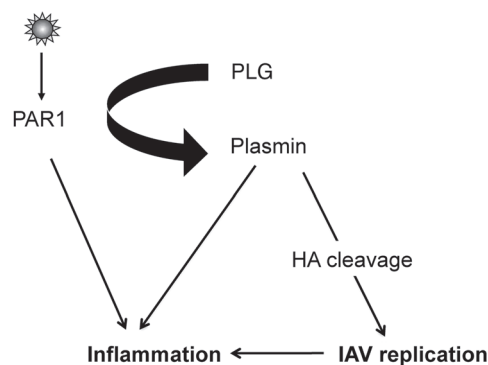
Our observation that a PAR1 agonist (43, 44) exacerbated the effects of IAV infection suggests that PAR1 activation is capable of promoting inflammation and tissue damage in this setting. Moreover, our observation that *Par1*<sup>-/-</sup> mice and SCH79797-treated mice were protected from IAV infection suggests that PAR1 activation contributes to the pathogenesis of IAV infection and that PAR1 is endogenously activated during IAV infection. Accordingly, the natural PAR1 activator thrombin was generated in IAV-infected lungs (45), and elevated levels of PAR1 were observed in the airways of IAV-infected mice (17). It is worth noting, however, that SCH79797 is known to have off-target effects on cell proliferation and survival (46, 47); thus, we cannot exclude PAR1-independent effect of SCH79797. However, SCH79797 was capable of inhibiting PAR1 signaling (Figure 4A and ref. 18), and the concordance of our KO and inhibitor studies — and the fact that their effects were opposite from those of PAR1-AP — suggest that the effects of SCH79797 in our model could be related to its ability to block PAR1 signaling.

Besides PAR1, other PARs may be involved in the pathogenesis of IAV infection (48–50). Identification of the exact nature and amount of proteases present at the site of infection, and how virus strain differences alter the immune response and its interactions with PARs, may advance our understanding of the pathogenesis of IAV infection.

Current treatments for IAV infection target the viral proteins M2 and NA. These drugs suffer from a number of disadvantages, including the rapid development of resistant virus variants as a result of selective pressure, which highlights the need for new pharmacological strategies against IAV infection. Because targeting host proteins would not be subject to resistance, and because severe infections with IAV are associated with a deleterious host inflammatory response, drugs regulating inflammation are appealing as potential treatments for IAV infection (51, 52). In our present study, blocking PAR1 signaling almost fully protected mice from a highly pathogenic, oseltamivir-resistant 2009 pandemic H1N1v virus isolated from a severely diseased oseltamivir-treated patient (34). Additionally, inhibition of PAR1 signaling up to 3 days after inoculation protected mice from a detrimental outcome of infection with various IAVs, including H1N1 and H3N2 strains. Because IAVs of the H1N1 and H3N2 subtypes are currently circulating in the human population, it is reasonable to assume that PAR1 antagonists are most likely also effective against seasonal influenza viruses. Interestingly, the PAR1 antagonist vorapaxar has been studied as a potential antithrombotic drug in approximately 40,000 patients over 3 years (53, 54). The most serious side effect, increased incidence of intracranial bleeding, occurred mainly in patients with a history of prior stroke. In the absence of such a history, the increase in the incidence of intracranial bleeding was less than 1 per 1,000 treatment-years. Thus, short periods of PAR1 antagonism would appear to be relatively safe. This observation, in consideration with our results, suggests that PAR1 antagonism

**Figure 7**

Proposed model for PAR1-mediated influenza virus pathogenesis. During IAV infection, PAR1 is activated and increases conversion of PLG into plasmin. On the one hand, plasmin cleaves and activates the viral HA, promoting IAV replication, which contributes to inflammation. On the other hand, plasmin directly promotes inflammation, and PAR1 promotes inflammation via mechanisms that are independent of PLG and virus. These likely interact with other host responses to viral infection to exacerbate inflammation and injury.





should be further explored for the treatment of IAV in additional preclinical models and, if appropriate, human studies.

## Methods

**Cells, virus strain, and reagents.** The NIH3T3 mouse cell line was a gift from D. Décimo (INSERM U758, Lyon, France). The human alveolar type II (A549) and MDCK cell lines used in this study were obtained from ATCC and grown as previously described (55). H1N1 (strain A/PR/8/34) was obtained from the ATCC. H3N2 (strain A/Hong-Kong/2/68) was obtained from the Dutch National Influenza Centre. The strain was originally obtained from the National Institute for Biological Standards and Control (NIBSC). The highly pathogenic H5N1 avian influenza virus (strain A/mallard/Bavaria/1/2006; also known as MB1) and the pandemic H1N1v influenza virus (strain A/Nordrhein-Westfalen/173/09) were used in this study. H1N1v, isolated from a severe H1N1pdm09 case and obtained through the German National Reference Centre for Influenza of the Robert Koch Institute, had acquired oseltamivir resistance during treatment (34). H5N1 was propagated in chicken eggs for 2 days, and the other viruses were propagated in confluent MDCK cells. After 2 days, cytopathic changes were complete, and culture supernatants were harvested and cleared by low-speed centrifugation and stored at  $-80^{\circ}\text{C}$ . PAR1-AP and control peptide (FTLLR-NH<sub>2</sub> and FTLLR-NH<sub>2</sub>, respectively) were purchased from Bachem. The PAR1 antagonist (SCH79797 dihydrochloride) was purchased from Axon Medchem. PLG was purchased from Sigma-Aldrich, and the following antibodies were used: monoclonal anti-HA (C102; Santa Cruz Biotechnology), monoclonal anti-tubulin (Sigma-Aldrich), and polyclonal anti-ERK and phospho-ERK (Cell Signaling Technology).

**In vitro stimulation.** A549 cells were preincubated for 5 minutes with 40  $\mu\text{M}$  PAR1-AP or control peptide or for 1 hour with 5  $\mu\text{M}$  SCH79797. Cells were then infected with H1N1 (MOI 0.001) in MEM supplemented with 0.5  $\mu\text{M}$  PLG (Sigma-Aldrich) in the presence of the drug. At the indicated times after stimulation, virus titers were analyzed by classical plaque assays as performed previously, using MDCK cells (56).

**Western blot analysis of ERK activation and HA cleavage.** A549 or NIH3T3 cells were stimulated or not with the indicated concentrations of PAR1-AP for 5 minutes at  $37^{\circ}\text{C}$ . Where indicated, cells were preincubated for 1 hour with SCH79797. Cells were then lysed, and proteins from the lysate were analyzed by Western blot for ERK activation, as previously described (57). For the HA cleavage experiments, A549 cells were stimulated or not with 40  $\mu\text{M}$  PAR1-AP and infected with IAV (MOI 0.5) for 16 hours in the presence or absence of 0.5  $\mu\text{M}$  PLG. Cells were then lysed, and proteins from the lysate were analyzed by Western blot, as described previously (57).

**Mice.** *Plg*<sup>-/-</sup> mice (with a disrupted *Plg* gene) and their WT littermates (58) and 6-week-old C57BL/6 female mice (Charles River Laboratories) were used in this study. *Par1*<sup>-/-</sup> mice (with a disrupted *Par1* gene) and their WT littermates were described previously (59). Heterozygous mice were crossed, and WT and KO offspring were used. Mouse ages ranged from 5 weeks to a maximum of 4 months, since the number of mice that could be obtained was limited. Male and female mice were used in the experiments. Groups of WT and KO mice were stratified for these differences in age and gender. Polymerase chain reaction of tail-tip genomic DNA was performed (60) for determination of the absence or presence of a functional *Plg* or *Par1* gene.

**Mouse infection and treatment.** Mice were anesthetized and inoculated intranasally with 25  $\mu\text{l}$  of a solution containing different doses of virus in the presence or absence of 50  $\mu\text{M}$  PAR1-AP, 50  $\mu\text{M}$  control peptide, and/or 50  $\mu\text{M}$  SCH79797. 500  $\mu\text{M}$  SCH79797 was also used for blocking experiments in Figure 4B. Intranasal treatments with PAR1-AP, control peptide, and/or SCH79797 were also repeated at days 2 and 3 after infection. Alternatively, mice were inoculated, and SCH79797 was administered on days 2–4 or days 3–5 after infection. Mice were then monitored for weight loss and mortality. For assessing virus replication, lungs were obtained from sacrificed mice, and infectious virus titers were determined by plaque assay as described previously (56).

**Cytokine detection by ELISA and PMN recruitment.** Production of the cytokines RANTES, IL-6, and KC in the lungs was determined by ELISA (R&D Systems), using BAL from mice, as previously described (60). For PMN recruitment, BAL was collected in PBS (Invitrogen) supplemented with 1 mM EDTA (Invitrogen). After cytocentrifugation, the percentage of PMNs was determined by counting a total of 500 cells per sample by microscopic examination of May-Grünwald- and Giemsa-stained cytocentrifuge slides.

**Lung histology.** At 3 days after virus inoculation and treatment, mice were killed, and lung tissue was harvested, fixed in 10% formaldehyde, and subsequently embedded in paraffin. Tissues were sectioned at 12  $\mu\text{M}$ , and sections were examined after staining with hematoxylin and eosin for histopathological changes.

**Statistics.** Mann-Whitney test was used for statistical analysis of lung virus titers and cytokine ELISA results. Kaplan-Meier test was used for statistical analysis of survival rates. XLSTAT software was used to analyze differences between groups; a *P* value less than 0.05 was considered statistically significant.

**Study approval.** Experiments were performed according to recommendations of the National Commission of Animal Experiment (CNEA) and the National Committee on the Ethic Reflexion of Animal Experiments (CNREEA) in compliance with European animal welfare regulation. The protocol was approved by the committee of animal experiments of the University Claude Bernard Lyon I (permit no. BH2008-13). All animal experiments were also carried out under the authority of licence issued by “la direction des services Vétérinaires” (accreditation no. 78-114). All efforts were made to minimize suffering.

## Acknowledgments

We are grateful to N. Lejal for technical assistance. This work was supported by the Agence Nationale de la Recherche (ANR; to B. Riteau); Inserm Avenir (to E. Camerer); Marie Curie actions (to E. Camerer); and Long-term structural funding—Methusalem by the Flemish government (to P. Carmeliet).

Received for publication November 7, 2011, and accepted in revised form October 4, 2012.

Address correspondence to: Beatrice Riteau, EMR 4610 Vir-Path, Virologie et Pathologie Humaine, Faculté de médecine RTH Laennec, Université Claude Bernard Lyon 1, Université de Lyon, F-69008, Lyon, France. Phone: 33.1.0478771008; Fax: 33.1.0478778751; E-mail: beatrice.riteau@univ-lyon1.fr.

1. La Gruta NL, Kedzierska K, Stambas J, Doherty PC. A question of self-preservation: immunopathology in influenza virus infection. *Immunol Cell Biol*. 2007;85(2):85–92.
2. Bouvier NM, Palese P. The biology of influenza viruses. *Vaccine*. 2008;26(suppl 4):D49–D53.
3. Kuiken T, Riteau B, Fouchier RA, Rimmelzwaan GF. Pathogenesis of influenza virus infections: the good, the bad and the ugly. *Curr Opin Virol*.

- 2012;2(3):276–286.
4. Webby RJ, Webster RG. Are we ready for pandemic influenza? *Science*. 2003;302(5650):1519–1522.
5. Foucault ML, Moules V, Rosa-Calatrava M, Riteau B. Role for proteases and HLA-G in the pathogenicity of influenza A viruses. *J Clin Virol*. 2011; 51(3):155–159.
6. Solorzano A, Song H, Hickman D, Perez DR. Pandemic influenza: preventing the emergence of novel

- strains and countermeasures to ameliorate its effects. *Infect Disord Drug Targets*. 2007;7(4):304–317.
7. Schmolke M, Garcia-Sastre A. Evasion of innate and adaptive immune responses by influenza A virus. *Cell Microbiol*. 2010;12(7):873–880.
8. de Jong MD, et al. Fatal outcome of human influenza A (H5N1) is associated with high viral load and hypercytokinemia. *Nat Med*. 2006;12(10):1203–1207.
9. Peiris JS, Cheung CY, Leung CY, Nicholls JM. Innate



- immune responses to influenza A H5N1: friend or foe? *Trends Immunol.* 2009;30(12):574–584.
10. Heutinck KM, ten Berge IJ, Hack CE, Hamann J, Rowshani AT. Serine proteases of the human immune system in health and disease. *Mol Immunol.* 2010;47(11–12):1943–1955.
11. Mackie EJ, Pagel CN, Smith R, de Niese MR, Song SJ, Pike RN. Protease-activated receptors: a means of converting extracellular proteolysis into intracellular signals. *IUBMB Life.* 2002;53(6):277–281.
12. Hollenberg MD. Proteinase-mediated signaling: proteinase-activated receptors (PARs) and much more. *Life Sci.* 2003;74(2–3):237–246.
13. Riteau B, de Vaureix C, Lefevre F. Trypsin increases pseudorabies virus production through activation of the ERK signalling pathway. *J Gen Virol.* 2006;87(pt 5):1109–1112.
14. Vu TK, Hung DT, Wheaton VI, Coughlin SR. Molecular cloning of a functional thrombin receptor reveals a novel proteolytic mechanism of receptor activation. *Cell.* 1991;64(6):1057–1068.
15. Coughlin SR. Thrombin signalling and protease-activated receptors. *Nature.* 2000;407(6801):258–264.
16. Coughlin SR, Camerer E. PARticipation in inflammation. *J Clin Invest.* 2003;111(1):25–27.
17. Lan RS, Stewart GA, Goldie RG, Henry PJ. Altered expression and in vivo lung function of protease-activated receptors during influenza A virus infection in mice. *Am J Physiol Lung Cell Mol Physiol.* 2004;286(2):L388–L398.
18. Ahn HS, Foster C, Boykow G, Stamford A, Manna M, Graziano M. Inhibition of cellular action of thrombin by N3-cyclopropyl-7-[[4-(1-methylethyl)phenyl]methyl]-7H-pyrrolo[3, 2-f]quinazoline-1,3-diamine (SCH 79797), a nonpeptide thrombin receptor antagonist. *Biochem Pharmacol.* 2000;60(10):1425–1434.
19. Goto S, Yamaguchi T, Ikeda Y, Kato K, Yamaguchi H, Jensen P. Safety and exploratory efficacy of the novel thrombin receptor (PAR-1) antagonist SCH530348 for non-ST-segment elevation acute coronary syndrome. *J Atheroscler Thromb.* 2010;17(2):156–164.
20. White HD. Oral antiplatelet therapy for atherothrombotic disease: current evidence and new directions. *Am Heart J.* 2011;161(3):450–461.
21. Oestreich J. SCH-530348, a thrombin receptor (PAR-1) antagonist for the prevention and treatment of atherothrombosis. *Curr Opin Investig Drugs.* 2009;10(9):988–996.
22. Shinohara Y, Goto S, Doi M, Jensen P. Safety of the novel protease-activated receptor-1 antagonist vorapaxar in Japanese patients with a history of ischemic stroke. *J Stroke Cerebrovasc Dis.* 2012;21(4):318–324.
23. LeBouder F, Lina B, Rimmelzwaan GF, Riteau B. Plasminogen promotes Influenza A virus replication through an annexin II-dependent pathway in absence of neuraminidase. *J Gen Virol.* 2010;91(pt 11):2753–2761.
24. LeBouder F, et al. Annexin II incorporated into influenza virus particles supports virus replication by converting plasminogen into plasmin. *J Virol.* 2008;82(14):6820–6828.
25. Wygrecka M, et al. Enolase-1 promotes plasminogen-mediated recruitment of monocytes to the acutely inflamed lung. *Blood.* 2009;113(22):5588–5598.
26. Gong Y, Hart E, Shchurin A, Hoover-Plow J. Inflammatory macrophage migration requires MMP-9 activation by plasminogen in mice. *J Clin Invest.* 2008;118(9):3012–3024.
27. Goto H, Wells K, Takada A, Kawaoka Y. Plasminogen-binding activity of neuraminidase determines the pathogenicity of influenza A virus. *J Virol.* 2001;75(19):9297–9301.
28. Goto H, Kawaoka Y. A novel mechanism for the acquisition of virulence by a human influenza A virus. *Proc Natl Acad Sci U S A.* 1998;95(17):10224–10228.
29. Peterson EA, Sutherland MR, Nesheim ME, Pryzdial EL. Thrombin induces endothelial cell-surface exposure of the plasminogen receptor annexin 2. *J Cell Sci.* 2003;116(pt 12):2399–2408.
30. McEachron TA, Pawlinski R, Richards KL, Church FC, Mackman N. Protease-activated receptors mediate crosstalk between coagulation and fibrinolysis. *Blood.* 2010;116(23):5037–5044.
31. Strande JL, Hsu A, Su J, Fu X, Gross GJ, Baker JE. SCH 79797, a selective PAR1 antagonist, limits myocardial ischemia/reperfusion injury in rat hearts. *Basic Res Cardiol.* 2007;102(4):350–358.
32. Cao C, Gao Y, Li Y, Antalis TM, Castellino FJ, Zhang L. The efficacy of activated protein C in murine endotoxemia is dependent on integrin CD11b. *J Clin Invest.* 2010;120(6):1971–1980.
33. Lo HM, Chen CL, Tsai YJ, Wu PH, Wu WB. Thrombin induces cyclooxygenase-2 expression and prostaglandin E2 release via PAR1 activation and ERK1/2- and p38 MAPK-dependent pathway in murine macrophages. *J Cell Biochem.* 2009;108(5):1143–1152.
34. Seyer R, et al. Synergistic adaptive mutations in the HA and PA lead to increased virulence of pandemic 2009 H1N1 influenza A virus in mice. *J Infect Dis.* 2012;205(2):262–271.
35. Su X, Camerer E, Hamilton JR, Coughlin SR, Marthay MA. Protease-activated receptor-2 activation induces acute lung inflammation by neuropeptide-dependent mechanisms. *J Immunol.* 2005;175(4):2598–2605.
36. Jenkins RG, et al. Ligand of protease-activated receptor 1 enhances alpha(v)beta6 integrin-dependent TGF-beta activation and promotes acute lung injury. *J Clin Invest.* 2006;116(6):1606–1614.
37. Mercer PF, Deng X, Chambers RC. Signaling pathways involved in proteinase-activated receptor-1-induced proinflammatory and profibrotic mediator release following lung injury. *Ann NY Acad Sci.* 2007;1096:86–88.
38. Chen D, et al. Protease-activated receptor 1 activation is necessary for monocyte chemoattractant protein 1-dependent leukocyte recruitment in vivo. *J Exp Med.* 2008;205(8):1739–1746.
39. Busuttill SJ, Ploplis VA, Castellino FJ, Tang L, Eaton JW, Plow EF. A central role for plasminogen in the inflammatory response to biomaterials. *J Thromb Haemost.* 2004;2(10):1798–1805.
40. Syrovets T, Tippler B, Rieks M, Simmet T. Plasmin is a potent and specific chemoattractant for human peripheral monocytes acting via a cyclic guanosine monophosphate-dependent pathway. *Blood.* 1997;89(12):4574–4583.
41. O'Connell PA, Surette AP, Liwski RS, Svenningsson P, Waisman DM. S100A10 regulates plasminogen-dependent macrophage invasion. *Blood.* 2010;116(7):1136–1146.
42. Sun X, Tse LV, Ferguson AD, Whittaker GR. Modifications to the hemagglutinin cleavage site control the virulence of a neurotropic H1N1 influenza virus. *J Virol.* 2010;84(17):8683–8690.
43. Zhao A, et al. Immune regulation of protease-activated receptor-1 expression in murine small intestine during *Nippostrongylus brasiliensis* infection. *J Immunol.* 2005;175(4):2563–2569.
44. Cunningham MA, Rondeau E, Chen X, Coughlin SR, Holdsworth SR, Tipping PG. Protease-activated receptor 1 mediates thrombin-dependent, cell-mediated renal inflammation in crescentic glomerulonephritis. *J Exp Med.* 2000;191(3):455–462.
45. Keller TT, et al. Effects on coagulation and fibrinolysis induced by influenza in mice with a reduced capacity to generate activated protein C and a deficiency in plasminogen activator inhibitor type 1. *Circ Res.* 2006;99(11):1261–1269.
46. Di Serio C, et al. Protease-activated receptor 1-selective antagonist SCH79797 inhibits cell proliferation and induces apoptosis by a protease-activated receptor 1-independent mechanism. *Basic Clin Pharmacol Toxicol.* 2007;101(1):63–69.
47. Pawlinski R, et al. Response to letter by Strande regarding article “Protease-activated receptor-1 contributes to cardiac remodeling and hypertrophy”. *Circulation.* 2008;117(24):e496.
48. Khoufache K, et al. Protective role for protease-activated receptor-2 against influenza virus pathogenesis via an IFN-gamma-dependent pathway. *J Immunol.* 2009;182(12):7795–7802.
49. Nhu QM, et al. Novel signaling interactions between proteinase-activated receptor 2 and Toll-like receptors in vitro and in vivo. *Mucosal Immunol.* 2010;3(1):29–39.
50. Feld M, et al. Agonists of proteinase-activated receptor-2 enhance IFN-gamma-inducible effects on human monocytes: role in influenza A infection. *J Immunol.* 2008;180(10):6903–6910.
51. Garcia CC, et al. Platelet-activating factor receptor plays a role in lung injury and death caused by Influenza A in mice. *PLoS Pathog.* 2010;6(11):e1001171.
52. Walsh KB, et al. Suppression of cytokine storm with a sphingosine analog provides protection against pathogenic influenza virus. *Proc Natl Acad Sci U S A.* 2011;108(29):12018–12023.
53. Tricoci P, et al. Thrombin-receptor antagonist vorapaxar in acute coronary syndromes. *N Engl J Med.* 2012;366(1):20–33.
54. Morrow DA, et al. Vorapaxar in the secondary prevention of atherothrombotic events. *N Engl J Med.* 2012;366(15):1404–1413.
55. Riteau B, et al. Characterization of HLA-G1, -G2, -G3, and -G4 isoforms transfected in a human melanoma cell line. *Transplant Proc.* 2001;33(3):2360–2364.
56. LeBouder F, et al. Immunosuppressive HLA-G molecule is upregulated in alveolar epithelial cells after influenza A virus infection. *Hum Immunol.* 2009;70(12):1016–1019.
57. Riteau B, Barber DF, Long EO. Vav1 phosphorylation is induced by beta2 integrin engagement on natural killer cells upstream of actin cytoskeleton and lipid raft reorganization. *J Exp Med.* 2003;198(3):469–474.
58. Ploplis VA, et al. Effects of disruption of the plasminogen gene on thrombosis, growth, and health in mice. *Circulation.* 1995;92(9):2585–2593.
59. Griffin CT, Srinivasan Y, Zheng YW, Huang W, Coughlin SR. A role for thrombin receptor signaling in endothelial cells during embryonic development. *Science.* 2001;293(5535):1666–1670.
60. Bernard D, et al. Costimulatory receptors in a teleost fish: typical CD28, elusive CTLA4. *J Immunol.* 2006;176(7):4191–4200.

## **Manuscrit n°2: Plasminogen Controls Inflammation and Pathogenesis of Influenza Virus Infection via Fibrinolysis.**

Fatma Berri, Guus F. Rimmerlzwaan, Michel Hanss, Emmanuel Albina, Marie-Laure Foucault-Grunenwald, Vuong B.Lê, Stella E.Vogelzang-Van Trierum, Patrica Gil, Eric Camerer, Dominique Martinez, Bruno Lina, Roger Lijnen, Peter Carmeliet, Beatrice Riteau.

**PlosPathogens. 2013. 9(3):e1003229. Doi: 10.1371/journal.ppat.1003229**

### **Résumé**

L'activation de l'hémostase aboutit à la formation d'un caillot de fibrine. Ce dernier doit disparaître pour que la cicatrisation soit effective et la fonction tissulaire restaurée. Le caillot de fibrine est donc éliminé grâce à la transformation du PLG en plasmine qui dégrade la fibrine (processus de fibrinolyse). Il a été préalablement démontré que la fibrinolyse était activée chez la souris durant les infections grippales (Keller 2006). Or, ce phénomène libère des produits de dégradation de la fibrine (FDP) qui sont des molécules pro-inflammatoires puissantes (Leavell et al 1996). Nous avons donc émis l'hypothèse que la dérégulation de ce processus pouvait contribuer à l'inflammation délétère des poumons durant les infections par les virus influenza. Pour cela, nous avons étudié le rôle du PLG, molécule clé de l'hémostase et dont l'activation est à l'origine de la fibrinolyse.

Afin d'étudier le rôle du PLG dans l'infection grippale, nous avons infecté des souris déficientes en PLG ou inhibé pharmacologiquement la transformation du PLG en plasmine, *in vivo*. Nous avons observé que les souris déficientes en PLG étaient protégées d'une inflammation délétère des poumons et de l'infection grippale, d'une manière indépendante de la souche virale (souches H1N1, et H5N1 hautement pathogènes), en comparaison avec des

souris sauvages. Cet effet a été aboli lorsque les souris ont été préalablement traitées avec de l'ancrod, un agent dégradant le fibrinogène. Ainsi, ces résultats ont démontré que l'hyperfibrinolyse médiée par l'activation du PLG en plasmine joue un rôle important dans l'inflammation délétère des poumons et la pathogénicité des virus influenza. De manière intéressante, le traitement des souris avec une molécule anti-fibrinolytique, le 6-AHA (6-Aminoheptanoic Acid, Amicar) les a protégées contre la mortalité induite par le VIA, également d'une manière indépendante de la souche virale. Nos résultats montrent donc que le PLG, via une hyperfibrinolyse, est délétère durant les infections grippales. Le 6-AHA, étant un principe actif administré pour d'autres applications chez l'homme et disponible sur le marché, nos résultats suggèrent donc que le système PLG/plasmine pourrait être une nouvelle cible thérapeutique contre les infections grippales.

# Plasminogen Controls Inflammation and Pathogenesis of Influenza Virus Infections via Fibrinolysis

Fatma Berri<sup>1</sup>, Guus F. Rimmelzwaan<sup>2</sup>, Michel Hanss<sup>3</sup>, Emmanuel Albina<sup>4</sup>, Marie-Laure Foucault-Grunenwald<sup>1</sup>, Vuong B. Lê<sup>1</sup>, Stella E. Vogelzang-van Trierum<sup>2</sup>, Patrica Gil<sup>4</sup>, Eric Camerer<sup>5,6</sup>, Dominique Martinez<sup>4</sup>, Bruno Lina<sup>1</sup>, Roger Lijnen<sup>7</sup>, Peter Carmeliet<sup>8,9</sup>, Béatrice Riteau<sup>1,10\*</sup>

**1** VirPath, EA4610 Virologie et Pathologie Humaine, Faculté de Médecine RTH Laennec, Université Claude Bernard Lyon 1, Lyon, France, **2** Department of Virology, Erasmus Medical Center, Rotterdam, The Netherlands, **3** Laboratoire d'Hématologie, CBPE, Hospices Civils de Lyon, Lyon, France, **4** CIRAD, UMR CMAEE, Montpellier, France INRA, UMR1309 CMAEE, Montpellier, France, **5** INSERM U970, Paris Cardiovascular Centre, Paris, France, **6** Université Paris-Descartes, Paris, France, **7** Center for Molecular and Vascular Biology, KU Leuven, Leuven, Belgium, **8** Laboratory of Angiogenesis & Neurovascular Link, Vesalius Research Center, VIB, Leuven, Belgium, **9** Laboratory of Angiogenesis & Neurovascular Link, Vesalius Research Center, KU Leuven, Leuven, Belgium, **10** INRA, Nouzilly, Indre-et-Loire, France

## Abstract

Detrimental inflammation of the lungs is a hallmark of severe influenza virus infections. Endothelial cells are the source of cytokine amplification, although mechanisms underlying this process are unknown. Here, using combined pharmacological and gene-deletion approaches, we show that plasminogen controls lung inflammation and pathogenesis of infections with influenza A/PR/8/34, highly pathogenic H5N1 and 2009 pandemic H1N1 viruses. Reduction of virus replication was not responsible for the observed effect. However, pharmacological depletion of fibrinogen, the main target of plasminogen reversed disease resistance of plasminogen-deficient mice or mice treated with an inhibitor of plasminogen-mediated fibrinolysis. Therefore, plasminogen contributes to the deleterious inflammation of the lungs and local fibrin clot formation may be implicated in host defense against influenza virus infections. Our studies suggest that the hemostatic system might be explored for novel treatments against influenza.

**Citation:** Berri F, Rimmelzwaan GF, Hanss M, Albina E, Foucault-Grunenwald M-L, et al. (2013) Plasminogen Controls Inflammation and Pathogenesis of Influenza Virus Infections via Fibrinolysis. *PLoS Pathog* 9(3): e1003229. doi:10.1371/journal.ppat.1003229

**Editor:** Andrew Pekosz, Johns Hopkins University - Bloomberg School of Public Health, United States of America

**Received:** September 22, 2012; **Accepted:** January 20, 2013; **Published:** March 21, 2013

**Copyright:** © 2013 Berri et al. This is an open-access article distributed under the terms of the Creative Commons Attribution License, which permits unrestricted use, distribution, and reproduction in any medium, provided the original author and source are credited.

**Funding:** This work was supported by the Agence Nationale de la Recherche (ANR, BR), Long term Structural funding - Methusalem by the Flemish Government (PC), and INSERM avenir (EC). The funders had no role in study design, data collection and analysis, decision to publish, or preparation of the manuscript.

**Competing Interests:** The authors have declared that no competing interests exist.

\* E-mail: beatrice.riteau@univ-lyon1.fr

## Introduction

Influenza A viruses (IAV) are an important cause of outbreaks of respiratory tract infections and are responsible for significant morbidity and mortality in the human population [1]. Upon infection with IAV, innate and adaptive immune responses are induced that restrict viral replication and that afford protection against infection with these viruses. However, excessive inflammation, particularly in the lower respiratory tract, may result in alveolar damage limiting respiratory capacity and deteriorate the clinical outcome of IAV infections [2,3]. Dys-regulation of cytokine production in the lungs is thus often associated with a fatal outcome of IAV [4]. The sites of virus replication in the respiratory tract represent complex microenvironments, in which extracellular proteases are present abundantly [5,6]. Some of these proteases can play a role in innate immune responses since they are important mediators of inflammatory processes [7] and influence virus replication [8,9]. To date, however, the elucidation of host proteases contributing to pathogenesis of IAV infections *in vivo* has been hampered by the lack of experimental models.

One of the proteases of interest is plasmin, which is a serine protease involved in fibrinolysis, the biological process of dissolving fibrin polymers into soluble fragments. Plasmin is generated through cleavage of the proenzyme plasminogen, produced in the liver and present in the blood. Specific binding and conversion of

plasminogen into plasmin by IAV may afford the virus an alternative protease for cleavage of its hemagglutinin molecule [10,11]. This is an essential step in the virus replication cycle and this may contribute to the pathogenesis of IAV infection [12,13]. In addition, plasminogen/plasmin plays a central role in fibrinolysis-mediated inflammation [14] and there is evidence of fibrinolysis activation during IAV infections [15]. Thus, plasminogen could contribute to the pathogenesis of IAV infections by promoting virus replication or by inducing a fibrinolysis-dependent harmful inflammatory response in the respiratory tract. At present it is unknown whether one or both of these two mechanisms of plasminogen activity contribute to pathogenesis of IAV infections *in vivo*. In the present study we address this research question and using plasminogen-deficient mice (PLG-KO) and pharmacological approaches the role of plasminogen during IAV infections was investigated.

Our findings show that plasminogen plays an important role in lung inflammation upon IAV infections, mainly through fibrinolysis. Therefore, targeting host factors, such as the fibrinolytic molecule plasminogen may be of interest for the development of new therapeutics against IAV infections.

## Author Summary

Influenza viruses, including H5N1 bird influenza viruses continue to form a major threat for public health. Available antiviral drugs for the treatment of influenza are effective to a limited extent and the emergence of resistant viruses may further undermine their use. The symptoms associated with influenza are caused by replication of the virus in the respiratory tract and the host immune response. Here, we report that a molecule of the fibrinolytic system, plasminogen, contributes to inflammation caused by influenza. Inhibiting the action of plasminogen protected mice from severe influenza infections, including those caused by H5N1 and H1N1 pandemic 2009 viruses and may be a promising novel strategy to treat influenza.

## Results

### Plasminogen promotes IAV pathogenesis

To explore the role of plasminogen in IAV pathogenesis, we investigated the consequence of plasminogen-deficiency. Plasminogen +/– mice were intercrossed to generate wild-type (WT) and plasminogen –/– (PLG-KO) mice, which were infected with IAV A/PR/8/34 (H1N1; 50,000 or 500 PFU) and weight loss and survival rates were monitored. As shown in Figure 1A, compared to WT mice, PLG-KO mice were significantly more resistant to IAV-induced weight loss and death. In PLG-KO mice substantial protection was also observed against infection with 2009 pandemic virus A/Netherlands/602/09 (30,000 PFU, Figure 1B) and highly pathogenic H5N1 virus A/chicken/Ivory-Coast/1787/2006 (10 EID<sub>50</sub> H5N1, Figure 1C). Of note, the latter was not adapted to replicate in mammals, which could explain the delay in weight loss observed upon infection, as also observed by others [16]. Thus, we concluded that without plasminogen, pathogenesis of IAV infections was dampened and mortality reduced in a subtype-independent manner.

### Protection conferred by PLG-deficiency is independent on virus replication

To gain further insight into the role of plasminogen in virus replication, A549 cells were infected with IAV in the absence or presence of plasminogen. Interestingly, plasminogen supported the replication of IAV A/PR/8/34 but not that of A/Netherlands/602/09 (Figure 2A). In contrast, trypsin supported replication of both viruses while no replication was observed in absence of proteases. Since plasminogen promotes IAV replication through HA cleavage [11], plasminogen-mediated HA cleavage of both viruses was compared (Figure 2B). In absence of proteases (–), HA0 precursor protein was detected in A549 cells infected with either virus. In presence of plasminogen (PLG), an additional band, corresponding to HA2 [11] was detected at 25 kDa in A/PR/8/34, but not in A/Netherlands/602/09 infected cells. In presence of trypsin (Try), HA2 was detected in cells infected with either virus. Similar levels of tubulin were detected, which was included as control cellular protein. Thus, plasminogen promotes cleavage of HA of IAV A/PR/8/34 but not that of A/Netherlands/602/09, which correlated with differences in replicative capacity of these viruses in presence of plasminogen.

On day 2 post-inoculation with IAV A/PR/8/34, mean lung virus titer of PLG-KO mice was significantly lower than that of WT mice (Figure 2C). This difference was not observed for IAV A/Netherlands/602/09. For both viruses, and at the other days post-infection, no significant differences in lung virus titers were observed between PLG-KO and WT mice. Thus, *in vivo*,

plasminogen promoted early virus replication of IAV A/PR/8/34 but not of A/Netherlands/602/09. Since the absence of plasminogen protected mice against both viruses, the deleterious effect of plasminogen was most likely independent of virus replication in the lungs.

### Pulmonary injury and virus dissemination

To assess possible other contributions of plasminogen to the pathogenesis of IAV infections, inflammation of the lungs and viral dissemination were examined after infection of mice with IAV A/PR/8/34 or A/Netherlands/602/09. At day 3 post-infection, extensive alveolar damage and marked cellular infiltrates were observed in lungs of WT mice in contrast to those of PLG-KO mice (HE) after A/PR/8/34 virus infection (Figure 3A, left panel). This difference was also observed upon infection with A/Netherlands/602/09 virus, at day 5 (Figure 3A, right panel) but not at day 3 post-inoculation (data not shown). For all conditions, in WT and PLG-KO mice, similar numbers of IAV-infected cells were detected by immunohistochemistry (IHC). Also, no lesions were observed in Mock-infected mice (data not shown). Thus, plasminogen-deficiency protected mice against inflammation induced by A/PR/8/34 and A/Netherlands/602/09 viruses, showing that plasminogen plays a deleterious role in lung inflammation, independent of virus replication in the lungs.

To investigate the difference in pulmonary inflammation between PLG-KO and WT mice, cytokine levels in the bronchoalveolar lavages (BALs) were assessed by ELISA (Figure 3B) or a luminex-based cytokine detection assays (Figure 4A) at various time point post-infection. Upon inoculation of A/PR/8/34 virus, both in PLG-KO and WT mice, BAL cytokine levels increased 2 and 5 days post-inoculation. However, in BAL of PLG-KO mice cytokine levels were considerably and significantly lower than in those of WT littermates (see scale differences for Figure 4A), which correlated with reduced IAV-induced lung inflammation in absence of plasminogen. Upon A/Netherlands/602/09 virus infection, release of cytokines in the BAL was also significantly higher in WT mice compared to PLG-KO mice at day 5 but not at day 2 post-inoculation (Figure 3B, right panel). Thus in concordance with the histological analysis, plasminogen promoted lung inflammation of IAV A/PR/8/34 and A/Netherlands/602/09 viruses, showing that the effect is most likely independent of virus replication in the lungs. Furthermore, in PLG-KO mice the virus failed to disseminate to extra pulmonary organs unlike in WT mice, upon intranasal infection with A/PR/8/34 virus (500 PFU) (Figure 4B). Especially high virus titers were detected in the liver, the source of plasminogen. Collectively, these results suggest that plasminogen plays an important role in promoting the inflammatory response and virus dissemination to extra-pulmonary organs during IAV-infection.

### Fibrinolysis and IAV pathogenesis

Since degradation of fibrin is one of the main functions of plasminogen/plasmin, we hypothesized that the host fibrinolytic system plays a role in the pathogenesis of IAV infection. First, we investigated whether IAV infection induced fibrinolysis. To this end, mice were inoculated with IAV A/PR/8/34 and at various time points post-inoculation, the level of fibrinolysis markers in BALs was assessed by ELISA (Figure 5A). Plasminogen and active plasmin levels were barely detectable in the BAL of uninfected mice but their levels significantly increased during the course of infection. Levels of fibrinogen also significantly increased at day 4 post-infection and then dropped at days 5 and 6, suggesting a recruitment of fibrinogen to the lungs and a rapid consumption of

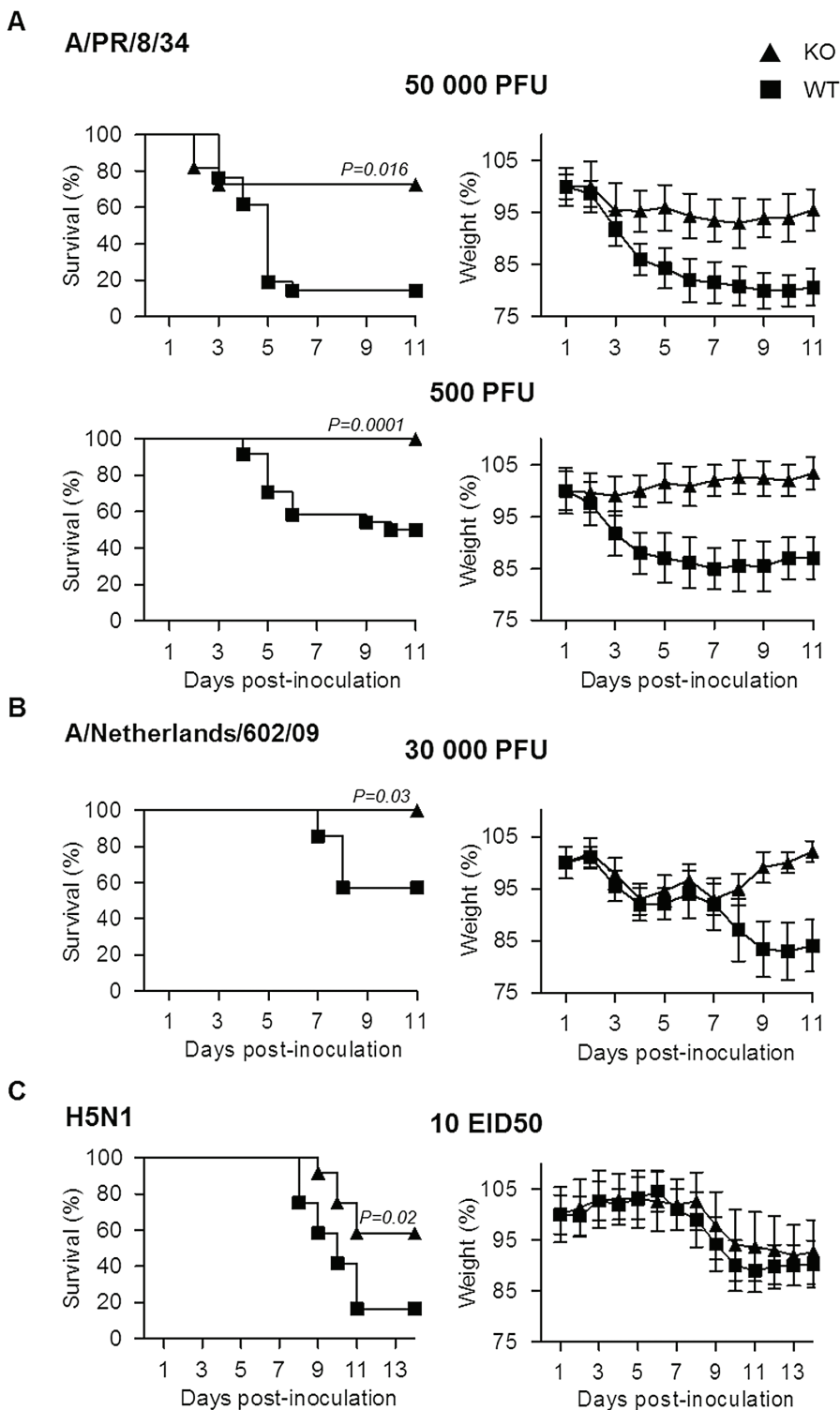


**Figure 1. Plasminogen contributes to influenza pathogenesis.** Survival and weight loss of PLG-KO (triangles) and WT (squares) mice infected with (A) IAV A/PR/8/34 (50,000 PFU; n=11–21 or 500 PFU; n=23–24), (B) A/Netherlands/602/09 (30,000 PFU; n=7) or (C) A/chicken/Ivory-Coast/1787/2006 (10 EID50; n=12). The proportion of survival was determined based on euthanasia criteria. Animals that lost 20% of their body weight were considered to have reached humane endpoints and were sacrificed according to the study protocol. It is of note that upon WT mice infection with A/chicken/Ivory-Coast/1787/2006, all infected mice lost weight but died before reaching –20% of their body weight, in contrast to PLG-KO mice, which explains the difference in mortality but not in weight loss. Weight loss data represent weight average  $\pm$  s.e.m of the above indicated number of mice. n=mice per group.  
 doi:10.1371/journal.ppat.1003229.g001

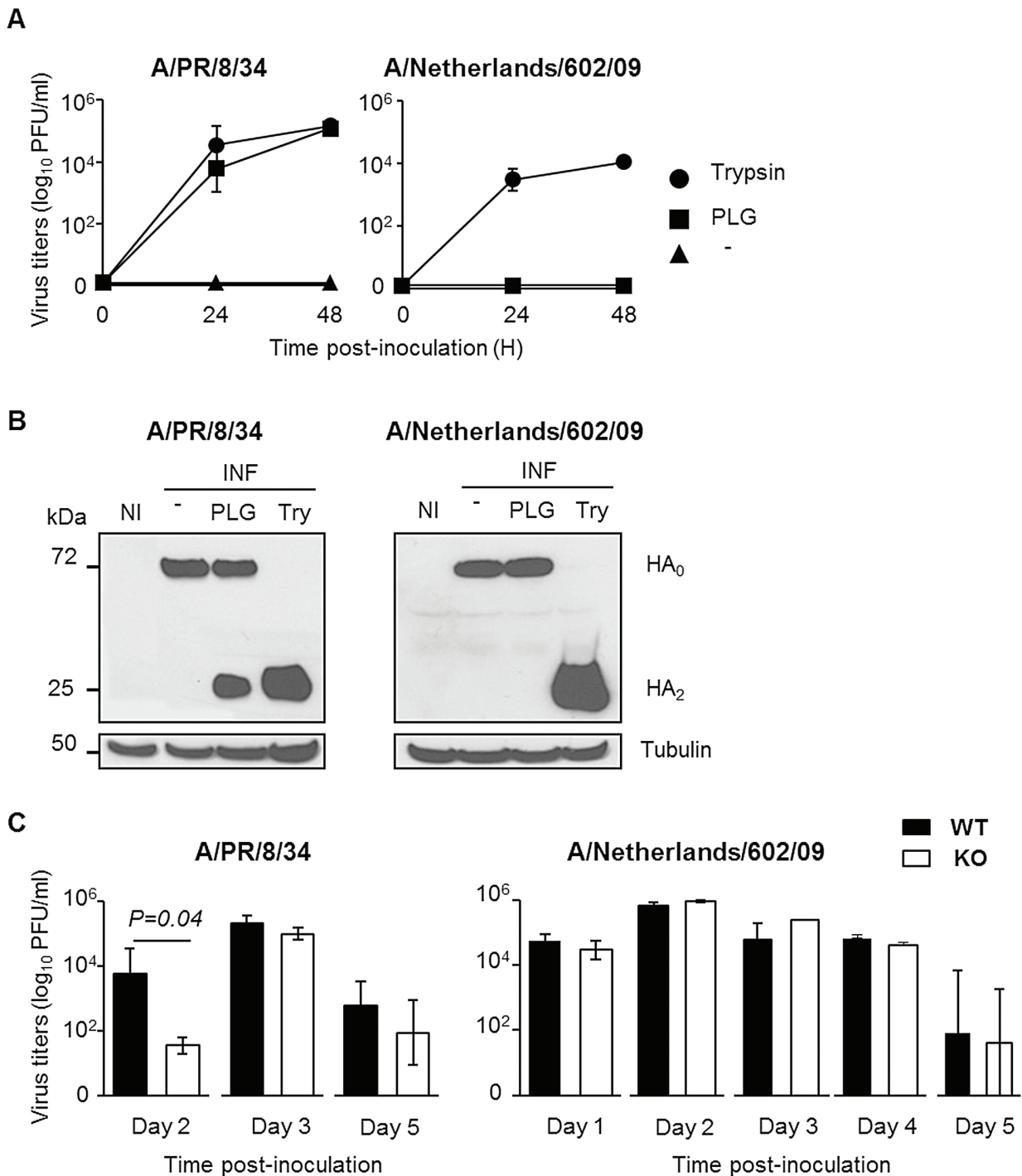


**Figure 2. The deleterious role of plasminogen is independent on virus replication.** (A) Virus replication of IAV A/PR/8/34 and A/Netherlands/602/09 after inoculation of A549 cells in presence or absence (triangle) of plasminogen (square) or trypsin (circle). Data represent mean  $\pm$  s.e.m of three independent experiments. (B) Western blot analysis of A/PR/8/34 and A/Netherlands/602/09 HA cleavage after infection of A549 cells in presence or absence of plasminogen (PLG) or trypsin (Try). Membranes were probed with anti-HA and anti-tubulin antibodies. kDa (apparent molecular weight). NI stands for uninfected. (C) Infectious A/PR/8/34 (n = 3–5) and A/Netherlands/602/09 (n = 3) lung virus titers at the indicated time points post-inoculation of WT (black bars) or PLG-KO mice (white bars). Data represent mean  $\pm$  s.e.m of 3–5 individual mice per group. n = mice per group and per time-point. doi:10.1371/journal.ppat.1003229.g002

the molecule and fibrinolysis. Finally, levels of FDP and D-dimers, degradation products of fibrinolysis, significantly increased upon infection, reaching 45 and 13 ng/ml respectively on day 6 post-

inoculation. Similar results were also obtained upon infection with influenza virus A/Netherlands/602/09 (Figure 5A). As expected, in the BAL of infected PLG-KO mice, used as negative control,

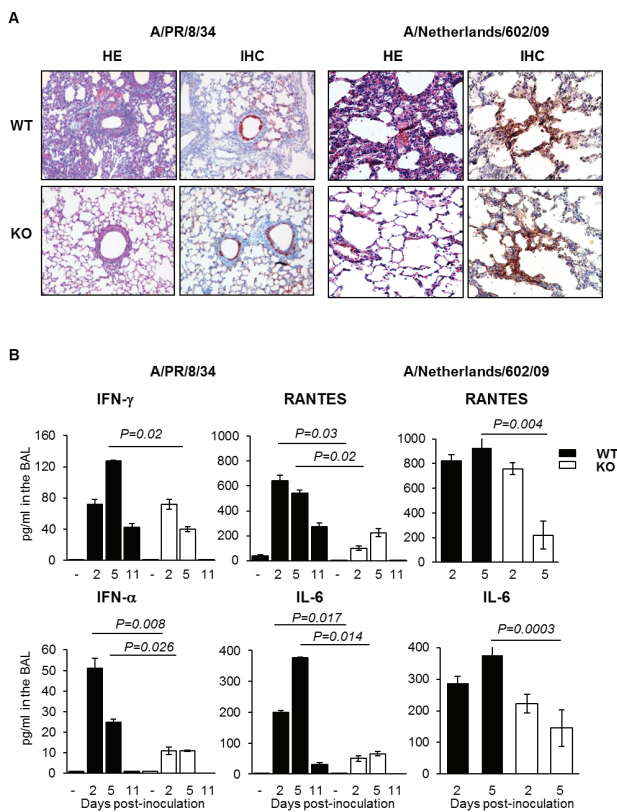


**Figure 3. Plasminogen-deficiency prevents severe inflammation.** (A) Histopathological analysis of lungs from infected WT and PLG-KO mice inoculated with A/PR/8/34 virus (day 3 post-infection) or A/Netherlands/602/09 virus (day 5 post-infection). Thin sections of lungs obtained from infected and uninfected WT and PLG-KO mice (as indicated) were stained with hematoxylin end eosin (HE) to evaluate histopathological changes. Note the marked infiltration of inflammatory cells in the lungs of infected WT mice, which was largely absent in the lungs of PLG-KO mice. The results shown are representative for two-three mice for both groups. Immunohistochemistry (IHC) using a monoclonal antibody for the influenza A virus nucleoprotein was used to detect virus-infected cells. Cells positive for the presence of viral antigen stained red. (B) Cytokine levels in BAL were assessed by ELISA on the indicated days post inoculation of WT (black bars) and PLG-KO mice (white bars) with IAV A/PR/8/34 or A/Netherlands/602/09. Data represent mean  $\pm$  s.e.m. of 3–6 mice per group. doi:10.1371/journal.ppat.1003229.g003

fibrinolysis markers were barely detectable. Thus, IAV infection induced fibrinolysis. These results were confirmed by Western blot analysis using an antibody directed against the mouse A $\alpha$  chain of fibrinogen (Figure 5B), which recognizes purified mouse fibrinogen at a molecular weight of 66 kDa (data not shown). Compared to uninfected mice (–), fibrinogen was readily detectable 2–6 days post-inoculation in the lungs of infected mice. In the tissues, no marked fibrinogen consumption was detected but during the course of IAV infection, additional smaller bands corresponding to FDP were observed in mouse lungs. These findings confirmed that fibrinolysis took place during IAV infections *in vivo*.

To simulate the depletion of fibrin (and therefore fibrinolysis), mice were treated with the snake venom Ancrod, a thrombin-like protease that cleaves the A $\alpha$  chain of fibrinogen, enhancing its degradation and severely reducing its plasma levels (Figure 5C). Treatment with Ancrod significantly increased IAV-induced weight loss and mortality compared to vehicle-treated mice, but had no effect on uninfected control mice (Figure 6A). This

increased mortality was also associated with an increase in inflammation of the lungs, as detected by elevated cytokine levels in the BAL (Figure 6B, WT). Of particular interest, the level of interferon-gamma was barely detectable in untreated mice but severely increased upon ancrod treatment. Thus, degradation of fibrin(ogen) contributed to inflammation and increased pathogenicity of IAV infection.

### Plasminogen promotes IAV pathogenesis through fibrinolysis

Next, we investigated whether Ancrod treatment could reverse the protective effect of plasminogen-deficiency in terms of inflammation and mortality rate. Again, PLG-KO mice were protected from lung inflammation ( $p < 0.05$ , between WT versus PLG-KO), as judged from cytokine responses (Figure 6B) and from IAV-induced mortality (Figure 6C). Interestingly, Ancrod-treatment reversed the protection observed in the absence of plasminogen and cytokine responses and mortality rates were similar to those of Ancrod treated WT mice (Figure 6B and C,  $p > 0.05$ , between WT-treated and PLG-KO-treated ancrod). Ancrod had no effect in uninfected mice (Figure S1). Thus, fibrinolysis contributes to inflammation and pathogenesis of IAV infections, which is mediated by plasminogen.

To further confirm if the deleterious role of plasminogen is caused by fibrinolysis, we tested the outcome of infection of mice after treatment with Ancrod and/or 6-aminohexanoic acid (6-AHA). Indeed, 6-AHA is a lysine analogue that binds to the lysine binding sites of plasminogen, inhibiting plasminogen-binding to fibrin(ogen) and plasmin-mediated fibrinolysis [17]. First, 6-AHA treated mice inoculated with 5,000 or 500 PFU of A/PR/8/34 were significantly more resistant to infection than untreated mice (Figure 7A) and this protection correlated with reduced inflammation in 6-AHA treated animals (Figure S2). Also, lung virus titers were significantly lower in 6-AHA-treated mice compared to untreated mice, at day 2 but not at days 3 or 5 post-infection (Figure 7B). Thus, inhibition of plasminogen fibrinolytic activity protected mice from developing pneumonitis and severe disease. Furthermore, Ancrod-treatment of 6-AHA treated mice over-rode the protective effect of 6-AHA, again resulting in IAV-induced mortality (Figure 7A, lower panel). Administration of Ancrod and/or 6-AHA had no effect in uninfected mice (Figure S3). Thus, the protective effect of 6-AHA was reversed by Ancrod-mediated fibrinogen degradation, demonstrating that plasminogen contributed to pathogenesis of IAV infection through fibrinolysis activation.

### 6-AHA protects against influenza

Preventing deleterious inflammation after IAV infection could be a promising new strategy to treat IAV infections. Therefore, we investigated whether blocking the fibrinolytic activity of plasminogen by 6-AHA administration at a later time point post-inoculation was still protective. WT mice were inoculated with IAV A/PR/8/34 and treated or not with 6-AHA, two days later. As shown in Figure 7C, treatment with 6-AHA improved the outcome of infection and prevented mortality. 6-AHA treatment also protected mice from infection with A/Netherlands/602/09 and highly pathogenic H5N1 viruses (Figure 7C, lower panels). Thus, blocking plasminogen-mediated fibrinolysis protected mice against infections with various and highly pathogenic IAVs.

### Discussion

The present study showed for the first time that fibrinolysis plays a central role in the inflammatory response and the pathogenesis

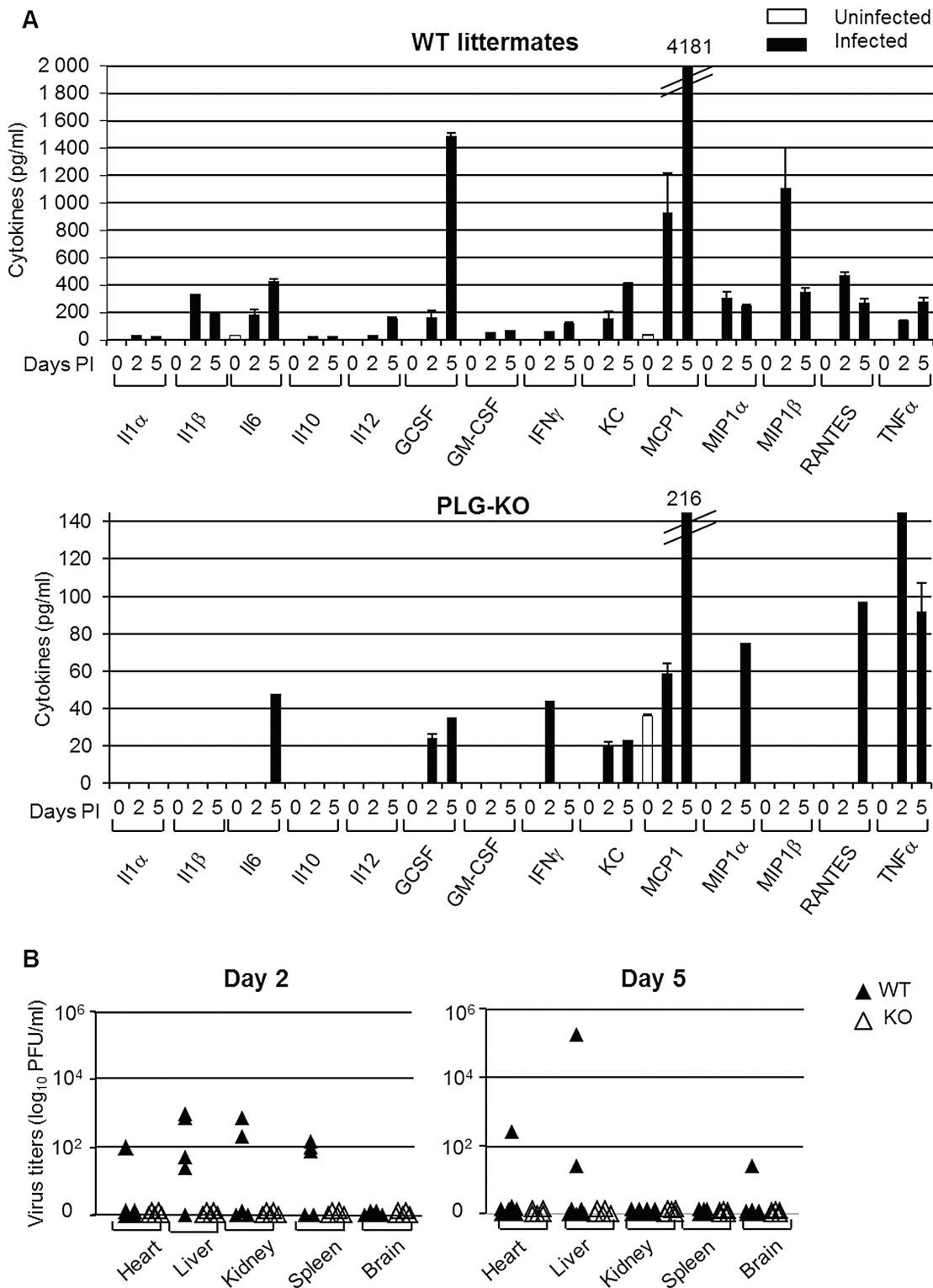


**Figure 4. Plasminogen-deficiency prevents severe inflammation and virus dissemination.** (A) Cytokine levels in BAL were assessed by 23-multiplex Luminex kit (uninfected, white bars; infected, black bars) on the indicated days post inoculation of WT (top panel) and PLG-KO mice (bottom panel) with IAV A/PR/8/34. The levels of IL-2, IL-3, IL-4, IL-5, IL-9, IL-12(p70), IL-13, IL-17 and eotaxin were below the detection limit (not shown). Data represent mean  $\pm$  s.e.m. of 2 individual mice per group from one experiment and is representative of 2 individual experiments (total  $n=3-6$  mice per group). (B) A/PR/8/34 virus titers in the indicated organs of WT (closed symbols) and PLG-KO mice (open symbols) was assessed 2 and 5 days post-inoculation.

doi:10.1371/journal.ppat.1003229.g004

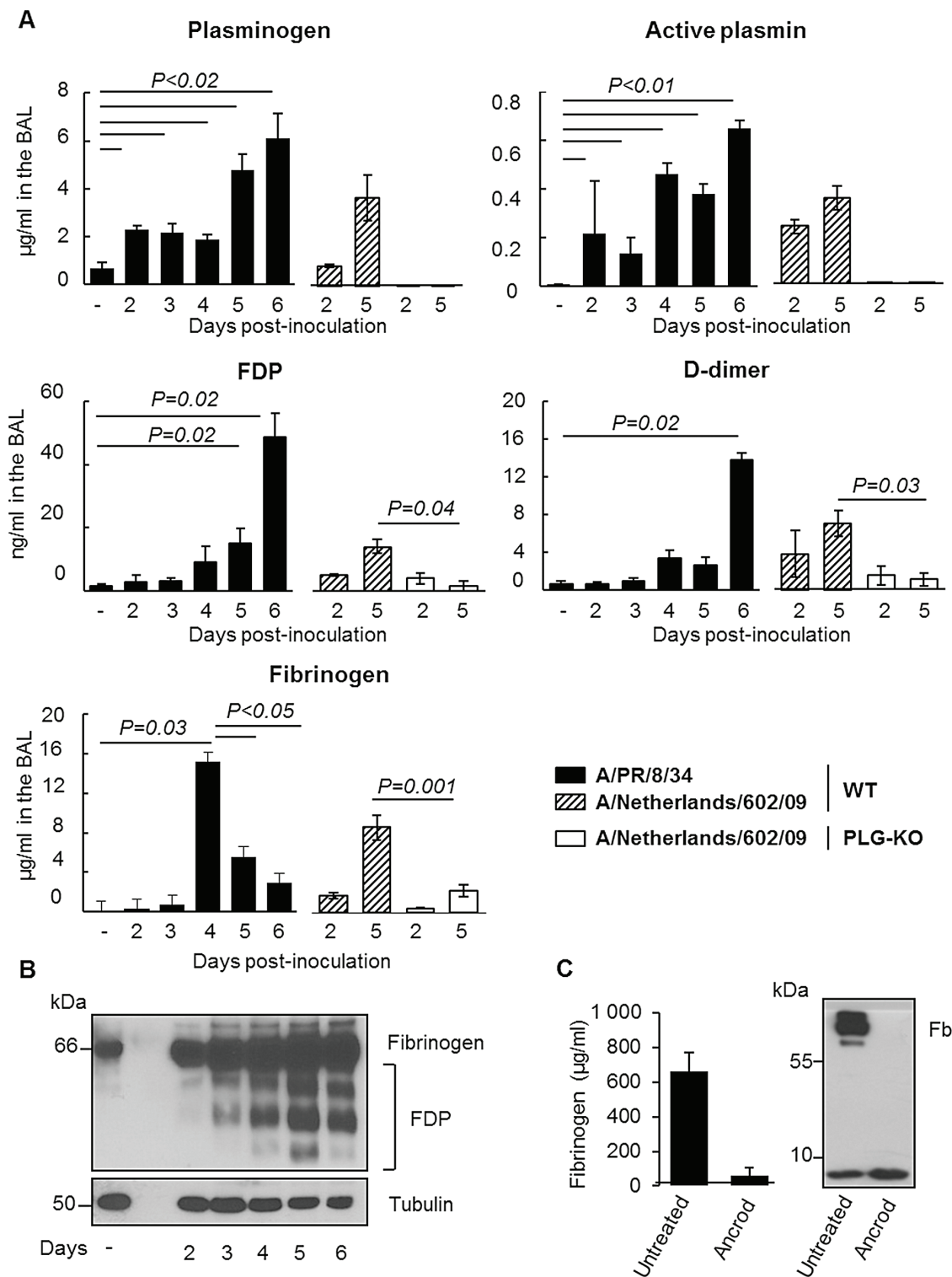


**Figure 5. Fibrinolysis is induced following severe influenza infections.** (A) Levels of Plasminogen, Active Plasmin, FDP, D-dimer and Fibrinogen, were determined by ELISA in the BAL of A/PR/8/34 infected or uninfected (–) C57BL/6 mice after the indicated days post-inoculation. Markers were also evaluated in the BAL of WT or PLG-KO mice infected with A/Netherlands/602/09 virus. Data represent mean  $\pm$  s.e.m of n=3–6 mice per group. (B) Western blot analysis for the detection of fibrinogen and FDP in the lungs of IAV-infected mice on the indicated days post inoculation (representative of n=3). kDa: apparent molecular weight. n=mice per group. (C) Presence of fibrinogen was assessed in the blood of mice treated or not with Ancrod by ELISA (left panel) or Western blot analysis (right panel). The results represent the mean values  $\pm$  s.e.m from 3 individual animals per group for the ELISA. The western blot analysis is representative for results of 3 mice per group. doi:10.1371/journal.ppat.1003229.g005

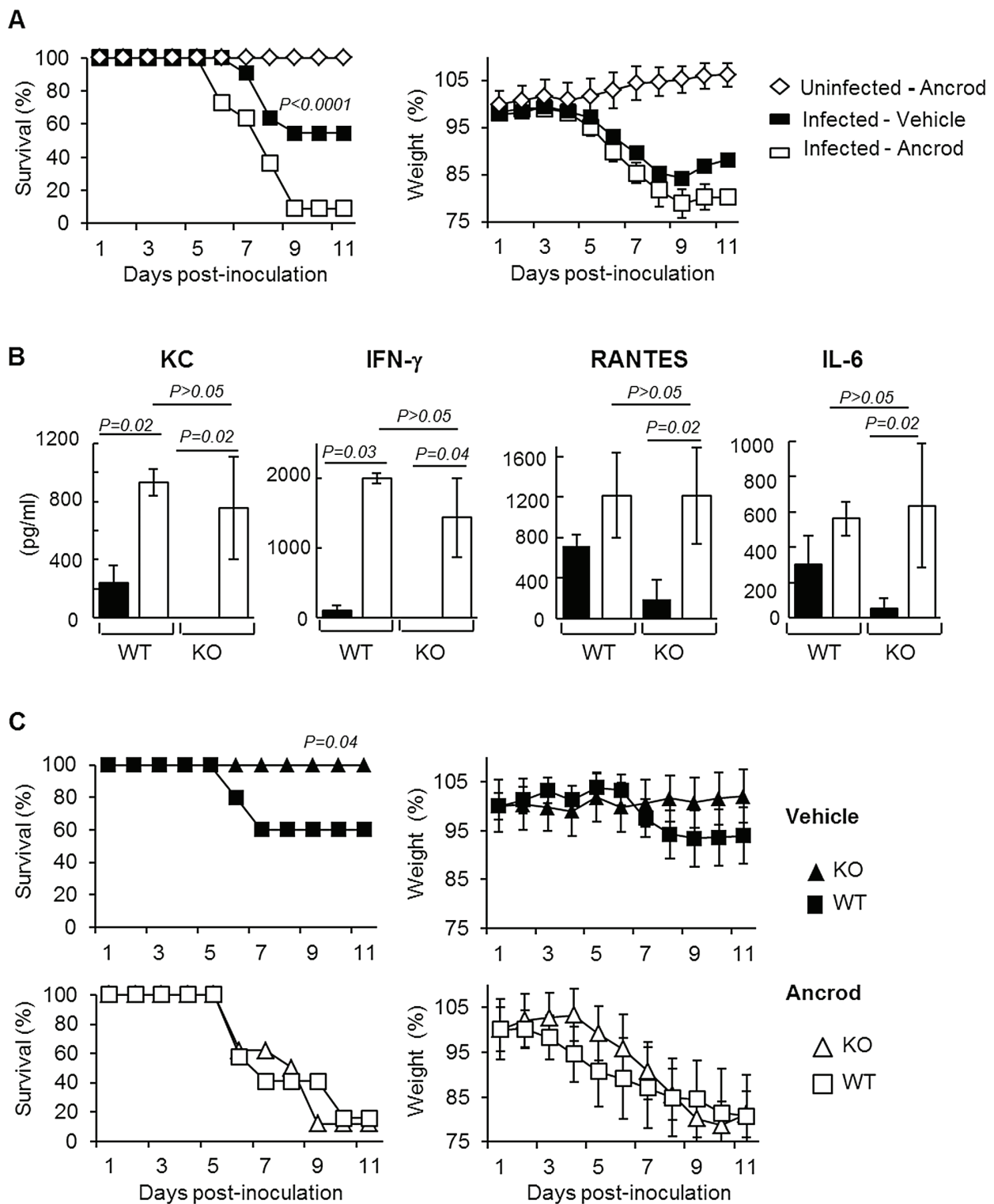


**Figure 6. Effect of Ancrod treatment on inflammation and IAV pathogenesis.** (A) Survival and weight loss of mice treated with Ancrod (open symbols,  $n=11$ ) or not (closed symbols,  $n=11$ ) after infection with IAV A/PR/8/34 (squares) or uninfected mice (diamonds,  $n=5$ ). Weight loss data represent weight average  $\pm$  s.e.m. of the above indicated number of mice. (B) Cytokines levels in the BAL were measured by ELISA after A/PR/8/34 infection of WT and PLG-KO (KO) mice treated with Ancrod (white bars) or not (black bars). Data represent mean  $\pm$  s.e.m. of  $n=4$  mice per group. (C) Survival rate (left panels) and weight loss (right panels) of WT (squares) and PLG-KO (triangles) mice treated with Ancrod (open symbols) or not (closed symbols) after intranasal inoculation with IAV A/PR/8/34 ( $n=8-10$  mice per group). Weight loss data represent weight average  $\pm$  s.e.m. of the above indicated number of mice.  
doi:10.1371/journal.ppat.1003229.g006

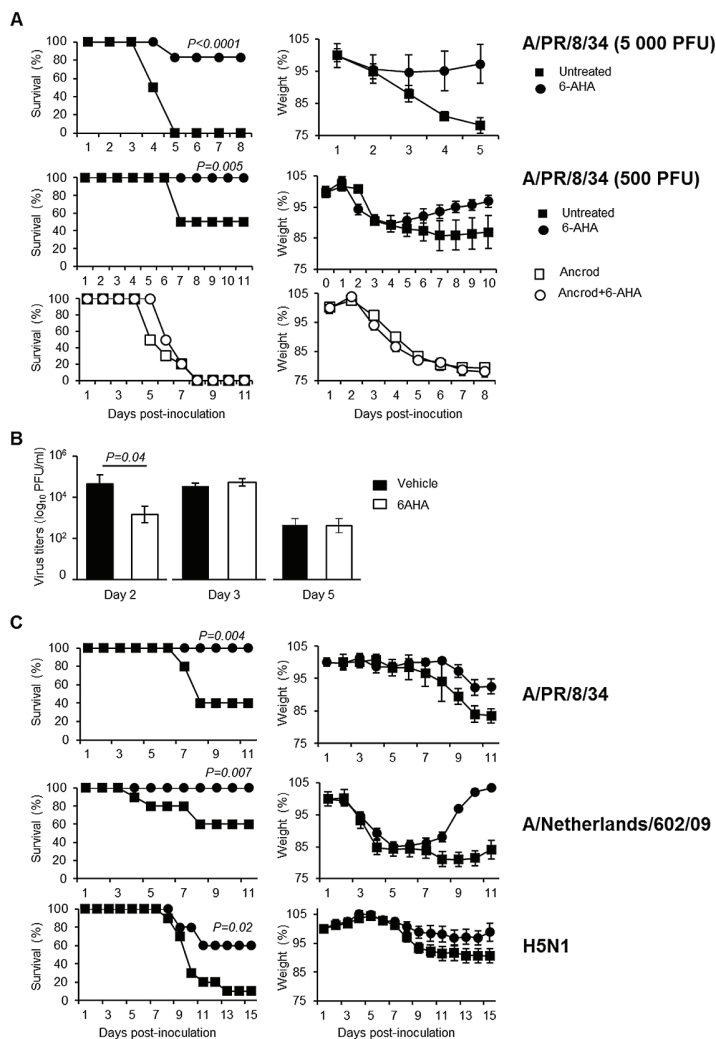


**Figure 7. Effect of 6-aminohexanoic acid and/or Ancrod treatment on the course of IAV infection.** Survival and weight loss of IAV inoculated C57BL/6 mice treated with 6-AHA (circle) or not (squares). (A) Mice were inoculated with IAV A/PR/8/34 (5,000 PFU, n = 28 or 500 PFU; n = 11) in presence (open symbols) or absence (closed symbols) of Ancrod. 6-AHA treatment was initiated on the day of inoculation. (B) Infectious A/PR/8/34 lung virus titers in 6-AHA treated or untreated mice. Data represent mean  $\pm$  s.e.m of 3 individual mice per group. (C) Mice were inoculated with IAV A/PR/8/34 (n = 10), A/Netherlands/602/09 (n = 16) or A/chicken/Ivory-Coast/1787/2006 (n = 10) as indicated. 6-AHA treatment was initiated two days post-inoculation. n = per group. Weight loss data represent weight average  $\pm$  s.e.m of the above indicated number of mice. doi:10.1371/journal.ppat.1003229.g007

of IAV infections. Consistently, evidence is accumulating that the fibrinolytic molecule plasminogen and plasmin are critical host factors for immune cell infiltration and cytokine production upon injury [18–20]. The absence of plasminogen blunts inflammation in response to several inflammatory stimuli and suppresses development of lesions [21–23]. In our study, absence of plasminogen also considerably reduced the extent of lung inflammation upon IAV infection. Since severe inflammation contributes to the pathogenicity of IAV infections of humans [2,4], most likely the proinflammatory properties of plasminogen play a role in the pathogenesis of these infections. IAV have the capacity to bind plasminogen and convert it into its active form plasmin through viral or cellular proteins like annexin-2 [11,12]. However, the extent of plasminogen activation is strain-dependent [11], which may explain differences in pathogenicity of IAV strains.

Mechanistically, the mode of action of plasminogen-driven lung inflammation was through fibrinolysis. Indeed, degradation of

fibrinogen by Ancrod treatment increased pathogenicity of IAV infection and compensated the protective effect in PLG-KO mice or in mice in which plasminogen fibrinolytic activity was blocked by 6-AHA treatment. Consistently, Keller et al showed an activation of the fibrinolytic system during non-pathogenic IAV infection in mice [15]. Remarkably, in humans increased production of D-dimer, a marker of fibrinolysis was found to be a risk factor for fatal outcome of H5N1 and pandemic H1N1 virus infections [24,25]. Furthermore, IAV infections have been associated with bleeding medical disorders [26,27]. Thus, as for bacteria [28], the dysregulation of hemostasis by virus infections may cause serious complications. Consistent with our results, it was recently demonstrated that endothelial cells are central orchestrators of cytokine amplification during IAV infections [29]. Interestingly, plasminogen-dependent inflammation appears early after infection with influenza virus A/PR/8/34, of which virus replication is promoted by plasminogen. In contrast,

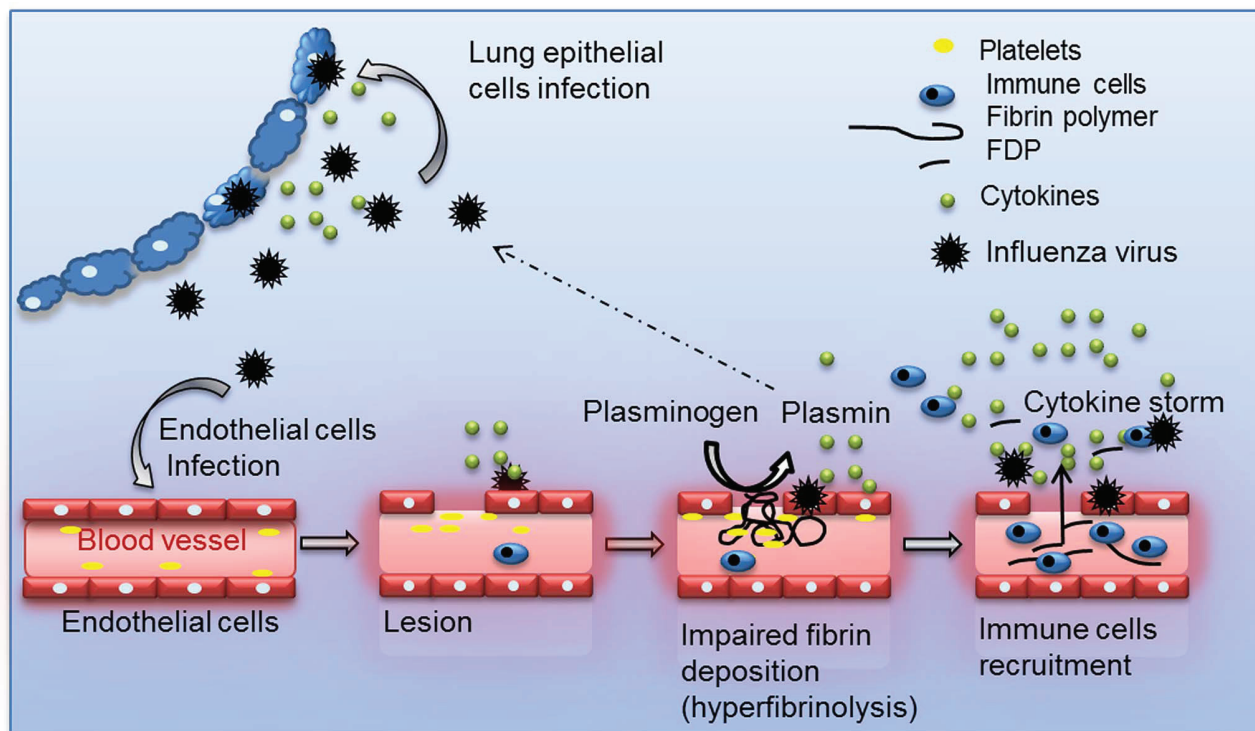


**Figure 8. Schematic overview of the proposed model for Plasminogen-mediated influenza virus pathogenesis.** During IAV infection, plasminogen is converted into plasmin. On the one hand, plasmin cleaves and activates the viral hemagglutinin, promoting IAV replication for some influenza strains. On the other hand, plasmin promotes inflammation via fibrinolysis and increases permeability. doi:10.1371/journal.ppat.1003229.g008

replication of influenza virus A/Netherlands/602/09 is independent of plasminogen and control of plasminogen activity has a delayed impact on inflammation and disease. Thus, the capability of plasminogen to cleave HA and promote virus replication may also contribute to lung inflammation for some IAV strains. Possibly, a sustained high degree of inflammation is deleterious for the host.

Collectively, we propose a model (Figure 8) in which plasminogen-mediated fibrinolysis increases FDP production and vascular permeability allowing increase recruitment of inflammatory cells at the site of infection. As a positive feedback loop, plasminogen mediated virus replication may also further contribute to lung inflammation. Fibrinolysis may also allow systemic haematogenous spread of virus. Consistently, we and others detected IAV replication in extrapulmonary organs in plasminogen-competent mice [30]. Since plasminogen is omnipresent in the blood, it may provide certain IAV an alternative mechanism of HA cleavage in extra-pulmonary organs [10,11]. For example, the plasminogen-binding property of the neuraminidase of A/WSN/33 strain is a determinant of its neurotropism and pathogenicity in mice [12,13]. Interestingly, particular high virus titers were found in the liver, which is the primary source of plasminogen. This may explain why IAV can replicate in hepatocarcinoma liver HEPG-2 cells in the absence of exogenous proteases (Figure S4). Whether plasminogen-dependent IAV replication contributes to damage of the liver or other extra-pulmonary organs, as observed in Reye's syndrome or other postinfluenza complications [31] requires further investigation. Interestingly, differences in virus replication were not at the basis of plasminogen-dependent differences in pathogenesis of IAV infection although it also can contribute to

exacerbation of inflammation. Indeed, A/Netherlands/602/09 virus replication in the lungs was not affected by plasminogen deficiency, while infected PLG-KO mice were protected from infection. This is consistent with a recent report showing that presence of critical residues in HA, necessary for cleavage by plasmin is strain-dependent [32]. In addition, the HA of A/chicken/Ivory-Coast/1787/2006 contains a polybasic site, which is cleaved by furin-type proteases. This suggests that plasminogen plays a minor role in replication of this virus, while plasminogen deficiency still protected from infection with this virus. Alternative proteases may thus play a more dominant role in HA cleavage and virus replication *in vivo* than plasminogen [33–36].

For the clinical management of influenza patients, a limited number of antiviral drugs are available. The use of these currently available drugs is compromised by the emergence of virus strains that developed resistance to these drugs. Therefore, intervention strategies that aim at preventing deleterious inflammatory responses after IAV infection are of interest and do not suffer from resistance to antiviral drugs. Specifically, blocking protease activity may be an efficient way to achieve this, as previously suggested [37–39]. Our results are consistent with these studies but differ in term of mechanism of action. Indeed, our results suggest a more predominant role for proteases in lung hemostasis compared to virus replication and HA cleavage.

In summary, our findings reveal a previously unrecognized role for fibrinolysis and plasminogen in the pathogenesis of IAV infections. Thus, targeting plasminogen, its conversion into plasmin or regulating fibrinolysis may be a venue for the development of novel intervention strategies for the treatment of severe IAV infections.

## Materials and Methods

### Ethics statement

Experiments were performed according to recommendations of the “National Commission of Animal Experiment (CNEA)” and the “National Committee on the Ethic Reflexion of Animal Experiments (CNREEA)”. The protocol was approved by the committee of animal experiments of the University Claude Bernard Lyon I (Permit number: BH2008-13). All animal experiments were also carried out under the authority of license issued by “la direction des services Vétérinaires” (accreditation number 78–114). All efforts were made to minimize suffering.

### Reagent

Viruses, cells, and reagents used, were: IAV A/Netherlands/602/09 [40], A/chicken/Ivory-Coast/1787/2006 [41], A/PR/8/34 (American Type Culture Collection, ATCC), A549 cells (ATCC), Madin-Darby Canine Kidney cells (MDCK, ATCC), trypsin (Becton Dickinson), plasminogen and 6-AHA (Sigma), Ancrod (NIBSC), 23-Plex Mouse Cytokine Assay (Bio-Rad), ELISA kits for mouse -IL-6, -KC, -RANTES, -IFN- $\alpha$  -IFN- $\gamma$  (R&D Systems), -plasminogen (Mybiosource), -active plasmin (Kordia), -D-dimer, -fibrinogen and -FDP (Genway), antibodies anti-HA (Santa Cruz), anti-tubulin (Sigma), anti-NP (ATCC), anti-fibrinogen (Genway).

### In vitro experiments and proteins detection

Blood fibrinogen and lung proteins were extracted as described [42,43] and proteins were analyzed by western blot [44]. A549 experiments were performed as described previously [11].

### Mice

Mice with a disrupted PLG gene (PLG-KO) and their WT littermates were bred as described previously [45]. Briefly, PLG heterozygous mice (C57BL/6 and 25% 129Sv) were crossed and WT and PLG-KO mice offspring were genotyped by polymerase chain reaction, which was performed, as previously described [46] using primers amplifying the WT PLG gene (5'ACTGCTGCC-CACTGTTTGGAG 3' and 5' GATAACCTTGTAGAATT-CAGGTC3') or the inactivated PLG gene (5'ATGAACTGCAG-GACGAGGCAG3' and 5' GCGAACAGTTCGGCTGGCGC 3'). Most of the experiments were performed using 5–6 weeks old mice. Also, males and females were used in the experiments. Groups between WT and PLG KO mice were homogenized for these different parameters. Except when PLG-WT and PLG-KO mice were used, experiments were performed with six-week-old C57BL/6 female mice (Charles River Laboratories).

### Mice infection and treatment

Mice were anesthetized with ketamine (42,5 mg/kg) and inoculated by the intranasal route with the indicated IAV in a volume of 25  $\mu$ l. Upon inoculation, survival rates and loss of body weight was scored daily, as previously described [47]. For weight loss curves, the last measured value was carried forward until the end of the observation period. Alternatively, mice were sacrificed at various pre-fixed time points post-inoculation to perform bronchoalveolar lavages

## References

- Knipe DM, Howley PM, editors (2006) *Fields Virology*. 5<sup>th</sup> edition. Philadelphia (Pennsylvania): Lippincott, Williams, & Wilkins.
- Kuiken T, Riteau B, Fouchier RA, Rimmelzwaan GF (2012) Pathogenesis of influenza virus infections: the good, the bad and the ugly. *Curr Opin Virol* 2: 276–286.
- La Gruta NL, Kedzierska K, Stambas J, Doherty PC (2007) A question of self-preservation: immunopathology in influenza virus infection. *Immunol Cell Biol* 85: 85–92.
- de Jong MD, Simmons CP, Thanh TT, Hien VM, Smith GJ, et al. (2006) Fatal outcome of human influenza A (H5N1) is associated with high viral load and hypercytokinemia. *Nat Med* 12: 1203–1207.
- Reed CE, Kita H (2004) The role of protease activation of inflammation in allergic respiratory diseases. *J Allergy Clin Immunol* 114: 997–1008; quiz 1009.
- Sokolova E, Reiser G (2007) A novel therapeutic target in various lung diseases: airway proteases and protease-activated receptors. *Pharmacol Ther* 115: 70–83.

(BAL) or to sample organs. Virus titers in organs were determined by classical plaque assay using MDCK cells [47]. ELISA and luminex assays were performed according to the instructions of the manufacturer and virus titers were assessed as described [48]. Lungs histology and immunohistochemistry were performed as described [49]. Treatment with 6-AHA was injected intraperitoneally (30 mg per mouse in 200  $\mu$ l of physiological serum) every 6 hours for 4 days. Ancrod was injected (1.75 unit per mouse) intraperitoneally two days before infection for 7 days at 10 hours intervals.

### Statistical analysis

Kaplan-Meier test was used for statistical analysis of survival rates and Mann-Whitney's test was used for lung virus titers and ELISA results,  $p$  values < 0.05, were considered statistically significant. Two-tails analysis was performed. The number (n) of animals per experimental group is mentioned in the figure legends. Experiments were stratified in terms of weight, gender and age of the mice.

## Supporting Information

**Figure S1 Effect of Ancrod treatment on uninfected PLG-KO mice.** Survival and weight loss of uninfected PLG-KO mice treated with Ancrod (open triangle, n = 3). (TIF)

**Figure S2 Effect of 6-AHA on cytokine levels in the BAL.** Cytokine levels in the BAL of IAV-infected C57BL/6 mice, treated or not (upper panel) with 6-AHA (lower panel) was evaluated by multiplex assay four days post-inoculation. Only detectable levels are shown. n = 3 mice per group. Please note the difference in scale of y-axis between treated and untreated animals. (TIF)

**Figure S3 Effect of Ancrod treatment and/or 6-AHA treatment on uninfected mice.** Survival and weight loss of uninfected C57BL/6 mice treated with Ancrod and 6-AHA (open circles, n = 5) or 6-AHA only (closed circles, n = 5). (TIF)

**Figure S4 IAV replication kinetics in HEPG-2 cells.** Replication kinetics of IAV A/PR/8/34 and A/Udorn/72 in absence of proteases was assessed after inoculating HEPG-2 cells at a MOI of 0.001. (TIF)

## Acknowledgments

We thank Renata de Almeida for assistance and discussions, Emmanuel Couacy-Hymann for providing the Avian H5N1 influenza strain and Martine Jandrot-Perrus for discussions.

## Author Contributions

Conceived and designed the experiments: FB BR. Performed the experiments: FB EA MLFG VBL SEVV PG. Analyzed the data: FB GFR MH EC BL RL PC BR. Contributed reagents/materials/analysis tools: GFR MH DM PC. Wrote the paper: BR.

7. Steinhoff M, Buddenkotte J, Shpacovitch V, Rattenholl A, Moormann C, et al. (2005) Proteinase-activated receptors: transducers of proteinase-mediated signaling in inflammation and immune response. *Endocr Rev* 26: 1–43.
8. Bradley LM, Douglass MF, Chatterjee D, Akira S, Baaten BJ (2012) Matrix metalloproteinase 9 mediates neutrophil migration into the airways in response to influenza virus-induced toll-like receptor signaling. *PLoS Pathog* 8: e1002641.
9. Khoufache K, Berri F, Nacken W, Vogel AB, Delenne M, et al. (2013) PAR1 contributes to influenza A virus pathogenicity in mice. *J Clin Invest* 123: 206–214.
10. LeBouder F, Morello E, Rimmelzwaan GF, Bosse F, Pechoux C, et al. (2008) Annexin II incorporated into influenza virus particles supports virus replication by converting plasminogen into plasmin. *J Virol* 82: 6820–6828.
11. LeBouder F, Lina B, Rimmelzwaan GF, Riteau B (2010) Plasminogen promotes influenza A virus replication through an annexin 2-dependent pathway in the absence of neuraminidase. *J Gen Virol* 91: 2753–2761.
12. Goto H, Kawaoka Y (1998) A novel mechanism for the acquisition of virulence by a human influenza A virus. *Proc Natl Acad Sci U S A* 95: 10224–10228.
13. Goto H, Wells K, Takada A, Kawaoka Y (2001) Plasminogen-binding activity of neuraminidase determines the pathogenicity of influenza A virus. *J Virol* 75: 9297–9301.
14. van Hinsbergh VW (2012) Endothelium—role in regulation of coagulation and inflammation. *Semin Immunopathol* 34: 93–106.
15. Keller TT, van der Sluijs KF, de Kruijff MD, Gerdes VE, Meijers JC, et al. (2006) Effects on coagulation and fibrinolysis induced by influenza in mice with a reduced capacity to generate activated protein C and a deficiency in plasminogen activator inhibitor type 1. *Circ Res* 99: 1261–1269.
16. Manz B, Brunotte L, Reuther P, Schwemmle M (2012) Adaptive mutations in NEP compensate for defective H5N1 RNA replication in cultured human cells. *Nat Commun* 3: 802.
17. Prentice C (1980) Basis of antifibrinolytic therapy. *J Clin Pathol* 33: 35–40.
18. Gong Y, Hart E, Shchurin A, Hoover-Plow J (2008) Inflammatory macrophage migration requires MMP-9 activation by plasminogen in mice. *J Clin Invest* 118: 3012–3024.
19. Wygrecka M, Marsh LM, Morty RE, Henneke I, Guenther A, et al. (2009) Enolase-1 promotes plasminogen-mediated recruitment of monocytes to the acutely inflamed lung. *Blood* 113: 5588–5598.
20. Syrovets T, Tippler B, Rieks M, Simmet T (1997) Plasmin is a potent and specific chemoattractant for human peripheral monocytes acting via a cyclic guanosine monophosphate-dependent pathway. *Blood* 89: 4574–4583.
21. O'Connell PA, Surette AP, Liwski RS, Svenningsson P, Waisman DM (2010) S100A10 regulates plasminogen-dependent macrophage invasion. *Blood* 116: 1136–1146.
22. Ploplis VA, French EL, Carmeliet P, Collen D, Plow EF (1998) Plasminogen deficiency differentially affects recruitment of inflammatory cell populations in mice. *Blood* 91: 2005–2009.
23. Moons L, Shi C, Ploplis V, Plow E, Haber E, et al. (1998) Reduced transplant arteriosclerosis in plasminogen-deficient mice. *J Clin Invest* 102: 1788–1797.
24. Soepandi PZ, Burhan E, Mangunegoro H, Nawas A, Aditama TY, et al. (2010) Clinical course of avian influenza A(H5N1) in patients at the Persahabatan Hospital, Jakarta, Indonesia, 2005–2008. *Chest* 138: 665–673.
25. Wang ZF, Su F, Lin XJ, Dai B, Kong LF, et al. (2011) Serum D-dimer changes and prognostic implication in 2009 novel influenza A(H1N1). *Thromb Res* 127: 198–201.
26. Urso R, Bevilacqua N, Gentile M, Biagioli D, Lauria FN (2011) Pandemic 2009 H1N1 virus infection associated with purpuric skin lesions: a case report. *J Med Case Reports* 5: 132.
27. Okayama S, Arakawa S, Ogawa K, Makino T (2011) A case of hemorrhagic colitis after influenza A infection. *J Microbiol Immunol Infect* 44(6): 480–483.
28. Degen JL, Bugge TH, Goguen JD (2007) Fibrin and fibrinolysis in infection and host defense. *J Thromb Haemost* 5 Suppl 1: 24–31.
29. Teijaro JR, Walsh KB, Cahalan S, Fremgen DM, Roberts E, et al. (2011) Endothelial Cells Are Central Orchestrators of Cytokine Amplification during Influenza Virus Infection. *Cell* 146: 980–991.
30. Fislva T, Gocnik M, Sladkova T, Durmanova V, Rajcani J, et al. (2009) Multiorgan distribution of human influenza A virus strains observed in a mouse model. *Arch Virol* 154: 409–419.
31. Sanchez-Lamier M, Davis LE, Blisard KS, Woodfin BM, Wallace JM, et al. (1991) Influenza A virus in the mouse: hepatic and cerebral lesions in a Reye's syndrome-like illness. *Int J Exp Pathol* 72: 489–500.
32. Sun X, Tse LV, Ferguson AD, Whittaker GR (2010) Modifications to the hemagglutinin cleavage site control the virulence of a neurotropic H1N1 influenza virus. *J Virol* 84: 8683–8690.
33. Zhirnov OP, Ikizler MR, Wright PF (2002) Cleavage of influenza A virus hemagglutinin in human respiratory epithelium is cell associated and sensitive to exogenous antiproteases. *J Virol* 76: 8682–8689.
34. Bertram S, Glowacka I, Blazejewska P, Soilleux E, Allen P, et al. (2010) TMPRSS2 and TMPRSS4 facilitate trypsin-independent influenza virus spread in Caco-2 cells. *J Virol* 84: 10016–10025.
35. Botcher E, Matrosovich T, Beyerle M, Klenk HD, Garten W, et al. (2006) Proteolytic activation of influenza viruses by serine proteases TMPRSS2 and HAT from human airway epithelium. *J Virol* 80: 9896–9898.
36. Chaipan C, Kobasa D, Bertram S, Glowacka I, Steffen I, et al. (2009) Proteolytic activation of the 1918 influenza virus hemagglutinin. *J Virol* 83: 3200–3211.
37. Zhirnov OP, Klenk HD, Wright PF (2011) Aprotinin and similar protease inhibitors as drugs against influenza. *Antiviral Res* 92: 27–36.
38. Botcher-Friebertshauer E, Freuer C, Sielaff F, Schmidt S, Eickmann M, et al. (2010) Cleavage of influenza virus hemagglutinin by airway proteases TMPRSS2 and HAT differs in subcellular localization and susceptibility to protease inhibitors. *J Virol* 84: 5605–5614.
39. Zhirnov OP, Ovcharenko AV, Bukrinskaya AG (1982) Protective effect of protease inhibitors in influenza virus infected animals. *Arch Virol* 73: 263–272.
40. Munster VJ, de Wit E, van den Brand JM, Herfst S, Schrauwen EJ, et al. (2009) Pathogenesis and transmission of swine-origin 2009 A(H1N1) influenza virus in ferrets. *Science* 325: 481–483.
41. Couacy-Hymann E, Danho T, Keita D, Bodjo SC, Kouakou C, et al. (2009) The first specific detection of a highly pathogenic avian influenza virus (H5N1) in Ivory Coast. *Zoonoses Public Health* 56: 10–15.
42. Hanss MM, Ffrench PO, Mornex JF, Chabuet M, Biot F, et al. (2003) Two novel fibrinogen variants found in patients with pulmonary embolism and their families. *J Thromb Haemost* 1: 1251–1257.
43. Luyendyk JP, Sullivan BP, Guo GL, Wang R (2010) Tissue factor-deficiency and protease activated receptor-1-deficiency reduce inflammation elicited by diet-induced steatohepatitis in mice. *Am J Pathol* 176: 177–186.
44. Bernard D, Riteau B, Hansen JD, Phillips RB, Michel F, et al. (2006) Costimulatory receptors in a teleost fish: typical CD28, elusive CTLA4. *J Immunol* 176: 4191–4200.
45. Ploplis VA, Carmeliet P, Vazirzadeh S, Van Vlaenderen I, Moons L, et al. (1995) Effects of disruption of the plasminogen gene on thrombosis, growth, and health in mice. *Circulation* 92: 2585–2593.
46. Riteau B, Moreau P, Menier C, Khalil-Daher I, Khosrotehrani K, et al. (2001) Characterization of HLA-G1, -G2, -G3, and -G4 isoforms transfected in a human melanoma cell line. *Transplant Proc* 33: 2360–2364.
47. Khoufache K, LeBouder F, Morello E, Laurent F, Riffault S, et al. (2009) Protective role for protease-activated receptor-2 against influenza virus pathogenesis via an IFN-gamma-dependent pathway. *J Immunol* 182: 7795–7802.
48. LeBouder F, Khoufache K, Menier C, Mandouri Y, Keffous M, et al. (2009) Immunosuppressive HLA-G molecule is upregulated in alveolar epithelial cells after influenza A virus infection. *Hum Immunol* 70: 1016–1019.
49. Riteau B, Faure F, Menier C, Viel S, Carosella ED, et al. (2003) Exosomes bearing HLA-G are released by melanoma cells. *Hum Immunol* 64: 1064–1072.

**Manuscrit n°3: Annexin V Incorporated into Influenza Virus Particles  
Inhibits Gamma Interferon Signaling and Promotes Viral replication.**

Fatma Berri, Ghina Haffar, Vuong Ba Lê, Anne Sadewasser, Katharina Paki, Bruno Lina, Thorsten Wolff, Béatrice Riteau.

**J. Virol. 2014, 88(19):11215.**

**Résumé**

La réplication virale constitue un facteur de virulence pour les virus influenza de type A (VIAs). Lors du bourgeonnement, les VIAs incorporent dans leur enveloppe, en plus des protéines virales, plusieurs protéines de la cellule hôte (LeBouder et al 2008, Shaw et al 2008). Cependant, le rôle de ces protéines d'origine cellulaire n'a pas reçu beaucoup d'attention.

Dans cette étude nous nous sommes intéressés au rôle de la protéine cellulaire, annexine 5 (A5), dans la réplication virale, *in vitro*. Nos résultats montrent que l'infection des cellules par les VIAs induit l'expression de l'A5 à la surface des cellules infectées et qu'une quantité de protéine A5 est également retrouvée dans les radeaux lipidiques, site de bourgeonnement des VIAs. Par ailleurs, des analyses par immunoempreinte et de marquages par billes d'or de l'A5 sur virus hautement purifiés ont également montré la présence de l'A5 dans les particules virales. Ainsi, les virions incorporent de l'A5, lors du bourgeonnement cellulaire. D'une manière significative, l'incubation des cellules THP-1 différenciées en macrophages, avec des virus purifiés, inhibe la production de l'IP-10 (*INF-γ inducible protein 10*) et la phosphorylation de STAT1, induits par l'IFN-γ. Cependant, le blocage de l'A5 par un anticorps spécifique à la surface des virions ou l'utilisation de virions produits sur cellules

exprimant peu d'A5, par la technique d'extinction des gènes, restaure l'inhibition de STAT1 et la production d'IP-10 en présence d'IFN- $\gamma$ . Cela induit également une inhibition de la réplication virale *in vitro*. Ces résultats montrent que l'A5 incorporée dans les particules du VIA inhibe l'effet antiviral médié par l'IFN- $\gamma$ . Le rôle de l'A5 dans l'échappement du virus à la signalisation par l'IFN- $\gamma$  a également été confirmé *in vivo*, chez la souris. Ainsi, nos résultats suggèrent que l'incorporation de l'A5 dans les virions est une voie d'échappement du virus au système immunitaire.

# Annexin V Incorporated into Influenza Virus Particles Inhibits Gamma Interferon Signaling and Promotes Viral Replication

Fatma Berri,<sup>a</sup> Ghina Haffar,<sup>a</sup> Vuong Ba Lê,<sup>a</sup> Anne Sadewasser,<sup>b</sup> Katharina Paki,<sup>b</sup> Bruno Lina,<sup>a</sup> Thorsten Wolff,<sup>b</sup> Béatrice Riteau<sup>a,c</sup>

VirPath, EMR4610 Virologie et Pathologie Humaine, Faculté de Médecine RTH Laennec, Université Claude Bernard Lyon 1, Université de Lyon, Lyon, France<sup>a</sup>; Division of Influenza Viruses and Other Respiratory Viruses, Robert Koch Institute, Berlin, Germany<sup>b</sup>; INRA, Tours, France<sup>c</sup>

## ABSTRACT

During the budding process, influenza A viruses (IAVs) incorporate multiple host cell membrane proteins. However, for most of them, their significance in viral morphogenesis and infectivity remains unknown. We demonstrate here that the expression of annexin V (A5) is upregulated at the cell surface upon IAV infection and that a substantial proportion of the protein is present in lipid rafts, the site of virus budding. Western blotting and immunogold analysis of highly purified IAV particles showed the presence of A5 in the virion. Significantly, gamma interferon (IFN- $\gamma$ )-induced Stat phosphorylation and IFN- $\gamma$ -induced 10-kDa protein (IP-10) production in macrophage-derived THP-1 cells was inhibited by purified IAV particles. Disruption of the IFN- $\gamma$  signaling pathway was A5 dependent since downregulation of its expression or its blockage reversed the inhibition and resulted in decreased viral replication *in vitro*. The functional significance of these results was also observed *in vivo*. Thus, IAVs can subvert the IFN- $\gamma$  antiviral immune response by incorporating A5 into their envelope during the budding process.

## IMPORTANCE

Many enveloped viruses, including influenza A viruses, bud from the plasma membrane of their host cells and incorporate cellular surface proteins into viral particles. However, for the vast majority of these proteins, only the observation of their incorporation has been reported. We demonstrate here that the host protein annexin V is specifically incorporated into influenza virus particles during the budding process. Importantly, we showed that packaged annexin V counteracted the antiviral activity of gamma interferon *in vitro* and *in vivo*. Thus, these results showed that annexin V incorporated in the viral envelope of influenza viruses allow viral escape from immune surveillance. Understanding the role of host incorporated protein into virions may reveal how enveloped RNA viruses hijack the host cell machinery for their own purposes.

Influenza is an ineradicable contagious disease that constitutes a major public health problem, occurring as a seasonal epidemic of variable impact or sporadic pandemic outbreaks (1, 2). The etiological agents of the disease, the single-stranded RNA influenza viruses, are classified into three types (A, B, and C), of which influenza A virus (IAV) is clinically the most important. Annually, IAV causes 3 to 5 million clinical infections and 200,000 to 500,000 fatal cases (3). Thus, these viruses are of great concern to human health and impose a considerable socioeconomic burden. Important factors in the pathogenesis of influenza include the efficient replication of the virus in the respiratory tract and the host immune response, traits that are dependent on each other (4–6). While the immune response aims to control the spread of the virus, IAV has developed strategies for subverting host defenses, thereby facilitating their spread (7–10). Further knowledge into how IAV escapes the host immunosurveillance is critical for the design of new treatments that are able to control the disease.

Similarly to other enveloped viruses, IAV exits the host cell by budding from a cellular membrane (11, 12). Thereby, particles released from infected cells can incorporate many host cellular proteins during the assembly and budding steps of morphogenesis. Earlier study identified 36 host-encoded proteins in purified IAV particles in addition to viral virion components (13). Among them, the annexin family of proteins that bind to negatively charged phospholipids is well represented (13, 14). However, the functional significance of host protein incorporation has not been determined yet, except for the role of annexin II, which promotes viral replication when incorporated into a virus particle (14, 15).

One protein of interest is annexin V (A5), which has recently been found to play a role in the regulation of the immune response (16, 17). We address here the specific incorporation of A5 into IAV particles and its functional relevance in viral replication.

We found that the host protein A5 was incorporated into IAV particles and inhibited gamma interferon (IFN- $\gamma$ )-induced signaling and antiviral activity both *in vitro* and *in vivo*. Collectively, these results show that incorporation of A5 into IAV virions supports influenza virus escape from immunosurveillance.

## MATERIALS AND METHODS

**Viruses and reagents.** IAV A/PR/8/34 (H1N1) was a gift from G. F. Rimmelzwaan (Erasmus University, Rotterdam, Netherlands), and A/WSN/33 (H1N1) and A/Udorn/72 (H3N2) IAV were a gift from N. Naffakh (Pasteur Institute, Paris, France). The following reagents were used in the study: small interfering RNA (siRNA) targeting A5 (Santa Cruz Biotechnology), recombinant mouse IFN- $\gamma$  (Sigma-Aldrich), recombinant human IFN- $\gamma$  and IFN- $\alpha$  (R&D Systems), trypsin (Becton Dickinson), an enzyme-linked immunosorbent assay (ELISA) kit for

Received 14 May 2014 Accepted 14 July 2014

Published ahead of print 16 July 2014

Editor: B. Williams

Address correspondence to Béatrice Riteau, beatrice.riteau@laposte.net.

F.B. and G.H. contributed equally to this article.

Copyright © 2014, American Society for Microbiology. All Rights Reserved.

doi:10.1128/JVI.01405-14

IFN- $\gamma$ -induced 10-kDa protein (IP-10) and interleukin-1 $\beta$  (IL-1 $\beta$ ; R&D Systems), cholera toxin B subunit (Sigma-Aldrich, France), monoclonal anti-tubulin (Sigma), polyclonal anti-A5 (Santa Cruz Biotechnology), monoclonal anti-M2 (Santa Cruz Biotechnology), monoclonal anti-hemagglutinin (anti-HA; Santa Cruz Biotechnology), polyclonal anti-ERK (Cell Signaling Technology, Saint Quentin, France), monoclonal anti-Stat1 (Santa Cruz Biotechnology), and polyclonal anti-p-Stat1 (R&D Systems) antibodies. Rabbit polyclonal anti-A/PR/8/34 virus cross-reacting with A/WSN/33 virus proteins (referred to as polyclonal anti-influenza) was a gift from G. F. Rimmelzwaan (Erasmus University). Phorbol myristate acetate (PMA; Sigma) was used for human monocytic cell line (THP-1) differentiation.

**Cell culture and raft isolation.** The human monocytic THP-1, human alveolar A549, human epithelial kidney 293T, HeLa, and Madin-Darby canine kidney (MDCK) cell lines used in the present study were obtained from the American Type Culture Collection. MDCK cells were cultured in Eagle minimal essential medium (EMEM; Lonza, France) supplemented with 5% fetal bovine serum (FBS; Lonza), 2 mM L-glutamine, and 100 international units (IU)/ml penicillin-streptomycin (PS). A549 and 293T cells were grown in Dulbecco modified Eagle medium (DMEM; Lonza) supplemented with 10% FBS, 2 mM L-glutamine, and 100 IU/ml PS. THP-1 cells were cultured in RPMI (Lonza) supplemented with 10% FBS, 2 mM L-glutamine, 100 IU/ml PS, 5 ml of pyruvate sodium, 5 ml of amino acids, and  $\beta$ -mercaptoethanol. Raft isolations were performed as previously described (18).

**Virus production, titration, and purification.** MDCK cells were seeded at  $13 \times 10^6$  cells per 175-cm<sup>2</sup> tissue culture flask and then incubated at 37°C overnight. The next day, based on previous evaluations, cell confluence was evaluated at  $20 \times 10^6$  cells per 175 cm<sup>2</sup>, and the cells were infected with IAV at a multiplicity of infection (MOI) of  $10^{-3}$  in EMEM containing 1  $\mu$ g of trypsin/ml. At 2 days postinfection, the supernatant was harvested and then clarified using low-speed centrifugation, and the virus particles were titrated as previously described (19). Briefly, MDCK cells were infected with IAV for 1 h at 37°C. After viral adsorption, the cells were overlaid with medium containing 2% agarose and 1  $\mu$ g of trypsin/ml, followed by incubation for 3 days at 37°C. Viral plaques were then visualized using bromophenol blue staining. To purify the virus particles, the supernatants were clarified and concentrated 100-fold by ultracentrifugation at  $60,000 \times g$  for 105 min at 4°C. Concentrated viruses were then purified by centrifugation for 2 h at  $80,000 \times g$  at 4°C in a 20 to 60% sucrose density gradient. The virus particles were then separated into two different tubes for pretreatment with 20  $\mu$ g of either blocking anti-A5 antibody (referred to as "AV-V") or isotype control antibody (referred to as "V")/ml for 1 h at 4°C. Viruses were then washed by ultracentrifugation at  $31,000 \times g$  for 2 h and suspended in medium. Infectious virus titers were then evaluated in both virus preparations and used for experiments. AV-V or V particles were then used in the experiments.

**Identification and quantification of cell surface proteins by SILAC (stable isotope labeling by amino acids in cell culture)-based mass spectrometric (MS) analysis.** A549 cells were grown in stable isotope-labeled DMEM (SILAC-DMEM, PAA) supplemented with 10% dialyzed FBS (Invitrogen), 2 mM L-glutamine, and antibiotics at 37°C with 5% CO<sub>2</sub>. Cells were either cultivated in SILAC medium containing light (R0K0: R = <sup>12</sup>C<sub>6</sub>, <sup>14</sup>N<sub>4</sub>; K = <sup>12</sup>C<sub>6</sub>, <sup>14</sup>N<sub>2</sub>) or heavy (R10K8: R = <sup>13</sup>C<sub>6</sub>, <sup>15</sup>N<sub>4</sub>; K = <sup>13</sup>C<sub>6</sub>, <sup>15</sup>N<sub>2</sub>) arginine and lysine for at least six cell doublings prior to infection. A total of  $4 \times 10^7$  heavy-labeled cells (R10K8) were infected with IAV A/PR/8/34 (H1N1) at an MOI of 5, while the same number of light-labeled cells (R0K0) served as a mock control. At 16 h postinfection (hpi) cells were washed with phosphate-buffered saline (PBS) and incubated with 1 mg/ml Sulfo-NHS-SS-Biotin (Thermo Fisher Scientific)/PBS for 40 min at 4°C, followed by quenching with 10 mM glycine-PBS buffer. After biotinylation of cell surface proteins, the cell extract of each population (heavy or light) was prepared in 1 ml of lysis buffer (50 mM Tris-HCl [pH 8], 150 mM NaCl, 1% Nonidet P-40, 2 mM Na<sub>3</sub>VO<sub>4</sub>, 1 mM Pefabloc) and cleared by centrifugation. The protein concentration of each lysate was

determined by a BCA protein assay (Thermo Fisher Scientific), and the lysates were mixed at a 1:1 heavy/light ratio, followed by selection of biotinylated proteins on a streptavidin-agarose resin (Thermo Fisher Scientific) at 4°C for 16 h. The beads were washed once with 50 mM Tris-HCl (pH 7.4)–150 mM NaCl–5 mM EDTA, twice with 50 mM Tris-HCl (pH 7.4)–500 mM NaCl–5 mM EDTA, three times with 20 mM Tris-HCl (pH 7.4)–500 mM NaCl, and once with 10 mM Tris-HCl (pH 7.4). The precipitated proteins were eluted in 4 $\times$  sodium dodecyl sulfate (SDS) sample buffer–20%  $\beta$ -mercaptoethanol for 30 min at 37°C. Affinity-purified proteins were reduced and alkylated by the addition of 10 mM dithiothreitol (2 min, 95°C) and 50 mM iodacetamid (30 min, 22°C, in the dark), respectively. Proteins were separated by SDS–12.5% PAGE, and the gel lane was cut into six slices, which were then subjected to in-gel tryptic digest using a trypsin profile IGD kit (Sigma). The resulting peptides were separated using a C<sub>18</sub> capillary analytical column (10 cm [inner diameter, 75  $\mu$ m]; Thermo Fisher Scientific) with a linear gradient over 95 min (solvent A = 1% FA, 99% H<sub>2</sub>O and solvent B = 80% ACN, 1% FA) at a constant flow rate of 300 nl/min using an Easy Nano liquid chromatography II system coupled to an LTQ Orbitrap discovery XL (Thermo Fisher Scientific). Eluting peptides were ionized by electrospray ionization at 1.4 kV and a capillary temperature of 200°C. Mass spectra ( $m/z$  range, 300 to 2000) were measured with a resolution of  $M/\Delta M = 30,000$  at  $m/z$  400. The top five precursor peptide ions were fragmented by collision-induced dissociation (normalized collision energy, 35%; activation Q, 0.250, activation time, 30 ms) with a dynamic exclusion time of 30 s. The data were acquired using Xcalibur software. Raw data files were evaluated using Proteome Discoverer (PD) software (version 1.4; Thermo Fisher Scientific). Proteins were identified by searching against the UniProt/Swiss-Prot Human and Influenza A/PR/8/34 database (89,454 entries) using SEQUEST algorithm and the following search parameters: carbamidomethylation of cysteine (+57.021) as a fixed modification, oxidation of histidine, methionine, and tryptophan (+15.995); phosphorylation of serine, threonine, and tyrosine (+79.966) and appropriate SILAC labels as variable modifications; tryptic digestion with a maximum of two missed cleavages; a peptide precursor mass tolerance of 10 ppm; and a fragment mass tolerance of 0.8 Da. The decoy database search option was enabled and all peptides were filtered with a maximum false discovery rate (FDR) of 1%. Protein quantification was performed with at least two unique and labeled peptides per protein and a mass precision of 4 ppm. The relative abundance of a protein at cell surface was derived from its heavy/light (H/L) ratio in the differently labeled cell populations. Quantification values outside the range from 0.01 to 100 were recorded as 0.01 (ratio  $\leq$  0.01) and 100 (ratio  $\geq$  100). Proteins were grouped by PD annotation software tool and selected according to the gene ontology cellular component (GOCC) categories "membrane," "cell surface," or "extracellular" (20). An H/L ratio of  $>2$  for a given protein was considered to signal increased surface abundance.

**Depletion of A5 from virions by siRNA-mediated knockdown.** Specific siRNA targeting A5 was used to knock down protein expression in 293T cells. These cells were chosen because of their high transfection efficiency. Nontargeted siRNA was used as a control. According to the manufacturer's instructions, 293T cells (60 to 80% confluence, i.e.,  $2 \times 10^5$  cells per 10 cm<sup>2</sup>) were transfected with siRNA targeting A5 (1  $\mu$ g/ $2 \times 10^5$  cells) or control-siRNA, diluted in transfection reagent (confidential lipidic composition from Santa Cruz). At 24 h posttransfection, DMEM containing 20% fetal calf serum, PS (200 IU/ml), and L-glutamine (4 mM) was added to the cells, followed by incubation at 37°C for additional 48 h. At this step, Western blot analysis was performed to verify the transfection efficiency (data not shown). Alternatively, cells were infected with IAV (MOI = 1), and supernatants containing the virus particles were harvested at 16 hpi. The virus titers were evaluated by plaque assay and used in experiments. Similar ratios of the different viral proteins in both preparations and reduced expression of packaged A5 in the virions released in the supernatant of A5-specific siRNA-treated cells (referred to as A5 siRNA v) compared to control viruses (referred to as Ctrl siRNA v) were

confirmed by loading 20  $\mu$ l of the corresponding supernatants on a gel, followed by Western blot analysis. Of note, the downregulation of A5 by siRNAs had no effect on the release of infectious particles (data not shown).

**Flow cytometry, immunocytochemistry, and Western blot analysis.** A549 or MDCK cells either were left uninfected or were infected with A/PR8/34, A/Udorn/72, or A/WSN/33 (MOI of 1 or 10) for 24 h, and the expression of A5 was assessed by using flow cytometry analysis or cytochemistry, as previously described (8, 21). For the kinetic experiments, A549 cells were infected with IAV A/WSN/33 (MOI of  $10^{-2}$ ) in the presence of trypsin (0.5  $\mu$ g/ml), and A5 expression was assessed by flow cytometry at 6, 24, and 48 hpi. For experiments assessing virus attachment to the cells, differentiated THP-1 cells were incubated with the indicated IAV (MOI of 1) for 5 min at 37°C or for 30 min at 4°C; the cells were then washed, and virus binding to the cells was analyzed by flow cytometry using anti-HA antibody. For internalization experiments, differentiated-THP1 cells were first incubated with “Ctl siRNA v” or “A5 siRNA v” at 4°C for 30 min. The cells were then shifted to 37°C for 1 h to allow virus internalization. Back at 4°C, the cells were then fixed and permeabilized or not to assess the percentage of internalized versus cell surface bound viruses by flow cytometry using anti-HA antibody. For intracytoplasmic staining, the cells were fixed with 0.5% paraformaldehyde for 10 min and permeabilized 10 min with 0.1% Triton X-100 at 4°C (22). For the Western blot analysis, purified virions or cells were lysed in ice-cold lysis buffer (1% Triton X-100, 100 mM Tris-HCl [pH 7.4], 1.5 M NaCl, and 5 mM EDTA in the presence of a complete proteinase inhibitor mixture), and the proteins were analyzed as previously described (19).

**Stat activation experiments.** THP-1 cells were incubated with PMA for 48 h at 37°C (differentiated THP-1 cells). After differentiation into macrophages, the cells were incubated with or without AV-V or V (strain A/WSN/33) or A5 siRNA v or Ctl siRNA v for 5 min, 1 h, or 16 h and either left unstimulated or stimulated with human IFN- $\alpha$  or IFN- $\gamma$  (1,000 IU) for 5 min at 37°C. Alternatively, HeLa cells were used in the experiments. The cells were then lysed for 45 min on ice, and proteins from the lysate were analyzed by Western blotting. For the dose-response analysis, differentiated THP-1 cells were stimulated for 5 min with the indicated dose of IFN- $\gamma$ , and the cells were lysed before Western blot analysis.

**IP-10 and IL-1 $\beta$  production experiments.** Differentiated THP-1 cells were preincubated with or without AV-V or V (strain A/WSN/33) or A5 siRNA v or Ctl siRNA v at an MOI of 1 for 5 min at 37°C. The cells were then either left unstimulated or stimulated with 1,000 IU of IFN- $\alpha$  or IFN- $\gamma$  for 3 h or 24 h at 37°C. Subsequently, supernatants were harvested, and IP-10 or IL-1 $\beta$  production was quantified by ELISA.

**Immunogold analysis.** Immunogold labeling of A5 was performed on gradient-purified virus particles by the flotation of grids on drops of reactive media. To prevent nonspecific binding, the grids were coated with 1% bovine serum albumin (BSA) in 50 mM Tris-HCl (pH 7.4) for 10 min at room temperature. Thereafter, the grids were incubated for 4 h at 4°C in a wet chamber with a polyclonal antibody raised against A5 (dilution 1/50) in 1% BSA–50 mM Tris-HCl (pH 7.4). The grids were successively washed once in 50 mM Tris-HCl at pH 7.4 and pH 8.2 at room temperature and then incubated in a wet chamber for 45 min at room temperature in 1% BSA–50 mM Tris-HCl (pH 8.2) for 10 min at room temperature. The grids were labeled with a goat anti-rabbit gold-conjugated IgG (10 nM; Tebu Bio) diluted 1:80 in 1% BSA–50 mM Tris-HCl (pH 8.2) and then successively washed once in 50 mM Tris-HCl (pH 8.2) and 50 mM Tris-HCl (pH 7.4) at room temperature and once in filtered distilled water. The grids with the suspension were then labeled with 2% phosphotungstic acid for 2 min and observed on a transmission electron microscope (1400 JEM; JEOL, Tokyo, Japan), equipped with a Gatan camera (Orius 600) and digital micrograph software.

**In vitro replication.** To test the susceptibility of differentiated THP-1 cells to IAV infection, cells were infected with A/WSN/33 virus (MOI of 1), and infectious virus titers were determined at the indicated time point postinfection by plaque assay titration. To determine the role of packaged

A5 in the antiviral activity mediated by IFN- $\gamma$ , differentiated THP-1 cells were incubated with either AV-V or V (strain A/WSN/33) or A5 siRNA v or Ctl siRNA v (MOI of 1) for 5 min at 37°C. The cells were then washed, and 1 ml of RPMI medium without serum, containing or not 1,000 IU of rIFN- $\gamma$ , was added to cells, followed by incubation for 24 h at 37°C. Infectious virus titers were then evaluated by plaque assay in the supernatant of the cells.

**Mice.** C57BL/6 Mice were infected intranasally with IAV (500 PFU) in a volume of 25  $\mu$ l as previously described (23, 24). Once all of the mice were infected, the animals were still anesthetized, and they were then administered intranasally with vehicle or mouse recombinant IFN- $\gamma$  ( $8 \times 10^4$  IU/25  $\mu$ l). Mice were sacrificed at 2 days postinfection to sample the lungs. Virus titers in lung homogenates were then determined by plaque assay as described above. Animal experiments were performed according to recommendations of the National Commission of Animal Experiment (CNEA) and the National Committee on the Ethic Reflection of Animal Experiments (CNREEA). Experiments were approved by the Animal Ethics Committee (permit BH2008-13; Lyon University) and carried out under the license accreditation 78-114.

**Statistical analysis.** The Mann-Whitney test was used for statistical analysis. The results were considered statistically significant at a *P* value of <0.05 (\*). All bars in the figures represent the mean values  $\pm$  the standard deviations (SD) from the indicated number of experiments.

## RESULTS

**An MS-based approach detects increased annexin V levels on the surfaces of IAV-infected cells.** First, changes in cell surface protein composition after IAV virus infection were investigated by using SILAC-based MS analysis. Proteins accessible at the cell surface to amine-reactive thiol-cleavable biotin ester were compared in mock-treated (light amino acids) and influenza A/PR8/34 virus-infected A549 cells (heavy amino acid) at 16 hpi. Cell lysates were prepared, mixed, and subjected to affinity selection using streptavidin-agarose. Subsequently, proteins were eluted from the matrix and identified by MS analysis. Alterations in cell surface protein expression due to IAV infection correspond to changes in heavy/light (H/L) ratio (Table 1). As expected, the viral surface proteins HA, NA, and M2 were detected exclusively in infected cells. Table 1 also depicts cellular surface and membrane proteins with the most prominent increases in response to virus infection, including A5, as well as four other proteins (annexin 2, ezrin, annexin 1, and alpha-enolase) that were previously also detected as the cell surface increased or in purified influenza virions (13–15, 25).

**Annexin V upregulation at the cell surface upon IAV infection is independent on the strain and the cell type.** In our further analysis we focused on the role of A5. As shown in Fig. 1A, fluorescence-activated cell sorting analysis confirmed increased cell surface expression of A5 after the infection of epithelial A549 cells with A/PR8/34 (H1N1), A/Udorn/72 (H3N2), or A/WSN/33 (H1N1) viruses. Upregulation of A5 was independent of the cell type, since similar results were also observed after IAV infection of MDCK cells (Fig. 1B). The viral protein M2 was included as a positive control and was only detected after virus infection. Relative to the M2 protein, cells infected with A/WSN/33 virus showed the strongest A5 upregulation in terms of median fluorescence intensity for both cell types, suggesting that A5 upregulation at the cell surface differs between IAV strains. To confirm these results, A549 cells were infected with IAV, and A5 expression was visualized using immunofluorescence confocal microscopy (Fig. 2A). In the IAV-infected cells, A5 expression was mainly observed at the plasma membrane, while in uninfected cells A5 was mainly pres-

TABLE 1 Upregulated cell surface proteins upon IAV infection compared to noninfected cells identified by LC-MS/MS<sup>a</sup>

Protein (accession no.)	Description	Score	Coverage (%)	H/L ratio	H/L count	H/L variability (%)
P60903	Protein S100-A10 (S100-A10)	31.21	36.08	5.319	6	4.9
Q9BQE5	Apolipoprotein L2 (APOL2)	8.89	13.06	4.747	3	17.5
P07355	Annexin A2 (ANXA2)	534.01	69.62	4.352	84	12.2
P08758	Annexin A5 (ANXA5)	10.30	11.25	4.072	3	24.9
Q9HCC0	Methylcrotonoyl-CoA carboxylase beta chain, mitochondrial (MCCC2)	17.35	18.29	2.940	8	12.6
E7EQR4 <sup>b</sup>	Ezrin (EZR)	5.77	6.14	2.872	3	33.6
O95994	Anterior gradient protein 2 homolog (AGR2)	9.26	24.57	2.743	4	11.1
O00220	Tumor necrosis factor receptor superfamily member 10A (TNFRSF10A)	50.86	19.02	2.716	10	7.3
P30510 <sup>b</sup>	HLA class I histocompatibility antigen, Cw-14 alpha chain (HLA-C)	262.98	39.88	2.595	9	5.0
P04083	Annexin A1 (ANXA1)	65.75	46.82	2.444	17	12.6
O60218	Aldo-keto reductase family 1 member B10 (AKR1B10)	91.28	60.76	2.406	21	9.8
P06733	Alpha-enolase (ENO1)	29.77	21.89	2.310	6	10.0
P06821	Matrix protein 2 {influenza A virus[(A/Puerto Rico/8/34(H1N1))]}	176.41	39.18	100.000	7	0.0
P03452	Hemagglutinin {influenza A virus [A/Puerto Rico/8/34(H1N1)]}	87.22	46.83	100.000	31	0.0
P03468	Neuraminidase {influenza A virus [A/Puerto Rico/8/34(H1N1)]}	38.28	19.38	100.000	13	0.0

<sup>a</sup> A549 cells were infected with A/PR/8/34 virus at an MOI of 5 and, at 16 h postinoculation, upregulated cell surface proteins were identified by liquid chromatography-tandem MS (LC-MS/MS). Heavy/light (H/L) ratios of cellular proteins are organized from the potential strongest change in cell surface abundance to minor changes upon IAV infection. The accession numbers, descriptions, and total scores for the cellular and three viral proteins are shown. The total score is the sum of the scores of the individual peptides that identified the protein. "Coverage" indicates the percentage of the protein sequence covered by the identified peptides. The H/L count indicates the number of peptide ratios that were actually used to calculate a particular protein ratio, whereas H/L variability indicates the variability of these peptide ratios from the particular H/L protein ratio.

<sup>b</sup> Uniprot accession number.

ent in the cytoplasm. As controls, the infected but not uninfected cells displayed detectable HA proteins. Also, nuclei were stained with DAPI, and the merged images are shown (Fig. 2A). We then further investigated whether total A5 expression or simply its lo-

calization was affected by the infection. A549 cells were left uninfected or infected with influenza A/WSN/33 virus, and total A5 expression was assessed by flow cytometry analysis on permeabilized cells (Fig. 2B, left panel). The results indicated that total A5

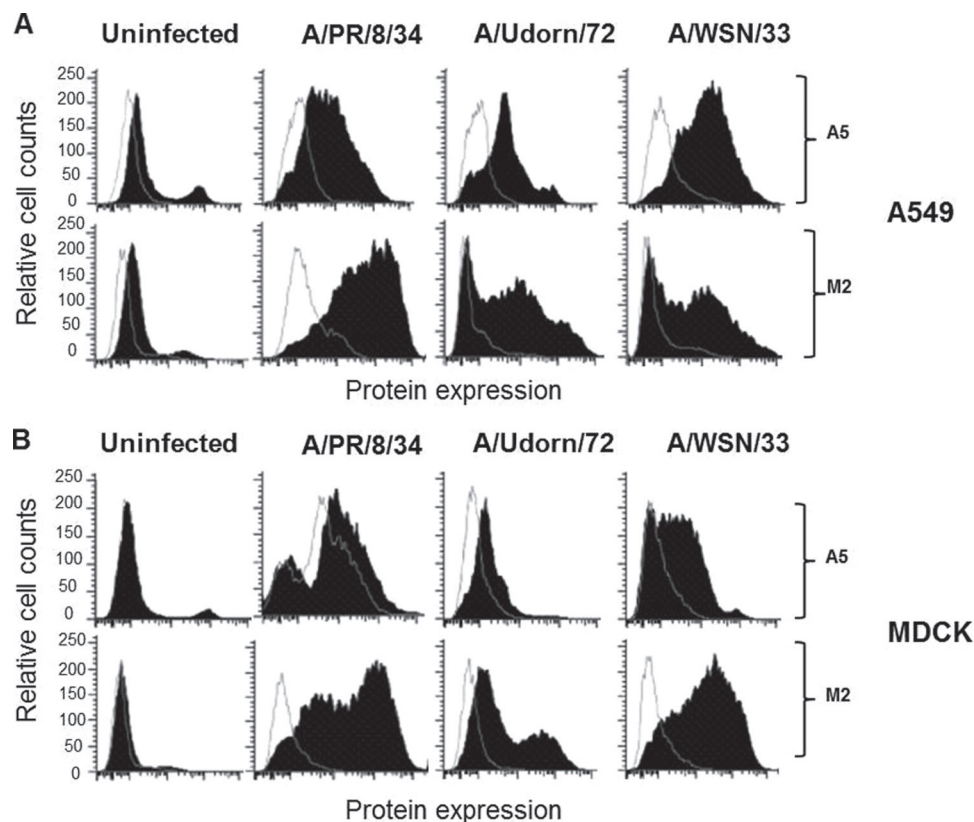
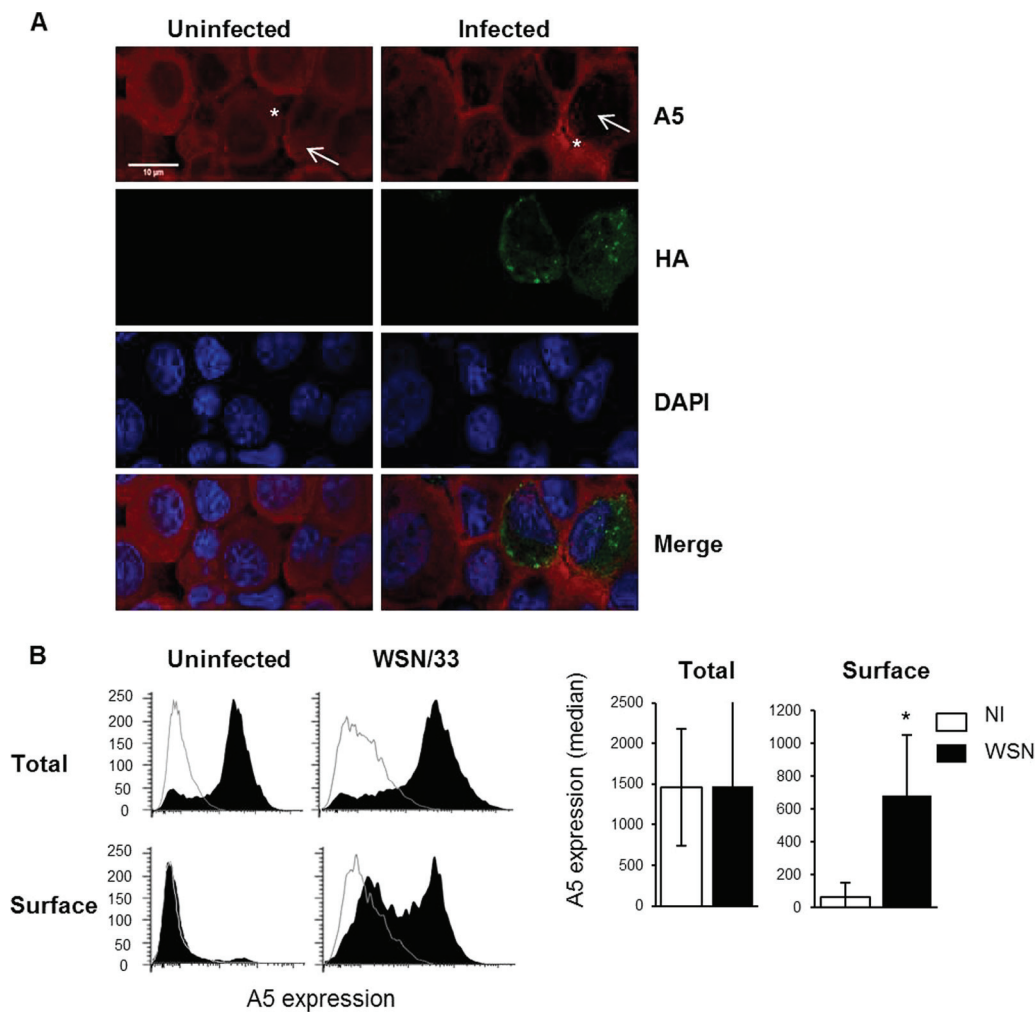


FIG 1 The host cellular protein A5 is upregulated at the cell surface after IAV infection. A549 (A) or MDCK (B) cells were either left uninfected or infected with A/PR/8/34, A/Udorn/72, or A/WSN/33 viruses (MOI of 10). At 24 hpi, flow cytometry analysis was performed with an anti-A5 antibody (closed histograms) or an isotype control (open histograms). The viral protein M2 was used as a positive control for viral infection. The results are representative of two independent experiments.



**FIG 2** The host cellular protein A5 is translocated to the cell surface. (A) A549 cells were either left uninfected or infected with IAV A/WSN/33 virus (MOI of 1). At 24 hpi, cellular A5 or viral HA proteins were visualized by immunofluorescence microscopy, using anti-A5 and anti-HA specific antibodies, respectively. The nuclei were stained with DAPI (4',6'-diamidino-2-phenylindole), and the merged images are shown (original magnification,  $\times 189$ ). The results are representative of two independent experiments. Please note the presence of A5 labeling in the cytoplasm in uninfected cells, which is largely absent in the infected ones (arrows) but rather detected at the plasma membrane (stars). (B) A549 cells were either left uninfected or infected with A/WSN/33 virus (MOI of 10). At 24 hpi, flow cytometry analysis was performed using an anti-A5 antibody (closed histograms) or an isotype control (open histograms). Labeling of A5 was performed either on unpermeabilized cells, showing cell surface A5 proteins, or on permeabilized cells, showing total A5 proteins (left panel). Quantification of the mean fluorescence intensity of A5 expression  $\pm$  the SD from five independent experiments is shown on the right panel. \*,  $P < 0.05$  (NI versus WSN).

protein levels were similar in infected compared to uninfected cells. In marked contrast, cytometry analysis performed on unpermeabilized cells, which only revealed cell surface protein, confirmed a specific increase of A5 at the cell surface upon IAV infection. These results are highlighted in the right panel of Fig. 2B by the quantification of the mean fluorescence intensity (MFI) of A5 labeling. Altogether, these results indicated that IAV infection induced A5 translocation to the cell surface, without affecting total cellular A5 levels.

**Cell surface expression of annexin V is dependent on viral replication.** Although we observed that upon IAV infection all strains increased A5 expression at the cell surface, the levels of A5 translocation differed between IAV strains. Thus, possibly, cell surface A5 translocation was dependent on the rate of IAV replication, which could differ between IAV strains. To test this hypothesis, we investigated whether A5 localization at the cell membrane would increase in a replication-dependent manner. A549

cells were thus infected with IAV A/WSN/33 at a low MOI ( $10^{-2}$ ) in the presence of trypsin. Cell surface expression of A5 was then assessed by flow cytometry experiments at 6, 24, and 48 hpi (Fig. 3A). The results showed that, in marked contrast to noninfected cells (NI), upon infection (INF) A5 was translocated at the cell surface in a time course-dependent manner, showing that translocation of A5 to the cell surface increases with multiple rounds of replication. In these experiments, M2 expression was assessed as a positive control for IAV infection. Thus, translocation of A5 to the cell surface is dependent on viral replication.

**A substantial proportion of annexin V is present in lipid rafts.** Due to the functional importance of lipid rafts in IAV infection and budding, we then investigated the association between A5 and these domains. Clustered rafts were thus floated by sucrose density gradient centrifugation, which by definition isolates detergent-resistant membrane (DRM or lipid raft) domains, and gradient fractions were analyzed by Western blotting (Fig. 3B).

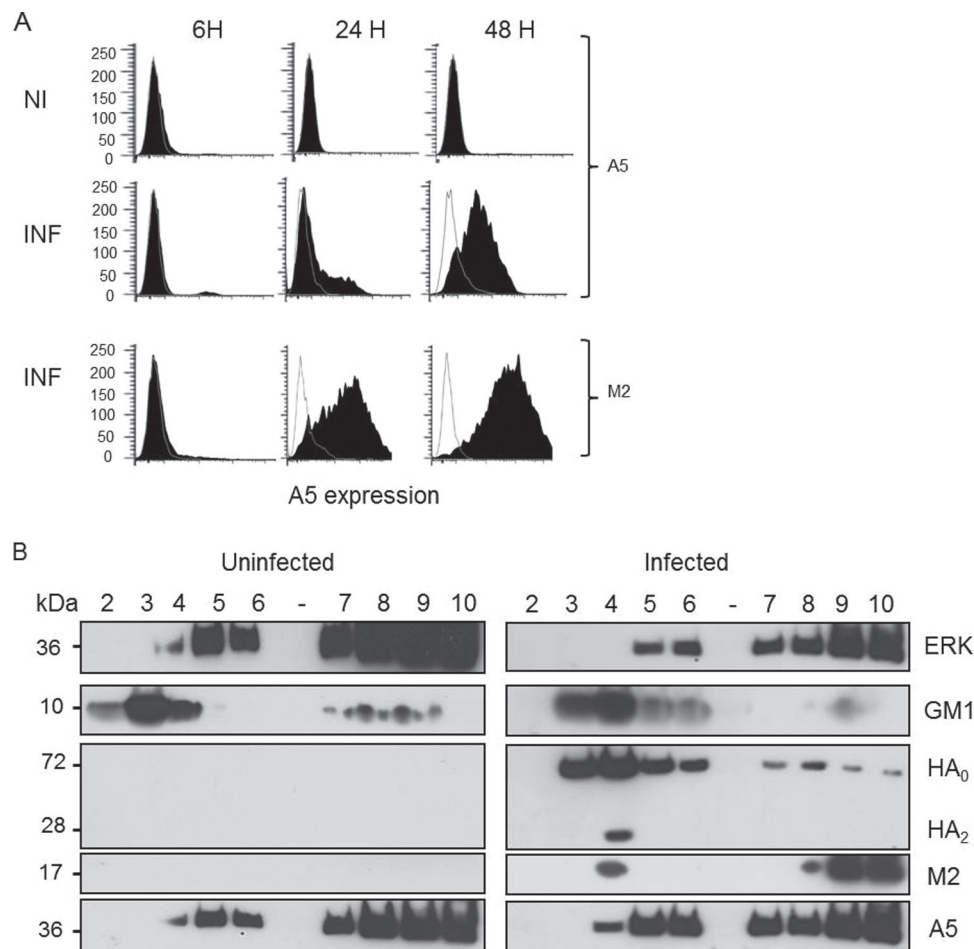


**FIG 3** Kinetic of cell surface expression of A5 after IAV infection and its expression in DRM fractions. (A) Time course experiment of cell surface expression of A5 upon infection of A549 cells with A/WSN/33 virus (MOI of  $10^{-2}$  in the presence of trypsin). Expression of the viral M2 protein was used as a positive control of viral infection. (B) A549 cells were either left uninfected or infected with A/WSN/33 virus (MOI of 10) for 16 h. Cells were then lysed, and the DRM domains were isolated by sucrose gradient ultracentrifugation. After centrifugation, 1-ml fractions were collected from the top of the tube and characterized by Western blot analysis (fractions 1 to 10). Blots were probed with anti-ERK antibody (ERK), cholera toxin B subunit (GM1), and anti-HA ( $HA_0$ - $HA_2$ ), anti-M2 (M2), and anti-A5 (A5) antibodies. Fractions 3 to 5 correspond to the DRMs, whereas the soluble fractions correspond to fractions 7 to 10. The results are representative of two independent experiments.

ERK1/2 was present in the detergent-soluble fractions (Fig. 3B, lanes 7 to 10), while the ganglioside GM1, a resident raft component, detected by cholera toxin B subunit, was present in the DRM fractions (Fig. 3B, lanes 3 and 4). Only infected cells displayed detectable viral HA and M2 proteins. HA protein ( $HA_0$  or  $HA_2$ ) was found almost exclusively in association with the DRM, while M2 protein was predominantly associated with the soluble membrane fraction. More importantly, A5 was indifferently found in the soluble membrane fraction and with the DRM in uninfected cells or infected cells. Therefore, a substantial proportion of A5 is present in lipid rafts, although influenza virus infection did not alter its localization.

**Annexin V is incorporated into virus particles.** IAVs bud from lipid rafts, and a substantial proportion of A5 is located in these domains. Thus, we investigated whether A5 could be packaged into virions when released from the infected cell. To investigate this point, IAV A/PR/8/34, A/Udorn/72, and A/WSN/33 were purified from culture supernatants of infected MDCK cells, and the resulting purified virions were probed by Western blotting

with anti-A5, anti-M2, and anti-ERK antibodies (Fig. 4A). MDCK cells were used because of their high susceptibility to infection with various IAV strains, allowing us to obtain a sufficient amount of virus particles in the supernatant for subsequent purification. The results showed the presence of A5 in all purified virions, in addition to the viral protein M2. In contrast, the cytoplasmic protein extracellular signal-regulated kinase (ERK) was not detected in the virions but was present in the lysates of uninfected or A/PR/8/34 virus-infected MDCK cells, excluding a nonspecific incorporation of cellular proteins into virus particles. It is of note that higher quantities of purified A/PR/8/34 and A/Udorn/72 particles were loaded onto the gel to detect A5 within these virions. Most likely, the level of A5 incorporation into virus particles is strain dependent. To confirm that A5 was not a copurified contaminant of cellular origin, electron microscopic immunogold labeling was performed on purified virions with anti-A5 and secondary gold antibodies, followed by negative staining. Immunogold staining confirmed that A5 was indeed associated with the A/PR/8/34, A/Udorn/72, and A/WSN/33 IAV strains (Fig. 4B). Altogether,

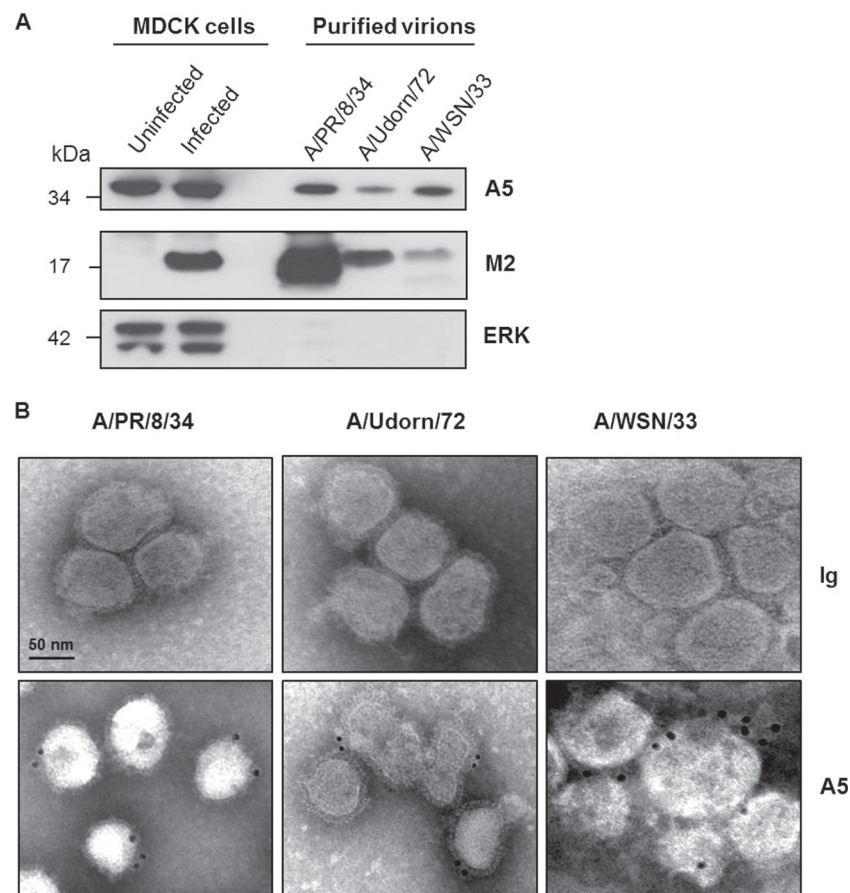


**FIG 4** Cellular A5 protein is incorporated into IAV particles. (A) A/PR/8/34, A/Udorn/72, and A/WSN/33 viruses, produced on MDCK cells, were purified by sucrose ultracentrifugation and analyzed by Western blotting with anti-A5, anti-M2, and anti-ERK antibodies. Aliquots of total proteins from MDCK cells either left uninfected or infected for 16 h with A/PR/8/34 strain were used as controls. The molecular mass is indicated in kilodaltons. (B) Electron microscopic immunogold labeling was performed on purified virions using A5-specific antibodies or isotype control. Scale bar, 50 nm. The results presented in both panels are representative of three independent experiments.

these data demonstrated that the cellular protein A5 is incorporated into IAV particles.

**Packaged A5 inhibits IFN- $\gamma$  receptor signaling.** A5 associates with the IFN- $\gamma$  receptor and downregulates its signaling (16). We therefore investigated whether A5 incorporated into IAV particles (A/WSN/33 strain) could modulate the IFN- $\gamma$  response in differentiated THP-1 macrophages, which express the IFN- $\gamma$  receptor at the cell surface (data not shown). Although productive infection of IAV by macrophages is a matter of debate (26–28), we found that differentiated THP-1 macrophages were highly susceptible to IAV infection (Fig. 5A). First, stimulation of these cells with recombinant IFN- $\gamma$  activated the Jak/Stat pathway in a dose-dependent manner, as demonstrated by increased Stat1 phosphorylation by Western blot analysis (Fig. 5B). The maximal effect was observed at around 1,000 IU of IFN- $\gamma$ , which was the concentration used in subsequent experiments. When differentiated THP-1 cells were preincubated with purified A/WSN/33 virions (V), Stat1 phosphorylation triggered by IFN- $\gamma$  was strongly inhibited (Fig. 5C). Thus, purified virions inhibited IFN- $\gamma$ -induced Stat1 phosphorylation. This effect was not observed when A5 on purified virions was masked with a specific neutralizing antibody (AV-V), showing that inhibition of stat phosphorylation was A5 dependent. In the absence of IFN- $\gamma$ , purified virions had no effect

on Stat phosphorylation. Thus, we concluded that A5 incorporated into virus particles inhibits IFN- $\gamma$ -induced signaling.

Signal transduction via the Jak/Stat pathway initiated by IFN- $\gamma$  receptors leads to the release of C-X-C motif chemokine 10 (CXCL10), also known as IP-10 (29). Therefore, to confirm that A5 blocked IFN- $\gamma$  receptor signaling, we next investigated whether packaged A5 could also interfere with IFN- $\gamma$ -induced IP-10 production. As expected, IFN- $\gamma$  triggered IP-10 production in differentiated THP-1 cells (Fig. 5D). Cells preincubated with purified A/WSN/33 virus particles inhibited this response. However, such an inhibition was not observed in the presence of purified A/WSN/33 viruses, in which packaged A5 was masked with a specific antibody. In the absence of IFN- $\gamma$ , IP-10 release was barely detectable. Importantly, flow cytometry experiments showed comparable attachment of the cells by the two viruses, V versus AV-V, as revealed by similar HA staining in both groups (Fig. 5E, left panel). Quantification of MFI labeling of HA is shown on the right panel (Fig. 5E). Also, both virus preparations displayed identical infectivity (Fig. 5F). Thus, we concluded that A5 incorporated into virus particles inhibits IFN- $\gamma$ -induced stat activation and IP-10 release.

These findings were further confirmed by an approach using siRNA, allowing us to obtain viruses with reduced A5 levels (referred to as A5 siRNA v) compared to control viruses (referred to

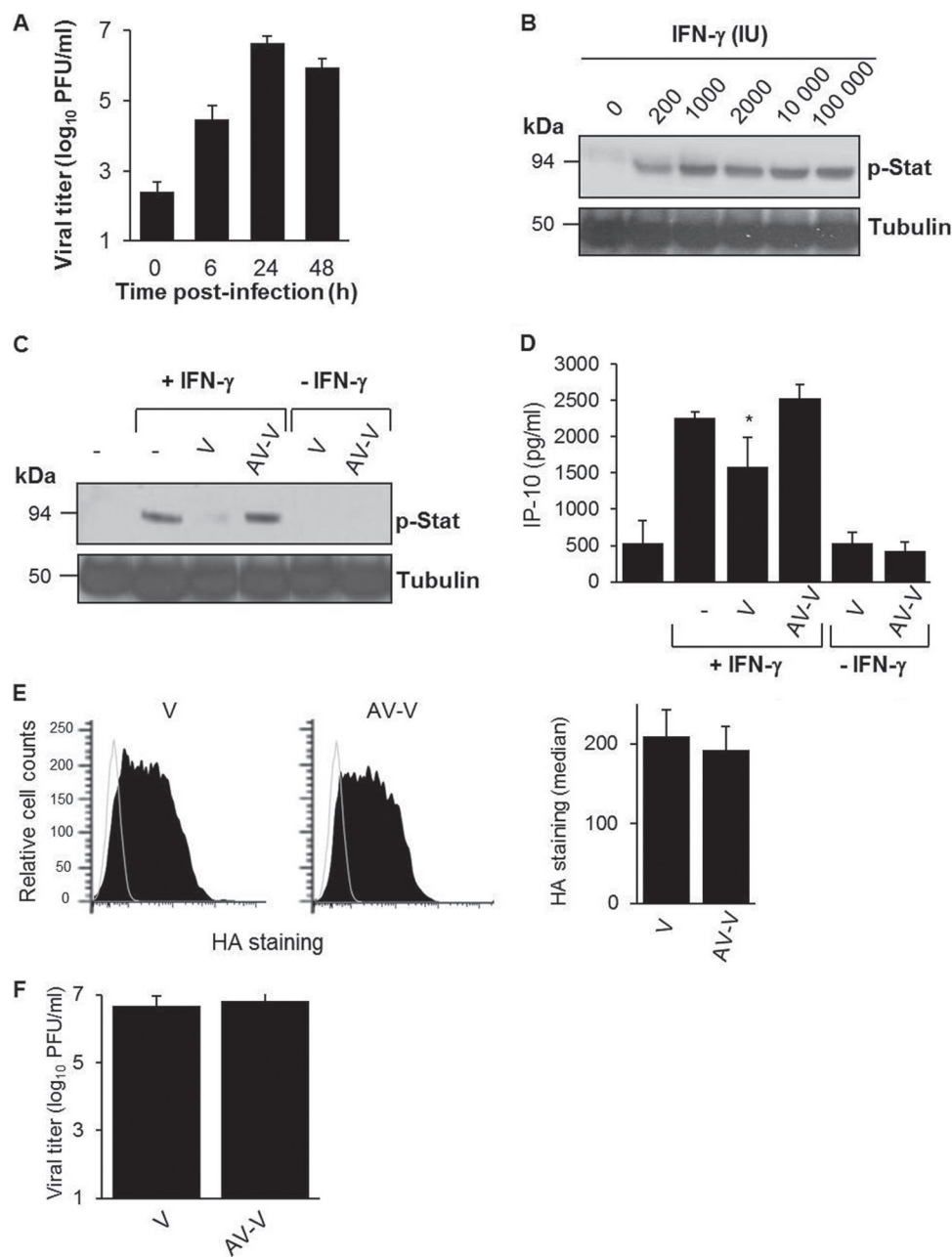


**FIG 5** Packaged A5 inhibits IFN- $\gamma$  receptor signaling. (A) Macrophage-differentiated THP-1 cells were infected with A/WSN/33 virus (MOI of 1), and virus titers were determined in the supernatants of the cells at the indicated time points postinoculation. (B) Macrophage-differentiated THP-1 cells were treated with different doses of human rIFN- $\gamma$  for 5 min at 37°C. The cells were lysed, and Stat phosphorylation was analyzed by Western blotting with an anti-phospho Stat antibody (p-Stat). Tubulin was used as a control for loading. (C and D) Differentiated THP-1 cells were incubated for 5 min with purified A/WSN/33 particles (MOI of 1), which were either pretreated (AV-V) or not pretreated (V) with an anti-A5 antibody. The cells were then either left unstimulated or stimulated with IFN- $\gamma$  (1,000 IU). (C) After 5 min, the cells were lysed, and Stat phosphorylation was analyzed by Western blotting. (D) Alternatively, IP-10 release was evaluated in the supernatant at 3 h poststimulation by classical ELISA. \*,  $P < 0.05$  (between “-” versus “V” and “V” versus “AV-V”). The results in panels A to D are representative of at least two independent experiments. (E) Differentiated THP-1 cells were incubated for 5 min with purified A/WSN/33 particles (MOI of 1), which were either pretreated (AV-V) or not pretreated (V) with an anti-A5 antibody. The cells were then analyzed for virus binding by flow cytometry with an anti-HA antibody (left panel). The MFI for HA staining was obtained from three replicates (right panel). (F) Infectious titers of V and AV-V preparations.

as Ctl siRNA v) (Fig. 6A). Both virus preparations displayed identical infectivity (Fig. 6B) and similar ratios of the different virus proteins, as shown by Western blot analysis with a polyclonal anti-influenza virus antibody (Fig. 6C). When differentiated THP-1 cells were preincubated for 5 min with Ctl siRNA v, Stat phosphorylation triggered by IFN- $\gamma$  was again inhibited. In marked

contrast, no effect was observed in the presence of A5 siRNA v (Fig. 6D). Similar results were obtained in HeLa cells, suggesting that the inhibitory effect of virion-associated A5 was independent of the cell type (Fig. 6E). Packaged A5 also interfered with IFN- $\gamma$ -induced IP-10 production at 3 h poststimulation, but this effect was lost after 24 h (Fig. 6F). In contrast, no effect of packaged A5

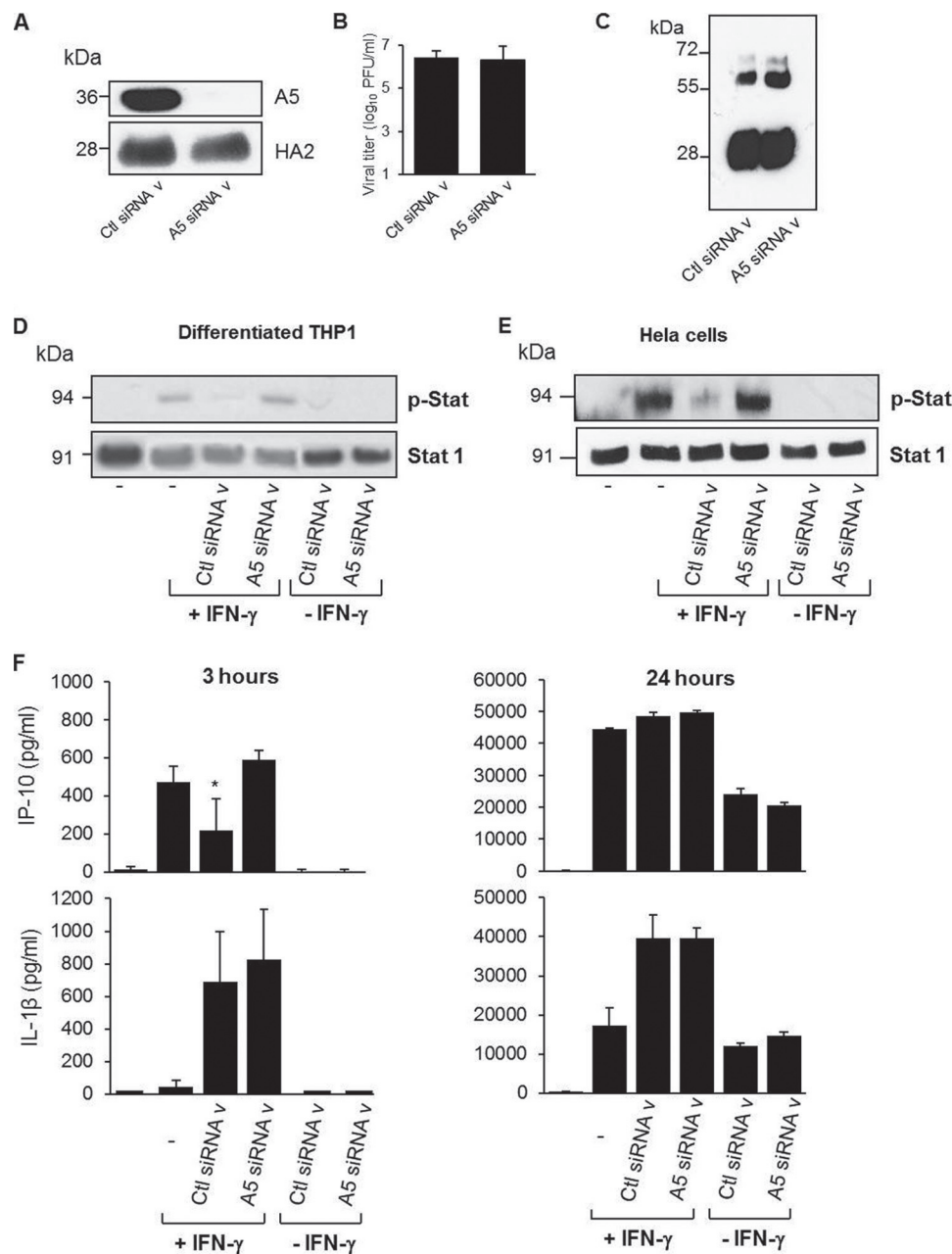


**FIG 6** Packaged A5 inhibits IFN- $\gamma$  receptor signaling. (A) Western blot analysis of virions produced from 293T cells transfected with nontargeted siRNA (Ctl siRNA v) or specific siRNA targeting A5 (A5 siRNA v), using an anti-A5 antibody. Anti-HA antibody was used as a positive control for virus detection. (B) Infectious titers of Ctl siRNA v and A5 siRNA v preparations. (C) Western blot analysis of control siRNA v and A5 siRNA v, using a polyclonal anti-influenza virus antibody. (D to F) Differentiated THP-1 cells (D) or HeLa cells (E) were incubated for 5 min with Ctl siRNA v or A5 siRNA v (MOI of 1). Cells were then either left unstimulated or stimulated with IFN- $\gamma$  (1 IU). After 5 min, the cells were lysed, and Stat phosphorylation was analyzed by Western blotting. (F) Alternatively, IP-10 release was evaluated in the supernatant at 3 or 24 h poststimulation by classical ELISA. \*,  $P < 0.05$  (between “–” versus “Ctl siRNA v” and “Ctl siRNA v” versus “A5 siRNA v”). The results are representative of at least two independent experiments.

was observed upon IL-1 $\beta$  release (Fig. 6F). Comparable attachment of the cells by the two viruses, A5 siRNA v versus Ctl siRNA v, was confirmed by flow cytometry experiments (Fig. 7A) after binding assays for 5 min at 37°C or 1 h at 4°C. Indeed, quantification of the MFI showed similar A5 labeling (Fig. 7B). Also, after internalization assays for 30 min at 37°C, cell surface-bound viruses decreased, and both viruses showed similar internalization within the cells (Fig. 7C, left panel). Quantification of the MFI of

cell surface versus the total (cell surface and internalized) viruses is shown in Fig. 7D. More importantly, inhibition mediated by packaged A5 on IFN- $\gamma$  receptor signaling was specific, and such an effect was not detected in the presence of IFN- $\alpha$  (Fig. 7E and F). Altogether, these observations strengthen the previous findings showing that A5 incorporated into virus particles specifically blocks intracellular signaling mediated by IFN- $\gamma$ .

**Virus replication *in vitro*.** IFN- $\gamma$  mediates a cellular antiviral

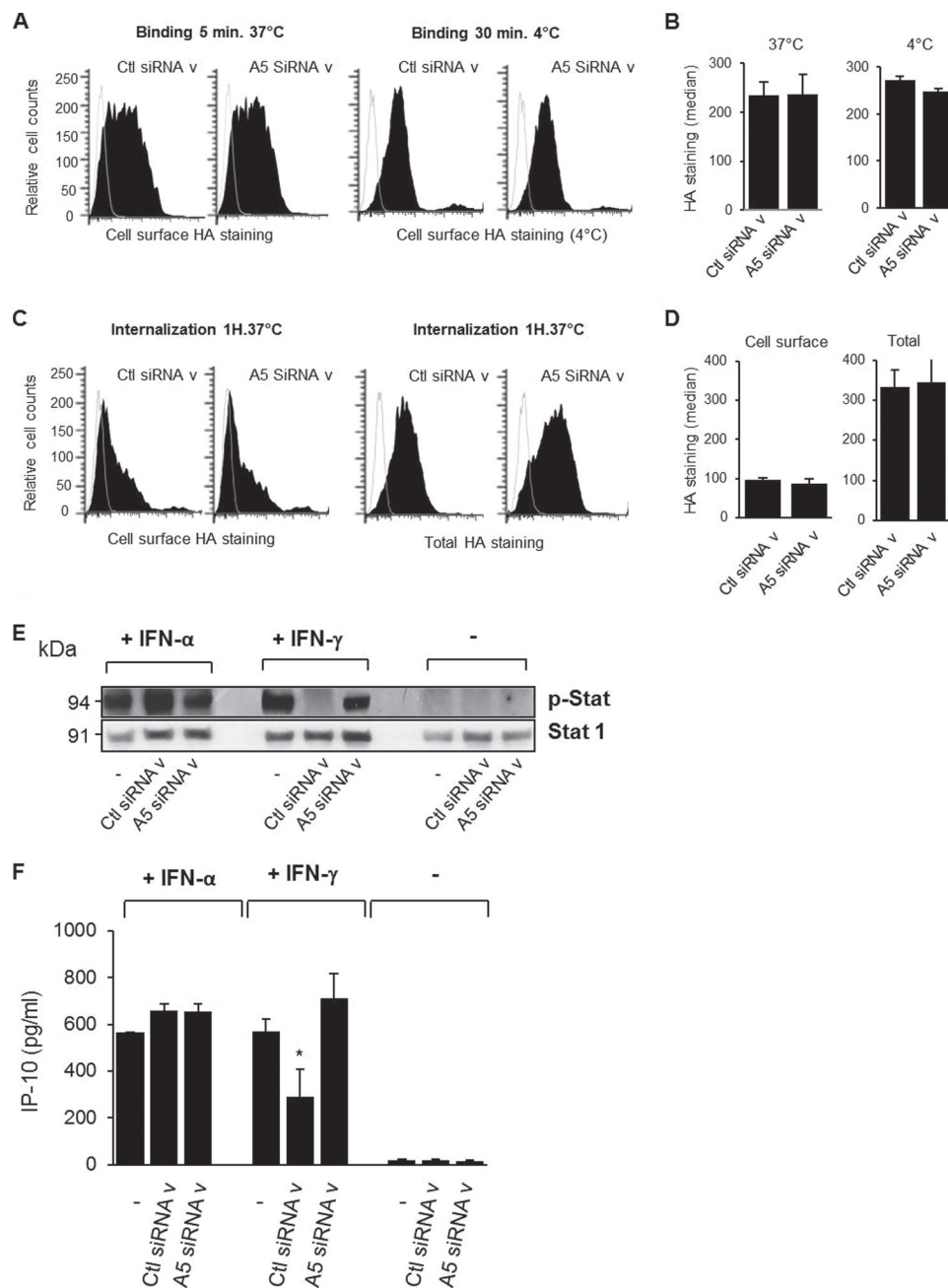


**FIG 7** Packaged A5 does not inhibit IFN- $\alpha$  receptor signaling. (A) Differentiated THP-1 cells were incubated with Ctl siRNA v or A5 siRNA v (MOI of 1) for 5 min at 37°C or for 30 min at 4°C. (B) The cells were then analyzed for virus binding by flow cytometry with an anti-HA antibody, and the MFI of HA staining was obtained from three triplicates. (C) Alternatively, cells were incubated with the virus for 30 min at 4°C and with a shift to 37°C to allow virus internalization. Labeling of HA was performed either on unpermeabilized cells, showing cell surface-bound viruses (left panel), or on permeabilized cells, showing total viruses, including the cell surface and internalized ones (right panel). (D) The MFI of HA staining was obtained from three triplicates. (E and F) Differentiated THP-1 cells were incubated for 5 min with Ctl siRNA v or A5 siRNA v (MOI of 1). The cells were then either left unstimulated or stimulated with IFN- $\alpha$  (1,000 IU) or IFN- $\gamma$  (1,000 IU). (E) After 5 min, the cells were lysed, and Stat1 phosphorylation was analyzed by Western blotting. (F) Alternatively, IP-10 release was evaluated in the supernatant at 3 h poststimulation by classical ELISA. \*,  $P < 0.05$  (between “-” versus “Ctl siRNA v” and “Ctl siRNA v” versus “A5 siRNA v”). The results are representative of two independent experiments (B and C).

state that prevents further viral spread (30). Since packaged A5 inhibits IFN- $\gamma$  receptor signaling, we then investigated whether it could also block the antiviral activity of IFN- $\gamma$  and promote viral replication. To address this point, viral growth was evaluated in the supernatant of differentiated THP-1 cells infected with IAV particles (Fig. 8). In the presence of IFN- $\gamma$  treatment, masking A5

with a specific antibody on A/WSN/33 virus particles inhibited viral replication in differentiated THP-1 cells. Also, A5 siRNA v replicated less efficiently than Ctl siRNA v in the presence of IFN- $\gamma$ . Altogether, these results showed that A5 incorporated into IAV particles triggers an intracellular process leading to increased virus production in the presence of IFN- $\gamma$ .

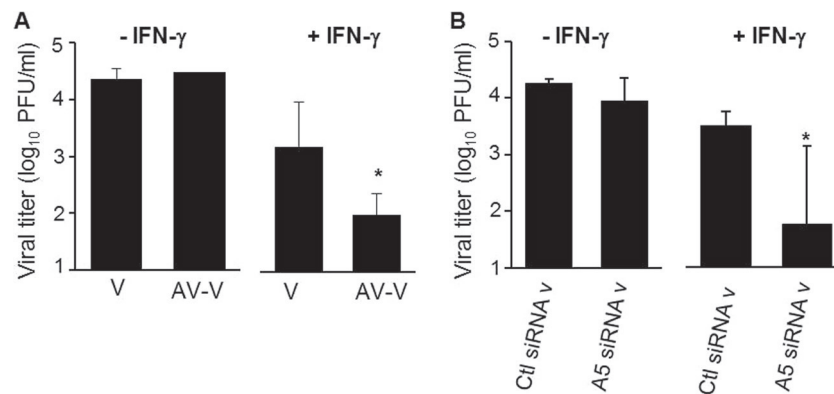


**FIG 8** Packaged A5 inhibits the antiviral activity mediated by IFN- $\gamma$  *in vitro*. PMA-differentiated THP-1 macrophages were infected with purified A/WSN/33 particles, in which A5 was previously masked (AV-V) or not masked (V) with anti-A5 antibody (A), or the supernatant of A/WSN/33-infected 293T cells, in which expression of A5 was downregulated by siRNA (A5 siRNAv) or not downregulated (Ctl siRNAv) (B). All viruses were used at an MOI of 1. The cells were either left in the presence or in the absence of rIFN- $\gamma$ . Infectious virus titers were then evaluated in the supernatant of the cells at 24 hpi. The results represent mean virus titers  $\pm$  the SD from three independent experiments. \*,  $P < 0.05$  (between “V” versus “AV-V” and “Ctl siRNA v” versus “A5 siRNA v”). The results are representative of three independent experiments.

**Virus replication *in vivo*.** Next, we investigated whether packaged A5 could also promote viral replication by subverting the IFN- $\gamma$  response *in vivo*. First, infectious virus titers were determined in lungs collected from infected mice treated with different concentrations of rIFN- $\gamma$ . On day 2 postinoculation with IAV, the mean lung virus titers in mice treated with IFN- $\gamma$  was lower than that of untreated mice, and this effect was dose dependent. A significant inhibition at  $8 \times 10^4$  IU of rIFN- $\gamma$  per mouse was observed (Fig. 9A). Thus, *in vivo*, the administration of rIFN- $\gamma$  inhibits virus production in mouse lungs. Next, mice were infected with a high dose of purified IAV particles that were preincubated with or without anti-A5 neutralizing antibodies. At 2 days postinfection, the lung virus titers were evaluated. When purified virions (V) were used for infection, IFN- $\gamma$  treatment inhibited the mean lung virus titers obtained compared to untreated mice. However, this inhibition was much greater when purified virions in which A5 was blocked were used to infect the mice (Fig. 9B). No difference was observed in lung virus titers obtained from mice infected with V or AV-V in the absence of rIFN- $\gamma$  treatment. Thus, we

concluded that A5 incorporated into IAV particles increases lung viral replication in the presence of IFN- $\gamma$  *in vivo*.

## DISCUSSION

Previous works have shown that virus infection can alter the contingent of proteins exposed at the surface of the host cell (31). It is interesting that 5 of the 12 proteins with the strongest increase in surface abundance in influenza virus-infected cells have been previously detected in purified IAV virions. Therefore, it is tempting to speculate that their augmented display at the cell surface is not merely an incidental event but may be rather stimulated by the infection to support virus propagation. In the present study, we have demonstrated that incorporation of the host cellular protein A5 into IAV particles provided the virus with a means to inhibit IFN- $\gamma$  signaling and increase its replication *in vitro* and *in vivo*. The *in vitro* data showed increased A5 cell surface expression after IAV infection. Cellular programmed cell death is activated by IAV and, during such event, phosphatidylserine becomes exposed to the cell surface (32). A5 has a strong affinity for phosphatidylser-

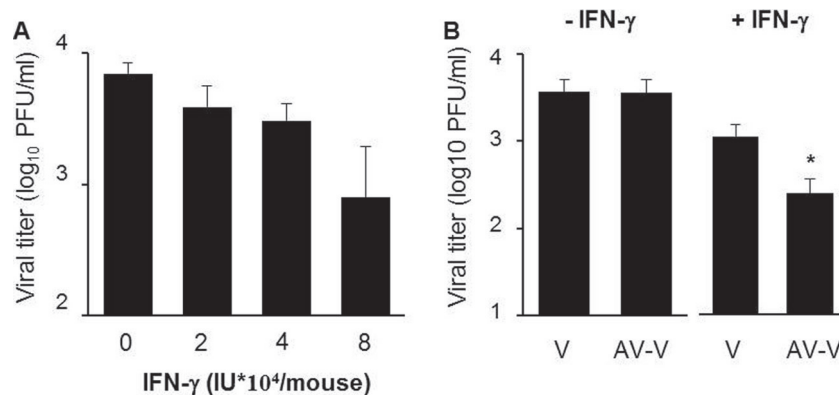


**FIG 9** Packaged A5 inhibits the antiviral activity mediated by IFN- $\gamma$  *in vivo*. (A) Mice were infected with purified A/PR/8/34 virus (500 PFU) and treated with the indicated quantities of mouse rIFN- $\gamma$  by intranasal administration. At 2 days postinfection, virus titers were evaluated in the lungs by classical plaque assay. (B) Mice ( $n = 5$  per group) were treated with  $8 \times 10^4$  IU of rIFN- $\gamma$  and infected with purified A/PR/8/34 viruses, in which A5 was previously blocked with anti-A5 antibody (AV-V) or not blocked (V). At 2 days postinfection, lung virus titers were evaluated by plaque assay. \*,  $P < 0.05$  (between “V” and “AV-V”). The results are representative of two independent experiments.

ine (33), making it a useful probe for the detection of apoptotic cells (34). Thus, most likely, cellular A5 is translocated from the cytoplasm to the cell surface through phosphatidylserine binding and flip-flop transmembrane translocation of lipids (35). Interestingly, a substantial proportion of A5 was located in cholesterol-rich membrane domains, referred to as lipid rafts. HA was enriched in these domains, whereas M2 and the host ERK molecule were rather excluded, which is in line with other reports (36). It has been demonstrated that these domains are the platforms for IAV assembly and budding (36, 37). Since the viral envelope of IAV is derived from the host cell plasma membrane, it is likely that enveloped viruses incorporate proteins enriched in lipid rafts from the host cell. Accordingly, we were able to detect A5 in highly purified IAV preparations by Western blot analysis, as well as by immunogold labeling, indicating that cellular contaminants are probably not responsible for the detection of A5. Consistently, along with annexin 2, A5 has also been detected by matrix-assisted laser desorption ionization–time of flight analysis of purified IAV particles previously (data not shown; 14). These results are in accordance with results obtained by others and show that A5 is one of the 36 host proteins incorporated into influenza virus particles (13). Interestingly, A5 is also associated with other enveloped viruses, such as human cytomegaloviruses (38), human immunodeficiency viruses (39), herpes simplex viruses (40), vaccinia viruses (41), and porcine reproductive and respiratory syndrome viruses (42). Thus, the acquisition of A5 from the host cell membrane during the budding process is not specific to IAV. However, to our knowledge, the present study is the first to show a functional role for packaged A5 in the context of viral infection. Indeed, our results showed that A5-associated with IAV inhibited IFN- $\gamma$  receptor signaling and allowed for an increase in viral replication, *in vitro*, using differentiated THP-1 macrophages and HeLa cells. These results were not observed in epithelial A549 cells, which surprisingly did not express the IFN- $\gamma$  receptor at the cell surface (data not shown). Interestingly, however, we were able to confirm the role of packaged A5 on virus replication *in vivo* after 48 h of IFN- $\gamma$  administration in mice, a period during which its biological activity remains stable (43).

In our study, the role of packaged A5 was detected when the virus was preincubated for 5 min but not 1 or 16 h before IFN- $\gamma$  treatment (data not shown). Preincubation for 5 min most likely corresponds to virus binding to the cells, whereas after 1 h the virus may be internalized and after 16 h the virus may have undergone replication. Thus, virus binding to the cells, but not endocytosis or replication, was required for inhibition of IFN- $\gamma$  receptor signaling. These results are consistent with a previous report which showed that A5 associates with the IFN- $\gamma$  receptor and negatively regulates IFN- $\gamma$  signaling (16).

IFN- $\gamma$  plays an important role in recovery from IAV infection by helping to clear the virus (44–46). Thus, the incorporation of A5 into IAV particles provides the virus a way to escape from host immune IFN- $\gamma$  responses and therefore is an opportunity for the virus to become more infectious. In line with this hypothesis, it has been shown that IAV abrogates the IFN- $\gamma$  response to evade its antiviral activity (47). Thus, as previously suggested, strategies attempting to restore IFN- $\gamma$  function may be of interest for therapeutic effects against IAV pathogenesis in humans (46).

We found that downregulation of A5 expression in 293T cells or in A549 epithelial cells had no effect on viral replication (data not shown), showing that A5 has no role in the viral replication

cycle, at least in our conditions. These results differ from a previous study, which suggested that A5 could serve as a second receptor for viral entry (48). The precise physiological role of A5 remains to be determined. However, it has been proposed that A5 inhibits blood coagulation by competing for phosphatidylserine binding sites with prothrombin (49–51). Recently, we found that the thrombin protease-activated receptor 1 (PAR1) and hemostasis deregulation play a pivotal role in the inflammation and cytokine storm induced during severe virus infections (5, 23, 24, 52). Thus, the modulating function of A5 during IAV could go beyond IFN- $\gamma$ . Possibly, by modulating hemostasis, A5 expression may also play a role in the inflammation and cytokine storm that occur during severe cases of influenza.

Altogether, this report suggests that specific incorporation of A5 into virus particles is a strategy adopted by IAV for subverting host defenses, thereby facilitating viral spread. The differential capacity of IAV to upregulate A5 at the surfaces of infected cells and to incorporate A5 during the budding process may be an additional factor for differences in the virulence of IAV.

#### ACKNOWLEDGMENTS

This study was supported by the Agence Nationale de la Recherche (grant ANR-13-BSV3-0011 HemoFlu to B.R.), the VIROSIGN project funded by the German Ministry of Education and Research (to T.W.), and the German Research Foundation (grant DFG SFB-TR84 to T.W.).

We are grateful to G. F. Rimmelzwaan (Erasmus University, Rotterdam, Netherlands) and N. Naffakh (Pasteur Institute, Paris, France) for the IAV strains and to T. Schwecke (Robert Koch Institute) for initial help with the MS analysis.

#### REFERENCES

1. Fukuyama S, Kawaoka Y. 2011. The pathogenesis of influenza virus infections: the contributions of virus and host factors. *Curr. Opin. Immunol.* 23:481–486. <http://dx.doi.org/10.1016/j.coi.2011.07.016>.
2. Webby RJ, Webster RG. 2003. Are we ready for pandemic influenza? *Science* 302:1519–1522. <http://dx.doi.org/10.1126/science.1090350>.
3. Stohr K. 2002. Influenza: WHO cares. *Lancet Infect. Dis.* 2:517. [http://dx.doi.org/10.1016/S1473-3099\(02\)00366-3](http://dx.doi.org/10.1016/S1473-3099(02)00366-3).
4. Kuiken T, Riteau B, Fouchier RA, Rimmelzwaan GF. 2012. Pathogenesis of influenza virus infections: the good, the bad, and the ugly. *Curr. Opin. Virol.* 2:276–286. <http://dx.doi.org/10.1016/j.coviro.2012.02.013>.
5. Berri F, Le VB, Jandrot-Perrus M, Lina B, Riteau B. 2014. Switch from protective to adverse inflammation during influenza: viral determinants and hemostasis are caught as culprits. *Cell. Mol. Life Sci.* 71:885–898. <http://dx.doi.org/10.1007/s00018-013-1479-x>.
6. Foucault ML, Moules V, Rosa-Calatrava M, Riteau B. 2011. Role for proteases and HLA-G in the pathogenicity of influenza A viruses. *J. Clin. Virol.* 51:155–159. <http://dx.doi.org/10.1016/j.jcv.2011.04.013>.
7. Kochs G, Garcia-Sastre A, Martinez-Sobrido L. 2007. Multiple anti-interferon actions of the influenza A virus NS1 protein. *J. Virol.* 81:7011–7021. <http://dx.doi.org/10.1128/JVI.02581-06>.
8. LeBouder F, Khoufache K, Menier C, Mandouri Y, Keffous M, Lejal N, Krawiec-Radanne I, Carosella ED, Rouas-Freiss N, Riteau B. 2009. Immunosuppressive HLA-G molecule is upregulated in alveolar epithelial cells after influenza A virus infection. *Hum. Immunol.* 70:1016–1019. <http://dx.doi.org/10.1016/j.humimm.2009.07.026>.
9. Garcia-Sastre A. 2011. Induction and evasion of type I interferon responses by influenza viruses. *Virus Res.* 162:12–18. <http://dx.doi.org/10.1016/j.virusres.2011.10.017>.
10. Le Gal FA, Riteau B, Sedlik C, Khalil-Daher I, Menier C, Dausset J, Guillet JG, Carosella ED, Rouas-Freiss N. 1999. HLA-G-mediated inhibition of antigen-specific cytotoxic T lymphocytes. *Int. Immunol.* 11:1351–1356. <http://dx.doi.org/10.1093/intimm/11.8.1351>.
11. Nayak DP, Balogun RA, Yamada H, Zhou ZH, Barman S. 2009. Influenza virus morphogenesis and budding. *Virus Res.* 143:147–161. <http://dx.doi.org/10.1016/j.virusres.2009.05.010>.
12. Nayak DP, Hui EK, Barman S. 2004. Assembly and budding of influenza

- virus. *Virus Res.* 106:147–165. <http://dx.doi.org/10.1016/j.virusres.2004.08.012>.
13. Shaw ML, Stone KL, Colangelo CM, Gulcicek EE, Palese P. 2008. Cellular proteins in influenza virus particles. *PLoS Pathog.* 4:e1000085. <http://dx.doi.org/10.1371/journal.ppat.1000085>.
  14. LeBouder F, Morello E, Rimmelzwaan GF, Bosse F, Pechoux C, Delmas B, Riteau B. 2008. Annexin II incorporated into influenza virus particles supports virus replication by converting plasminogen into plasmin. *J. Virol.* 82:6820–6828. <http://dx.doi.org/10.1128/JVI.00246-08>.
  15. LeBouder F, Lina B, Rimmelzwaan GF, Riteau B. 2010. Plasminogen promotes influenza A virus replication through an annexin 2-dependent pathway in the absence of neuraminidase. *J. Gen. Virol.* 91:2753–2761. <http://dx.doi.org/10.1099/vir.0.023804-0>.
  16. Leon C, Nandan D, Lopez M, Moenrezakhanlou A, Reiner NE. 2006. Annexin V associates with the IFN- $\gamma$  receptor and regulates IFN- $\gamma$  signaling. *J. Immunol.* 176:5934–5942. <http://dx.doi.org/10.4049/jimmunol.176.10.5934>.
  17. Yan X, Doffek K, Yin C, Krein M, Phillips M, Sugg SL, Johnson B, Shilyansky J. 2012. Annexin V promotes anti-tumor immunity and inhibits neuroblastoma growth in vivo. *Cancer Immunol. Immunother.* 61:1917–1927. <http://dx.doi.org/10.1007/s00262-012-1250-4>.
  18. Riteau B, Barber DF, Long EO. 2003. Vav1 phosphorylation is induced by  $\beta$ 2 integrin engagement on natural killer cells upstream of actin cytoskeleton and lipid raft reorganization. *J. Exp. Med.* 198:469–474. <http://dx.doi.org/10.1084/jem.20021995>.
  19. Riteau B, de Vaureix C, Lefevre F. 2006. Trypsin increases pseudorabies virus production through activation of the ERK signalling pathway. *J. Gen. Virol.* 87:1109–1112. <http://dx.doi.org/10.1099/vir.0.81609-0>.
  20. Ashburner M, Ball CA, Blake JA, Botstein D, Butler H, Cherry JM, Davis AP, Dolinski K, Dwight SS, Eppig JT, Harris MA, Hill DP, Issel-Tarver L, Kasarskis A, Lewis S, Matese JC, Richardson JE, Ringwald M, Rubin GM, Sherlock G. 2000. Gene ontology: tool for the unification of biology. *Nat. Genet.* 25:25–29.
  21. Riteau B, Moreau P, Menier C, Khalil-Daher I, Khosrotehrani K, Bras-Goncalves R, Paul P, Dausset J, Rouas-Freiss N, Carosella ED. 2001. Characterization of HLA-G1, -G2, -G3, and -G4 isoforms transfected in a human melanoma cell line. *Transplant Proc.* 33:2360–2364. [http://dx.doi.org/10.1016/S0041-1345\(01\)02021-8](http://dx.doi.org/10.1016/S0041-1345(01)02021-8).
  22. Zilberman S, Schenowitz C, Agaugue S, Benoit F, Riteau B, Rouzier R, Carosella ED, Rouas-Freiss N, Menier C. 2012. HLA-G1 and HLA-G5 active dimers are present in malignant cells and effusions: the influence of the tumor microenvironment. *Eur. J. Immunol.* 42:1599–1608. <http://dx.doi.org/10.1002/eji.201141761>.
  23. Berri F, Rimmelzwaan GF, Hanss M, Albina E, Foucault-Grunenwald ML, Le VB, Vogelzang-van Trierum SE, Gil P, Camerer E, Martinez D, Lina B, Lijnen R, Carmeliet P, Riteau B. 2013. Plasminogen controls inflammation and pathogenesis of influenza virus infections via fibrinolysis. *PLoS Pathog.* 9:e1003229. <http://dx.doi.org/10.1371/journal.ppat.1003229>.
  24. Khoufache K, Berri F, Nacken W, Vogel AB, Delenne M, Camerer E, Coughlin SR, Carmeliet P, Lina B, Rimmelzwaan GF, Planz O, Ludwig S, Riteau B. 2013. PAR1 contributes to influenza A virus pathogenicity in mice. *J. Clin. Invest.* 123:206–214. <http://dx.doi.org/10.1172/JCI61667>.
  25. Sagara J, Tsukita S, Yonemura S, Tsukita S, Kawai A. 1995. Cellular actin-binding ezrin-radixin-moesin (ERM) family proteins are incorporated into the rabies virion and closely associated with viral envelope proteins in the cell. *Virology* 206:485–494. [http://dx.doi.org/10.1016/S0042-6822\(95\)80064-6](http://dx.doi.org/10.1016/S0042-6822(95)80064-6).
  26. Mok CK, Lee DC, Cheung CY, Peiris M, Lau AS. 2007. Differential onset of apoptosis in influenza A virus H5N1- and H1N1-infected human blood macrophages. *J. Gen. Virol.* 88:1275–1280. <http://dx.doi.org/10.1099/vir.0.82423-0>.
  27. Perrone LA, Plowden JK, Garcia-Sastre A, Katz JM, Tumpey TM. 2008. H5N1 and 1918 pandemic influenza virus infection results in early and excessive infiltration of macrophages and neutrophils in the lungs of mice. *PLoS Pathog.* 4:e1000115. <http://dx.doi.org/10.1371/journal.ppat.1000115>.
  28. Yu WC, Chan RW, Wang J, Travanty EA, Nicholls JM, Peiris JS, Mason RJ, Chan MC. 2011. Viral replication and innate host responses in primary human alveolar epithelial cells and alveolar macrophages infected with influenza H5N1 and H1N1 viruses. *J. Virol.* 85:6844–6855. <http://dx.doi.org/10.1128/JVI.02200-10>.
  29. Liu M, Guo S, Hibbert JM, Jain V, Singh N, Wilson NO, Stiles JK. 2011. CXCL10/IP-10 in infectious diseases pathogenesis and potential therapeutic implications. *Cytokine Growth Factor Rev.* 22:121–130.
  30. Garcia-Sastre A, Biron CA. 2006. Type 1 interferons and the virus-host relationship: a lesson in detente. *Science* 312:879–882. <http://dx.doi.org/10.1126/science.1125676>.
  31. Gudleski-O'Regan N, Greco TM, Cristea IM, Shenk T. 2012. Increased expression of LDL receptor-related protein 1 during human cytomegalovirus infection reduces virion cholesterol and infectivity. *Cell Host Microbe* 12:86–96. <http://dx.doi.org/10.1016/j.chom.2012.05.012>.
  32. Demchenko AP. 2012. The change of cellular membranes on apoptosis: fluorescence detection. *Exp. Oncol.* 34:263–268.
  33. van Engeland M, Nieland LJ, Ramaekers FC, Schutte B, Reutelingsperger CP. 1998. annexin V-affinity assay: a review on an apoptosis detection system based on phosphatidylserine exposure. *Cytometry* 31:1–9. [http://dx.doi.org/10.1002/\(SICI\)1097-0320\(19980101\)31:1<1::AID-CYTO1>3.0.CO;2-R](http://dx.doi.org/10.1002/(SICI)1097-0320(19980101)31:1<1::AID-CYTO1>3.0.CO;2-R).
  34. Niu G, Chen X. 2010. Apoptosis imaging: beyond annexin V. *J. Nucl. Med.* 51:1659–1662. <http://dx.doi.org/10.2967/jnumed.110.078584>.
  35. Boon JM, Lambert TN, Sisson AL, Davis AP, Smith BD. 2003. Facilitated phosphatidylserine (PS) flip-flop and thrombin activation using a synthetic PS scramblase. *J. Am. Chem. Soc.* 125:8195–8201. <http://dx.doi.org/10.1021/ja029670q>.
  36. Leser GP, Lamb RA. 2005. Influenza virus assembly and budding in raft-derived microdomains: a quantitative analysis of the surface distribution of HA, NA and M2 proteins. *Virology* 342:215–227. <http://dx.doi.org/10.1016/j.virol.2005.09.049>.
  37. Rossman JS, Lamb RA. 2011. Influenza virus assembly and budding. *Virology* 411:229–236. <http://dx.doi.org/10.1016/j.virol.2010.12.003>.
  38. Varnum SM, Streblov DN, Monroe ME, Smith P, Auberry KJ, Pasa-Tolic L, Wang D, Camp DG, 2nd, Rodland K, Wiley S, Britt W, Shenk T, Smith RD, Nelson JA. 2004. Identification of proteins in human cytomegalovirus (HCMV) particles: the HCMV proteome. *J. Virol.* 78:10960–10966. <http://dx.doi.org/10.1128/JVI.78.20.10960-10966.2004>.
  39. Chertova E, Chertov O, Coren LV, Roser JD, Trubey CM, Bess JW, Jr, Sowder RC, II, Barsov E, Hood BL, Fisher RJ, Nagashima K, Conrads TP, Veenstra TD, Lifson JD, Ott DE. 2006. Proteomic and biochemical analysis of purified human immunodeficiency virus type 1 produced from infected monocyte-derived macrophages. *J. Virol.* 80:9039–9052. <http://dx.doi.org/10.1128/JVI.01013-06>.
  40. Loret S, Guay G, Lippe R. 2008. Comprehensive characterization of extracellular herpes simplex virus type 1 virions. *J. Virol.* 82:8605–8618. <http://dx.doi.org/10.1128/JVI.00904-08>.
  41. Jensen ON, Houthaevae T, Shevchenko A, Cudmore S, Ashford T, Mann M, Griffiths G, Krijnsen Locker J. 1996. Identification of the major membrane and core proteins of vaccinia virus by two-dimensional electrophoresis. *J. Virol.* 70:7485–7497.
  42. Zhang C, Xue C, Li Y, Kong Q, Ren X, Li X, Shu D, Bi Y, Cao Y. 2010. Profiling of cellular proteins in porcine reproductive and respiratory syndrome virus virions by proteomics analysis. *Virol. J.* 7:242. <http://dx.doi.org/10.1186/1743-422X-7-242>.
  43. Miyakawa N, Nishikawa M, Takahashi Y, Ando M, Misaka M, Watanabe Y, Takakura Y. 2011. Prolonged circulation half-life of interferon gamma activity by gene delivery of interferon gamma-serum albumin fusion protein in mice. *J. Pharm. Sci.* 100:2350–2357. <http://dx.doi.org/10.1002/jps.22473>.
  44. Karupiah G, Chen JH, Mahalingam S, Nathan CF, MacMicking JD. 1998. Rapid interferon gamma-dependent clearance of influenza A virus and protection from consolidating pneumonitis in nitric oxide synthase 2-deficient mice. *J. Exp. Med.* 188:1541–1546. <http://dx.doi.org/10.1084/jem.188.8.1541>.
  45. Wiley JA, Cerwenka A, Harkema JR, Dutton RW, Harmsen AG. 2001. Production of interferon-gamma by influenza hemagglutinin-specific CD8 effector T cells influences the development of pulmonary immunopathology. *Am. J. Pathol.* 158:119–130. [http://dx.doi.org/10.1016/S0002-9440\(10\)63950-8](http://dx.doi.org/10.1016/S0002-9440(10)63950-8).
  46. Khoufache K, LeBouder F, Morello E, Laurent F, Riffault S, Andrade-Gordon P, Boullier S, Rousset P, Vergnolle N, Riteau B. 2009. Protective role for protease-activated receptor-2 against influenza virus pathogenesis via an IFN- $\gamma$ -dependent pathway. *J. Immunol.* 182:7795–7802. <http://dx.doi.org/10.4049/jimmunol.0803743>.
  47. Uetani K, Hiroi M, Meguro T, Ogawa H, Kamisako T, Ohmori Y, Erzurum SC. 2008. Influenza A virus abrogates IFN- $\gamma$  response in respiratory epithelial cells by disruption of the Jak/Stat pathway. *Eur. J. Immunol.* 38:1559–1573. <http://dx.doi.org/10.1002/eji.200737045>.

48. Huang RT, Lichtenberg B, Rick O. 1996. Involvement of annexin V in the entry of influenza viruses and role of phospholipids in infection. *FEBS Lett.* 392:59–62. [http://dx.doi.org/10.1016/0014-5793\(96\)00783-1](http://dx.doi.org/10.1016/0014-5793(96)00783-1).
49. Rand JH, Wu XX, Quinn AS, Taatjes DJ. 2010. The annexin A5-mediated pathogenic mechanism in the antiphospholipid syndrome: role in pregnancy losses and thrombosis. *Lupus* 19:460–469. <http://dx.doi.org/10.1177/0961203310361485>.
50. Rand JH. 2000. The pathogenic role of annexin V in the antiphospholipid syndrome. *Curr. Rheumatol. Rep.* 2:246–251. <http://dx.doi.org/10.1007/s11926-000-0086-7>.
51. Joseph JE, Harrison P, Mackie IJ, Isenberg DA, Machin SJ. 2001. Increased circulating platelet-leucocyte complexes and platelet activation in patients with antiphospholipid syndrome, systemic lupus erythematosus and rheumatoid arthritis. *Br. J. Haematol.* 115:451–459. <http://dx.doi.org/10.1046/j.1365-2141.2001.03101.x>.
52. Aerts LHM, Rhéaume C, Lavigne S, Couture C, Kim W, Susan-Resiga D, Prat A, Seidah NG, Vergnolle N, Riteau B, Boivin G. 2013. Modulation of protease activated receptor 1 influences human metapneumovirus disease severity in a mouse model. *PLoS One* 28:e72529. <http://dx.doi.org/10.1371/journal.pone.0072529>.

## Chapitre 3 : Discussions & Conclusions

## **Discussions et conclusions**

Les infections grippales sont l'une des causes les plus importantes des maladies des voies respiratoires. Ces infections engendrent des épidémies saisonnières et des pandémies sporadiques chez l'homme affectant tous les ans, plusieurs dizaines de millions de personnes dans le monde. Les infections grippales constituent donc un véritable enjeu de santé publique, au niveau mondial (Fiers et al 2004, To et al 2010). Par ailleurs, l'émergence récente de virus aviaires contaminant l'homme et les infections humaines récurrentes par les virus de sous-type H5N1 hautement pathogènes ainsi que les récentes infections par les virus de sous-type H7N7, mettent en exergue la menace permanente d'une pandémie grippale (Webster et al 2006). En ce qui concerne le virus hautement pathogène H5N1, dont le taux de mortalité peut atteindre les 60-70%, seules 4 mutations sont suffisantes à une transmission inter-furets (Herfst S 2012, Masaki Imai 2012). Le furet représente un modèle représentatif de la maladie grippale chez l'homme en termes de transmission et donc ces données suggèrent un risque potentiel de transmission interhumaine du virus hautement pathogène H5N1. Nos recherches ont eu pour objectif de mieux comprendre les relations hôte-pathogène afin de déterminer de nouvelles cibles thérapeutiques.

Lors des cas graves d'infection grippale, il a été démontré que la réponse immunitaire était dérégulée et excessive, engendrant probablement des dommages collatéraux des poumons qui impactent la capacité respiratoire du patient (Kuiken et al 2012, Morens & Fauci 2007). L'ensemble de nos résultats suggèrent que l'hémostase est à la base de cette dérégulation. Nous avons ainsi montré que le récepteur activé par la thrombine, PAR1 et l'activation excessive de la fibrinolyse, jouent un rôle délétère dans la dérégulation de l'inflammation induite par les VIA.

Puisque le VIA a un fort endothéliotropisme (Feldmann et al 2000, Reperant et al 2012), il est probable que durant les infections grippales, les cellules endothéliales soient lésées, ce qui expliquerait l'activation de l'hémostase, dans le but de réparer la lésion. Des molécules clés de l'hémostase telles que PAR1 sont alors mises en jeu et lorsque cette activation est tempérée, ceci est protecteur pour l'organisme. Ainsi, Antoniak et ses collaborateurs ont montré, contrairement à nos résultats, que PAR1 aurait un effet protecteur contre les infections grippales (Antoniak et al 2013). De manière intéressante, il semblerait que les conditions d'infection utilisée dans cette étude, soit des conditions de faible infection. En effet, les taux de cytokines observées dans les lavages broncho-alvéolaire des souris infectée est très faible en comparaison avec nos études, suggérant que la réponse immunitaire est contrôlée. Par ailleurs, ces auteurs suggèrent que l'effet protecteur de PAR1 agit via le récepteur TLR3, ce qui est en accord avec un rôle important de la réponse immunitaire. Cependant lors des infections graves, le rôle de TLR3 est plutôt délétère (Le Goffic et al 2006). Si PAR1 est directement relié à l'activation de TLR3 durant les infections influenza, alors il doit probablement exister un seuil au-delà duquel l'activation de l'hémostase et des PRRs passe de protecteur à délétère. Ceci expliquerait pourquoi dans nos études, le rôle de PAR1 augmente la pathogénicité des VIA. En accord avec nos résultats, la majorité des études montrent plutôt un rôle néfaste de PAR1 dans les maladies inflammatoires, notamment dans les maladies respiratoires aiguës (Jenkins et al 2006, Mercer et al 2007, Mercer et al 2014), dans le sepsis (Tressel et al 2011), les pneumonies induites par les métapneumovirus (Aerts et al 2013) ou les bactéries streptocoques (Schouten et al 2012).

Nos études sont aussi en accord avec le récent rapport de Teijaro et ses collaborateurs montrant que les cellules endothéliales orchestrent l'avalanche cytokinique durant les infections influenza (Teijaro et al 2011). Dans cette étude, il a été démontré que l'activation du récepteur à S1P1 jouait un rôle important. Or, comme nous l'avons mentionné, PAR1 joue

un rôle ambivalent. A de faibles concentrations de thrombine, il coactive le récepteur S1P1 et induit un effet anti-inflammatoire (Feistritzer C 2005). A de fortes concentrations de thrombine, PAR1 se dissocie du récepteur à la PC et agit en tant que pro-inflammatoire. Probablement, plus l'infection par le virus influenza est importante, plus les taux de thrombine sont élevés. Ainsi, ces données pourraient indiquer que lors des infections graves par le VIA, PAR1 ne serait plus activé par la PCa mais directement par la thrombine. De ce fait, PAR1 ne co-activerait plus le récepteur S1P1, jouant ainsi son rôle pro-inflammatoire et délétère.

Au vu des données de la littérature montrant un endothéliotropisme des VIA (Feldmann et al 2000, Reperant et al 2012), l'infection des cellules endothéliales pourrait induire une lésion de l'endothélium et activer l'hémostase. Alternativement, l'environnement inflammatoire induit lors de la réponse initiale de l'hôte suite à l'infection des cellules épithéliales par le VIA pourrait être la cause de la lésion endothéliale (Narasaraju et al 2011, Visseren et al 2000). Dans les deux cas, les facteurs responsables de l'activation des cellules endothéliales dans certains cas d'infection seulement, restent à être identifiés. Il est possible que des virus qui seraient hautement réplicatifs augmenteraient d'autant plus l'activation de PRR et induiraient plus d'inflammation initiale ou auraient une capacité plus importante à infecter les cellules endothéliales. Nous avons également observé que le VIA développait des stratégies pour échapper au système immunitaire. Ainsi, l'incorporation d'A5 dans la particule virale permet au virus de bloquer la signalisation induite par les IFN- $\gamma$  et permet au virus de mieux se répliquer (article 3). Donc, les capacités intrinsèque des sous-types de virus mais aussi leur capacité à exploiter le système de l'hôte pourraient contribuer à la pathogénicité des VIA et à la dérégulation de l'hémostase.

Bien que les études soient relativement récentes, de nombreuses études ont montré que l'hémostase est activée durant les infections grippales. Tout d'abord, une étude a montré que

suite à une infection influenza, chez la souris et chez l'homme, les plaquettes étaient activées (Boilard E 2014, Garcia et al 2010). Ensuite, Keller et ses collaborateurs ont montré chez la souris, que le VIA induisait une production de thrombine et que la fibrinolyse était activée (Keller 2006). Ces résultats ont été confirmés chez le furet également (Goeijenbier et al 2014). Au vu de nos résultats, une dérégulation à ce niveau pourrait donc avoir lieu. Nous avons montré, lors de ma thèse, que le plasminogène et l'hyperfibrinolyse étaient délétères durant les infections grippales (article 2). Nos résultats montrant un effet délétère de la fibrinolyse dans les infections grippales sont en accord avec des études cliniques montrant que l'augmentation accrue de D-Dimer, marqueurs de la fibrinolyse, était un facteur de risque durant des infections induites par des virus hautement pathogènes H5N1 et des virus H1N1 pandémiques (Soepandi et al 2010, Wang et al 2011). Ceci pourrait expliquer pourquoi dans certains cas graves d'infection grippale, la pathogénicité des VIAs a été associée à des troubles de saignement (Urso et al 2011). Cet effet néfaste du PLG et de la fibrinolyse ne semble pas restreinte aux virus influenza puisque des effets similaires sont aussi observés durant les infections bactériennes (Degen et al 2007). Nous proposons ainsi un modèle (**Figure 11**, et annexe 1) dans lequel, durant les infections de grippe sévères, avant que le clou plaquettaire ne permette la réparation de la lésion, le caillot serait éliminé par une hyperfibrinolyse. L'activation du PLG et de la plasmine ainsi que les PDF, par leur activité chimoattractants, envahiraient le poumon et pourraient être responsables de l'orage cytokinique. Par ailleurs, au vu de nos résultats sur le rôle délétère des plaquettes durant les infections grippales (voir annexe 2), il est possible que ces dernières, présentes au niveau du site infectieux et associées aux leucocytes participent aussi à l'hypercytokinémie. Étant donné que PAR1 agit en amont de l'activation du PLG (voir article 1), il est probable que le rôle délétère de PAR1 passe par une augmentation d'une fibrinolyse incontrôlée.

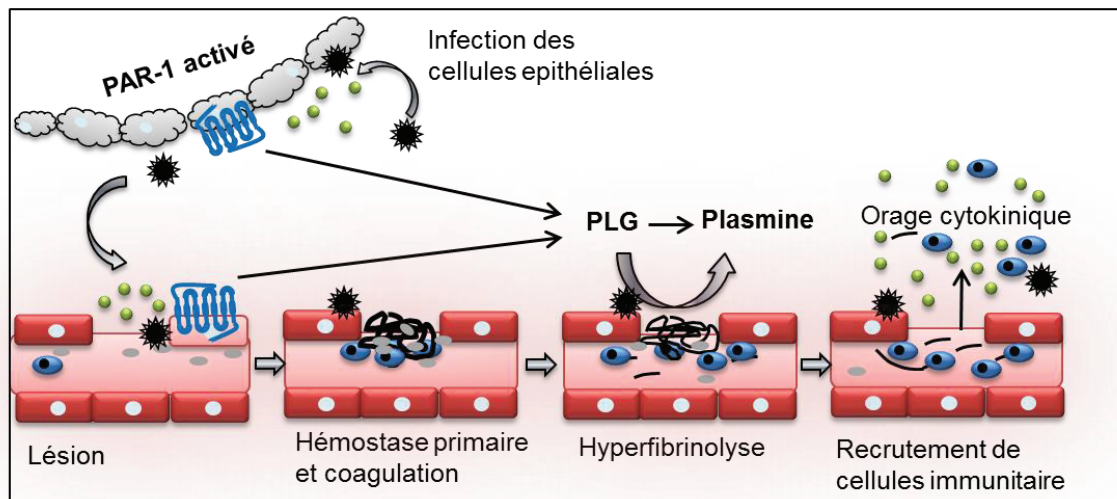


**Figure 12 : Modèle d'induction de l'avalanche cytokinique durant les infections grippales.**

Lors d'une infection grippale sévère, l'endothélium est agressé ou stimulé. Après activation de l'hémostase, l'activation excessive du plasminogène en plasmine induit une dérégulation de la fibrinolyse. La dissolution du caillot s'effectue avant que la réparation vasculaire n'ait lieu. La perméabilité vasculaire non restaurée conduit à l'avalanche de cytokines et au recrutement des leucocytes dans le poumon infecté. PAR1 agit en augmentant la fibrinolyse induite par les virus influenza.

Nos résultats pourraient avoir une forte répercussion sur la santé pour le bénéfice des patients. En effet, la principale raison de l'émergence de virus résistants est que la cible des antiviraux actuels est une protéine virale, la NA, dont le taux de mutation est extrêmement élevé. En ciblant une protéine de l'hôte, telle que la plasmine ou PAR1 et non le virus, cette stratégie ouvre la possibilité de réduire l'inflammation délétère des poumons, tout en réduisant l'émergence de virus résistants. Par ailleurs, en ciblant une protéine de l'hôte et non le virus, nos travaux apportent l'opportunité d'une alternative thérapeutique quelle que soit la souche du virus influenza. La preuve de concept de l'efficacité des molécules contre un spectre large de virus influenza a été apportée chez la souris, à la fois en ce qui concerne les antagonistes de PAR1 et les inhibiteurs du PLG. Nous avons en effet observé une protection contre des virus de sous-type H1N1, H3N2, H5N1 hautement pathogènes. De manière intéressante, certains principes actifs dont nous avons testé l'efficacité chez l'animal, sont commercialisés pour l'administration chez l'homme, tel que l'anti-fibrinolytique 6-

aminohexanoic acid (Amicar). Les PAR1 antagonistes, quant à eux, sont actuellement en phase III clinique pour d'autres applications thérapeutiques. Ces principes actifs pourraient donc être testés rapidement contre les infections grippales puisque leur effet secondaire chez l'homme a bien été étudié. En conclusion, nos résultats ouvrent des perspectives thérapeutique contre la grippe en ciblant la composante inflammatoire de la maladie et non le virus afin d'éviter les phénomènes de résistance virale et agir sur un spectre plus large de virus influenza.

## PERSPECTIVES

## Perspectives

Les perspectives actuelles sont de mieux comprendre le rôle de l'hémostase lors des infections grippales, notamment le rôle des plaquettes et de la coagulation. Un récent rapport montre que les plaquettes sont activées par la thrombine chez la souris. Il est donc possible que celle-ci soit à l'origine de ce défaut généralisé de la réponse de l'hôte. Nos résultats (voir article annexe 2, en révision dans AJRCCM) montrent que les plaquettes sont activées lors des infections grippales et ont un effet délétère chez la souris. Nos perspectives aujourd'hui, sont aussi de tester si des protéines virales et en particulier la protéine virale M2 pourraient favoriser cette dérégulation de l'hémostase. En effet, la protéine M2 est un canal à proton, nécessaire à la réplication virale. Plus récemment, il a été démontré que la protéine M2 jouait également un rôle dans l'activation du complexe inflammasome NLRP3/ASC/capase-1 (Ichinohe et al 2010) qui induit la production IL-18 et IL-1 $\beta$ , ces dernières étant des cytokines pro-inflammatoires multifonctionnelles notoires qui sont aussi fortement impliquée dans l'activation de l'hémostase (Yang et al 2013). Ainsi, la protéine virale M2 en modulant l'inflammasome pourrait via l'IL-1 $\beta$  induire à la fois (1) des modifications de l'intensité inflammatoire mais aussi (2) moduler l'hémostase et jouer un rôle important dans la résolution de l'inflammation. C'est dans l'objectif d'étudier cela que nous avons récemment produit par reverse génétique des virus influenza qui expriment des protéines M2 de virus hautement pathogènes (H5N1), faiblement pathogènes ou pandémiques dans deux fonds génétiques distincts : A/PR/8/34 (H1N1) et A/Memphis/14/98 (H3N2), en collaboration avec le Dr. DR Perez (Washington DC, USA).

*In vitro* sur cellules humaines, nos résultats préliminaires montrent que les virus exprimant la M2 des virus influenza aviaires hautement pathogènes (H5N1) et pandémiques induisent de manière significative beaucoup plus d'IL-1 $\beta$  (mais pas IL-6) en comparaison avec des virus exprimant des M2 de virus IAV moins pathogènes, alors que ces virus se

répliquent de la même manière. Nous souhaitons maintenant savoir si cette différence de production d'IL1 $\beta$  pourrait impacter l'activation de l'hémostase et notamment la production de thrombine. La thrombine étant à l'origine de l'activation des plaquettes, cela permettrait de comprendre quels sont les facteurs viraux et cellulaires à l'origine de l'activation, probablement incontrôlée des plaquettes.

## ANNEXES

**Annexe n°1: Switch from protective to adverse inflammation during influenza: viral determinants and hemostasis are caught as culprits**

Fatma Berri, Vuong Ba Le, Martine Jandrot-Perrus, Bruno Lina, Beatrice Riteau.

**CMLS, 2014. Doi: 10.1007/s00018-013-1479-x**

# Switch from protective to adverse inflammation during influenza: viral determinants and hemostasis are caught as culprits

Fatma Berri · Vuong Ba Lê · Martine Jandrot-Perrus ·  
Bruno Lina · Béatrice Riteau

Received: 28 May 2013 / Revised: 21 August 2013 / Accepted: 16 September 2013  
© European Union 2013

**Abstract** Influenza viruses cause acute respiratory infections, which are highly contagious and occur as seasonal epidemic and sporadic pandemic outbreaks. Innate immune response is activated shortly after infection with influenza A viruses (IAV), affording effective protection of the host. However, this response should be tightly regulated, as insufficient inflammation may result in virus escape from immunosurveillance. In contrast, excessive inflammation may result in bystander lung tissue damage, loss of respiratory capacity, and deterioration of the clinical outcome of IAV infections. In this review, we give a comprehensive overview of the innate immune response to IAV infection and summarize the most important findings on how the host can inappropriately respond to influenza.

**Keywords** Influenza virus · Inflammation · Hemostasis · Innate immune sensors · PAR1 · Plasminogen · Fibrinolysis · HLA-G

---

F. Berri · V. B. Lê · B. Lina · B. Riteau (✉)  
VirPath, EA4610 Virologie et Pathologie Humaine, Faculté de  
médecine RTH Laennec, Université Claude Bernard Lyon 1,  
Université de Lyon, 69008 Lyon, France  
e-mail: beatrice.riteau@univ-lyon1.fr

M. Jandrot-Perrus  
Inserm, U698, Paris, France

M. Jandrot-Perrus  
Université Paris 7, Paris, France

M. Jandrot-Perrus  
AP-HP, Hôpital Xavier Bichat, Paris, France

B. Riteau  
INRA, Nouzilly, France

## Introduction

Influenza is one of the most important causes of respiratory tract infection and is responsible for widespread morbidity and mortality every winter in moderate climate zones [1, 2]. Worldwide, influenza epidemics result in about 200,000–500,000 deaths each year. In addition to the epidemic outbreaks, a virus of animal origin (usually avian) can also be transmitted to humans and cause a pandemic, which can range from mild (200,000 deaths) to unusual but severe impacts in the population (40 million deaths for the Spanish 1918 pandemic). Thus, influenza is of great concern for human health.

The etiological agents of the disease, the enveloped single-stranded negative-sense RNA influenza viruses, are classified into three types (A, B, and C), of which influenza A virus (IAV) is clinically the most important [2–4]. IAV particles possess two viral surface glycoproteins, hemagglutinin (HA, organized in trimers) and neuraminidase (NA, organized in tetramers) and one matrix-2 protein (M2, organized in tetramers) (Fig. 1). Inside the virion, eight segments of negative-sense RNA are independently encapsidated by the viral nucleoprotein (NP) and a polymerase complex (PB2, PB1, PA), forming the ribonucleoprotein (RNP) complexes. The RNPs are surrounded by a layer of the matrix protein, M1, which line the envelope. In the initial phase of IAV infection, the homotrimer of HA binds to sialic acid on the surface of the host cell, allowing the endocytosis of the virus [4] (Fig. 2). In the endosome, under external acidic pH, the tetrameric channel of M2 proteins conducts protons into the virion, resulting in the dissociation of M1 from the RNP. Fusion of the viral and endosome membranes is mediated by the cleaved HA, which exposes its fusion peptide under acid pH. The vRNPs are then released from the endosome and transported to

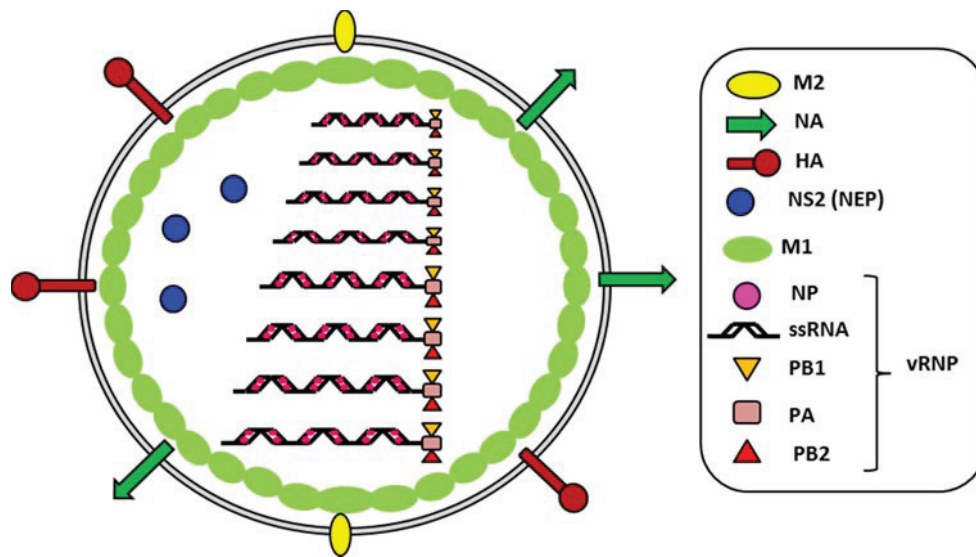


**Fig. 1** Structure of the IAV particle. The virion consists of 8 vRNP (ssRNA, NP, PB1, PB2, PA) surrounded by M1 proteins and an envelope derived from the plasma membrane of the host cell. The

viral HA, NA, and M2 as well as host proteins such as annexins (not shown) are incorporated into the envelope

the nucleus, where replication occurs. The newly synthesized viral RNAs are produced through a complementary positive stranded intermediate RNA (cRNA), which represents a full-length copy of the vRNA. In the nucleus, the polymerase also allows the transcription of the genome into mRNA, which is then transported back to the cytoplasm and translated into viral proteins. Each RNA segment (S) encodes one or two proteins. Proteins NP, PB1, PB2, and PA re-enter the nucleus to form the RNP complex with vRNA. M1 and NEP also re-enter the nucleus and their binding to the vRNPs allows their export to the cytoplasm. Instead, HA, NA, and M2 are transported to the plasma membrane via the reticulum/Golgi route. RNPs bud from the plasma membrane, which expresses the viral HA, NA, and M2 viral proteins to form the newly synthesized IAV virions [4] (Fig. 2). The glycoprotein content of viral proteins on the surface of IAV varies between IAV strains and is dependent on the viral genomic composition of the virus particles [5]. Also, because the envelope is derived from the plasma membrane of the host cell, host cellular proteins such as annexins are also incorporated into the virions [6, 7]. The neuraminidase plays an important role in the last steps of the budding, as it prevents direct re-association of the viral HA with sialic acid of the host cells, so IAV particles can be released [4]. The HA and NA of IAV exhibit a high sequence variability and based on their antigenic differences, IAV are divided into subtypes. To date, 17 HA and ten NA subtypes have been described for IAV [3]. While the bird is the reservoir of all IAV subtypes, only H1, H2, H3, and N1, N2 subtypes have caused infections in humans. Currently, only IAV of the H1N1 and H3N2

strains have established sustained human-to-human transmission. It is noteworthy that in addition to the epidemic outbreaks, a virus of animal origin (usually avian) can also be transmitted to humans and could cause a pandemic if the virus becomes transmissible from human to human. To date, recurrent human infections with IAV of the H5N1 virus subtype and more recently with the newly emerged H7N9 virus has highlighted the important threat caused by influenza [8–10].

Upon infection with IAV, immune responses are induced that protect the host efficiently [1]. However, when the response to the infection is inappropriately regulated, a deterioration of the respiratory capacity and the clinical outcome of IAV infections can be observed (Fig. 3) [11]. On one hand, if the response is low, the virus can escape immune-surveillance and replicate within the host, leading to a severe infection. On the other hand, hypercytokinemia and excessive recruitment of innate immune cells induce collateral damage of the lungs and increase the immunopathology of influenza. Thus, a better understanding of the mechanism by which inflammation is induced as well as how it fails or turns inappropriate for the host is necessary in order to develop more efficient means of treatment against influenza.

### The innate immune response to IAV infection

During the first days of IAV infection, viral replication, particularly in epithelial cells but also in monocytes, macrophages, or dendritic cells, initiates a cascade of signaling

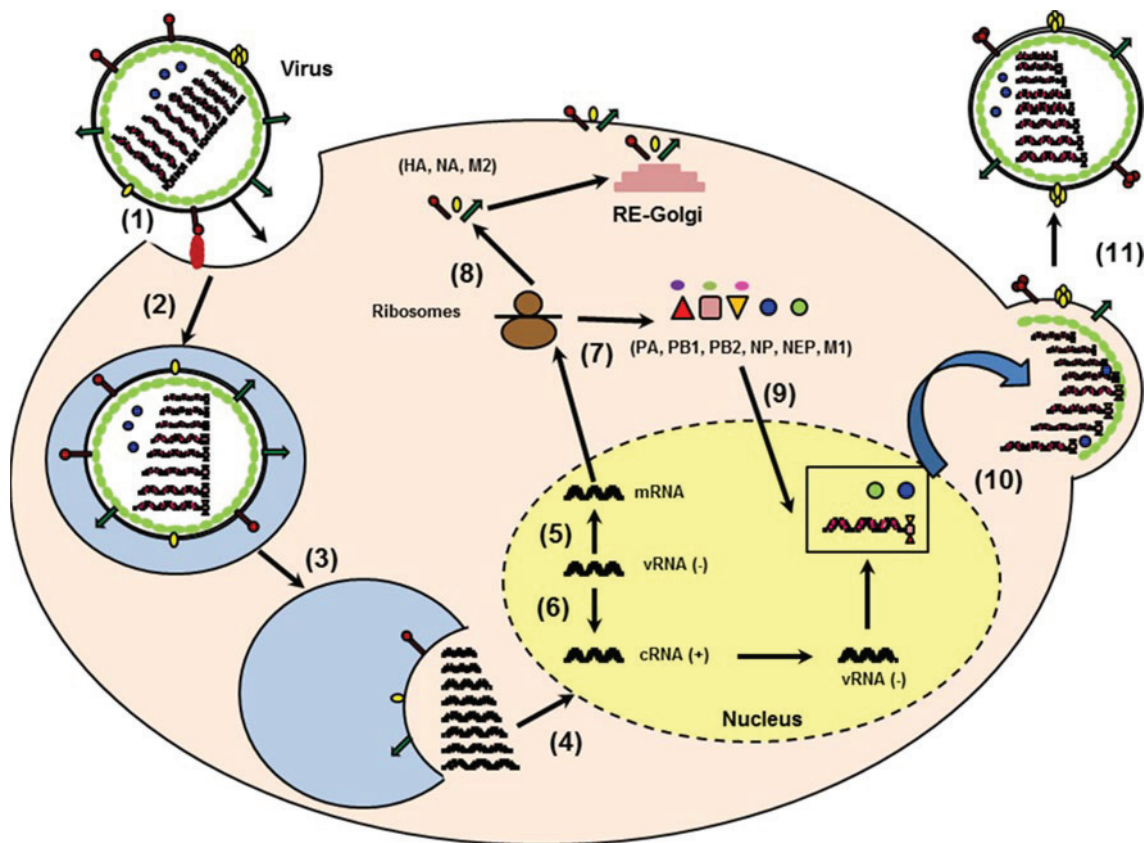


**Fig. 2** Schematic representation of the replication cycle of IAV. The viral HA binds to sialylated glycoprotein receptors (1) and upon binding the virus becomes endocytosed (2). From the endosome, the virus genome is released following a low PH-dependent fusion event mediated by HA (3). The RNPs are transported to the nucleus (4) where the transcription (5) and replication (6) occur. The newly synthesized viral RNAs are produced through a complementary positive-stranded intermediate RNA (cRNA). The mRNA are transported to the cyto-

plasm and translated into protein (7). HA, NA, and M2 are transported to the plasma membrane through the reticulum/Golgi route (8) while PB1, PB2, PA, NP, NEP, and M1 re-enter the nucleus (9). Association of M1 and NEP with the vRNA complex (vRNA, NP, PA, PB1, PB2) allows the translocation of the vRNPs (10). Budding of the vRNP/M1/NEP from the plasma membrane expressing host proteins and HA, NA, and M2 form the new virions (11)

pathways involving a myriad of innate immune sensors, called pattern-recognition receptors (PRRs) [12] (Fig. 4). Activation of these receptors results in the release of cytokines and chemokines, which promote a local antiviral state and the recruitment of immune cells to the site of infection. The innate immune response includes both the production of secretory molecules and the recruitment of the cellular components of the immune system. In this paragraph, we will summarize our current knowledge on the innate immune response to influenza.

#### Secretory molecules and pattern-recognition receptors activation

Secretory molecules are key mediators of antiviral immunity. Type I-IFN are the major cytokines that limit viral replication [13]. However, they are not sufficient for effective clearance of the virus, which evolved sophisticated

strategies to escape immune-surveillance [13]. Thus, local proinflammatory cytokines are also extremely important for immune cell recruitment to the site of infection and to promote adaptive immune response [1, 14]. Each cytokine is produced in a cell-type-dependent manner. Thus, the nature of the cytokines that are present in the respiratory tract varies as the infection progresses. It is also dependent on the strain of the virus since cell susceptibility is subtype-dependent. Although simplified, the first target of influenza is the epithelial cell and interleukin 6 (IL-6), IL-8 and regulated on activation, normal T cell expressed and secreted (RANTES) will be first release. Then, in addition to IL-6 and IL-8, infected alveolar macrophages will release macrophage inflammatory proteins (MIP), IL-1 and tumor necrosis factor- $\alpha$  (TNF- $\alpha$ ) while infected dendritic cells will produce additional TNF- $\alpha$ , IL-1, IL-6, and MIP [15]. Each cytokine has specific major functions and thus the relative level of each cytokine will drive the host response

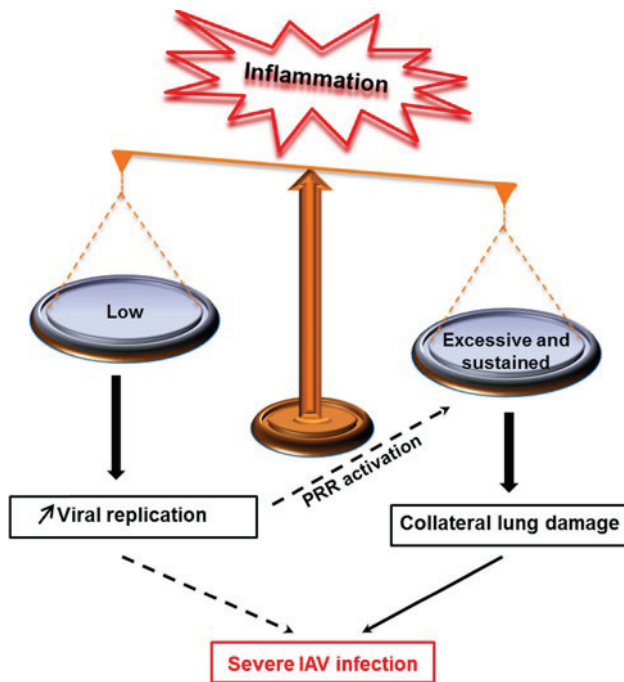


**Fig. 3** Model of unbalanced inflammation following influenza infection. When the response to influenza infection is low or excessive, immunopathology of influenza develops. Strong interplay may exist between insufficient versus excessive inflammation. Immune escape from immunosurveillance (low response) may increase viral replication, which in turn induces strong release of secretory molecules (intensity of infection). When excessive inflammation is sustained by an uncontrolled host response, collateral lung damage increases IAV pathogenesis

(Fig. 4). A high level of IL-1, IL-6, or TNF- $\alpha$  broadly provokes the inflammatory response and causes fever. In contrast, a high level of IL-8 (KC in mouse) or MIP proteins attract and activate neutrophils, while of MCP-1 promote monocytes recruitment [15]. Although the cytokines have specific functions and are released in a cell-type-dependent manner, all of them are produced/activated via a common mechanism involving the activation of PRRs (Fig. 4). Three PRRs detect influenza via pathogen-associated molecular patterns and initiate the release of secretory molecules. Those receptors are the Toll-like receptors (TLR), the RIG-I like receptors (RLR), and the Nod-like receptors (NLR). Thus, TLRs constitute the first group of PRRs that sense influenza and are themselves divided into two groups based on their localization and type of ligand. The first group includes TLR 1, 2, 4, 5, and 6 that are cell surface-expressed and are activated by non-nucleic acid pathogen components. The role of the first group in the defense against IAV infection was poorly investigated and remains controversial [16–18]. The second group includes TLR 3, 7, 8, and 9, which are endosome-localized receptors, recognizing nucleic acids. The intracellular localization of the

second group facilitates recognition of IAV, which enter host cells by endocytosis. All TLR, except TLR3 activate NF- $\kappa$ B (proinflammatory) and IRF3/7 (antiviral) through a common signaling adaptor MyD88. Instead, TLR3 recruits TRIF that can also be activated by TLR4. Upon IAV infection, TLR7 or MyD88-deficient dendritic cells are unable to release type-I IFN, in marked contrast to infected wild-type or TLR9-deficient cells [19, 20]. Thus, TLR 7 and 8, which specifically recognize ssRNA, are the main sensors of the ssRNA influenza virus [12, 19–21], while TLR9 does not seem to play a role. In contrast, the antiviral effect of TLR3 (that recognizes dsRNA intermediates) and TRIF remain obscure [22, 23].

The RLRs constitute the second group of PRRs, which sense influenza. RLR are cytoplasm-based receptors that recognize dsRNA and comprise three members; RIG-I, the melanoma differentiation-associated gene 5 (MDA5), and the laboratory of genetics and physiology 2 (LGP2). RLR signal through the mitochondrial antiviral-signaling protein (MAVS) signalosome leading to NF- $\kappa$ B and IRF3 activation. All three receptors contain a helicase domain while RIG-I and MDA 5 also contain a caspase recruitment domain, which allow them to overlap the role of inflammasome for IL1- $\beta$  release (please see below). Upon IAV infection, RIG-I, which detects 5' triphosphate RNA [24] and possibly containing short dsRNA structure motifs, but not MDA5, which recognizes stable dsRNA structures, are activated by IAV, while the role of LGP2 is not, so far, well defined. It was indeed demonstrated that RIG-I-deficiency but not MDA5-deficiency affects the release of IFN in response to IAV infection [25]. Finally, the cytosolic NLR receptors form the last group of PRRs that sense IAV. NLR are divided into subfamilies based on their difference in their effectors domains, leading to inflammatory response, autophagy, or cell death. Upon activation, NLR involved in inflammation assemble into platforms called inflammasomes to activate caspase-1 and trigger the maturation and secretion of IL-1 and IL-18, cytokines that play an important role during Flu infections [26]. Those cytokines are synthesized as inactive molecules, which upon enzymatic cleavage by caspase-1 become active and are secreted. So far, four members of the NLR family have been reported to initiate inflammasome multimeric protein platforms: NLRP1, NLRP3, NLRP6, and NLRC4. During macrophages infection by IAV, both the viral RNAs and the viral matrix 2 protein (M2) would be required to produce mature IL1- $\beta$  via activation of two signals (Fig. 5) [27]. Signal 1 allows pro-IL1 synthesis through TLR7 activation and signal 2 activates the complex NLRP3/ASC/caspase-1 for cleavage of pro-IL-1 into mature IL-1 by active caspase-1. The complex NLRP3/ASC/caspase-1 is activated when ionic concentration is modified by the proton channel activity of the viral M2 protein. In marked contrast to macrophages,

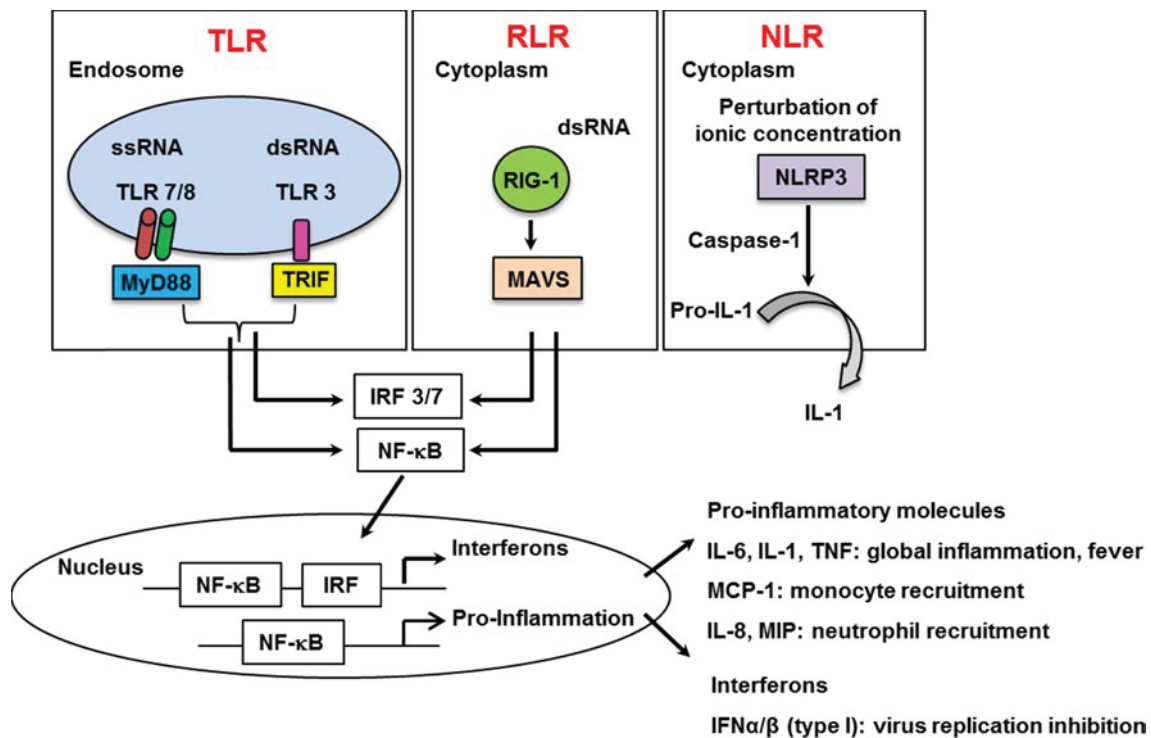


**Fig. 4** Pattern-recognition receptors (PRRs) sensing influenza viruses. Three groups of PRRs (TLR, RLR, and NLR) are able to sense influenza viruses. TLR7/8 and TLR3, endosome-expressed receptors, are activated by nucleic acids upon IAV infection. RIG-I,

expressed in the cytoplasm recognizes the 5'triphosphate genome of influenza. NLRP3 is activated upon modification of ionic concentration mediated by the viral M2 protein of influenza. Activation of PRRs allows the release of both pro-inflammatory cytokines and IFN

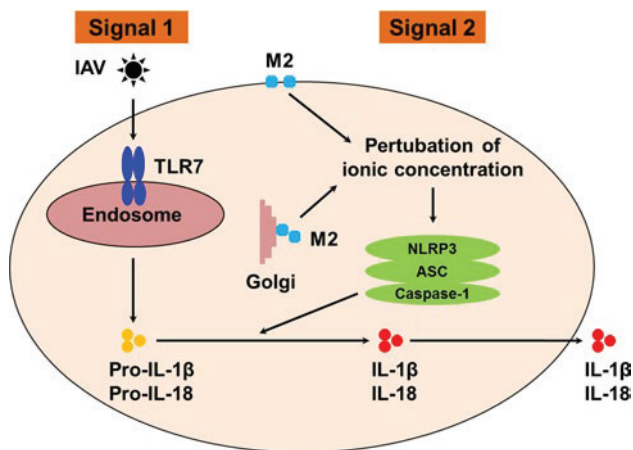


**Fig. 5** Signals required for IL1 and IL18 release in IAV-infected macrophages TLR7/8 senses influenza and initiates pro-IL-1β (and pro-IL18) synthesis (Signal 1). NLRP3 senses modification of ionic concentration mediated by the viral M2 protein upon IAV infection leading to the assembly of the complex NLRP3/ASC and caspase-1, which is then activated. Caspase1 activation cleaves the immature cytokines into mature IL1 and IL18

IL-1 secretion pathway is different in monocytes, where caspase-1 is constitutively active, and where signal 2 is not necessary [27]. However, the effect of NLRP3 in the

experimental model of IAV infection remains controversial. It was initially reported that caspase 1 and IL1-deficient mice (but not NLRP3-deficient mice) are more susceptible to influenza [28]. However, another report showed that NLRP3 deficiency increased influenza-induced mortality [29]. In addition, release of IL1-β by signal 2 may be more complex than a simple NLRP3 activation. Indeed, a recent report has provided evidence that a strong interplay between NLR, TLR, and RLR is necessary to ensure efficient IL1-β release upon IAV infections, at least in epithelial cells [30].

Altogether, PRRs are the way by which the host responds primarily to influenza. PRRs, however, are differently expressed between cell subtypes, and cellular tropism of IAV differs between virus subtypes. Thus, this adds complexity in the understanding of the regulation of cytokine production upon IAV infections. The most remarkable example of this complexity is that within one cell subtype, such as macrophages, marked differences can be observed as well. Resident macrophages produce fewer pro-inflammatory cytokines compared to blood-derived macrophages and the latter are also more susceptible to highly pathogenic influenza [31]. Altogether, the combination of all these events likely modulates the quality and the quantity of the cytokine response, which will subsequently drive the protective versus disruptive effect of inflammation.

## The cellular components of the inflammation

As mentioned above, cytokines and chemokines that are released upon infection contribute to the recruitment and activation of immune cells, thus facilitating the antiviral defense against the infection. Among the cellular components involved against influenza, three major components of the innate immune response *stricto sensu* can be mentioned; i.e., neutrophils, macrophages, and natural killer (NK) cells. First, (1) neutrophils recruited in large numbers to the respiratory tract upon influenza infections are implicated in the protection of the host [32, 33]. Depletion of these cells, in IAV-infected mice, increases viral replication, pulmonary inflammation, as well as mortality of the mice [32, 33]. Neutrophils eliminate the virus via different pathways, which include the phagocytosis of apoptotic IAV-infected cells and the degranulation and the production of reactive oxygen species, which assist in the clearance of infected cells [34, 35]. Another important additional weapon of neutrophils against pathogens is the release of neutrophil extracellular trap (NET), which arises from their nuclear contents into the extracellular space and are composed of decondensed chromatin and antimicrobial proteins. It was clearly demonstrated that NETs are formed upon IAV infections, although their role remains controversial [36, 37]. Altogether, neutrophils are important players against influenza. However, excessive recruitment of neutrophils to the lungs is also a major contributor of severe IAV infections and is typically observed upon mice infection with highly pathogenic H1N1 and H5N1 viruses [37, 38]. Their over-reaction further contributes to excessive lung inflammation and additional release of secretory molecules and particularly IL-1, TNF, or MIP proteins.

In addition to neutrophils, alveolar macrophages as well as newly recruited monocytes, which differentiate into macrophages, also contribute to innate immunity against influenza [32]. Macrophages eliminate cellular debris and apoptotic infected cells by phagocytosis. They also act as antigen-presenting cells and contribute to the induction of the adaptive immune response. Depletion of these cells increases lung viral replication as well as pathogenesis and death upon IAV infection [32, 39]. However, as for neutrophils, the presence of excessive macrophages in the lungs is a sign of severe IAV infection, suggesting that these cells could also contribute to the immunopathology of influenza [38]. Finally, the third innate cellular component recruited to the lungs upon IAV infection and playing a key role in IAV immune-surveillance are NK cells [40]. Upon activation, NK cells secrete cytokines and chemokines, and kill sensitive target cells by releasing the content of cytolytic granules [41, 42]. NK cell activation is orchestrated through a balance of inhibitory receptors (KIR) versus activatory (KAR) receptors

[43]. First, NK cells detect the loss of human-leukocyte antigen (HLA) at the surface of infected cells via absence of engagement of KIRs, an activation known as the missing self-signal. Secondly, NK cells sense infected targets that express ligands for activation receptors, known as the danger signal [44]. When positive signals tend to be dominant, the functional outcome is tilted in favor of NK responsiveness. Surprisingly, while most viruses down-regulate the expression of HLA molecules at the surface of infected cells, IAV does not alter HLA expression on infected target cells [45] or does so only slightly [46]. IAV even augments NK cell inhibition through reorganization of HLA molecules into lipid rafts [45]. Thus, activation of NK during influenza is not due to a missing self-signal. Instead, during influenza, the KARs, NKp44 and NKp46 (but not NKp30), are engaged by the HA of IAV, which leads to NK cell activation [47–49]. *In vivo*, mice deficient in NKp46 receptor are more susceptible to IAV infection, demonstrating the importance of NK cell function against influenza [50]. However, as for all the components of the innate immune system, NK cells function can turn deleterious for the host. It was indeed demonstrated that NK cells can also contribute to the pathogenesis of IAV infection [51, 52]. Altogether, this illustrates the importance to consider the severity of infection regarding a protective or deleterious role for any component of the immune response. For example, the role of other cell types of the immune system such as the mucosal-associated invariant T cells could be revised. Their function was initially shown to be restricted to bacterial infections [53] but their role during influenza may be crucial, depending on the type of infection and more importantly during IAV coinfection with bacteria.

## Viral escape from immunosurveillance

To evade the immune system, IAV has adopted strategies to efficiently replicate within the host [54]. Viral determinants such as the nonstructural protein 1 (NS1) and PB1-F2 block the antiviral IFN response and induce apoptosis of the recruited cellular components of the immune system, which enable them to react [55]. In addition, IAV upregulates the expression of the powerful immunotolerant human leukocyte antigen-G molecule (HLA-G) [56]. We will here highlight our current knowledge on how IAV manipulate these powerful molecules to escape immune-surveillance.

### Role of the NS1 viral protein

NS1 is a nonstructural viral protein that antagonizes host immune responses [13]. The segment 8 of influenza vRNA, also known as the NS gene, encodes two proteins. The

primary transcript generated encodes the NS1 protein. The second protein, NS2 (or NEP), is generated by alternative splicing of the primary transcript [57]. Recombinant viruses unable to express NS1 are viable but induce robust IFN secretion and show an attenuated phenotype *in vitro* and *in vivo*, which demonstrates the role of NS1 in the virulence of IAV [58]. The major function of NS1 is to limit the antiviral effect of IFN via different pathways. On one hand, NS1 blocks signaling by IRF3 and NF- $\kappa$ B [59, 60] and RIG-I activation [61, 62]. On the other hand, NS1 blocks IFN secretion at the posttranscriptional level with strong inhibition of IFN mRNA synthesis and post-transcriptional processing of IFN [63, 64]. In addition, NS1 is a key player in the manipulation of cell apoptotic machinery [65]. It was demonstrated that NS1 interact with tubulin, leading to disruption of normal cell division and apoptosis [66]. The length of NS1 is variable and strain-specific. In particular, at the C-terminus of NS1, truncations or extensions were observed [3]. While NS1 predominantly localizes in the nucleus and cytoplasm, those modifications may have consequences in its localization and most likely in its function [67]. The fact that NS1 is a virulence factor of IAV makes it a good target to attenuate these viruses. Several studies demonstrated that IAV with partial deletions in NS1 proteins are attenuated and do not cause disease, but induce a protective immune response in different species. These IAV variants are excellent live-attenuated influenza vaccine candidates, which could be of high interest in the future [68].

#### Role of PB1-F2

PB1-F2 is a proapoptotic viral protein that is expressed from an alternative open reading frame in the PB1 gene of IAV [69]. Some influenza strains do not express PB1-F2 and thus it is not required for viral replication. Nevertheless, PB1-F2 has been established as an important factor of virulence of influenza [70, 71]. Recombinant viruses unable to express PB1-F2 protein are less pathogenic in mice [72]. In addition, viruses with a single mutation in PB1-F2 (N66S) are highly pathogenic in mice as a consequence of increased viral replication [71]. The way by which PB1-F2 mediates increased viral replication is through inhibition of RIG-I-mediated type I IFN production at the level of the MAVS pathway [73–75]. The serine at position 66 (66S) in PB1-F2 further enhances IFN antagonism activity. PB1-F2 also induces apoptosis. After phosphorylation by protein kinase C, PB1-F2 interacts with the inner mitochondrial membrane adenine nucleotide translocase 3 and the outer mitochondrial membrane voltage-dependent anion channel 1, leading to permeabilization and destabilization of mitochondrial membrane, which results in cell death [74–76]. Also, another interesting characteristic of PB1-F2 is its

contribution to the virulence of subsequent secondary bacterial pneumonia [77].

#### Role of the nonclassical host HLA-G molecule

The major histocompatibility complex molecule, HLA-G, is a non-classical antigen, which expression is mainly restricted to the cytotrophoblast, during pregnancy [78]. Several isoforms of HLA-G have been described that exhibit immunotolerant properties and are key factors in maternal-fetal tolerance [78–80]. HLA-G inhibits the lytic activity of NK cells [81, 82] as well as antigen-specific cytotoxic T cells directed against influenza (CTL) and allogeneic proliferative responses [83–85]. Recently, HLA-G has emerged as a key molecule in the evasion of immune response to several pathologic situations, such as tumors [86–90] and bacterial and viral infections, including influenza [56, 91–95]. HLA-G is upregulated at the surface of IAV-infected cells in a strain-dependent manner, at both the mRNA and protein levels [96]. These results suggest that the virulence of IAV may be caused by the differential capability of different strains to upregulate HLA-G. In line with this report, elevated HLA-G expression was ectopically observed in pandemic and seasonal IAV-infected patients [97]. HLA-G has been found to play an important role in several other viral infections and its expression has been correlated with increased severity of infection and poor survival of infected patients [92–95]. Given its broad immune-tolerant properties, by upregulating HLA-G, IAV may efficiently escape from immune surveillance and this likely contributes to IAV pathogenesis.

#### Uncontrolled deleterious inflammation

Resolution of inflammation is an integral component of the program of acute inflammation. It is absolutely required to protect healthy cells from tissue damage and is a prerequisite for the return of tissue homeostasis. When inflammation is inappropriately regulated, it becomes persistent and excessive. This deregulated inflammation, known as a “cytokine storm”, exacerbates the immunopathology of influenza [98]. Compared to uncomplicated patients, abnormal elevated levels of cytokines and chemokines are commonly detected in severe influenza infections [11]. Here, we will discuss the possible mechanism leading to the uncontrolled inflammation associated with severe influenza infections.

#### Role of the viral determinants

The role of viral replication in the virulence of IAV is still debated. Clinical studies showed that in severe influenza

cases, a high level of virus replication and an excessive inflammatory response can be observed [11]. Whether a direct correlation exists between viral replication and the deregulated immune response remains an open question. An emerging idea is that a high level of virus replication likely contributes but is not the only culprit of excessive inflammation during influenza. The so-called “cytokine storm” would result from two components, which are (1) a high intensity of inflammation mediated by increased viral replication and PRR activation and (2) a sustained inflammation that results from an improper host response. Thus, some viral determinants are assumed to be associated with increased viral replication as well as excessive inflammation. Not surprisingly, chimeric viruses expressing strong activity of the polymerase complex (PA, PB1, and PB2) replicate more efficiently and are a potent inducer of pro-inflammatory cytokines and chemokines [99]. Also, the PA gene of a highly pathogenic H5N1 virus contributes to its virulence through increased viral replication and subsequent induction of an excessive innate immune response [100]. Another viral determinant that could impact viral replication and cytokine/chemokine release is the presence of a multibasic site in the HA of IAV [56]. After entry into the cell, the virus genome is released from the endosome following a low pH-dependent fusion event mediated by HA, and this fusion occurs only when HA is cleaved. The HA of low pathogenic strains contain a monobasic site that can only be cleaved by extracellular trypsin-like proteases, which thus represent a restricted factor for viral replication. In contrast, the HA of highly pathogenic IAV contain a polybasic site that is cleaved by intracellular furin-type proteases that are present ubiquitously, facilitating viral replication [101]. Indeed, the production of excessive proinflammatory molecules was reported for strains with multibasic cleavage site in HA [102].

Also, as described above, viral proteins NS1 and PB1-F2 are also important determinants that can promote the deregulation of inflammation.

#### Role of host determinants and hemostasis deregulation

As just mentioned, virus replication is unlikely to be solely responsible for deregulation of innate immunity upon IAV infection. In particular, the crosstalk between the pathogen and the host is a crucial factor driving immunopathogenesis of IAV.

#### *Role of PAR1 in the transition between protective versus deleterious inflammation*

Proteases and their receptors have recently emerged as a contributor of immunopathogenesis during viral infections [56, 103, 104]. Protease-activated-receptor 1 (PAR1), a G

protein-coupled receptor, is activated as a result of proteolytic cleavage by thrombin, a protease central to the coagulation process. At a high concentration of thrombin, PAR1 plays a proinflammatory role, while at low concentration of thrombin, PAR1 mediates anti-inflammatory effects [105]. Using a mild IAV infection (observed by low levels of cytokine release in the broncho-alveolar lavages of infected WT mice), PAR1 was recently proposed to cooperate with TLR for IFN production [106]. Thus, according to the antiviral effect of TLR and IFN during IAV infections, these results are consistent with a potential protective effect of PAR1 during IAV infections (Fig. 6). The role of PAR1 in promoting innate immunity is platelet-independent, which is in favor of the presence of low concentration of thrombin and a moderate activation of endothelial cells [106]. Interestingly, and in marked contrast, we recently reported that during a severe lethal IAV infection, in which activation of the coagulation is likely to occur, resulting in high thrombin concentrations, PAR1 signaling was deleterious for the host [104]. Administration of PAR1 antagonists or PAR1 deficiency protected mice from lethal inflammation of the lungs. In contrast, activating PAR1 with specific agonists increased the cytokine storm and decreased survival. In addition, during severe infections, a cooperation between the activation of PAR1 and of the fibrinolytic system appeared to promote lethal inflammation [107] (Fig. 6 and discussed below). Similar deleterious role of PAR1 was also during meta-pneumovirus infections [108]. Thus, the severity of the infection likely determines the extent of IAV infection (epithelial versus endothelial cells) and the protective versus deleterious role of PAR-1-triggered anti versus pro-inflammatory responses. Accordingly, endothelial cells have recently emerged at the center of the uncontrolled inflammatory response induced by influenza [109]. The S1P1 receptor has a key position in the control of endothelial cell integrity and the routing of PAR1 towards anti-inflammatory versus proinflammatory responses [105]. At a low concentration of thrombin, PAR1 mediates endothelial barrier protection and anti-inflammatory effects through cross-activation of S1P1 receptor [105]. At a high concentration of thrombin, S1P1 is no longer activated and PAR1 signaling turns pro-inflammatory [105]. In fact, several reports showed that administration of S1P1 receptor (S1P1R) agonists blunt influenza-induced cytokine storm in mice and protect them from mortality induced by several IAV strains [109–111]. Altogether, it is tempting to speculate that modulation of the interactions between PAR1 and S1P1 contributes to regulate and orchestrate inflammation during influenza. More complex regulations of PAR1 may also involve cross-activation of (1) PAR2 [112], previously shown to protect against influenza [113] or (2) endothelial protein C receptor (EPCR) [114], although its role remains to be fully demonstrated [115, 116].

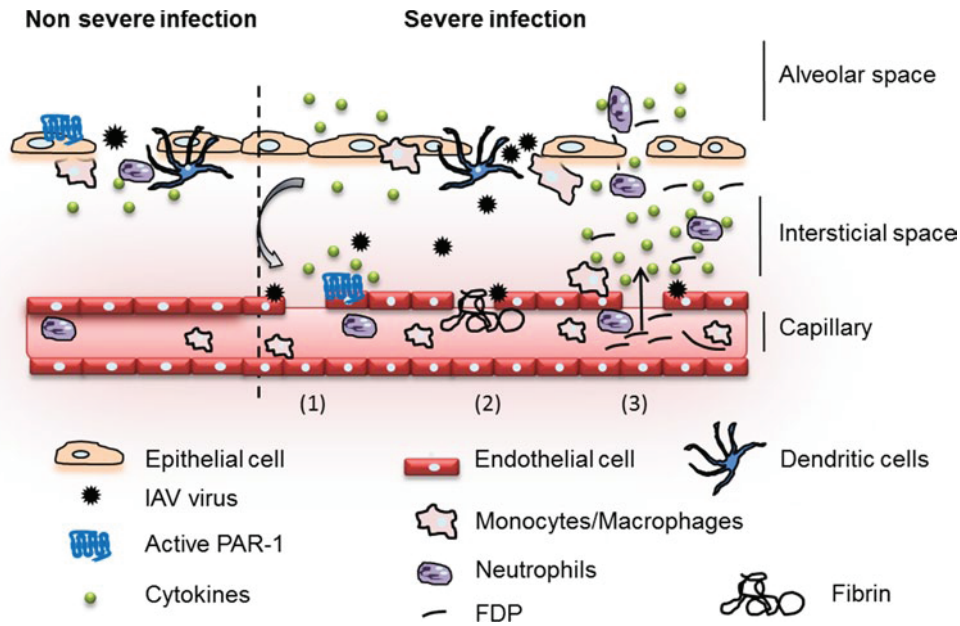


**Fig. 6** Model of protective and destructive inflammation during influenza. Upon IAV infection (non-severe infection), epithelial cells are infected and release secretory molecules promoting activation of the host immune response. Initial immune system activation is protective and aims at the elimination of the invading pathogen. PAR1, expressed at the surface of epithelial cells, cooperates with PRRs for effective activation of innate immunity against influenza. However, if

the infection is not controlled (severe infection), endothelial cells are injured (1). Hemostasis is activated (2) and deregulation of fibrinolysis through hyperactivation of plasminogen/plasmin promotes excessive and deleterious inflammation (3). PAR1, which is also expressed at the surface of the endothelium, cooperates with plasminogen and further exacerbates inflammation and injury

### Role of plasminogen and hyperfibrinolysis

Plasminogen is a zymogen that is activated into its active form plasmin by urokinase and tissue plasminogen activators (uPA, tPA). The main function of plasmin is to break down blood clots by dissolving fibrin polymers into soluble fragments, a process called fibrinolysis. Pericellular plasmin contributes to the remodeling of the extracellular matrix directly or indirectly via the activation of metalloproteases and could lead to cell anoikis when excessive [117]. The generation of plasmin activity is a tightly regulated process. However, since ever, pathogens have exploited the function of plasminogen/plasmin for their own benefit. Particularly, activation of plasminogen by bacteria increases extracellular matrix degradation and fibrinolysis, a way by which the pathogen disseminates within the host. At the same time, this dysregulation of plasminogen activation and fibrinolysis has been associated with excessive inflammation [118]. Not only bacteria but also viruses and IAV in particular have evolved several strategies to sequester and activate plasminogen, through viral or cellular proteins [6, 119, 120]. Neuraminidase of the IAV strain A/WSN/33 can bind plasminogen, conferring this strain with the capacity to replicate efficiently in the brain [119, 121]. IAV can also activate plasminogen through the host cellular protein annexin 2 (A2), which is upregulated at the

surface of infected cells and which is incorporated into the virions [6, 120]. Recently, we provided the first evidence that plasminogen plays a central role in influenza pathogenesis and cytokine storm [107]. We found that plasminogen-deficient mice or pharmacological inhibition of plasminogen activation in vivo protected mice from influenza infections and cytokine storm. Furthermore, pharmacological depletion of fibrinogen, the main target of plasmin had a profound deleterious effect on the survival of IAV-infected mice and this whether or not plasminogen activation is triggered (WT versus plasminogen-deficient mice), suggesting that fibrin is rather protective. Thus, these results pointed out for the first time that uncontrolled activation of the plasminergic system drives vascular permeability and excessive lung inflammation upon IAV infections. These results are consistent with clinical reports showing that fibrinolysis deregulation could be associated with fatal outcome of IAV infections in humans [122, 123]. In addition to fibrinolysis, it is well known that plasmin also promotes, in a strain-dependent manner, the proteolytic cleavage of the viral hemagglutinin, an essential step for the infectivity of IAV [2]. In vivo, viruses where HA can be cleaved by plasminogen replicate more efficiently in the lungs of plasminogen-competent mice compared to the ones of plasminogen-deficient mice [107]. Likely, this increased plasminogen-dependent virus replication also contributes to more

PPR activation, which may further nourish the vicious circle of inflammation. Thus, these results point to a role for plasminergic and hemostasis deregulation in the control of the deleterious inflammation induced by influenza.

## Conclusions

Influenza still causes significant morbidity and mortality associated with severe immunopathology of the lungs, related to excessive innate immune response. However, the mechanisms of such immunopathogenesis remain poorly understood. Based on our recent understanding, a model of inflammation in response to influenza can be proposed (Fig. 6). First, infected epithelial cells sense influenza and activate the innate immune response. Cytokines and chemokines are released and immune cells are recruited to the site of infection to clear the virus (protective immunity). In this context and at the epithelial level, some molecules such as PAR1 cooperate with PPR for protective innate immunity activation. A local and limited formation of fibrin could also be protective by limiting the diffusion of the infection. If the protective barriers are overwhelmed by the infection, endothelial cells are injured. Endothelium injury can result from (1) the acute phase of inflammation leading to increased endothelial cell permeability or (2) a direct infection of endothelial cells by IAV. In these conditions, protective molecules turn deleterious for the host. Deregulation of hemostasis, activation of PAR-1, or of the plasminergic system, then feed a vicious circle leading to malignant inflammation. This recent demonstration of the involvement of unbalanced hemostasis in the pathogenesis of influenza has to be replaced in a broader context. Indeed fibrinolysis plays a fundamental role in the clearance of blood clots and the clearance of extravascular fibrin. The major manifestation of plasminogen deficiency is the absence of fibrin resorption leading to the formation of pseudomembranes on inflamed mucosal surfaces in human [124] and impaired wound healing in mice [125]. In the context of sepsis, impairment of fibrin clearance is assumed to be pivotal in the pathogenesis of microvascular thrombosis and disseminated intravascular coagulation (DIC) [126]. Given the dual role of fibrinolysis, which may depend on the severity of the infection, our results suggest that it will be essential to define in the next future specific markers of non-severe versus severe IAV infections to direct therapeutics against influenza. During non-severe infections, one could use the current and novel antivirals against influenza aiming at slowing down viral growth. In contrast, during severe IAV infections, where the hallmark of pathogenesis is the deleterious inflammation of the lungs, blocking viral replication may have no effect. Instead, targeting hemostasis looks to be a promising novel strategy for the

future. Future research will aim at more precisely elucidating the immune mechanism of protection and deregulation in order to design new intervention strategies against influenza. From our current knowledge, PAR1 antagonists, PAR2 agonists, plasminogen inhibitors, or SIP1 agonists might be explored as a new treatment for influenza. By maintaining the inflammatory responses in their protective role against viral replication, these new strategies would provide protection against severe IAV infections, without encouraging the emergence of virus resistance.

## References

1. Kuiken T, Riteau B, Fouchier RA, Rimmelzwaan GF (2012) Pathogenesis of influenza virus infections: the good, the bad and the ugly. *Curr Opin Virol* 2(3):276–286
2. Horimoto T, Kawaoka Y (2005) Influenza: lessons from past pandemics, warnings from current incidents. *Nat Rev Microbiol* 3(8):591–600
3. Palese P, Shaw ML (2007) Orthomyxoviridae: the viruses and their replication. In: Knipe DM, Howley PM (eds) *Fields virology*, vol 2, 5th edn. Lippincott Williams & Wilkins, Philadelphia, pp 1647–1689
4. Lamb RAKR (2001) Orthomyxoviridae: the viruses and their replication. In: Knipe DM, Howley PM, Griffin DE (eds) *Fields virology*. Lippincott Williams and Wilkins, Philadelphia, pp 1487–1531
5. Moules V, Terrier O, Yver M, Riteau B, Moriscot C, Ferraris O, Julien T, Giudice E, Rolland JP, Erny A, Bouscambert-Duchamp M, Frobert E, Rosa-Calatrava M, Pu Lin Y, Hay A, Thomas D, Schoehn G, Lina B (2011) Importance of viral genomic composition in modulating glycoprotein content on the surface of influenza virus particles. *Virology* 414(1):51–62
6. LeBouder F, Morello E, Rimmelzwaan GF, Bosse F, Pechoux C, Delmas B, Riteau B (2008) Annexin II incorporated into influenza virus particles supports virus replication by converting plasminogen into plasmin. *J Virol* 82(14):6820–6828
7. Shaw ML, Stone KL, Colangelo CM, Gulcicek EE, Palese P (2008) Cellular proteins in influenza virus particles. *PLoS Pathog* 4(6):e1000085
8. Gao R, Cao B, Hu Y, Feng Z, Wang D, Hu W, Chen J, Jie Z, Qiu H, Xu K, Xu X, Lu H, Zhu W, Gao Z, Xiang N, Shen Y, He Z, Gu Y, Zhang Z, Yang Y, Zhao X, Zhou L, Li X, Zou S, Zhang Y, Li X, Yang L, Guo J, Dong J, Li Q, Dong L, Zhu Y, Bai T, Wang S, Hao P, Yang W, Zhang Y, Han J, Yu H, Li D, Gao GF, Wu G, Wang Y, Yuan Z, Shu Y (2013) Human infection with a novel avian-origin influenza A (H7N9) virus. *N Engl J Med* 368(20):1888–1897
9. Herfst S, Schrauwen EJ, Linster M, Chutinimitkul S, de Wit E, Munster VJ, Sorrell EM, Bestebroer TM, Burke DF, Smith DJ, Rimmelzwaan GF, Osterhaus AD, Fouchier RA (2012) Airborne transmission of influenza A/H5N1 virus between ferrets. *Science* 336(6088):1534–1541
10. Imai M, Watanabe T, Hatta M, Das SC, Ozawa M, Shinya K, Zhong G, Hanson A, Katsura H, Watanabe S, Li C, Kawakami E, Yamada S, Kiso M, Suzuki Y, Maher EA, Neumann G, Kawaoka Y (2012) Experimental adaptation of an influenza H5 HA confers respiratory droplet transmission to a reassortant H5 HA/H1N1 virus in ferrets. *Nature* 486(7403):420–428
11. de Jong MD, Simmons CP, Thanh TT, Hien VM, Smith GJ, Chau TN, Hoang DM, Chau NV, Khanh TH, Dong VC, Qui PT, Cam BV, Ha do Q, Guan Y, Peiris JS, Chinh NT, Hien TT,

- Farrar J (2006) Fatal outcome of human influenza A (H5N1) is associated with high viral load and hypercytokinemia. *Nat Med* 12(10):1203–1207
12. Ichinohe T (2010) Respective roles of TLR, RIG-I and NLRP3 in influenza virus infection and immunity: impact on vaccine design. *Expert Rev Vaccines* 9(11):1315–1324
  13. Garcia-Sastre A (2011) Induction and evasion of type I interferon responses by influenza viruses. *Virus Res* 162(1–2):12–18
  14. Pascale F, Contreras V, Bonneau M, Courbet A, Chilmonczyk S, Bevilacqua C, Epardaud M, Niborski V, Riffault S, Balazuc AM, Foulon E, Guzylack-Piriou L, Riteau B, Hope J, Bertho N, Charley B, Schwartz-Cornil I (2008) Plasmacytoid dendritic cells migrate in afferent skin lymph. *J Immunol* 180(9):5963–5972
  15. La Gruta NL, Kedzierska K, Stambas J, Doherty PC (2007) A question of self-preservation: immunopathology in influenza virus infection. *Immunol Cell Biol* 85(2):85–92
  16. Shinya K, Ito M, Makino A, Tanaka M, Miyake K, Eisfeld AJ, Kawaoka Y (2012) The TLR4-TRIF pathway protects against H5N1 influenza virus infection. *J Virol* 86(1):19–24
  17. Imai Y, Kuba K, Neely GG, Yaghubian-Malhami R, Perkmann T, van Loo G, Ermolaeva M, Veldhuizen R, Leung YH, Wang H, Liu H, Sun Y, Pasparakis M, Kopf M, Mech C, Bavari S, Peiris JS, Slutsky AS, Akira S, Hultqvist M, Holmdahl R, Nicholls J, Jiang C, Binder CJ, Penninger JM (2008) Identification of oxidative stress and Toll-like receptor 4 signaling as a key pathway of acute lung injury. *Cell* 133(2):235–249
  18. Shirey KA, Lai W, Scott AJ, Lipsky M, Mistry P, Pletneva LM, Karp CL, McAlees J, Gioannini TL, Weiss J, Chen WH, Ernst RK, Rossignol DP, Gusovsky F, Blanco JC, Vogel SN (2013) The TLR4 antagonist Eritoran protects mice from lethal influenza infection. *Nature* 497(7450):498–502. doi:10.1038/nature12118
  19. Lund JM, Alexopoulou L, Sato A, Karow M, Adams NC, Gale NW, Iwasaki A, Flavell RA (2004) Recognition of single-stranded RNA viruses by Toll-like receptor 7. *Proc Natl Acad Sci USA* 101(15):5598–5603
  20. Diebold SS, Kaisho T, Hemmi H, Akira S, Reis e Sousa C (2004) Innate antiviral responses by means of TLR7-mediated recognition of single-stranded RNA. *Science* 303(5663):1529–1531
  21. Geeraedts F, Goutagny N, Hornung V, Severa M, de Haan A, Pool J, Wilschut J, Fitzgerald KA, Huckriede A (2008) Superior immunogenicity of inactivated whole virus H5N1 influenza vaccine is primarily controlled by Toll-like receptor signalling. *PLoS Pathog* 4(8):e1000138
  22. Le Goffic R, Balloy V, Lagranderie M, Alexopoulou L, Escriou N, Flavell R, Chignard M, Si-Tahar M (2006) Detrimental contribution of the Toll-like receptor (TLR)3 to influenza A virus-induced acute pneumonia. *PLoS Pathog* 2(6):e53
  23. Zhao J, Wohlford-Lenane C, Zhao J, Fleming E, Lane TE, McCray PB Jr, Perlman S (2012) Intranasal treatment with poly(I\*<sup>3</sup>C) protects aged mice from lethal respiratory virus infections. *J Virol* 86(21):11416–11424
  24. Rehwinkel J, Tan CP, Goubau D, Schulz O, Pichlmair A, Bier K, Robb N, Vreede F, Barclay W, Fodor E, Reis e Sousa C (2010) RIG-I detects viral genomic RNA during negative-strand RNA virus infection. *Cell* 140(3):397–408
  25. Kato H, Takeuchi O, Sato S, Yoneyama M, Yamamoto M, Matsui K, Uematsu S, Jung A, Kawai T, Ishii KJ, Yamaguchi O, Otsu K, Tsujimura T, Koh CS, Reis e Sousa C, Matsuura Y, Fujita T, Akira S (2006) Differential roles of MDA5 and RIG-I helicases in the recognition of RNA viruses. *Nature* 441(7089):101–105
  26. Bauernfeind F, Ablasser A, Bartok E, Kim S, Schmid-Burgk J, Cavlar T, Hornung V (2011) Inflammasomes: current understanding and open questions. *Cell Mol Life Sci* 68(5):765–783
  27. Netea MG, Simon A, van de Veerndonk F, Kullberg BJ, Van der Meer JW, Joosten LA (2010) IL-1beta processing in host defense: beyond the inflammasomes. *PLoS Pathog* 6(2):e1000661
  28. Ichinohe T, Lee HK, Ogura Y, Flavell R, Iwasaki A (2009) Inflammasome recognition of influenza virus is essential for adaptive immune responses. *J Exp Med* 206(1):79–87
  29. Allen IC, Scull MA, Moore CB, Holl EK, McElvania-TeKippe E, Taxman DJ, Guthrie EH, Pickles RJ, Ting JP (2009) The NLRP3 inflammasome mediates in vivo innate immunity to influenza A virus through recognition of viral RNA. *Immunity* 30(4):556–565
  30. Pothlichet J, Meunier I, Davis BK, Ting JP, Skamene E, von Messling V, Vidal SM (2013) Type I IFN triggers RIG-I/TLR3/NLRP3-dependent inflammasome activation in influenza A virus-infected cells. *PLoS Pathog* 9(4):e1003256
  31. van Riel D, Leijten LM, van der Eerden M, Hoogsteden HC, Boven LA, Lambrecht BN, Osterhaus AD, Kuiken T (2011) Highly pathogenic avian influenza virus H5N1 infects alveolar macrophages without virus production or excessive TNF-alpha induction. *PLoS Pathog* 7(6):e1002099
  32. Tumpey TM, Garcia-Sastre A, Taubenberger JK, Palese P, Swayne DE, Pantin-Jackwood MJ, Schultz-Cherry S, Solorzano A, Van Rooijen N, Katz JM, Basler CF (2005) Pathogenicity of influenza viruses with genes from the 1918 pandemic virus: functional roles of alveolar macrophages and neutrophils in limiting virus replication and mortality in mice. *J Virol* 79(23):14933–14944
  33. Tate MD, Deng YM, Jones JE, Anderson GP, Brooks AG, Reading PC (2009) Neutrophils ameliorate lung injury and the development of severe disease during influenza infection. *J Immunol* 183(11):7441–7450
  34. Hashimoto Y, Moki T, Takizawa T, Shiratsuchi A, Nakanishi Y (2007) Evidence for phagocytosis of influenza virus-infected, apoptotic cells by neutrophils and macrophages in mice. *J Immunol* 178(4):2448–2457
  35. Peake J, Suzuki K (2004) Neutrophil activation, antioxidant supplements and exercise-induced oxidative stress. *Exerc Immunol Rev* 10:129–141
  36. Hemmers S, Teijaro JR, Arandjelovic S, Mowen KA (2011) PAD4-mediated neutrophil extracellular trap formation is not required for immunity against influenza infection. *PLoS ONE* 6(7):e22043
  37. Narasaraaju T, Yang E, Samy RP, Ng HH, Poh WP, Liew AA, Phoon MC, van Rooijen N, Chow VT (2011) Excessive neutrophils and neutrophil extracellular traps contribute to acute lung injury of influenza pneumonitis. *Am J Pathol* 179(1):199–210
  38. Perrone LA, Plowden JK, Garcia-Sastre A, Katz JM, Tumpey TM (2008) H5N1 and 1918 pandemic influenza virus infection results in early and excessive infiltration of macrophages and neutrophils in the lungs of mice. *PLoS Pathog* 4(8):e1000115
  39. Kim HM, Lee YW, Lee KJ, Kim HS, Cho SW, van Rooijen N, Guan Y, Seo SH (2008) Alveolar macrophages are indispensable for controlling influenza viruses in lungs of pigs. *J Virol* 82(9):4265–4274
  40. Ennis FA, Meager A, Beare AS, Qi YH, Riley D, Schwarz G, Schild GC, Rook AH (1981) Interferon induction and increased natural killer-cell activity in influenza infections in man. *Lancet* 2(8252):891–893
  41. Bryceson YT, Long EO (2008) Line of attack: NK cell specificity and integration of signals. *Curr Opin Immunol* 20(3):344–352
  42. Riteau B, Barber DF, Long EO (2003) Vav1 phosphorylation is induced by beta2 integrin engagement on natural killer cells

- upstream of actin cytoskeleton and lipid raft reorganization. *J Exp Med* 198(3):469–474
43. Thielens A, Vivier E, Romagne F (2012) NK cell MHC class I specific receptors (KIR): from biology to clinical intervention. *Curr Opin Immunol* 24(2):239–245
  44. Orr MT, Lanier LL (2010) Natural killer cell education and tolerance. *Cell* 142(6):847–856
  45. Achdout H, Manaster I, Mandelboim O (2008) Influenza virus infection augments NK cell inhibition through reorganization of major histocompatibility complex class I proteins. *J Virol* 82(16):8030–8037
  46. Ronni T, Matikainen S, Sareneva T, Melen K, Pirhonen J, Keskinen P, Julkunen I (1997) Regulation of IFN- $\alpha$ / $\beta$ , MxA, 2',5'-oligoadenylate synthetase, and HLA gene expression in influenza A-infected human lung epithelial cells. *J Immunol* 158(5):2363–2374
  47. Mandelboim O, Lieberman N, Lev M, Paul L, Arnon TI, Bushkin Y, Davis DM, Strominger JL, Yewdell JW, Porgador A (2001) Recognition of haemagglutinins on virus-infected cells by NKp46 activates NK cell lysis by human NK cells. *Nature* 409(6823):1055–1060
  48. Ho JW, Hershkovitz O, Peiris M, Zilka A, Bar-Ilan A, Nal B, Chu K, Kudelko M, Kam YW, Achdout H, Mandelboim M, Altmeyer R, Mandelboim O, Bruzzone R, Porgador A (2008) H5-type influenza virus hemagglutinin is functionally recognized by the natural killer-activating receptor NKp44. *J Virol* 82(4):2028–2032
  49. Arnon TI, Lev M, Katz G, Chernobrov Y, Porgador A, Mandelboim O (2001) Recognition of viral hemagglutinins by NKp44 but not by NKp30. *Eur J Immunol* 31(9):2680–2689
  50. Gazit R, Gruda R, Elboim M, Arnon TI, Katz G, Achdout H, Hanna J, Qimron U, Landau G, Greenbaum E, Zakay-Rones Z, Porgador A, Mandelboim O (2006) Lethal influenza infection in the absence of the natural killer cell receptor gene *Ncr1*. *Nat Immunol* 7(5):517–523
  51. Zhou G, Juang SW, Kane KP (2013) NK cells exacerbate the pathology of influenza virus infection in mice. *Eur J Immunol* 43(4):929–938
  52. Abdul-Careem MF, Mian MF, Yue G, Gillgrass A, Chenoweth MJ, Barra NG, Chew MV, Chan T, Al-Garawi AA, Jordana M, Ashkar AA (2012) Critical role of natural killer cells in lung immunopathology during influenza infection in mice. *J Infect Dis* 206(2):167–177
  53. Le Bourhis L, Martin E, Peguillet I, Guihot A, Froux N, Core M, Levy E, Dusseaux M, Meyssonier V, Premel V, Ngo C, Riteau B, Duban L, Robert D, Rottman M, Soudais C, Lantz O (2010) Antimicrobial activity of mucosal-associated invariant T cells. *Nat Immunol* 11(8):701–708
  54. Garcia-Sastre A, Biron CA (2006) Type 1 interferons and the virus-host relationship: a lesson in detente. *Science* 312(5775):879–882
  55. Herold S, Ludwig S, Pleschka S, Wolff T (2012) Apoptosis signaling in influenza virus propagation, innate host defense, and lung injury. *J Leukoc Biol* 92(1):75–82
  56. Foucault ML, Moules V, Rosa-Calatrava M, Riteau B (2011) Role for proteases and HLA-G in the pathogenicity of influenza A viruses. *J Clin Virol* 51(3):155–159
  57. Robb NC, Jackson D, Vreede FT, Fodor E (2010) Splicing of influenza A virus NS1 mRNA is independent of the viral NS1 protein. *J Gen Virol* 91(Pt 9):2331–2340
  58. Garcia-Sastre A, Egorov A, Matassov D, Brandt S, Levy DE, Durbin JE, Palese P, Muster T (1998) Influenza A virus lacking the NS1 gene replicates in interferon-deficient systems. *Virology* 252(2):324–330
  59. Talon J, Horvath CM, Polley R, Basler CF, Muster T, Palese P, Garcia-Sastre A (2000) Activation of interferon regulatory factor 3 is inhibited by the influenza A virus NS1 protein. *J Virol* 74(17):7989–7996
  60. Wang X, Li M, Zheng H, Muster T, Palese P, Beg AA, Garcia-Sastre A (2000) Influenza A virus NS1 protein prevents activation of NF- $\kappa$ B and induction of  $\alpha$ / $\beta$  interferon. *J Virol* 74(24):11566–11573
  61. Guo Z, Chen LM, Zeng H, Gomez JA, Plowden J, Fujita T, Katz JM, Donis RO, Sambhara S (2007) NS1 protein of influenza A virus inhibits the function of intracytoplasmic pathogen sensor, RIG-I. *Am J Respir Cell Mol Biol* 36(3):263–269
  62. Mibayashi M, Martinez-Sobrido L, Loo YM, Cardenas WB, Gale M Jr, Garcia-Sastre A (2007) Inhibition of retinoic acid-inducible gene 1-mediated induction of beta interferon by the NS1 protein of influenza A virus. *J Virol* 81(2):514–524
  63. Kochs G, Garcia-Sastre A, Martinez-Sobrido L (2007) Multiple anti-interferon actions of the influenza A virus NS1 protein. *J Virol* 81(13):7011–7021
  64. Qiu Y, Krug RM (1994) The influenza virus NS1 protein is a poly(A)-binding protein that inhibits nuclear export of mRNAs containing poly(A). *J Virol* 68(4):2425–2432
  65. Schultz-Cherry S, Dybdahl-Sissoko N, Neumann G, Kawaoka Y, Hinshaw VS (2001) Influenza virus ns1 protein induces apoptosis in cultured cells. *J Virol* 75(17):7875–7881
  66. Han X, Li Z, Chen H, Wang H, Mei L, Wu S, Zhang T, Liu B, Lin X (2012) Influenza virus A/Beijing/501/2009(H1N1) NS1 interacts with beta-tubulin and induces disruption of the microtubule network and apoptosis on A549 cells. *PLoS ONE* 7(11):e48340
  67. Melen K, Kinnunen L, Fagerlund R, Ikonen N, Twu KY, Krug RM, Julkunen I (2007) Nuclear and nucleolar targeting of influenza A virus NS1 protein: striking differences between different virus subtypes. *J Virol* 81(11):5995–6006
  68. Talon J, Salvatore M, O'Neill RE, Nakaya Y, Zheng H, Muster T, Garcia-Sastre A, Palese P (2000) Influenza A and B viruses expressing altered NS1 proteins: a vaccine approach. *Proc Natl Acad Sci USA* 97(8):4309–4314
  69. Conenello GM, Palese P (2007) Influenza A virus PB1-F2: a small protein with a big punch. *Cell Host Microbe* 2(4):207–209
  70. Schmolke M, Manicassamy B, Pena L, Sutton T, Hai R, Varga ZT, Hale BG, Steel J, Perez DR, Garcia-Sastre A (2011) Differential contribution of PB1-F2 to the virulence of highly pathogenic H5N1 influenza A virus in mammalian and avian species. *PLoS Pathog* 7(8):e1002186
  71. Conenello GM, Zamarin D, Perrone LA, Tumpey T, Palese P (2007) A single mutation in the PB1-F2 of H5N1 (HK/97) and 1918 influenza A viruses contributes to increased virulence. *PLoS Pathog* 3(10):1414–1421
  72. Zamarin D, Ortigoza MB, Palese P (2006) Influenza A virus PB1-F2 protein contributes to viral pathogenesis in mice. *J Virol* 80(16):7976–7983
  73. Varga ZT, Ramos I, Hai R, Schmolke M, Garcia-Sastre A, Fernandez-Sesma A, Palese P (2011) The influenza virus protein PB1-F2 inhibits the induction of type I interferon at the level of the MAVS adaptor protein. *PLoS Pathog* 7(6):e1002067
  74. Zamarin D, Garcia-Sastre A, Xiao X, Wang R, Palese P (2005) Influenza virus PB1-F2 protein induces cell death through mitochondrial ANT3 and VDAC1. *PLoS Pathog* 1(1):e4
  75. Chen W, Calvo PA, Malide D, Gibbs J, Schubert U, Bacik I, Basta S, O'Neill R, Schickli J, Palese P, Henklein P, Benink JR, Yewdell JW (2001) A novel influenza A virus mitochondrial protein that induces cell death. *Nat Med* 7(12):1306–1312
  76. Chanturiya AN, Basanez G, Schubert U, Henklein P, Yewdell JW, Zimmerberg J (2004) PB1-F2, an influenza A virus-encoded proapoptotic mitochondrial protein, creates variably sized pores in planar lipid membranes. *J Virol* 78(12):6304–6312

77. McAuley JL, Hornung F, Boyd KL, Smith AM, McKeon R, Bennink J, Yewdell JW, McCullers JA (2007) Expression of the 1918 influenza A virus PB1-F2 enhances the pathogenesis of viral and secondary bacterial pneumonia. *Cell Host Microbe* 2(4):240–249
78. Rouas-Freiss N, Khalil-Daher I, Riteau B, Menier C, Paul P, Dausset J, Carosella ED (1999) The immunotolerance role of HLA-G. *Semin Cancer Biol* 9(1):3–12
79. Menier C, Riteau B, Dausset J, Carosella ED, Rouas-Freiss N (2000) HLA-G truncated isoforms can substitute for HLA-G1 in fetal survival. *Hum Immunol* 61(11):1118–1125
80. Riteau B, Moreau P, Menier C, Khalil-Daher I, Khosrotehrani K, Bras-Goncalves R, Paul P, Dausset J, Rouas-Freiss N, Carosella ED (2001) Characterization of HLA-G1, -G2, -G3, and -G4 isoforms transfected in a human melanoma cell line. *Transplant Proc* 33(3):2360–2364
81. Khalil-Daher I, Riteau B, Menier C, Sedlik C, Paul P, Dausset J, Carosella ED, Rouas-Freiss N (1999) Role of HLA-G versus HLA-E on NK function: HLA-G is able to inhibit NK cytotoxicity by itself. *J Reprod Immunol* 43(2):175–182
82. Riteau B, Menier C, Khalil-Daher I, Martinozzi S, Pla M, Dausset J, Carosella ED, Rouas-Freiss N (2001) HLA-G1 co-expression boosts the HLA class I-mediated NK lysis inhibition. *Int Immunol* 13(2):193–201
83. Riteau B, Menier C, Khalil-Daher I, Sedlik C, Dausset J, Rouas-Freiss N, Carosella ED (1999) HLA-G inhibits the allogeneic proliferative response. *J Reprod Immunol* 43(2):203–211
84. Le Gal FA, Riteau B, Sedlik C, Khalil-Daher I, Menier C, Dausset J, Guillet JG, Carosella ED, Rouas-Freiss N (1999) HLA-G-mediated inhibition of antigen-specific cytotoxic T lymphocytes. *Int Immunol* 11(8):1351–1356
85. Riteau B, Rouas-Freiss N, Menier C, Paul P, Dausset J, Carosella ED (2001) HLA-G2, -G3, and -G4 isoforms expressed as nonmature cell surface glycoproteins inhibit NK and antigen-specific CTL cytotoxicity. *J Immunol* 166(8):5018–5026
86. Paul P, Rouas-Freiss N, Khalil-Daher I, Moreau P, Riteau B, Le Gal FA, Avril MF, Dausset J, Guillet JG, Carosella ED (1998) HLA-G expression in melanoma: a way for tumor cells to escape from immunosurveillance. *Proc Natl Acad Sci USA* 95(8):4510–4515
87. Adrian Cabestre F, Moreau P, Riteau B, Ibrahim EC, Le Danff C, Dausset J, Rouas-Freiss N, Carosella ED, Paul P (1999) HLA-G expression in human melanoma cells: protection from NK cytotoxicity. *J Reprod Immunol* 43(2):183–193
88. Riteau B, Faure F, Menier C, Viel S, Carosella ED, Amigorena S, Rouas-Freiss N (2003) Exosomes bearing HLA-G are released by melanoma cells. *Hum Immunol* 64(11):1064–1072
89. Menier C, Riteau B, Carosella ED, Rouas-Freiss N (2002) MICA triggering signal for NK cell tumor lysis is counteracted by HLA-G1-mediated inhibitory signal. *Int J Cancer* 100(1):63–70
90. Zilberman S, Schenowitz C, Agaoglu S, Benoit F, Riteau B, Rouzier R, Carosella ED, Rouas-Freiss N, Menier C (2012) HLA-G1 and HLA-G5 active dimers are present in malignant cells and effusions: the influence of the tumor microenvironment. *Eur J Immunol* 42(6):1599–1608
91. Fainardi E, Castellazzi M, Stignani M, Morandi F, Sana G, Gonzalez R, Pistoia V, Baricordi OR, Sokal E, Pena J (2011) Emerging topics and new perspectives on HLA-G. *Cell Mol Life Sci* 68(3):433–451
92. Li C, Toth I, Schulze Zur Wiesch J, Pereyra F, Rychert J, Rosenberg ES, van Lunzen J, Lichterfeld M, Yu XG (2013) Functional characterization of HLA-G(+) regulatory T cells in HIV-1 infection. *PLoS Pathog* 9(1):e1003140
93. Larsen MH, Zinyama R, Kallestrup P, Gerstoft J, Gomo E, Thorner LW, Berg TB, Erikstrup C, Ullum H (2013) HLA-G 3' untranslated region 14-base pair deletion: association with poor survival in an HIV-1-infected Zimbabwean population. *J Infect Dis* 207(6):903–906
94. Segat L, Catamo E, Fabris A, Morgutti M, D'Agaro P, Campello C, Crovella S (2010) HLA-G\*0105N allele is associated with augmented risk for HIV infection in white female patients. *AIDS* 24(12):1961–1964
95. Shi WW, Lin A, Xu DP, Bao WG, Zhang JG, Chen SY, Li J, Yan WH (2011) Plasma soluble human leukocyte antigen-G expression is a potential clinical biomarker in patients with hepatitis B virus infection. *Hum Immunol* 72(11):1068–1073
96. LeBouder F, Khoufache K, Menier C, Mandouri Y, Keffous M, Lejal N, Krawice-Radanne I, Carosella ED, Rouas-Freiss N, Riteau B (2009) Immunosuppressive HLA-G molecule is upregulated in alveolar epithelial cells after influenza A virus infection. *Hum Immunol* 70(12):1016–1019
97. Chen HX, Chen BG, Shi WW, Zhen R, Xu DP, Lin A, Yan WH (2011) Induction of cell surface human leukocyte antigen-G expression in pandemic H1N1 2009 and seasonal H1N1 influenza virus-infected patients. *Hum Immunol* 72(2):159–165
98. Tsotsiashvili M, Levi R, Arnon R, Berke G (1998) Activation of influenza-specific memory cytotoxic T lymphocytes by Concanavalin A stimulation. *Immunol Lett* 60(2–3):89–95
99. Li OT, Chan MC, Leung CS, Chan RW, Guan Y, Nicholls JM, Poon LL (2009) Full factorial analysis of mammalian and avian influenza polymerase subunits suggests a role of an efficient polymerase for virus adaptation. *PLoS ONE* 4(5):e5658
100. Hu J, Hu Z, Song Q, Gu M, Liu X, Wang X, Hu S, Chen C, Liu H, Liu W, Chen S, Peng D, Liu X (2013) The PA-gene-mediated lethal dissemination and excessive innate immune response contribute to the high virulence of H5N1 avian influenza virus in mice. *J Virol* 87(5):2660–2672
101. Zeng H, Pappas C, Belsler JA, Houser KV, Zhong W, Wadford DA, Stevens T, Balczon R, Katz JM, Tumpey TM (2012) Human pulmonary microvascular endothelial cells support productive replication of highly pathogenic avian influenza viruses: possible involvement in the pathogenesis of human H5N1 virus infection. *J Virol* 86(2):667–678
102. Suguitan AL Jr, Matsuoka Y, Lau YF, Santos CP, Vogel L, Cheng LI, Orandle M, Subbarao K (2012) The multibasic cleavage site of the hemagglutinin of highly pathogenic A/Vietnam/1203/2004 (H5N1) avian influenza virus acts as a virulence factor in a host-specific manner in mammals. *J Virol* 86(5):2706–2714
103. Riteau B, de Vaureix C, Lefevre F (2006) Trypsin increases pseudorabies virus production through activation of the ERK signalling pathway. *J Gen Virol* 87(Pt 5):1109–1112
104. Khoufache K, Berri F, Nacken W, Vogel AB, Delenne M, Camerer E, Coughlin SR, Carmeliet P, Lina B, Rimmelzwaan GF, Planz O, Ludwig S, Riteau B (2013) PAR1 contributes to influenza A virus pathogenicity in mice. *J Clin Invest* 123(1):206–214
105. Feistritzer C, Riewald M (2005) Endothelial barrier protection by activated protein C through PAR1-dependent sphingosine 1-phosphate receptor-1 crossactivation. *Blood* 105(8):3178–3184
106. Antoniak S, Owens AP 3rd, Baunacke M, Williams JC, Lee RD, Weithauser A, Sheridan PA, Malz R, Luyendyk JP, Esserman DA, Trejo J, Kirchhofer D, Blaxall BC, Pawlinski R, Beck MA, Rauch U, Mackman N (2013) PAR-1 contributes to the innate immune response during viral infection. *J Clin Invest* 123(3):1310–1322
107. Berri F, Rimmelzwaan GF, Hanss M, Albina E, Foucault-Grunenwald ML, Le VB, Vogelzang-van Trierum SE, Gil P, Camerer E, Martinez D, Lina B, Lijnen R, Carmeliet P, Riteau B (2013) Plasminogen controls inflammation and

- pathogenesis of influenza virus infections via fibrinolysis. *PLoS Pathog* 9(3):e1003229
108. Aerts L, Hamelin MÈ, Rhéaume C, Lavigne S, Couture C, Kim W, Susan-Resiga D, Prat A, Seidah NG, Vergnolle N, Riteau B, Boivin G (2013) Modulation of protease activated receptor 1 influences human metapneumovirus disease severity in a mouse model. *Plos One* 8:e72529
  109. Teijaro JR, Walsh KB, Cahalan S, Fremgen DM, Roberts E, Scott F, Martinborough E, Peach R, Oldstone MB, Rosen H (2011) Endothelial cells are central orchestrators of cytokine amplification during influenza virus infection. *Cell* 146(6):980–991
  110. Walsh KB, Teijaro JR, Wilker PR, Jatzek A, Fremgen DM, Das SC, Watanabe T, Hatta M, Shinya K, Suresh M, Kawaoka Y, Rosen H, Oldstone MB (2011) Suppression of cytokine storm with a sphingosine analog provides protection against pathogenic influenza virus. *Proc Natl Acad Sci USA* 108(29):12018–12023
  111. Marsolais D, Hahm B, Walsh KB, Edelmann KH, McGavern D, Hatta Y, Kawaoka Y, Rosen H, Oldstone MB (2009) A critical role for the sphingosine analog AAL-R in dampening the cytokine response during influenza virus infection. *Proc Natl Acad Sci USA* 106(5):1560–1565
  112. O'Brien PJ, Prevost N, Molino M, Hollinger MK, Woolkalis MJ, Woulfe DS, Brass LF (2000) Thrombin responses in human endothelial cells. Contributions from receptors other than PAR1 include the transactivation of PAR2 by thrombin-cleaved PAR1. *J Biol Chem* 275(18):13502–13509
  113. Khoufache K, LeBouder F, Morello E, Laurent F, Riffault S, Andrade-Gordon P, Boullier S, Rousset P, Vergnolle N, Riteau B (2009) Protective role for protease-activated receptor-2 against influenza virus pathogenesis via an IFN-gamma-dependent pathway. *J Immunol* 182(12):7795–7802
  114. Esmon CT (2012) Protein C anticoagulant system—anti-inflammatory effects. *Semin Immunopathol* 34(1):127–132
  115. Schouten M, Sluijs KF, Gerlitz B, Grinnell BW, Roelofs JJ, Levi MM, van't Veer C, Poll T (2010) Activated protein C ameliorates coagulopathy but does not influence outcome in lethal H1N1 influenza: a controlled laboratory study. *Crit Care* 14(2):R65
  116. Schouten M, van't Veer C, Levi M, Esmon CT, van der Poll T (2011) Endogenous protein C inhibits activation of coagulation and transiently lowers bacterial outgrowth in murine *Escherichia coli* peritonitis. *J Thromb Haemost* 9(5):1072–1075
  117. Meilhac O, Ho-Tin-Noe B, Houard X, Philippe M, Michel JB, Angles-Cano E (2003) Pericellular plasmin induces smooth muscle cell anoikis. *FASEB J* 17(10):1301–1303
  118. Degen JL, Bugge TH, Goguen JD (2007) Fibrin and fibrinolysis in infection and host defense. *J Thromb Haemost* 5(Suppl 1):24–31
  119. Goto H, Kawaoka Y (1998) A novel mechanism for the acquisition of virulence by a human influenza A virus. *Proc Natl Acad Sci USA* 95(17):10224–10228
  120. LeBouder F, Lina B, Rimmelzwaan GF, Riteau B (2010) Plasminogen promotes influenza A virus replication through an annexin 2-dependent pathway in the absence of neuraminidase. *J Gen Virol* 91(Pt 11):2753–2761
  121. Goto H, Wells K, Takada A, Kawaoka Y (2001) Plasminogen-binding activity of neuraminidase determines the pathogenicity of influenza A virus. *J Virol* 75(19):9297–9301
  122. Wang ZF, Su F, Lin XJ, Dai B, Kong LF, Zhao HW, Kang J (2011) Serum D-dimer changes and prognostic implication in 2009 novel influenza A(H1N1). *Thromb Res* 127(3):198–201
  123. Soepandi PZ, Burhan E, Mangunegoro H, Nawas A, Aditama TY, Partakusuma L, Isbaniah F, Ikhsan M, Swidarmoko B, Sutiyo A, Malik S, Benamore R, Baird JK, Taylor WR (2010) Clinical course of avian influenza A(H5N1) in patients at the Persahabatan Hospital, Jakarta, Indonesia, 2005–2008. *Chest* 138(3):665–673
  124. Mehta R, Shapiro AD (2008) Plasminogen deficiency. *Haemophilia* 14(6):1261–1268
  125. Bugge TH, Kombrinck KW, Flick MJ, Daugherty CC, Danton MJ, Degen JL (1996) Loss of fibrinogen rescues mice from the pleiotropic effects of plasminogen deficiency. *Cell* 87(4):709–719
  126. Gando S (2013) Role of fibrinolysis in sepsis. *Semin Thromb Hemost* 39(4):392–399

**Annexe n°2: Platelet dysfunction promotes the cytokine storm during severe influenza**

Vuong Ba Lê, Jochen G. Schneider, Yvonne Boergeling, Fatma Berri, Mariette Ducatez, Jean-Luc Guerin, Iris Adrian, Bruno Lina, Jean-Claude Bordet, Martine Jandrot-Perrus, Stephan Ludwig, Béatrice Riteau.

**En révision dans, American Journal of Respiratory And Critical Care Medicine (AJRCCM)**

1 **Platelet dysfunction promotes influenza pathogenesis: Toward the Development of a**  
2 **Universal Therapy**

3

4 Vuong Ba Lê<sup>1</sup>, Jochen G. Schneider<sup>2,3</sup>, Yvonne Boergeling<sup>4</sup>, Fatma Berri<sup>1</sup>, Mariette Ducatez<sup>5,6</sup>,  
5 Jean-Luc Guerin<sup>5,6</sup>, Iris Adrian<sup>3</sup>, Bruno Lina<sup>1</sup>, Jean-Claude Bordet<sup>7</sup>, Martine Jandrot-Perrus<sup>8</sup>,  
6 Stephan Ludwig<sup>4</sup>, Béatrice Riteau<sup>1,9\*</sup>

7

8 <sup>1</sup>EA4610, Lyon, France; <sup>2</sup>Luxembourg Centre for Systems Biomedicine, Esch-Sur-Alzette,  
9 Luxembourg ; <sup>3</sup>Saarland University Medical Center, Homburg/Saar, Germany; <sup>4</sup>Institute  
10 Molecular Virology, ZMBE, Münster, Germany; <sup>5</sup>UMR 1225, IHAP, INRA Toulouse, France;  
11 <sup>6</sup>INP, ENVT, Toulouse France; <sup>7</sup>Unité d'Hémostase Clinique, Lyon, France; <sup>8</sup>INSERM  
12 UMR\_S1148, Paris Diderot, CHU Xavier Bichat, Paris, France; <sup>9</sup>INRA Nouzilly, France

13 \* **correspondance to Beatrice Riteau:** EA4610, Université Lyon INRA, France. Phone :  
14 04.78.77.87.11 - Fax: 04.78.77.87.51 [beatrice.riteau@laposte.net](mailto:beatrice.riteau@laposte.net).

15 **Author contributions:** VBL, JGS, JCB, MJP, SL, BR designed the experiments. VBL, YB,  
16 FB, IA performed the experiments. FB, JGS, SL, BL critically read the manuscript. VBL, MJP  
17 and BR wrote the manuscript. **Support:** BR and MJP acquired funding from ANR HemoFlu  
18 and JGS from DFG, FNR Core Itgb3VascIn. **Short Head:** Platelet dysfunction during  
19 influenza; **Classification:** 10.15 Treatment.

20 **Commentary:** Our research shows that platelets play a key role in the pathogenesis of  
21 influenza-induced acute lung injury. This may have strong impact for the development of novel  
22 drugs for the treatment of these diseases. This article has an online data supplement, which is  
23 accessible from this issue's table of content online at [www.atsjournals.org](http://www.atsjournals.org). Total word count:

24 3436

25 **Abstract**

26 **Rationale:** The hallmark of severe influenza virus infections is an excessive inflammation of  
27 the lungs. Platelets are activated during influenza but their role in influenza pathogenesis and  
28 cytokine storm is unknown.

29 **Objectives:** To determine the role of platelet during influenza virus infections and propose new  
30 therapeutics against influenza.

31 **Methods:** We used targeted gene deletion approaches and pharmacological interventions to  
32 investigate the role of platelets during influenza virus infection, in mice.

33 **Measurements and Main Results:** Lungs of infected mice were massively infiltrated by  
34 aggregates of activated platelets that have engulfed influenza viruses. Deficiency in the major  
35 platelet receptor glycoprotein IIIa (GPIIIa) protected mice from death caused by influenza viruses.  
36 In contrast, activating Protease-Activated Receptor 4 (PAR4), a receptor crucial for platelet  
37 activation exacerbated influenza-induced acute lung injury and death. Mechanistically, platelet  
38 dysfunction was at the basis of this process since this effect was abolished in mice treated with  
39 the specific anti-platelet drug eptifibatide or in mice deficient in GPIIIa. More interestingly,  
40 mice treated with anti-platelet molecules (antagonists of PAR4 or eptifibatide) were protected  
41 from severe lung injury and lethal infections induced by several influenza strains.

42 **Conclusions:** The intricate relationship between hemostasis and inflammation has major  
43 consequences in influenza virus pathogenesis and anti-platelet drugs might be explored for  
44 developing universal treatments against influenza virus infections. The anti-platelet drug  
45 eptifibatide (Integrilin®), that was tested in this study is commercialized and used in humans,  
46 permitted us to expect that such anti-platelet molecules would combine efficacy and safety in  
47 humans.

48 **Key words:** Lung injury, novel drugs, Flu pathogenesis, pneumonia. **Words:** 245

49

50 **Introduction**

51 Influenza is one of the most common infectious diseases in humans, occurring as sporadic  
52 pandemic and seasonal epidemic outbreaks, leading to significant fatal cases. Influenza  
53 pathogenesis is a complex process involving both viral determinants and the immune system  
54 (1-3). During severe influenza, dysregulation of cytokine production contributes to collateral  
55 damage of the lungs, possibly leading to organ failure and death (4-7). The endothelium, which  
56 lines the interior surface of blood vessels is thought to orchestrate the crescendo in cytokine  
57 accumulation, although the mechanism involved is not fully identified (8).

58 Upon endothelial injury, platelets are recruited by inflamed endothelial cells, where they adhere  
59 and get activated (9). Simultaneously, Protease-Activated Receptor (PAR) mediates activation  
60 of platelets by thrombin. These events lead to the conformational change of the platelet  
61 glycoprotein IIb/IIIa (GPIIb/IIIa) receptor for fibrinogen that bridges platelets, leading to their  
62 aggregation and a reinforcement of their activation. Importantly, platelet activation is strongly  
63 associated with enhanced inflammatory responses. Activated platelets release potent  
64 inflammatory molecules and play a key role in leukocyte recruitment (10). Platelet activation  
65 is finely tuned but its dysfunction is pathogenic and contributes to inflammatory disorders (11-  
66 13). Thus, uncontrolled platelet activation could contribute to the pathogenesis of IAV  
67 infections by fuelling a harmful inflammatory response in the respiratory tract. However, the  
68 role of platelets in the context of IAV infection has never been investigated. In the present study,  
69 using pharmacological and gene deletion approaches, we investigated the role of platelets in  
70 IAV pathogenesis, *in vivo*. Our findings showed that platelets feed the cytokine storm and  
71 contribute to influenza virus pathogenicity in mice. More importantly, commercially available  
72 anti-platelets drugs efficiently protected mice from IAV pathogenesis, induced by several  
73 influenza strains. Because such a strategy targeting the host rather than the virus would limit  
74 the emergence of virus resistance and would be universal, these results suggest that inhibitors

75 of platelet function should be explored for the development of a novel treatment of IAV  
76 infections.  
77

78 **METHODS**

79

80 **Cells, Viruses, Antibodies, and Reagents**

81 A549 cells and MDCK cells were purchased from ATCC. IAV A/PR/8/34 virus (H1N1),  
82 A/HK/1/68 (H3N2) and A/NL/602/2009 (H1N1) (ATCC) were gifts from GF. Rimmelzwaan  
83 (Erasmus, Rotterdam, Netherlands). Highly pathogenic avian influenza virus  
84 A/FPV/Bratislava/79 (H7N7) was from the IMV Münster, Germany. The following reagents  
85 were used: DAPI (Life Technologies), Alexa Fluo® secondary antibodies (Life Technologies),  
86 eptifibatide (Integrilin®, GlaxoSmithKline), PAR4 antagonist pepducin p4pal-10 (Polypeptide  
87 Laboratories), PAR4 agonist peptide (AYPGKF-NH<sub>2</sub>, Bachem), PAR4 control peptide  
88 (YAPGKF-NH<sub>2</sub>, Bachem); antibodies: monoclonal anti-neutrophil Ly6G (Cedarlane),  
89 polyclonal anti-platelet CD41 (Bioss), monoclonal anti-viral HA (Santa Cruz Biotechnology),  
90 monoclonal anti-IAV NP (kind gift from Dr GF. Rimmelzwaan), monoclonal anti-p-Selectin  
91 FITC-conjugated (Emfret), monoclonal anti-CD41/61 PE-conjugated (Emfret); Vectastain®  
92 ABC kit (Vector Laboratories), 3,3'-diaminobenzidine (DAB) peroxidase substrate (Vector  
93 Laboratories), ketamine/xylazine anesthesia (Virbac, Bayer HealthCare), May-Grünwald and  
94 Giemsa solutions (Merck), Hematoxylin and Eosin solutions (Diapath), ELISA kits for mouse  
95 IL-6, IL-1 $\beta$ , IFN- $\gamma$ , MIP-2, RANTES (R&D Systems), serotonin (BlueGene), TXB2  
96 (Elabscience) and sP-selectin (Qayee-Bio). Total protein was evaluated by using the Coomassie  
97 Bradford Protein assay kit (Thermo Scientific).

98

99 **Mice**

100 Experiments were performed in accordance with the Guide for the Care and Use of Laboratory  
101 Animals of “la Direction des Services Vétérinaires (DSV)”, the French regulations to which  
102 our animal care and protocol adhered. Licence authority was issued by the DSV and Lyon

103 university (accreditation 78-114). Protocols were approved by the Committee on Ethics of  
104 Animal Experiments of Lyon University (Permit BH2008-13).  
105 Balb/c, female, 7weeks old were used for H7N7 virus infections. Otherwise, 6-week-old  
106 C57BL/6 female mice (Charles River Laboratories, Arbresle, France) and GPIIIa<sup>-/-</sup> mice or  
107 wild-type littermates on a C57BL/6 background were used in this study. For the latter,  
108 heterozygous mice were crossed, and WT and KO offspring (males and females) were used.  
109 Polymerase chain reaction of tail-tip genomic DNA was performed (14) for determination of  
110 the absence or presence of GPIIIa gene. Infection experiments were performed as previously  
111 described (15). Mice were anesthetized with ketamine/xylazine (42.5/5 mg/kg) and inoculated  
112 intranasally with IAV. Eptifibatide was injected intraperitoneally (10µg /200 µl per mouse)  
113 every 3 days until the end of the experiment. For PAR4 stimulation experiments, mice were  
114 anesthetized every day for 3 days. The first day, anesthetized mice were infected intranasally  
115 in the presence or absence of PAR4-AP or control peptide (100 µg/mouse). Intranasal peptide  
116 treatments were also repeated at days 2 and 3 after infection. For PAR4 antagonist treatment,  
117 pepducin p4pal-10 was given intraperitoneally (0.5 mg/kg) two days post-infection and  
118 treatments were repeated on the next two days. Upon inoculation, survival rates were followed.  
119 Alternatively, mice were sacrificed at prefixed time points to perform BAL or harvest lungs.  
120 ELISA was performed according to the manufacturer's instructions and virus titers were  
121 assessed by plaque assay using MDCK cells as previously described (16). Lung histology and  
122 immunohistochemistry were also performed as previously (17).

123

#### 124 **Electron Microscopy**

125 For ultrastructural analysis, lung tissues were cut into 1 mm<sup>3</sup> pieces, fixed in 2% glutaraldehyde  
126 at 4°C and tissues were washed in 0.2 M cacodylate-HCl buffer containing 0.4 M saccharose  
127 and post-fixed in 0.3 M cacodylate-HCl buffer containing 2% osmium tetroxide for 1 hour.

128 After dehydration in a graded alcohol series, tissue samples were impregnated with 75% Epon  
129 A/25% Epon B/1.7% DMP30 mixture. Tissue embedding was performed by polymerization at  
130 60°C for 72 hours. Ultrathin sections (approximately 70 nm thick) were made using a Reichert  
131 ultracut ultramicrotome (Leica Microsystems), mounted on 200 mesh copper grids coated with  
132 1:1,000 polylysine, stabilized for 24 hours at room temperature and contrasted with uranyl  
133 acetate/citrate. Sections were examined using a transmission electron microscope.

134

### 135 **Immungold Staining**

136 Immunogold staining was then performed, using the anti-HA antibody followed by 10 nm gold-  
137 conjugated secondary antibody, as previously described (18).

### 138 **Evaluation of platelet and leukocyte numbers**

139 Numbers of platelets were assessed using the Vet ABC™ Hematology Analyzer (SCIL).  
140 Leukocytes and neutrophils in the BAL were determined by May-Grünwald Giemsa stained  
141 cytospin preparations, as previously performed (15).

### 142 **Flow Cytometry of blood platelets**

143 Blood was collected by cardiac puncture in ACD buffer. CD41-positive cells and platelet  
144 activation in whole blood were evaluated using FITC-conjugated P-selectin and PE-conjugated  
145 CD41/CD61 antibodies, as previously described (19, 20).

146

### 147 **Statistical Analysis**

148 Kaplan-Meier test was used for statistical analysis of survival rates and the Mann-Whitney test  
149 for lung virus titers and results of ELISA and total protein quantifications. Probabilities \* ( $p$ ) <  
150 0.05, \*\* ( $p$ ) < 0.01 were considered statistically significant.

151 **RESULTS**

152

153 **Platelet recruitment to the lungs upon IAV infection**

154 Platelet recruitment to the lungs was first examined after infection of mice with a sublethal or  
155 a 50% lethal dose (LD<sub>50</sub>) of IAV A/PR/8/34. Immunohistochemistry of the lungs, using  
156 monoclonal antibodies for IAV nucleoprotein (NP) and CD41, was used to detect virus-infected  
157 cells and platelets, respectively (Figure 1A). At both doses, extensive numbers of IAV-infected  
158 cells and marked platelet infiltrates were detected in the lungs of infected mice compared to  
159 uninfected mice. To confirm these results, platelet counts in the broncho-alveolar lavages  
160 (BAL) of infected (LD<sub>50</sub>) versus uninfected mice were assessed using a blood cell counter  
161 (Figure 1B). In the BAL of infected mice, platelet levels were significantly higher than in those  
162 of uninfected mice, reaching  $50 \times 10^9$  cells/L on day 6 post-inoculation. These results show that  
163 platelets are massively recruited to the lungs upon IAV infection.

164

165 **Engulfment of viral particles by platelets**

166 Next, we investigated whether platelets recruited to the lungs of IAV infected mice would  
167 engulf IAV particles. To this end, the presence of IAV particles in platelets from the BAL of  
168 infected mice was investigated, by immunofluorescence staining, using the platelet-specific  
169 anti-CD41 and viral anti-hemagglutinin (HA) antibodies. Nuclei were counterstained with  
170 DAPI. In contrast to uninfected mice (NI), upon infection (LD<sub>50</sub>), CD41-positive DAPI-  
171 negative platelets, stained positively for viral HA, demonstrating that platelets engulfed IAV  
172 particles, *in vivo* (Figure 1C). CD41-negative/DAPI-positive cells were used as controls for  
173 antibody specificity. To confirm these results, immunogold labeling of ultrathin cryosections  
174 of lungs of uninfected or infected mice was performed using a specific anti-HA antibody.  
175 Examination of platelets clearly showed a positive and specific staining of viruses, which were

176 located predominantly within platelet granules (Figure 1D). Altogether, these results show that  
177 platelets recruited to the lungs take up IAV particles in the specific subcellular compartments  
178 of granules.

179

### 180 **Platelet activation and aggregation**

181 Upon injury, platelets become immobilized, activate, secrete their granule content, and  
182 aggregate. Thus we next analyzed these responses in the lungs of infected mice (sublethal or  
183 LD<sub>50</sub>). Upon activation, serotonin is released from platelet dense granules and P-selectin is  
184 rapidly translocated from the alpha granules to the plasma membrane and shed. Serotonin and  
185 soluble P-selectin (sP-selectin) levels were respectively measured in BAL and plasma of the  
186 mice by ELISA (Figure 2A). Levels of serotonin and sP-selectin were significantly higher in  
187 the fluids of infected mice. Significant differences were only observed upon infection with IAV  
188 at the LD<sub>50</sub>. Thus, upon lethal IAV infection, the presence of platelet activation markers in the  
189 BAL and plasma indicates that platelets are activated in the lung. Furthermore, exposure of P-  
190 selectin at the surface of blood platelets isolated from IAV-infected mice was increased  
191 compared to those of uninfected mice (Figure 2B, left panel). The average % of P-selectin-  
192 positive platelets reached 23% upon infection, versus 5% in uninfected mice (Figure 2B, right  
193 panel). Moreover, transmission electron microscopic studies showed that platelets in the lungs  
194 of influenza virus-infected mice were tightly packed, forming large extravascular aggregates  
195 with signs of shape change and degranulation (Figure 2C). In contrast, in the lungs of uninfected  
196 mice, only a few isolated platelets were detected. Together, these results show that IAV  
197 infection induce infiltration of numerous activated platelets that form large aggregates within  
198 the lung tissue.

199

200

201 **Platelets contribute to influenza pathogenesis**

202 To explore the contribution of platelets to the severity of IAV infection, we then investigated  
203 the consequence of the deficiency of a major platelet receptor, GPIIIa. To this end, platelet  
204 GPIIIa<sup>+/-</sup> mice were intercrossed to generate wild-type (WT) and platelet GPIIIa<sup>-/-</sup> mice, which  
205 were then infected with IAV A/PR/8/34 and survival rates were monitored. As shown in Figure  
206 2D, compared to WT mice, GPIIIa<sup>-/-</sup> mice were significantly more resistant to IAV-induced  
207 death. Thus, in absence of platelet GPIIIa, the pathogenesis of IAV infection was dampened  
208 and mortality reduced, indicating that platelets contribute to the fatal outcome of severe IAV  
209 infections.

210

211 **PAR4 promotes pathogenesis of IAV infection in a platelet-dependent pathway**

212 In a complementary assay, we investigated the effect of promoting platelet activation. PAR4 is  
213 a major receptor for platelet activation in the mouse model. Therefore, mice were inoculated  
214 with a sublethal dose of IAV A/PR/8/34 and stimulated with 100 µg/mouse of the PAR4 agonist  
215 peptide, AYPGKF-NH<sub>2</sub> (PAR4-AP), or the inactive control peptide, YAPGKF-NH<sub>2</sub>. As  
216 expected, treatment with PAR4-AP increased platelet activation, as observed by increased  
217 serotonin and soluble P-selectin levels in the BAL and plasma of infected mice (Figure 3A).  
218 More interestingly, upon infection, mice treated with PAR4-AP displayed significantly higher  
219 mortality rates compared with mice treated with control peptide (Figure 3B). In contrast,  
220 treatment with PAR4-AP did not affect the survival of uninfected mice. The effect was platelet  
221 dependent, as treatment of mice with eptifibatide abrogated the deleterious effect of PAR4-AP  
222 (Figure 3C), as also did the platelet GPIIIa-deficiency (Figure 3D). Thus, platelet activation  
223 potentiates IAV pathogenesis. To assess whether PAR4 activation impacted virus replication,  
224 infectious virus titers were evaluated in the lungs of infected mice treated or not with PAR4-  
225 AP. No significant differences in lung virus titers were observed 3 or 6 days post-inoculation

226 between mice treated or not with PAR4-AP, showing that the deleterious effect of PAR4 was  
227 independent of virus replication in the lungs (Figure 3E). The contribution of PAR4 was further  
228 assessed by measuring the amounts of total protein and the cytokine levels in the BAL of  
229 infected mice treated or not with PAR4-AP. At day 6 post-infection, treatment with PAR4-AP  
230 significantly increased total proteins in the BAL (Figure 3F). Response levels of IL-6, IL-1 $\beta$   
231 and MIP-2 were also enhanced, while those of interferon (IFN)- $\gamma$ , RANTES and KC were  
232 unaffected (Figure 4A). At day 3 post-infection, no difference was observed. Thus, PAR4  
233 activation promoted IAV-induced inflammation of the lungs, at later time points post-infection.  
234 In agreement, staining of lung section at day 6 post-infection revealed marked cellular infiltrates  
235 of leukocytes (HE) and neutrophils (Ly6G) in the lungs of PAR4-AP-treated mice but not in  
236 controls (Figure 4B). Similar numbers of IAV-infected cells were detected by  
237 immunohistochemistry using an anti-viral NP antibody. No staining was observed in the lungs  
238 of uninfected mice, used as controls. Thus, PAR4 contributes to deleterious lung inflammation  
239 and IAV pathogenesis, via increased platelet activation.

240

#### 241 **PAR4 antagonism protects against influenza virus pathogenicity**

242 We next examined the effect of pharmacological inhibition of PAR4, using pepducin p4pal-10  
243 (21). When mice were infected with IAV A/PR/8/34 (LD<sub>50</sub>), treatment with pepducin p4pal-  
244 10 protected them from death (Figure 5A). Substantial protection was also observed against  
245 infection with an H3N2 virus, A/HK/1/68. The protection conferred by PAR4 antagonism  
246 correlated with the degree of inhibition of platelet activation. In the BAL of pepducin p4pal-  
247 10-treated mice, decreased levels of thromboxane B2 (TXB2), a specific marker of platelet  
248 activation, were observed (Figure 5B). In contrast, no difference in mean lung virus titers was  
249 detected on days 3 and 6 post-inoculation with IAV A/PR/8/34 (Figure 5C). However, treatment  
250 with pepducin p4pal-10 significantly reduced the recruitment of leucocytes (Figure 5D),

251 including neutrophils, in BAL at day 6 post-inoculation. Total proteins (Figure 5E) and levels  
252 of IL-6, IL-1 $\beta$  and MIP-2 (Figure 5F) were also decreased. Also, histopathological studies  
253 revealed that treatment with pepducin p4pal-10 reduced infiltration of inflammatory cells (HE),  
254 including neutrophils (Ly6G), in the lungs of infected mice (Figure 5G), while similar numbers  
255 of IAV-infected cells (NP) were detected by immunohistochemistry. Thus, inhibition of PAR4  
256 protects mice from IAV-induced pathogenesis.

257

### 258 **The anti-platelet drug eptifibatide protects mice from lethal influenza infection**

259 Preventing deleterious inflammation could be a promising new strategy to treat severe  
260 influenza. Therefore, we investigated whether inhibition of platelet aggregation with  
261 eptifibatide would have an incremental benefit on IAV infection outcome. Eptifibatide is an  
262 approved anti-platelet drug and therefore of particular interest for its potential repositioning as  
263 an anti-influenza treatment with accelerated regulatory registration. Mice were inoculated with  
264 IAV A/PR/8/34 (LD<sub>50</sub>) and treated or not with eptifibatide. Eptifibatide treatment had a  
265 dramatic effect on lung infiltration by platelets: platelet aggregation was totally prevented and  
266 only isolated platelets were observed (Figure 6A). This effect was accompanied by a decrease  
267 in the levels of TXB<sub>2</sub> present in the BAL of infected mice (Figure 6B), showing that inhibition  
268 of platelet aggregation also limited the extent of platelet activation. More importantly, treatment  
269 with eptifibatide improved the outcome of infection with A/PR/8/34 virus and prevented  
270 mortality of the mice (Figure 6C). Protection appeared to be independent of the strain, as it was  
271 also observed upon infection with IAV pandemic A/NL/602/09 (H1N1) and A/HK/1/68  
272 (H3N2). Similarly, a protective tendency was also observed upon infection with the highly  
273 pathogenic avian H7N7 virus (FPV). Protective effect was independent of virus replication in  
274 lungs (Figure 7A) but correlated with decreased total protein and cytokine levels in the BAL of  
275 eptifibatide-treated mice (Figure 7B-C). Immunohistochemistry confirmed that treatment by

276 eptifibatide prevented IAV-induced lung alveolar damage (HE) and neutrophil infiltration  
277 (Ly6G) but not viral replication (NP) at day 6 post-infection (Figure 7D). This effect was not  
278 observed at day 2 post-infection (data not shown). Thus, eptifibatide treatment prevented IAV-  
279 induced cytokine storm and protected mice against infection by various strains of IAV.

280

## 281 **DISCUSSION**

282 The present study shows that platelets play an active role in fuelling the cytokine storm and  
283 promote pathogenesis of influenza virus infections.

284 Histological analysis of lungs provided evidence that platelets massively infiltrate the lungs of  
285 infected mice. Also, IAV particles were detected within platelet granules. This finding confirms  
286 a previous report, showing that platelets engulf IAV particles, *in vitro* (22). This could consist  
287 of a passive passage of particles through the open canalicular system, the tortuous invaginations  
288 of platelet surface membrane tunnelling through the cytoplasm, in a manner similar to bacterial  
289 ingestion (23). Alternatively, uptake of IAV may be compared to phagocytosis by macrophages  
290 and neutrophils, as previously observed for human immunodeficiency viruses (24).

291 Ultrastructural analysis showed that features of platelets in the lungs of infected mice are those  
292 of aggregates made of activated platelets: platelets were tightly stacked without interplatelet  
293 spaces and with images of degranulation. Consistently, markers of platelet activation were  
294 detected in the fluids of infected mice. More recently, a recent report also showed platelet  
295 activation upon IAV infection (25). Platelets contribute to the host defence against bacterial  
296 infectious agents by limiting vascular lesions and induce repair of injury (12, 26, 27). However,  
297 platelet dysfunction may have pathological consequences. In our influenza model, platelet  
298 function was deleterious. First, mice deficient in GPIIIa, a major receptor required for platelet  
299 aggregation were protected from infections. Furthermore, stimulation of PAR4, a major  
300 receptor for platelet activation increased lung inflammation and the severity of IAV infections.

301 In contrast, PAR4 antagonists protected mice from death. Our results indicate that PAR4 acted  
302 through platelet activation since the effect of PAR4-AP was abrogated when infected mice were  
303 treated with the platelet specific inhibitor, eptifibatide (28), or when mice were deficient in  
304 platelet GPIIIa protein.

305 In several models of injury when platelet activation escapes control, it drives deleterious  
306 inflammation (29). Activated platelets release an arsenal of potent pro-inflammatory molecules  
307 (30, 31), which exacerbate neutrophil rolling, adhesion and recruitment (10, 32-34). In addition,  
308 the physical interaction between platelets and neutrophils further contributes to neutrophil  
309 retention and activation (35). Since cytokine storm is a hallmark of severe influenza virus  
310 infections, it was likely that platelets should have a pro-inflammatory effect with a key role in  
311 IAV pathogenesis.

312 Interestingly, exacerbation of cytokine production induced by platelet stimulation was only  
313 observed at later time points after infection. Upon injury, inflammation is induced to activate  
314 the repairing processes but should be resolved to allow recovery. Thus, it is possible that  
315 cytokine storm results from a default in the resolution of inflammation more than in its  
316 induction. Thus, cytokine storm could be depend on a loss of control of endothelial cells,  
317 hemostasis and wound healing, rather than virus replication (8, 36, 37). In this scenario,  
318 extravasation of large amounts of platelets and leucocytes would be at the basis of the defect in  
319 the resolution phase of the inflammation and cytokine storm, as in the model proposed in Figure  
320 8. Most likely this further promotes hemostasis dysregulation, such as fibrinolysis (19, 36) or  
321 PAR1 activation (38, 39), fuelling the vicious circle of inflammation (36, 40). In accord, in  
322 patients with severe IAV infection, dysregulation of hemostasis with thrombocytopenia and  
323 cardiovascular complications were often observed (41, 42). The dissociation of the aggregates  
324 should thus contribute to the restoration of pulmonary function.

325 Recurrent outbreaks of IAV that cause severe infections in humans have raised serious concern  
326 about therapeutic strategies available for these pathogens. Current treatments target viral protein  
327 that suffers from a number of disadvantages, including the rapid development of resistant virus  
328 variants as a result of selective pressure (43, 44). Because targeting the host rather than the virus  
329 would not easily lead to resistance, drugs regulating inflammation are appealing as potential  
330 treatments for IAV infection (15, 38, 40, 45-47). It is noteworthy that one of the drugs that was  
331 tested here, eptifibatid, is already commercialized and is currently in use clinically. This  
332 provides the potential for immediate therapeutic impact with the development of new drugs for  
333 treating influenza with an accelerated regulatory registration.

#### 334 **ACKNOWLEDGMENTS**

335 Authors are grateful to Dr. P. Clézardin (Inserm UMR S1033, France) and Dr. C. Dumontet  
336 (Cancer Center of Lyon, France) for help in immunohistochemistry and immunofluorescence.

337

#### 338 **REFERENCES**

339

- 340 **1. Kuiken T, Riteau B, Fouchier RA, Rimmelzwaan GF. Pathogenesis of influenza**  
341 **virus infections: The good, the bad and the ugly. *Curr Opin Virol* 2012;2:276-286.**
- 342 **2. Fukuyama S, Kawaoka Y. The pathogenesis of influenza virus infections: The**  
343 **contributions of virus and host factors. *Current opinion in immunology* 2011;23:481-486.**
- 344 **3. Foucault ML, Moules V, Rosa-Calatrava M, Riteau B. Role for proteases and hla-**  
345 **g in the pathogenicity of influenza a viruses. *J Clin Virol* 2011;51:155-159.**
- 346 **4. La Gruta NL, Kedzierska K, Stambas J, Doherty PC. A question of self-**  
347 **preservation: Immunopathology in influenza virus infection. *Immunol Cell Biol***  
348 **2007;85:85-92.**
- 349 **5. Cheung CY, Poon LL, Lau AS, Luk W, Lau YL, Shortridge KF, Gordon S, Guan**  
350 **Y, Peiris JS. Induction of proinflammatory cytokines in human macrophages by influenza**

- 351 a (h5n1) viruses: A mechanism for the unusual severity of human disease? *Lancet*  
352 2002;360:1831-1837.
- 353 6. de Jong MD, Simmons CP, Thanh TT, Hien VM, Smith GJ, Chau TN, Hoang DM,  
354 Chau NV, Khanh TH, Dong VC, Qui PT, Cam BV, Ha do Q, Guan Y, Peiris JS, Chinh  
355 NT, Hien TT, Farrar J. Fatal outcome of human influenza a (h5n1) is associated with high  
356 viral load and hypercytokinemia. *Nature medicine* 2006;12:1203-1207.
- 357 7. Kobasa D, Jones SM, Shinya K, Kash JC, Copps J, Ebihara H, Hatta Y, Kim JH,  
358 Halfmann P, Hatta M, Feldmann F, Alimonti JB, Fernando L, Li Y, Katze MG, Feldmann  
359 H, Kawaoka Y. Aberrant innate immune response in lethal infection of macaques with  
360 the 1918 influenza virus. *Nature* 2007;445:319-323.
- 361 8. Teijaro JR, Walsh KB, Cahalan S, Fremgen DM, Roberts E, Scott F,  
362 Martinborough E, Peach R, Oldstone MB, Rosen H. Endothelial cells are central  
363 orchestrators of cytokine amplification during influenza virus infection. *Cell*  
364 2011;146:980-991.
- 365 9. Rumbaut RE, Thiagarajan P. Platelet-vessel wall interactions in hemostasis and  
366 thrombosis. San Rafael (CA); 2010.
- 367 10. Duerschmied D, Suidan GL, Demers M, Herr N, Carbo C, Brill A, Cifuni SM,  
368 Mauler M, Cicko S, Bader M, Idzko M, Bode C, Wagner DD. Platelet serotonin promotes  
369 the recruitment of neutrophils to sites of acute inflammation in mice. *Blood*  
370 2013;121:1008-1015.
- 371 11. Cohen J. The immunopathogenesis of sepsis. *Nature* 2002;420:885-891.
- 372 12. Degen JL, Bugge TH, Goguen JD. Fibrin and fibrinolysis in infection and host  
373 defense. *J Thromb Haemost* 2007;5 Suppl 1:24-31.
- 374 13. Medcalf RL. Fibrinolysis, inflammation, and regulation of the plasminogen  
375 activating system. *J Thromb Haemost* 2007;5 Suppl 1:132-142.

- 376 14. Riteau B, Moreau P, Menier C, Khalil-Daher I, Khosrotehrani K, Bras-Goncalves  
377 R, Paul P, Dausset J, Rouas-Freiss N, Carosella ED. Characterization of hla-g1, -g2, -g3,  
378 and -g4 isoforms transfected in a human melanoma cell line. *Transplant Proc*  
379 2001;33:2360-2364.
- 380 15. Khoufache K, LeBouder F, Morello E, Laurent F, Riffault S, Andrade-Gordon P,  
381 Boullier S, Rousset P, Vergnolle N, Riteau B. Protective role for protease-activated  
382 receptor-2 against influenza virus pathogenesis via an ifn-gamma-dependent pathway. *J*  
383 *Immunol* 2009;182:7795-7802.
- 384 16. Riteau B, de Vaureix C, Lefevre F. Trypsin increases pseudorabies virus  
385 production through activation of the erk signalling pathway. *J Gen Virol* 2006;87:1109-  
386 1112.
- 387 17. Riteau B, Faure F, Menier C, Viel S, Carosella ED, Amigorena S, Rouas-Freiss N.  
388 Exosomes bearing hla-g are released by melanoma cells. *Hum Immunol* 2003;64:1064-  
389 1072.
- 390 18. LeBouder F, Morello E, Rimmelzwaan GF, Bosse F, Pechoux C, Delmas B, Riteau  
391 B. Annexin ii incorporated into influenza virus particles supports virus replication by  
392 converting plasminogen into plasmin. *J Virol* 2008;82:6820-6828.
- 393 19. LeBouder F, Lina B, Rimmelzwaan GF, Riteau B. Plasminogen promotes influenza  
394 a virus replication through an annexin 2-dependent pathway in the absence of  
395 neuraminidase. *J Gen Virol* 2010;91:2753-2761.
- 396 20. LeBouder F, Khoufache K, Menier C, Mandouri Y, Keffous M, Lejal N, Krawice-  
397 Radanne I, Carosella ED, Rouas-Freiss N, Riteau B. Immunosuppressive hla-g molecule  
398 is upregulated in alveolar epithelial cells after influenza a virus infection. *Hum Immunol*  
399 2009;70:1016-1019.

- 400 21. Covic L, Misra M, Badar J, Singh C, Kuliopulos A. Pepducin-based intervention  
401 of thrombin-receptor signaling and systemic platelet activation. *Nature medicine*  
402 2002;8:1161-1165.
- 403 22. Danon D, Jerushalmy Z, De Vries A. Incorporation of influenza virus in human  
404 blood platelets in vitro. Electron microscopical observation. *Virology* 1959;9:719-722.
- 405 23. White JG. Platelets are coverocytes, not phagocytes: Uptake of bacteria involves  
406 channels of the open canalicular system. *Platelets* 2005;16:121-131.
- 407 24. Youssefian T, Drouin A, Masse JM, Guichard J, Cramer EM. Host defense role of  
408 platelets: Engulfment of hiv and staphylococcus aureus occurs in a specific subcellular  
409 compartment and is enhanced by platelet activation. *Blood* 2002;99:4021-4029.
- 410 25. Boilard E, Pare G, Rousseau M, Cloutier N, Dubuc I, Levesque T, Borgeat P,  
411 Flamand L. Influenza virus h1n1 activates platelets through fcgammariia signaling and  
412 thrombin generation. *Blood* 2014;123:2854-2863.
- 413 26. Petaja J. Inflammation and coagulation. An overview. *Thromb Res* 2011;127 Suppl  
414 2:S34-37.
- 415 27. Engelmann B, Massberg S. Thrombosis as an intravascular effector of innate  
416 immunity. *Nat Rev Immunol* 2013;13:34-45.
- 417 28. Tardiff BE, Jennings LK, Harrington RA, Gretler D, Potthoff RF, Vorchheimer  
418 DA, Eisenberg PR, Lincoff AM, Labinaz M, Joseph DM, McDougal MF, Kleiman NS,  
419 Investigators P. Pharmacodynamics and pharmacokinetics of eptifibatide in patients with  
420 acute coronary syndromes: Prospective analysis from pursuit. *Circulation* 2001;104:399-  
421 405.
- 422 29. Henn V, Slupsky JR, Grafe M, Anagnostopoulos I, Forster R, Muller-Berghaus G,  
423 Kroczeck RA. Cd40 ligand on activated platelets triggers an inflammatory reaction of  
424 endothelial cells. *Nature* 1998;391:591-594.

- 425 30. Lindemann S, Tolley ND, Dixon DA, McIntyre TM, Prescott SM, Zimmerman GA,  
426 Weyrich AS. Activated platelets mediate inflammatory signaling by regulated interleukin  
427 1beta synthesis. *J Cell Biol* 2001;154:485-490.
- 428 31. von Hundelshausen P, Weber KS, Huo Y, Proudfoot AE, Nelson PJ, Ley K, Weber  
429 C. Rantes deposition by platelets triggers monocyte arrest on inflamed and atherosclerotic  
430 endothelium. *Circulation* 2001;103:1772-1777.
- 431 32. Diacovo TG, Roth SJ, Buccola JM, Bainton DF, Springer TA. Neutrophil rolling,  
432 arrest, and transmigration across activated, surface-adherent platelets via sequential  
433 action of p-selectin and the beta 2-integrin cd11b/cd18. *Blood* 1996;88:146-157.
- 434 33. Kuijper PH, Gallardo Torres HI, van der Linden JA, Lammers JW, Sixma JJ,  
435 Koenderman L, Zwaginga JJ. Platelet-dependent primary hemostasis promotes selectin-  
436 and integrin-mediated neutrophil adhesion to damaged endothelium under flow  
437 conditions. *Blood* 1996;87:3271-3281.
- 438 34. Mayadas TN, Johnson RC, Rayburn H, Hynes RO, Wagner DD. Leukocyte rolling  
439 and extravasation are severely compromised in p selectin-deficient mice. *Cell*  
440 1993;74:541-554.
- 441 35. Zarbock A, Polanowska-Grabowska RK, Ley K. Platelet-neutrophil-interactions:  
442 Linking hemostasis and inflammation. *Blood reviews* 2007;21:99-111.
- 443 36. Berri F, Le VB, Jandrot-Perrus M, Lina B, Riteau B. Switch from protective to  
444 adverse inflammation during influenza: Viral determinants and hemostasis are caught as  
445 culprits. *Cellular and molecular life sciences : CMLS* 2013.
- 446 37. O'Brien KB, Vogel P, Duan S, Govorkova EA, Webby RJ, McCullers JA, Schultz-  
447 Cherry S. Impaired wound healing predisposes obese mice to severe influenza virus  
448 infection. *J Infect Dis* 2012;205:252-261.

- 449 38. Khoufache K, Berri F, Nacken W, Vogel AB, Delenne M, Camerer E, Coughlin  
450 SR, Carmeliet P, Lina B, Rimmelzwaan GF, Planz O, Ludwig S, Riteau B. Par1  
451 contributes to influenza A virus pathogenicity in mice. *J Clin Invest* 2013;123:206-214.
- 452 39. Aerts L HM, Rhéaume C, Lavigne S, Couture C, Kim W, Susan-Resiga D, Prat A,  
453 Seidah NG, Vergnolle N, Riteau B, Boivin G. Modulation of protease activated receptor 1  
454 influences human metapneumovirus disease severity in a mouse model. *Plos One*  
455 2013;28;8(8):e72529.
- 456 40. Berri F, Rimmelzwaan GF, Hanss M, Albina E, Foucault-Grunenwald ML, Le VB,  
457 Vogelzang-van Trierum SE, Gil P, Camerer E, Martinez D, Lina B, Lijnen R, Carmeliet  
458 P, Riteau B. Plasminogen controls inflammation and pathogenesis of influenza virus  
459 infections via fibrinolysis. *PLoS Pathog* 2013;9:e1003229.
- 460 41. Warren-Gash C, Smeeth L, Hayward AC. Influenza as a trigger for acute  
461 myocardial infarction or death from cardiovascular disease: A systematic review. *Lancet*  
462 *Infect Dis* 2009;9:601-610.
- 463 42. Wiwanitkit V. Hemostatic disorders in bird flu infection. *Blood Coagul Fibrinolysis*  
464 2008;19:5-6.
- 465 43. Song MS, Hee Baek Y, Kim EH, Park SJ, Kim S, Lim GJ, Kwon HI, Pascua PN,  
466 Decano AG, Lee BJ, Kim YI, Webby RJ, Choi YK. Increased virulence of neuraminidase  
467 inhibitor-resistant pandemic H1N1 virus in mice: Potential emergence of drug-resistant  
468 and virulent variants. *Virulence* 2013;4:489-493.
- 469 44. Butler J, Hooper KA, Petrie S, Lee R, Maurer-Stroh S, Reh L, Guarnaccia T, Baas  
470 C, Xue L, Vitesnik S, Leang SK, McVernon J, Kelso A, Barr IG, McCaw JM, Bloom JD,  
471 Hurt AC. Estimating the fitness advantage conferred by permissive neuraminidase  
472 mutations in recent oseltamivir-resistant A(H1N1)pdm09 influenza viruses. *PLoS Pathog*  
473 2014;10:e1004065.

- 474 **45. Garcia CC, Russo RC, Guabiraba R, Fagundes CT, Polidoro RB, Tavares LP,**  
475 **Salgado AP, Cassali GD, Sousa LP, Machado AV, Teixeira MM. Platelet-activating factor**  
476 **receptor plays a role in lung injury and death caused by influenza a in mice. *PLoS Pathog***  
477 **2010;6:e1001171.**
- 478 **46. Walsh KB, Teijaro JR, Wilker PR, Jatzek A, Fremgen DM, Das SC, Watanabe T,**  
479 **Hatta M, Shinya K, Suresh M, Kawaoka Y, Rosen H, Oldstone MB. Suppression of**  
480 **cytokine storm with a sphingosine analog provides protection against pathogenic**  
481 **influenza virus. *Proc Natl Acad Sci U S A* 2011;108:12018-12023.**
- 482 **47. Lina B, Riteau B. [antagonists of par1: Towards a new antiviral strategy against**  
483 **flu]. *Med Sci (Paris)* 2013;29:107-109.**

484

#### 485 **FIGURE LEGENDS**

486 **Figure 1: Upon IAV infection, platelets infiltrate the lungs and engulf IAV particles. (A)**  
487 Immunohistochemistry analysis of lungs from uninfected (NI) or infected mice inoculated with  
488 A/PR/8/34 virus, at a sublethal dose or LD<sub>50</sub> (day 6 post-infection). Antibodies against the IAV  
489 nucleoprotein (NP) and CD41 were used to detect virus infected cells and platelets,  
490 respectively. The results shown are representative of three mice per group. (B) Platelet numbers  
491 in BAL were assessed using a Vet ABC™ Hematology Analyzer at day 6 post inoculation of  
492 mock or IAV-infected mice. Data are represented as means ± SEM of 4 mice per group. (C)  
493 Immunofluorescence staining of viral particles in platelets from BAL was performed with anti-  
494 influenza HA antibody. Platelets were detected with anti-CD41 antibody and the nuclei were  
495 counterstained with DAPI. The merged images are shown on the right panel. CD41-negative  
496 cells from BAL were used as a negative control. (D) Immunogold labeling of ultrathin  
497 cryosections of lungs of uninfected (NI) or A/PR/8/34 virus-infected mice (LD<sub>50</sub>, day 6 post-

498 infection) was performed using the specific anti-HA antibody. Black arrows indicate viral  
499 particles.

500

501 **Figure 2: Upon IAV infection, platelets are stimulated and contribute to influenza**

502 **pathogenesis.** (A) Levels of serotonin and sP-selectin were determined by ELISA in the BAL  
503 and plasma of Mock (NI) or A/PR/8/34 virus-infected mice, respectively, at day 6 post  
504 inoculation (sublethal dose or LD<sub>50</sub>). Data represent means  $\pm$  SEM of 4 mice per group. (B)  
505 Blood samples from uninfected (NI) or infected mice were double-stained with anti-P-selectin  
506 and anti-CD41 antibody as a platelet identifier. The mean percentage  $\pm$  SEM of activated  
507 platelets (CD41 and P-selectin-positive) from n = 5 mice per group is shown on the right panel.  
508 (C) Ultrastructural analysis of platelets in the lungs of uninfected and infected mice (A/PR/8/34,  
509 LD<sub>50</sub>). Note the aggregation of platelets in the lungs of infected mice along with their  
510 morphological change (arrows) and the absence of granules in some of them, which reflects  
511 their degranulation (asterisks). (D) Survival of platelet GPIIIa<sup>-/-</sup> mice and WT littermates after  
512 infection with A/PR/8/34 virus at a lethal dose (n=9-10 mice per group) or LD<sub>50</sub> (n = 6 mice per  
513 group).

514

515 **Figure 3: Effect of PAR4 activation on IAV pathogenicity, virus replication and**

516 **inflammation.** (A) Levels of serotonin and sP-selectin, were determined by ELISA,  
517 respectively in the BAL and plasma of infected mice (A/PR/8/34, sublethal dose) after treatment  
518 with PAR4-AP or control peptide, at day 6 post-inoculation. Columns represent means  $\pm$  SEM  
519 (n = 4-5). (B) Time course of IAV-induced death in mice in response to PAR4 stimulation.  
520 Mice were Mock-infected or inoculated with A/PR/8/34virus (Sublethal dose, n = 18-19 mice  
521 per group; LD<sub>50</sub>, n = 6-12 mice per group) and treated with either control peptide or PAR4-AP.  
522 (C) Time course of IAV-induced death in mice (A/PR/8/34virus) in response to PAR4

523 stimulation and after treatment or not with eptifibatide (n = 6-18 mice per group). (D) Time  
524 course of IAV-induced death in WT (n = 10 mice per group) and GPIIIa <sup>-/-</sup> mice (n = 7-9 mice  
525 per group) in response to PAR4 stimulation (A/PR/8/34virus). Same mice were used in panel  
526 A (dose LD<sub>50</sub>) (E) Lung virus titers after infection of mice with A/PR/8/34 virus (sublethal  
527 dose) stimulated or not with PAR4-AP. (F) Total protein quantification in BAL of infected mice  
528 in response to PAR4 stimulation. For E and F, columns represent means ± SEM (n= 3-5).

529 **Figure 4: PAR4-AP increases lung inflammation upon A/PR/8/34 virus infection.** (A)  
530 Cytokines in the BAL of infected mice (sublethal dose), treated with PAR4-AP or control  
531 peptide, were measured by ELISA 3 and 6 days after inoculation. Uninfected mice (NI) were  
532 used as control. Columns represent means ± SEM (n = 3-5). (B) Histopathological analysis of  
533 lungs from uninfected mice or mice infected with a sublethal dose of A/PR/8/34 virus after  
534 treatment with PAR4-AP or control peptide, at day 6 post-infection. Thin sections of lungs were  
535 stained with hematoxylin and eosin (HE). Note the marked infiltration of cells in the lungs of  
536 infected mice stimulated with PAR4-AP. Immunohistochemistry using antibodies against  
537 Ly6G, viral NP was used to detect neutrophils and virus-infected cells. Data are representative  
538 of three mice per group.

539

540 **Figure 5: PAR4 antagonist protects mice against IAV infection and deleterious lung**  
541 **inflammation.** (A) IAV-induced pathogenesis in mice treated or not with the PAR4 antagonist,  
542 pepducin p4pal-10 (pepducin). Mice were inoculated with A/PR/8/34 virus (LD<sub>50</sub> n = 13 mice  
543 per group) or A/HK/1/68 (LD<sub>50</sub>, n = 12 mice per group) and treated with pepducin or vehicle.  
544 Survival was then monitored for two weeks. (B) Levels of thromboxane B2 (TXB2) was  
545 determined by ELISA in the BAL of infected mice (A/PR/8/34, LD<sub>50</sub>) after treatment with  
546 pepducin or vehicle, at day 6 post-inoculation. Data represent mean ± SEM of 4-6 mice per  
547 group. (C) Lung virus titers after infection of mice with A/PR/8/34 virus (LD<sub>50</sub>) treated with

548 pepducin or vehicle. Columns represent means  $\pm$  SEM from 3 individual animals per group.  
549 (D) Relative leukocyte and neutrophil numbers in BAL from mice treated with pepducin or  
550 vehicle, determined by May-Grünwald-Giemsa staining 6 days after inoculation. Columns  
551 represent means  $\pm$  SEM from 6 individual mice per group. (E, F) Total proteins and levels of  
552 cytokines were determined by ELISA in the BAL of infected mice (A/PR/8/34, LD<sub>50</sub>) after  
553 treatment with pepducin or vehicle, at day 6 post-inoculation. Columns represent means  $\pm$  SEM  
554 of 4-6 mice per group. (G) Histopathological analysis of lungs from mice infected with  
555 A/PR/8/34 virus (LD<sub>50</sub>) after treatment with pepducin or vehicle, at day 6 post infection. Lung  
556 sections were stained with hematoxylin and eosin (HE). Immunohistochemistry using  
557 antibodies against Ly6G, viral NP was used to detect neutrophils and virus-infected cells. Data  
558 are representative of three mice per group.

559

560 **Figure 6: Eptifibatide protects mice against IAV infection, independently of the strain.**

561 (A) Ultrastructural analysis of platelets in the lungs of infected mice (A/PR/8/34, LD<sub>50</sub>), treated  
562 or not with eptifibatide, was performed by transmission electron microscopy. Note the  
563 aggregation of platelets in the lungs of infected mice, and their disaggregation after treatment  
564 of mice with eptifibatide. (B) Levels of thromboxane B2 (TXB2) were determined by ELISA  
565 in the BAL of infected mice (A/NL/602/09, LD<sub>50</sub>) after treatment with eptifibatide or vehicle.  
566 Columns represent means  $\pm$  SEM of 3-5 mice per group. (C) Survival of mice treated with  
567 eptifibatide or vehicle after infection with IAV A/PR/8/34 (n = 13 mice per group),  
568 A/NL/602/09 (n = 9-12 mice per group) or A/HK/1/68 (n = 12 mice per group) at their  
569 respective LD<sub>50</sub>. A/FPV/Bratislava/79 was used at 5 Pfu/mouse (n = 6-7 mice per group).

570

571 **Figure 7: Eptifibatide treatment prevents severe inflammation during influenza virus**

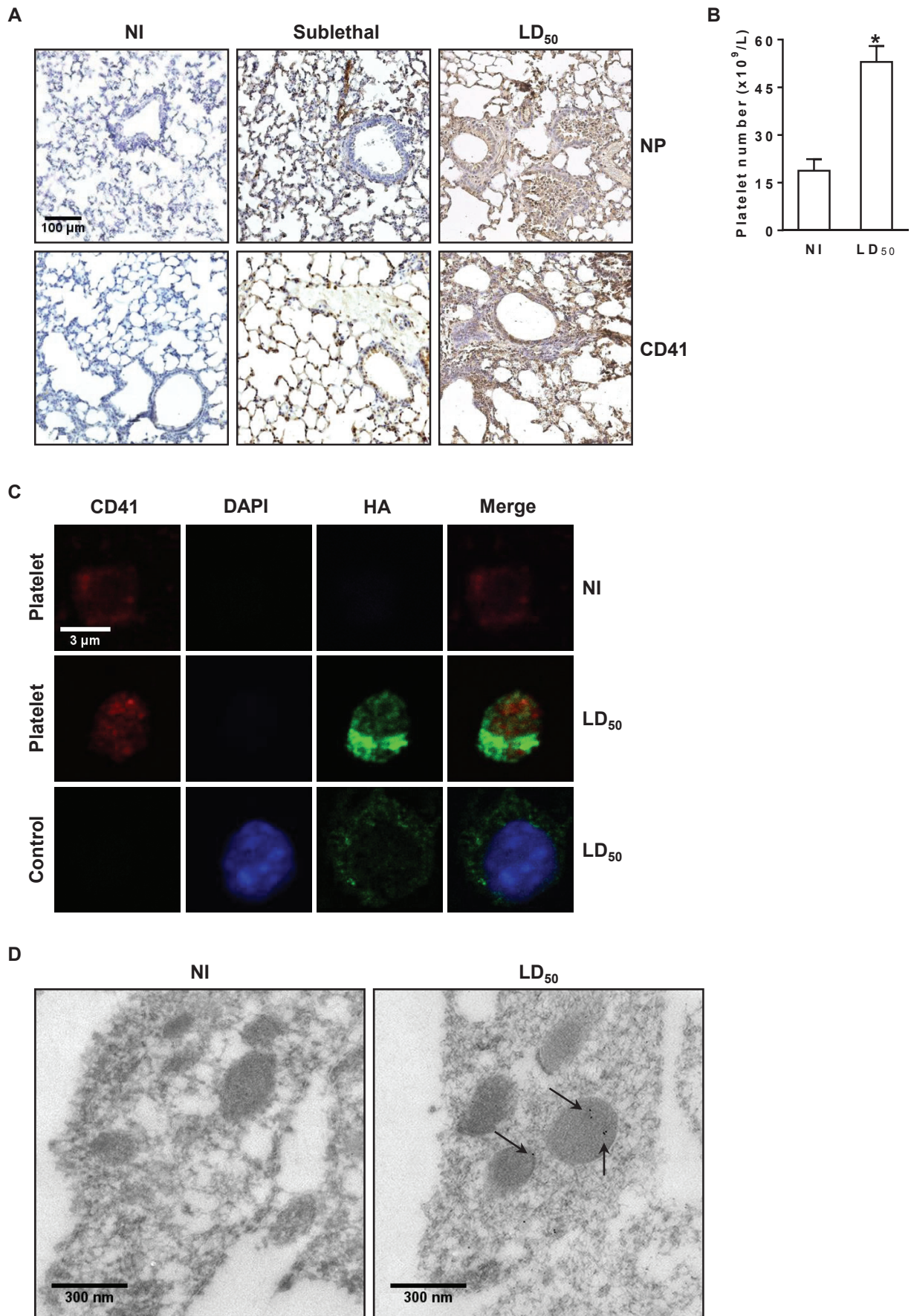
572 **infections.** (A) Lung virus titers after infection of mice with the A/NL/602/09 virus (LD<sub>50</sub>)

573 treated with eptifibatide or vehicle. Columns represent means  $\pm$  SEM from 3 individual animals  
574 per group. (B, C) Total proteins and levels of cytokines were determined by ELISA in the BAL  
575 of infected mice (A/NL/602/09, LD<sub>50</sub>) after treatment with eptifibatide or vehicle. Columns  
576 represent means  $\pm$  SEM of 3-5 mice per group. (D) Histopathological analysis of lungs from  
577 mice infected with A/NL/602/09 virus (LD<sub>50</sub>) after treatment with eptifibatide or vehicle, at day  
578 6 post-infection. Lung sections were stained with hematoxylin and eosin (HE).  
579 Immunohistochemistry using antibodies against Ly6G and viral NP was used to detect  
580 neutrophils and virus-infected cells. Data are representative of three mice per group.

581

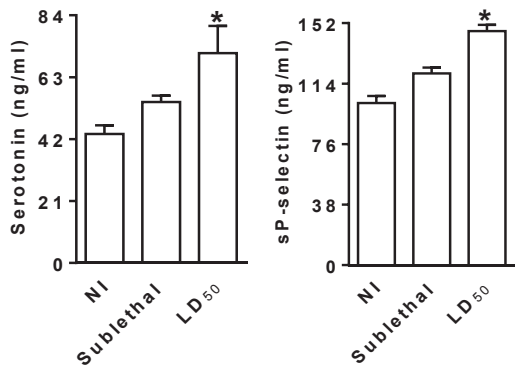
582 **Figure 8: Schematic overview of the proposed model for platelet-667 mediated influenza**  
583 **virus pathogenesis.** During severe IAV infection, endothelial cells are injured. Upon  
584 endothelium injury, platelets are immediately recruited by inflamed cells, where they adhere to  
585 and are activated by subendothelial proteins. Simultaneously, PAR4 mediates activation of  
586 platelets by thrombin. These events lead to the conformational change of the platelet  
587 glycoprotein IIb/IIIa (GPIIb/IIIa) receptor for fibrinogen that bridges platelets, leading to their  
588 aggregation and a reinforcement of their activation. This process is strongly associated with  
589 enhanced inflammatory responses, leading to cytokine storm, when platelets are hyperactivated.  
590 Anti-platelet treatment protects against influenza pathogenesis by controlling platelet function  
591 and restoring tissue hemostasis and wound healing.

Figure 1

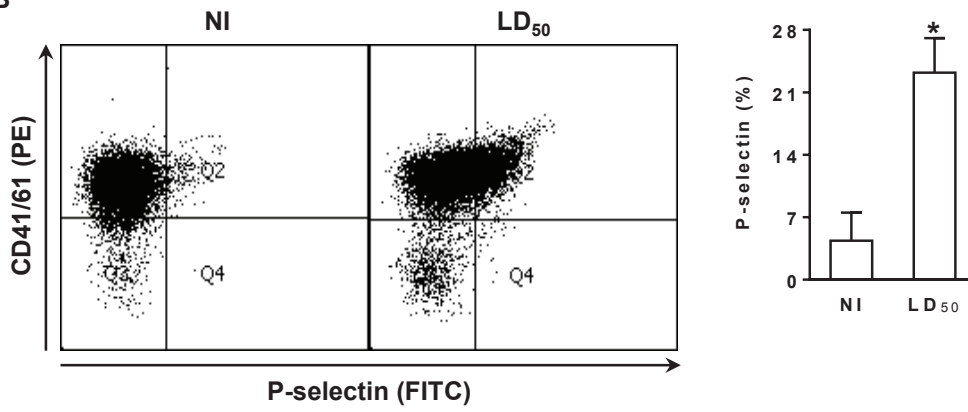


**Figure 2**

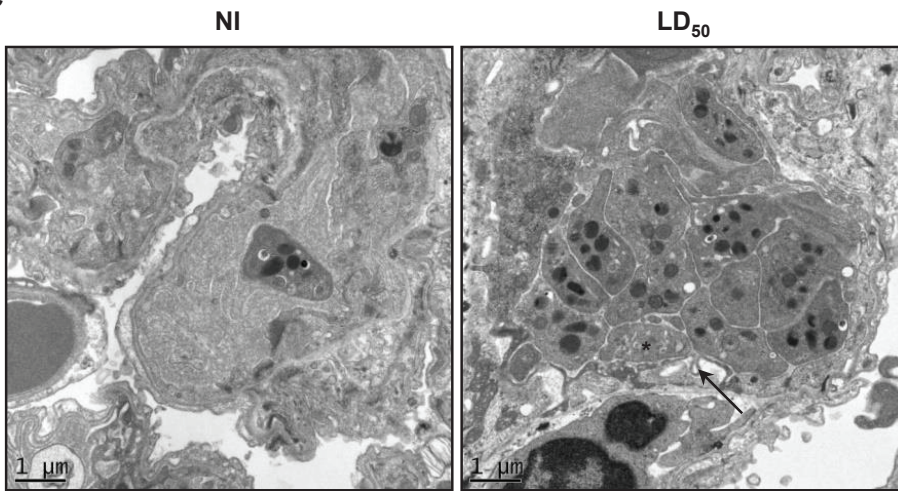
**A**



**B**



**C**



**D**

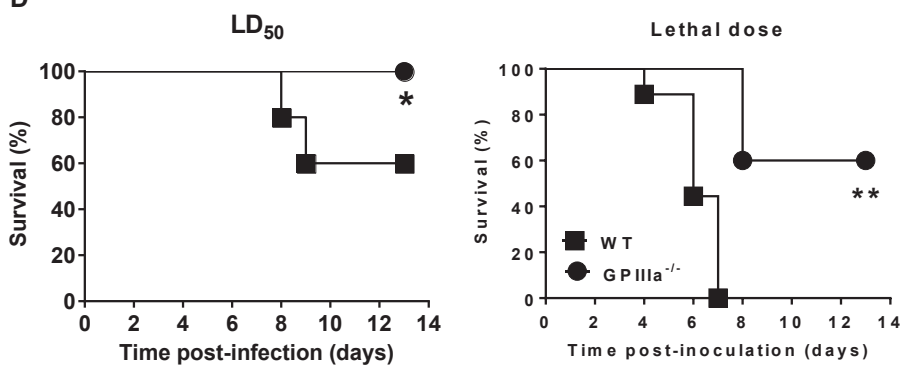


**Figure 3**

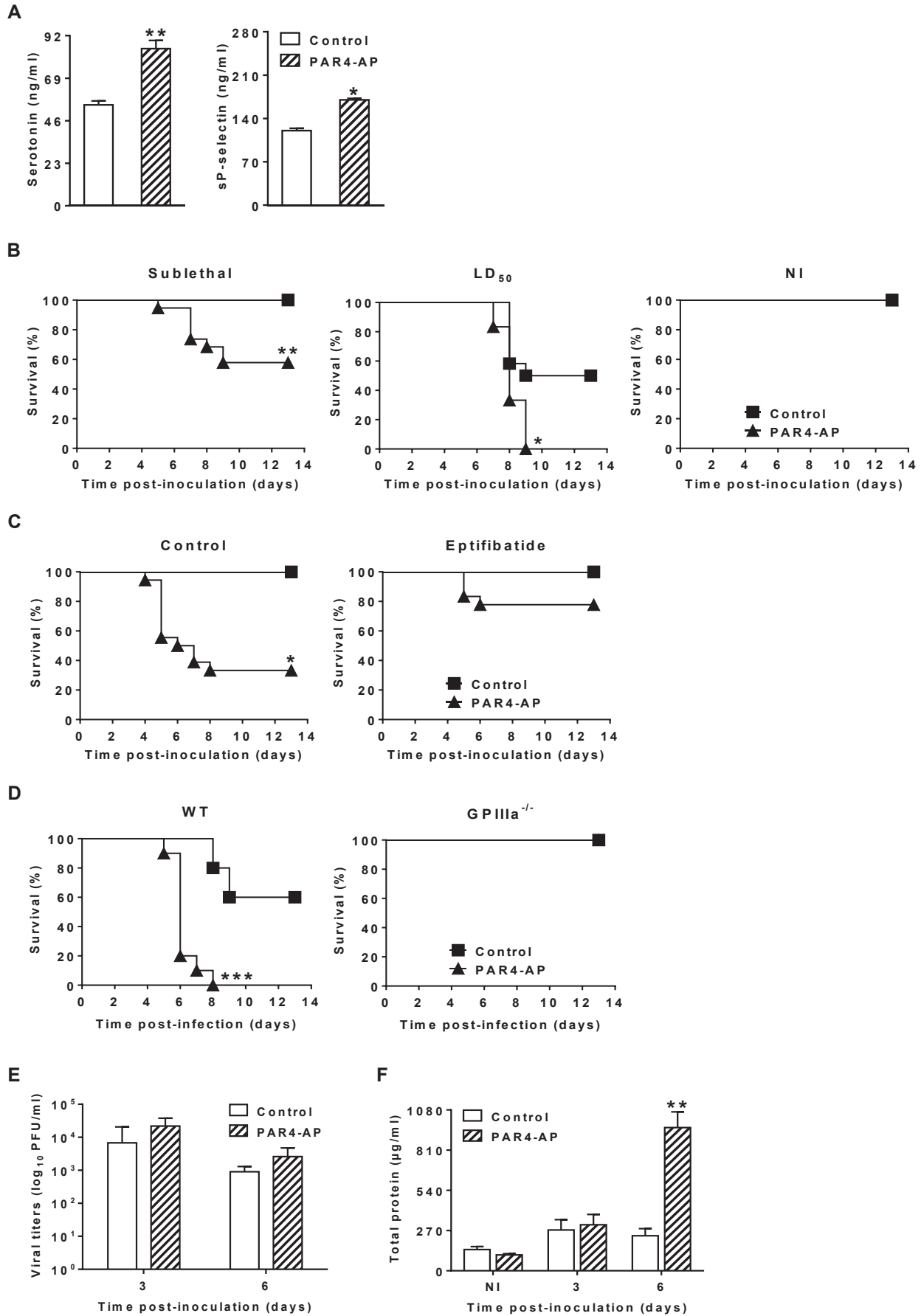


**Figure 4**

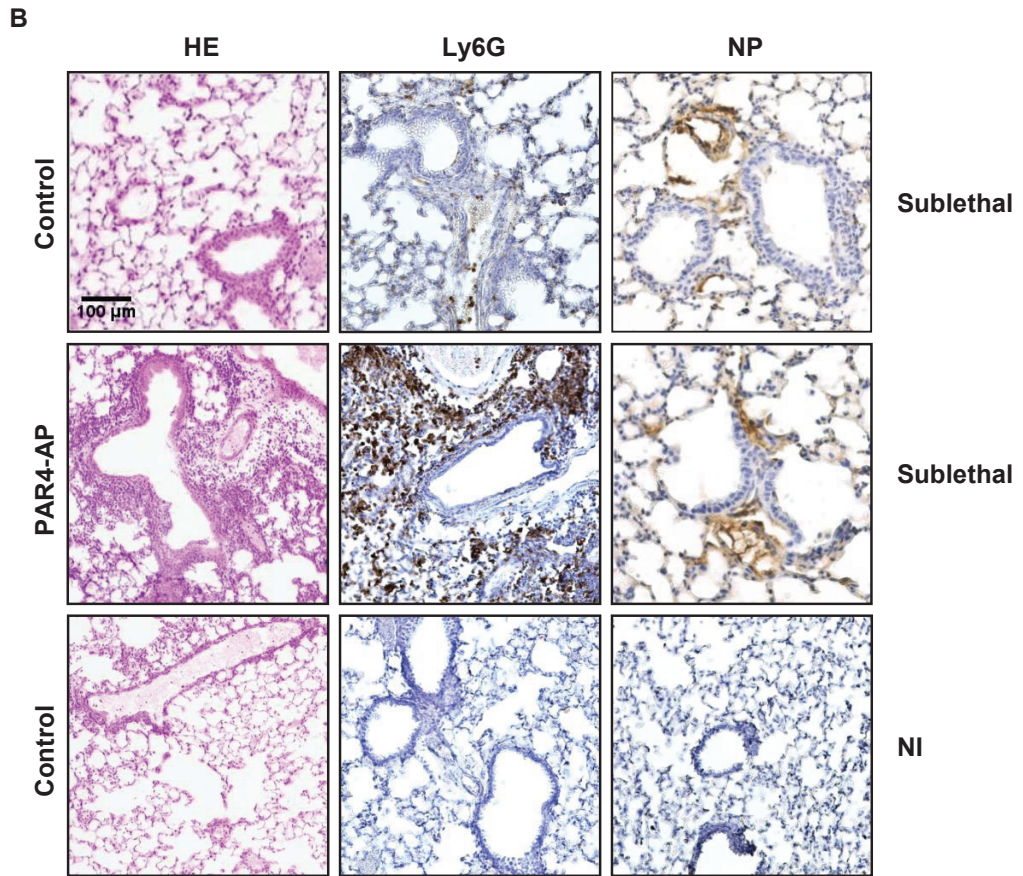
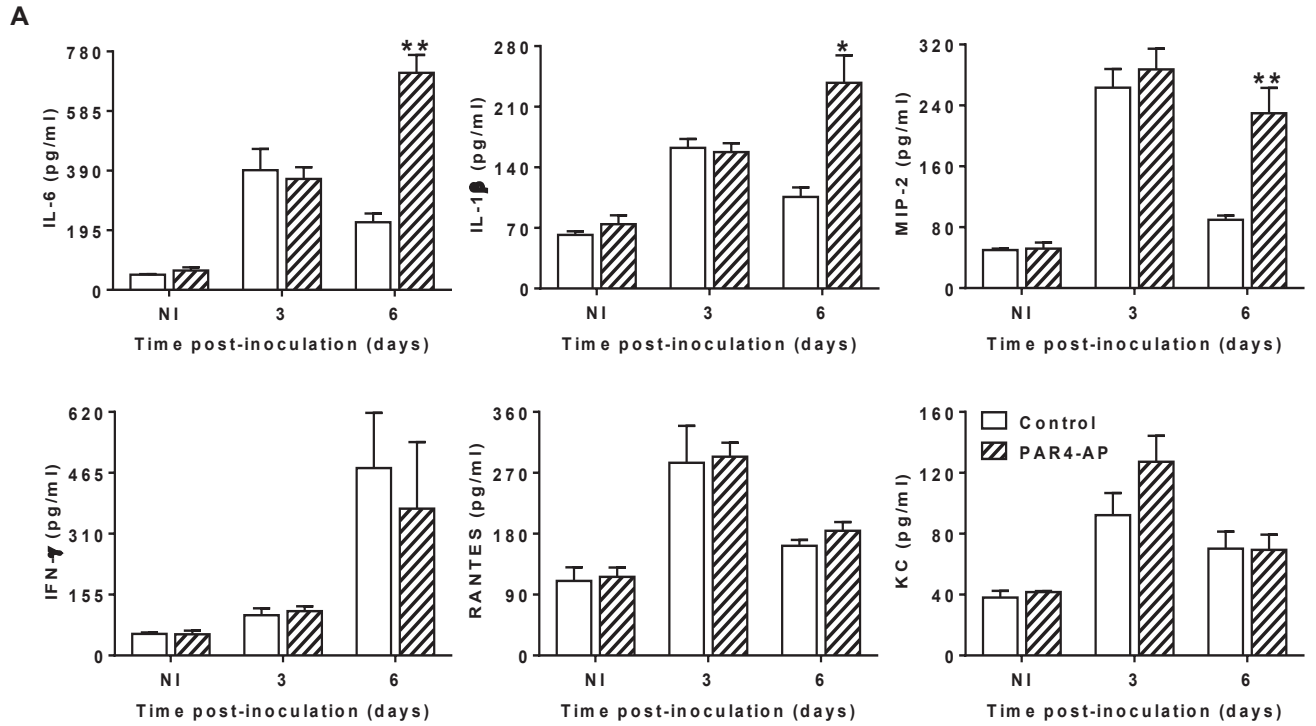


**Figure 5**

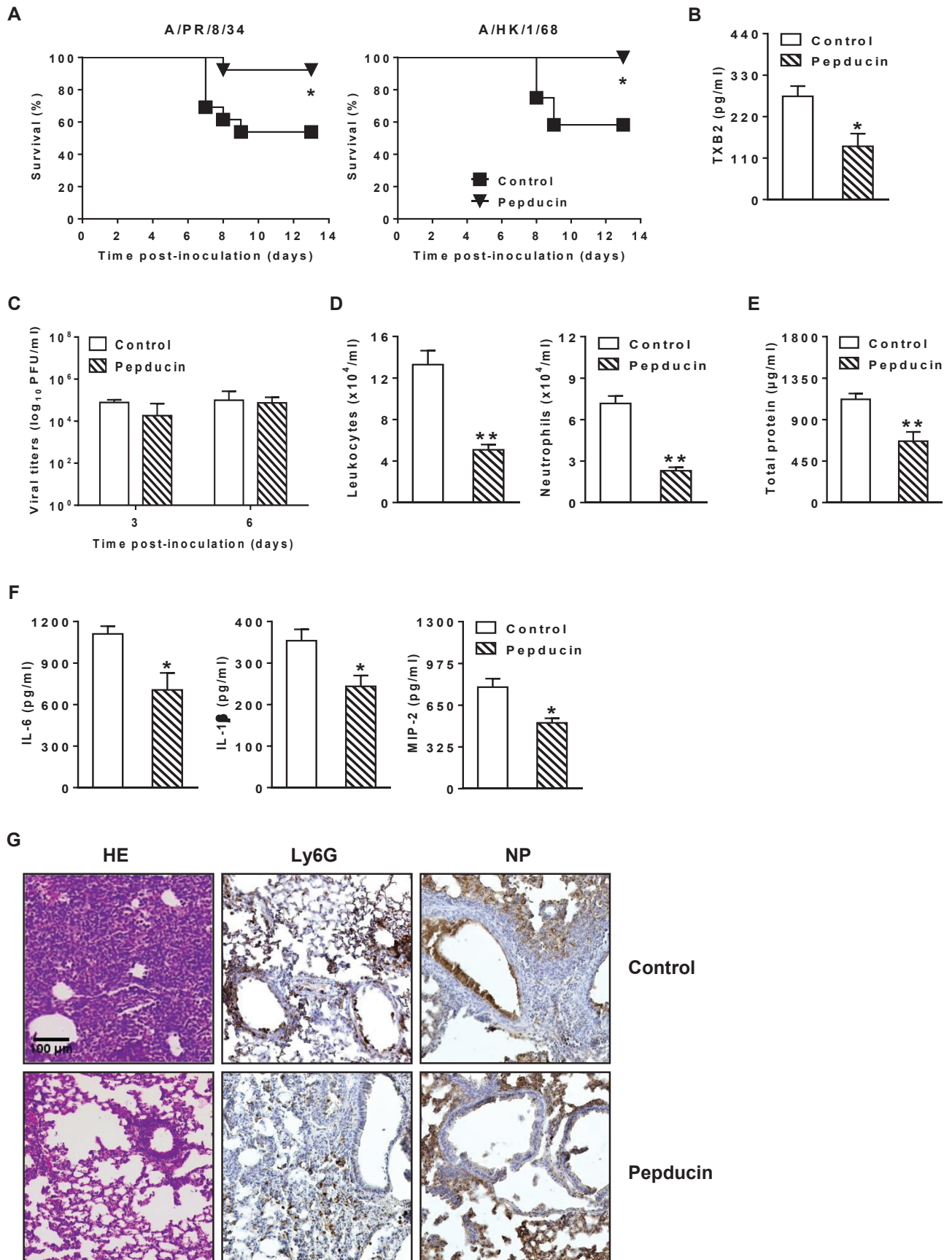
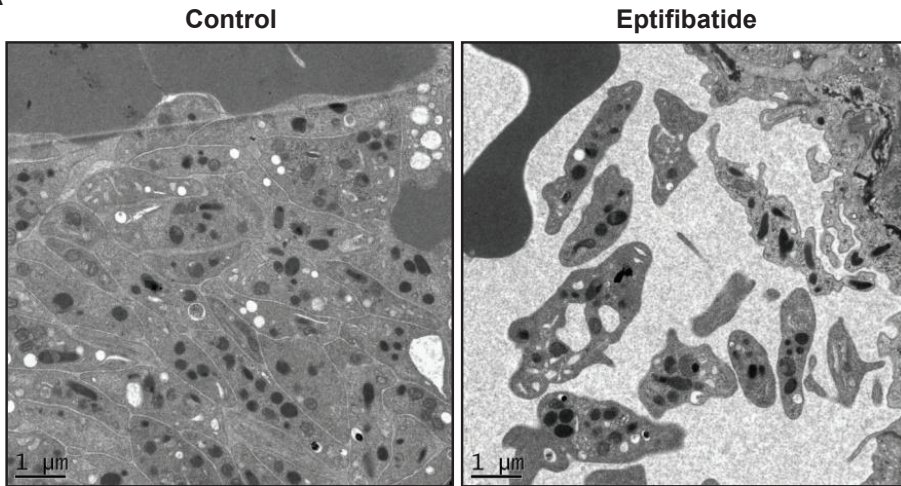
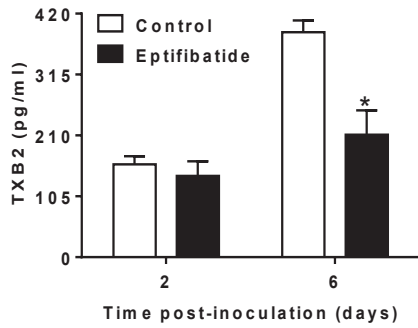


Figure 6

A



B



C

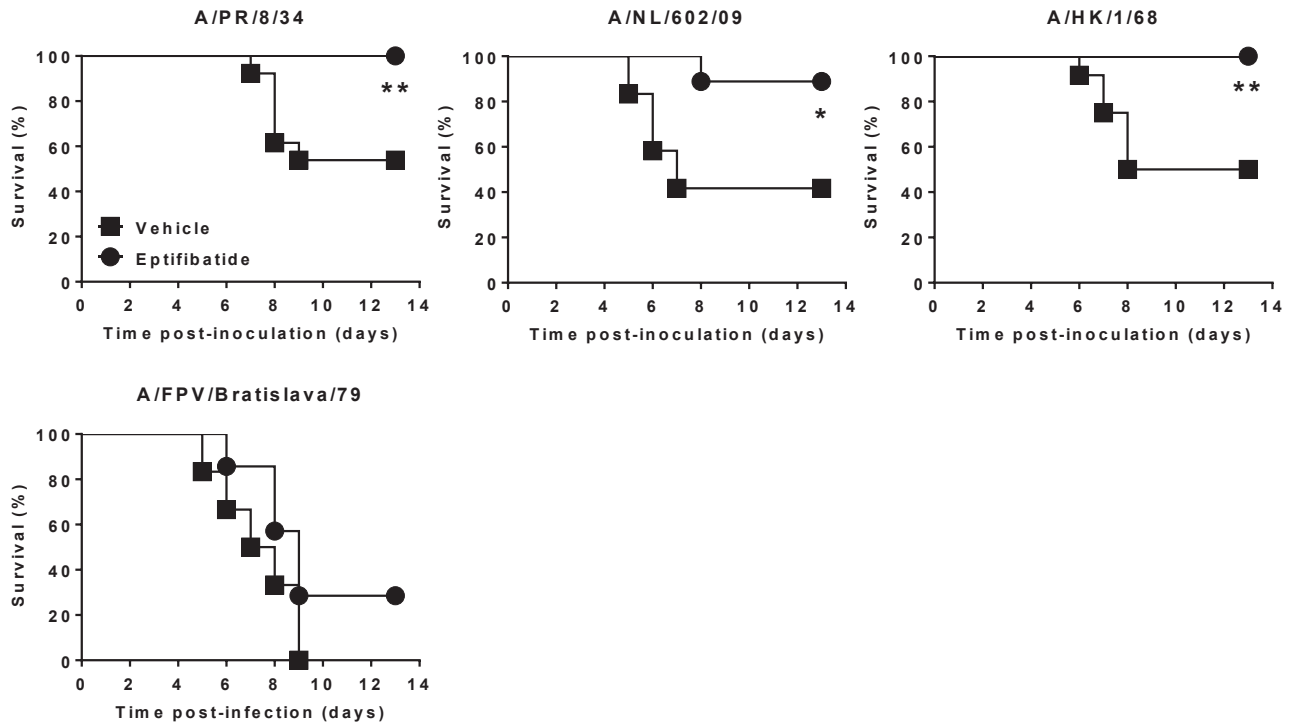
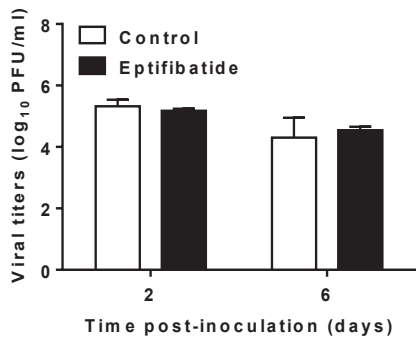
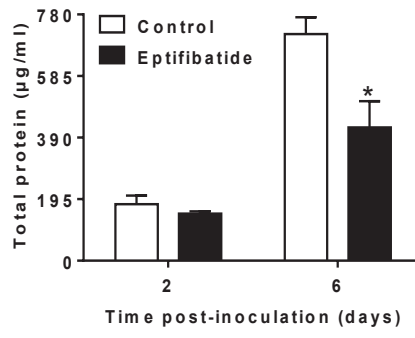


**Figure 7**

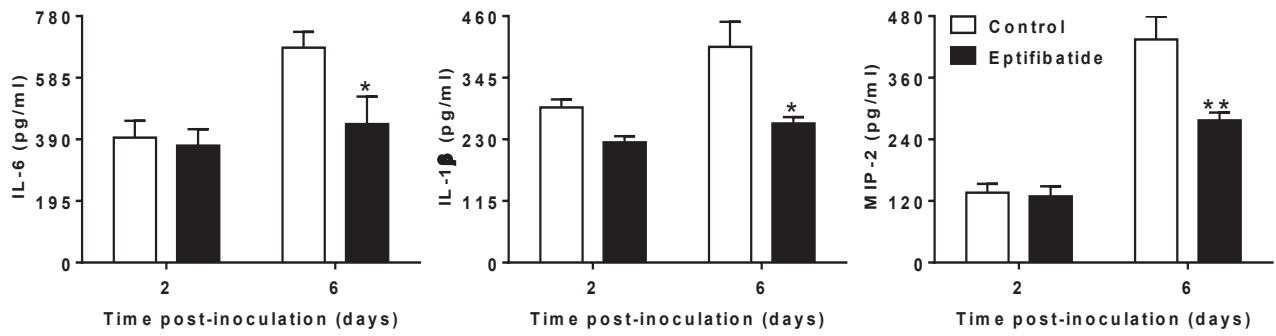
**A**



**B**



**C**



**D**

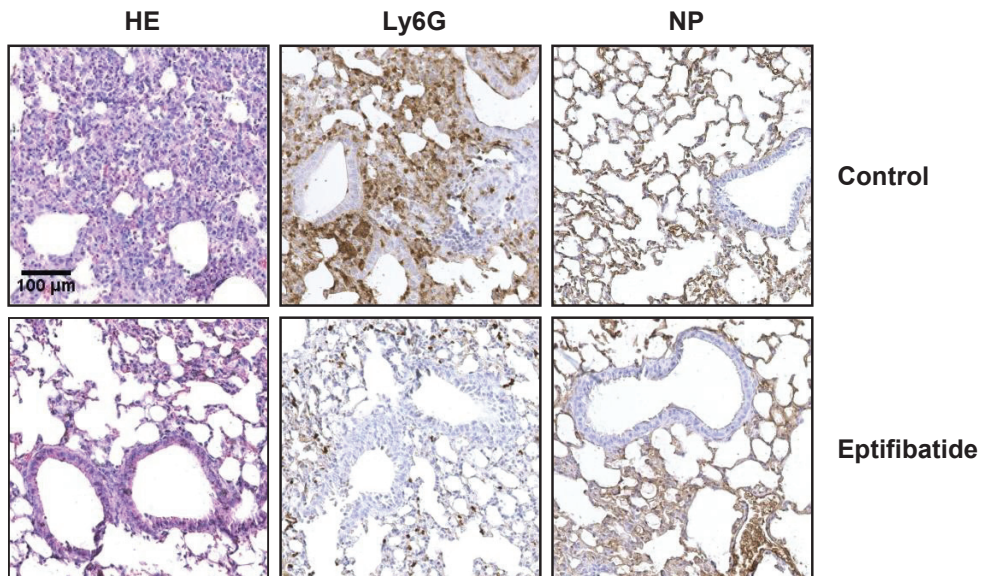
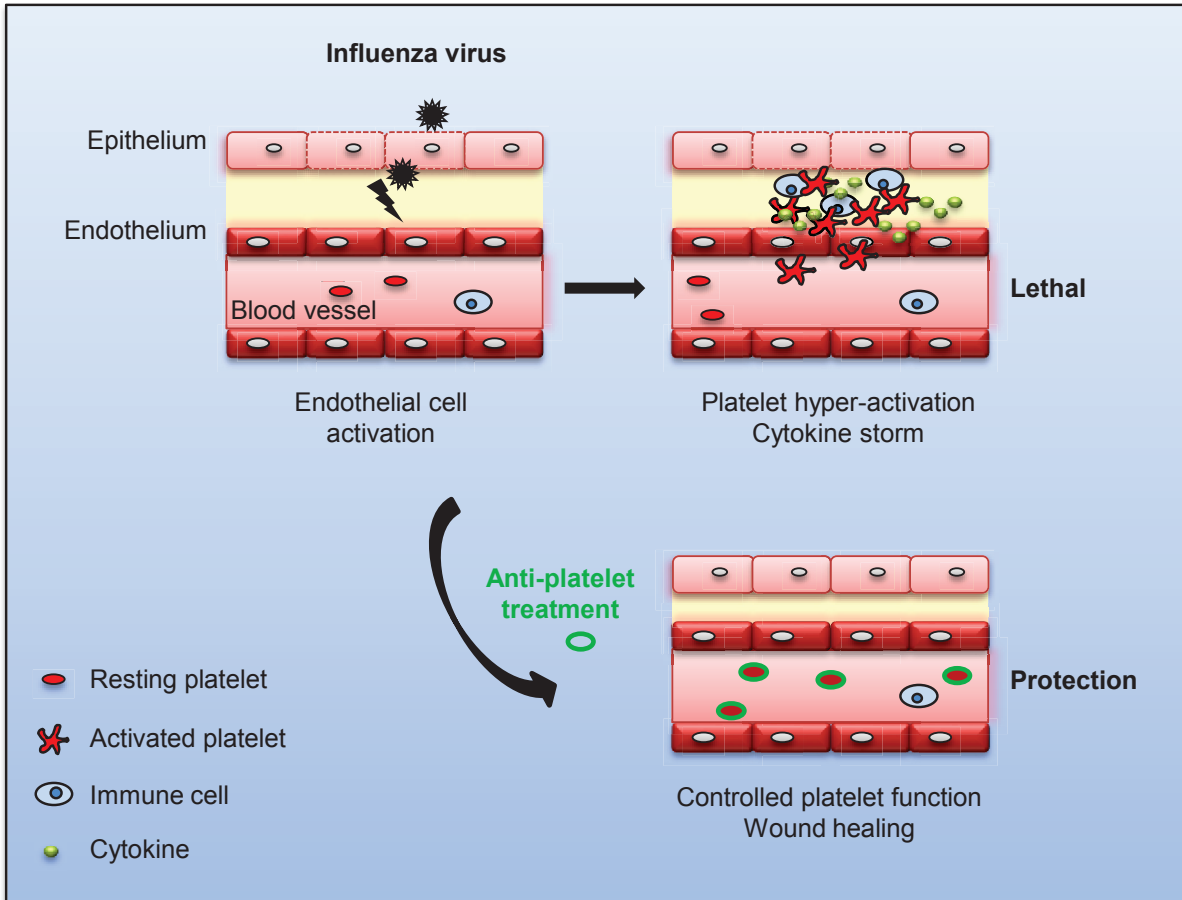


Figure 8



**Annexe n°3: *Ex Vivo* and *In Vivo* Inhibition of Human Rhinovirus  
Replication by a New Pseudosubstrate of Viral 2A Protease**

Nisrine Falah, Sébastien Violot, Didier Décimo, Fatma Berri, Marie-Laure Foucault-Grunenwald, Théophile Ohlmann, Isabelle Schuffenecker, Florence Morfin,d Bruno Lina, Béatrice Riteau, and Jean-Claude Cortay

**J.Virol, 2012. Doi: 10.1128/JVI.05263-11**

# Ex Vivo and In Vivo Inhibition of Human Rhinovirus Replication by a New Pseudosubstrate of Viral 2A Protease

Nisrine Falah,<sup>a</sup> Sébastien Violot,<sup>b</sup> Didier Décimo,<sup>c</sup> Fatma Berri,<sup>a</sup> Marie-Laure Foucault-Grunenwald,<sup>a</sup> Théophile Ohlmann,<sup>c</sup> Isabelle Schuffenecker,<sup>d</sup> Florence Morfin,<sup>d</sup> Bruno Lina,<sup>a,d</sup> Béatrice Riteau,<sup>a,e</sup> and Jean-Claude Cortay<sup>a</sup>

VirPath, EMR 4610, Virologie et Pathologie Humaine, Université Lyon 1, Université de Lyon, Faculté de Médecine Lyon-Est, Secteur Laennec, Lyon, France<sup>a</sup>; Biocristallographie et Biologie Structurale des Cibles Thérapeutiques, Université Lyon 1, Université de Lyon, Lyon, France, and CNRS, UMR 5086, Bases Moléculaires et Structurales des Systèmes Infectieux, Vercors, France<sup>b</sup>; Ecole Normale Supérieure de Lyon, Unité de Virologie Humaine, INSERM U758, Université Lyon 1, Université de Lyon, Lyon, France<sup>c</sup>; Laboratoire de Virologie, Hospices Civils de Lyon, Lyon, France<sup>d</sup>; and INRA, Tours, France<sup>e</sup>

**Human rhinoviruses (HRVs) remain a significant public health problem as they are the major cause of both upper and lower respiratory tract infections. Unfortunately, to date no vaccine or antiviral against these pathogens is available. Here, using a high-throughput yeast two-hybrid screening, we identified a 6-amino-acid hit peptide, LVLQTM, which acted as a pseudosubstrate of the viral 2A cysteine protease (2A<sup>Pro</sup>) and inhibited its activity. This peptide was chemically modified with a reactive electrophilic fluoromethylketone group to form a covalent linkage with the nucleophilic active-site thiol of the enzyme. Ex vivo and in vivo experiments showed that thus converted, LVLQTM was a strong inhibitor of HRV replication in both A549 cells and mice. To our knowledge, this is the first report validating a compound against HRV infection in a mouse model.**

Human rhinoviruses (HRVs) belong to the enterovirus group of the *Picornaviridae* family and are the main causative agents of the common cold, asthma exacerbations, and chronic obstructive pulmonary disease in humans (22). To date, there is no vaccine against HRV as there is almost no cross protection between the nearly 100 serotypes identified so far (21). Furthermore, no antiviral treatment against HRV is currently available on the market. Thus, there is an urgent need for validation of new compounds against HRV.

Among several antiviral strategies attempting to impair rhinovirus replication, one consists of blocking the activity of the viral HRV 2A protease (2A<sup>Pro</sup>). Targeting 2A<sup>Pro</sup> is of particular interest as it is a cysteine protease playing multifunctional roles necessary for viral replication. These roles include (i) autoprocessing by *cis* cleavage at the VP1-2A<sup>Pro</sup> junction; (ii) inhibition of the host cell translation through cleavage of the initiation factor eIF4G (17, 27) and the poly(A)-binding protein (PABP) (10); (iii) contribution to the deleterious overwhelming host cellular defense (3, 9, 23); and (iv) strengthening of viral polysome formation and stability (11, 12).

Several 2A<sup>Pro</sup> inhibitors have already been described and include alkylating agents such as iodoacetamide or *N*-ethylmaleimide that can react with the catalytic cysteine of the enzyme and that have been shown to reduce 2A<sup>Pro</sup> activity (15). Moreover, as the substrate-binding pocket of elastase is similar to that of 2A<sup>Pro</sup>, two substrate-derived elastase inhibitors, elastinal and methoxysuccinyl-Ala-Ala-Pro-Val-chloromethylketone have been reported to inhibit the *in vitro* proteolytic activity of 2A<sup>Pro</sup> and consequently reduce viral yields of HRV type 14 (HRV-14) and poliovirus type 1 (PV-1) (18). Furthermore, it has been demonstrated that the irreversible caspase inhibitor benzyloxycarbonyl-Val-Ala-Asp(methoxy)-fluoromethylketone (*z*-VAD-fmk) (7) is also able to directly inactivate HRV and coxsackie B virus type 4 (CBV4) 2A<sup>Pro</sup> enzymes (5). However, none of these compounds has ever been tested *in vivo*, thus impairing the validation of their efficacy in preclinical assays and the possibility to go further in the development of anti-HRV therapies.

The aim of this study was to design a peptide inhibitor of HRV-2 2A<sup>Pro</sup> and to test its antiviral activity *ex vivo* in A549 cells and *in vivo* in mice which are susceptible to infection by the minor HRV group member HRV-2.

Here, we report the identification of the LVLQTM peptide as a decoy substrate for 2A<sup>Pro</sup> that blocked enzyme activity upon binding and consequently affected HRV-2 replication *ex vivo* and *in vivo* when administered to infected mice. This is the first study validating such a compound *in vivo* in mice, opening new prospects for testing other drugs.

## MATERIALS AND METHODS

**Ethics statement.** Experiments were performed according to recommendations of the National Commission of Animal Experiment (CNEA) and the National Committee on the Ethic Reflexion of Animal Experiments (CNREEA). The protocol was approved by the Committee of Animal Experiments of the University Claude Bernard Lyon I (permit number BH2008-13). All animal experiments were also carried out under the authority of a license issued by la Direction des Services Vétérinaires (accreditation number 78-114). All efforts were made to minimize suffering.

**Yeast two-hybrid analysis.** Yeast two-hybrid screening was performed by Hybrigenics, S.A., Paris, France. The full-length coding sequence for HRV-2 2A<sup>Pro</sup> (GenBank accession number X02316) was amplified by PCR and cloned into pB27 plasmid as a C-terminal fusion to LexA (LexA-p2A). The construct was validated by sequencing and used as bait to screen a random-primed human placenta cDNA library constructed into pP6 plasmid. pB27 and pP6 plasmids were derived from the original pBTM116 and pGADGH plasmids, respectively (34).

A total of 53.1 million clones (6-fold the complexity of the library) were screened using a mating approach with Y187 (*mata*) and L40ΔGal4

Received 31 May 2011 Accepted 21 October 2011

Published ahead of print 9 November 2011

Address correspondence to Jean-Claude Cortay, cortay@univ-lyon1.fr.

Copyright © 2012, American Society for Microbiology. All Rights Reserved.

doi:10.1128/JVI.05263-11

(*mata*) *Saccharomyces cerevisiae* yeast strains, as previously described (6). Fifty-one His<sup>+</sup> colonies were selected on a medium lacking tryptophan, leucine, and histidine and supplemented with 100 mM 3-aminotriazole to suppress bait autoactivation. The prey fragments of the positive clones were then amplified by PCR and sequenced at their 5' and 3' junctions. The resulting sequences were used to identify the corresponding interacting proteins in the GenBank database (NCBI) using a fully automated procedure.

**Bacterial expression vectors and protein purification.** Synthetic genes (Eurofins MWG Operon) coding for HRV-2 2A<sup>Pro</sup> or echovirus 6 (EV-6) 2A<sup>Pro</sup> (GenBank accession number AY302558) were cloned between the NdeI and XhoI sites of the pSCodon1.2 vector (Eurogentec) in fusion with either a Strep●Tag (WSHPQFEK) or a (His)<sub>6</sub> tag at their C termini. Recombinant plasmids were used to transform the *Escherichia coli* B SE1 strain [F<sup>-</sup> Cm<sup>r</sup> *ompT lon hsdSB* (r<sub>B</sub><sup>-</sup> m<sub>B</sub><sup>-</sup>) *gal dcm* (DE3) (*lacI*, T7 polymerase under the control of the PlacUV5 promoter) *ccdB*<sup>+</sup>]. Bacteria were grown in the autoinduction medium ZYP-5052 (30) at 37°C for 5 to 6 h with vigorous shaking in baffled flasks, before growing to saturation at 20°C within 16 to 18 h. Subsequent purification steps were performed at 4°C. Cells were lysed with BugBuster protein extraction reagent (Novagen), and clarified supernatants were applied to the corresponding affinity chromatography resins. Strep●Tag proteins were purified using a StrepTrap HP resin (GE Healthcare) and His-tagged proteins were purified using a HIS-Select HF nickel resin (Sigma) according to the respective manufacturers' instructions. In each case, proteins were dialyzed against buffer D (100 mM Tris-HCl, pH 7.5, 200 mM NaCl, 4 mM dithiothreitol [DTT]) and concentrated using a Vivaspin centrifugal concentrator device (Sartorius Stedim Biotech). Enzymes were stored at -20°C in buffer D containing 50% glycerol.

**In vitro cleavage assays.** Different protease recognition site-coding sequences were inserted between the NheI and BglII sites in a short polypeptide linker that connects the native N and C termini of a circularly permuted firefly luciferase in the pGloSensor-10F linear vector (Promega). The resulting plasmids were then used as templates in a cell-free system for the expression of the corresponding GloSensor proteins containing the protease sites of interest. *In vitro* transcription/translation reactions were carried out in a TNT SP6 high-yield wheat germ master mix (Promega) supplemented with [<sup>35</sup>S]methionine according to the manufacturer's protocol. Reaction mixtures were incubated for 2 h at 25°C. Two micrograms of recombinant tobacco etch virus (TEV) protease, HRV-2 2A<sup>Pro</sup>, or EV-6 2A<sup>Pro</sup> was added to 13 μl of the *in vitro* translation reaction mixture and 13 μl of 2× digestion buffer (100 mM Tris-HCl, pH 8, 1 mM EDTA, 4 mM DTT [for TEV protease], 100 mM HEPES-NaOH, pH 7.9, 200 mM NaCl, 2 mM EDTA, 10 mM DTT [for HRV-2 2A<sup>Pro</sup>], 100 mM Tris-HCl, pH 7.5, 300 mM NaCl, and 10 mM DTT [for EV-6 2A<sup>Pro</sup>]) and incubated for 45 min at 30°C. Aliquots of total proteins were removed 0, 15, 30, and 45 min postincubation and separated in a 12% SDS-polyacrylamide gel. Autoradiography was performed after fluorography treatment. The 61-kDa band intensity was determined by densitometric analysis after background subtraction using Bio-Rad Quantity One one-dimension software. Luminescence detection was performed by diluting the remaining volume of each protease digestion and negative-control reaction mixture 1:20 in nuclease-free water, and 100 μl of these dilutions was added to each well of a white, flat-bottom 96-well plate. Each reaction was analyzed in triplicate. After addition of 100 μl Bright-Glo assay reagent to each well and incubation for 2 to 5 min at room temperature, luminescence was measured using a GloMax 96-well microplate luminometer. According to the manufacturer's instructions, the fold activation of each luciferase activity was calculated as follows: [(luminescence from tube A) - (luminescence from tube C)]/[(luminescence from tube B) - (luminescence from tube D)], where tube A contains a Plus-DNA TNT reaction mixture and HRV-2 2A<sup>Pro</sup>, tube B contains a Plus-DNA TNT reaction mixture only, tube C contains a no-DNA TNT reaction mixture and HRV-2 2A<sup>Pro</sup>, and tube D contains a no-DNA TNT reaction mixture only.

**Pulldown experiments.** For His pulldown assays, a PCR-amplified fragment corresponding to truncated proteins consisting of the C-terminal part (amino acids 274 to 520) of the functionally uncharacterized RBM6Δ6 protein (RBM6Δ6<sub>274-520</sub>) or RBM6<sub>274-660</sub> was inserted into the NcoI-XhoI sites of the expression vector pET-28 (Novagen). Translated proteins were synthesized *in vitro* using a T7 RNA polymerase-based TNT-coupled reticulocyte lysate system (Promega). HRV-2 2A<sup>Pro</sup>-(His)<sub>6</sub> fusion protein was bound to nickel nitrilotriacetic acid (Ni-NTA) magnetic agarose beads (Qiagen) and incubated for 1 h with 50 μl *in vitro*-translated [<sup>35</sup>S]methionine-labeled RBM6Δ6<sub>274-520</sub> or RBM6<sub>274-660</sub> in a total volume of 1 ml of incubation buffer (25 mM sodium phosphate, pH 8.0, 500 mM NaCl, 20 mM imidazole, and 0.005% Tween 20). Resin was collected with a magnetic separator and washed twice with 500 μl incubation buffer. Washed beads were resuspended in 40 μl of 2× SDS sample buffer, heated for 5 min, and pelleted in a microcentrifuge. Proteins from the supernatant were then subjected to a 12% SDS-PAGE. Gels were treated with Amplify reagent (GE Healthcare) for fluorography or subjected to Western blot analysis using a polyclonal antihistidine antibody (Cell Signaling). The amount of labeled proteins which coeluted with HRV-2 2A<sup>Pro</sup>-(His)<sub>6</sub> was quantified by densitometric analysis.

For Strep●Tag pulldown assays, the RBM6Δ6 LVLQTM-derived peptide-coding sequence was cloned in frame between two BsaI sites within the pET-SUMO vector (Invitrogen), allowing its expression in fusion with the C terminus of the SUMO protein. In addition, the Strep●Tag sequence WSHPQFEK was added at the N terminus of the fusion protein. This construct was transferred into the pSCodon1 vector, and recombinant Strep●Tag-SUMO-LVLQTM was expressed in the *E. coli* SE1 strain. Subsequent incubation reactions were performed under the same conditions described above, except that equal volumes of cleared lysates prepared from bacteria overproducing either Strep●Tag-SUMO-LVLQTM or HRV-2 2A<sup>Pro</sup>-(His)<sub>6</sub> proteins were mixed (to a 1-ml final volume) with Strep-Tactin magnetic beads (Qiagen). Proteins which were specifically bound to the washed beads were separated by 15% SDS-PAGE and visualized by staining with Coomassie brilliant blue R250. (His)<sub>6</sub>-tagged proteins were also revealed with a polyclonal antihistidine antibody (Cell Signaling).

**Cleavage of TRPIITTA-pNA substrate by HRV-2 2A<sup>Pro</sup>.** Cleavage of the TRPIITTA-p-nitroanilide (pNA) substrate by HRV-2 2A<sup>Pro</sup> was performed at 25°C for 10 min in a 1-ml reaction mix containing 50 mM HEPES-NaOH, pH 8.0, 100 mM NaCl, 1 mM EDTA, 10 mM DTT, and purified recombinant HRV-2 2A<sup>Pro</sup> (0.2 μM). The reaction was started by the addition of the TRPIITTA-pNA peptide (Eurogentec) at 25 μM and monitored continuously at 405 nm to characterize the initial velocity of the cleavage reaction. Peptide competition cleavage assays were performed under the same conditions, except that purified Strep●Tag-SUMO-LVLQTM protein (0 to 25 μM) was added to the reaction mix. Percent inhibition values were referred to as the ratio between initial velocity cleavage values measured with and without inhibitor. Data are expressed as means of three independent experiments, and standard deviations are indicated.

**Molecular modeling.** The crystal structure of the free HRV-2 2A<sup>Pro</sup> has been used (Protein Data Bank [PDB] accession number 2hrv) (24). The conformation of the LVLQTM peptide was modeled using the one in complex with the foot-and-mouth disease virus (FMDV) 3C<sup>Pro</sup> as a starting model (PDB accession number 2wv4) (35). Side chains from the FMDV 3C protease-bound peptide were replaced with the side chains of VLQTM and then energy minimized using a GROMOS96 43B1 force field (32).

**Cell culture and transient expression.** Human epithelial lung carcinoma A549 cells (CCL-185; ATCC) were grown in Dulbecco's modified Eagle's medium (DMEM; Lonza) and 1 g/liter glucose supplemented with 10% fetal calf serum, 2 mM L-glutamine, penicillin, and streptomycin. RBM6Δ6<sub>274-520</sub> and RBM6Δ6<sub>274-514</sub>-coding sequences were amplified by PCR and cloned into the multiple-cloning site of the pCI-neo vector (Promega) downstream from the following 2× Strep●Tag sequence: MASWSHPQFEKGGGSGGGSGGGWSHPQFEK (where the underlining indi-

cates the Strep-Tag sequence). All plasmid constructs were transfected into cells using NanoJuice transfection reagents (Novagen), according to the manufacturer's instructions.

**Western blotting.** Proteins were separated by SDS-PAGE and transferred onto nitrocellulose membranes. The membranes were incubated for 1 h in Tris-buffered saline containing 0.1% Tween 20 and 5% nonfat milk powder at room temperature. Membranes were then incubated overnight at 4°C with a polyclonal antihistidine antibody (reference no. 2365; Cell Signaling) or an antiserum recognizing the C-terminal domain of eIF4G (19). These antibodies were revealed using the horseradish peroxidase-coupled goat antirabbit antibody, followed by chemiluminescence detection using the SuperSignal West Pico chemiluminescent substrate from Pierce.

**In vitro transcription and RNA transfection.** Plasmids containing the 2A protease-coding region were constructed by inserting the respective coding sequences into the pGlobin-*Renilla* vector (29). For *in vitro* transcription, DNA templates were linearized at the EcoRI site downstream from a synthetic poly(A) tail. Capped RNAs were transcribed using the T7 RNA polymerase as previously described (25) and treated with RQ1 DNase (Promega). The integrity of the RNAs was checked by electrophoresis on nondenaturing agarose gels, and the concentration was quantified by spectrophotometry at 260 nm using a Nanodrop apparatus (Nanodrop Technologies).

Two days before RNA transfection, A549 cells were seeded into 48-well plates at 75,000 cells per well to reach about 180,000 cells at the time of transfection. RNA transfection was performed with 100 ng of 2A<sup>Pro</sup>-coding RNA and the TransIT kit (Mirus Bio) for 2 h and 50 ng of *Renilla*-coding RNA for additional 3 h. The cells were then harvested, and luciferase activity was quantified using the *Renilla* luciferase (R-Luc) assay system from Promega and a Veritas microplate luminometer (Turner BioSystems). Transfection efficiency was evaluated by transfecting the green fluorescent protein (GFP)-coding RNA under the same conditions and counting the number of green fluorescent cells by fluorescence-activated cell sorter (FACS) analysis. Over 70% of A549 cells expressed GFP.

**Virus infection.** HRV-2 (GenBank accession number X02316) and HRV-14 (GenBank accession number K02121) were provided by the WHO/National Reference Centre for Enteroviruses (Lyon, France). A549 cells (90% confluence) were infected with HRV-2 or HRV-14 at a multiplicity of infection (MOI) of 1 in DMEM containing 2% fetal calf serum, 2 mM L-glutamine, penicillin, and streptomycin and incubated at 34°C. Virus titer was quantified by the 50% tissue culture infectious dose (TCID<sub>50</sub>) assay using MRC5 cells according to the method of Reed and Muench (26).

**Infection and mouse treatment.** Six-week-old BALB/c female mice were purchased from Charles River Laboratories, and experiments were undertaken as previously described (13). On the day of infection, a three-step protocol was used for peptide administration: (i) first, mice were anesthetized by intraperitoneal injection of ketamine (42.5 mg/kg of body weight), (ii) then, a 25- $\mu$ l volume of HRV-2 suspension containing 100,000 PFU was injected dropwise to the external nares of the mice using a micropipette, and (iii) finally, a 25- $\mu$ l volume of the indicated concentration of peptide solution dissolved in 1% dimethyl sulfoxide (DMSO) was administered in the same way either right after infection or at 12 h postinoculation. Lungs were harvested at different time points postinfection and ground in the Tissue Lyser LT device from Qiagen. After centrifugation at 12,000  $\times$  g for 5 min at 4°C, supernatants were collected and virus titers were determined as described above. Ten mice were used for each experimental condition.

**Statistical analysis.** The Mann-Whitney U test was used to evaluate statistical significance ( $P < 0.05$ ) of viral replication *in vivo*.

## RESULTS

**Yeast two-hybrid screening for proteins interacting with HRV-2 2A<sup>Pro</sup>.** In order to identify partners and potential inhibitors of

CL27/	TVSTYIHIQQTQVDFYAGKSEMPVCR	L R L K N	L <sub>(COOH)</sub>
CL35/	PNGFRPFCCHTQQTMGWAFRPSQGHQG	L R L R N	L <sub>(COOH)</sub>
CL45/	LRLHACKVK	I K L V T	L <sub>(COOH)</sub>
CL52/	GRKQS	L S L V T	L <sub>(COOH)</sub>
CL41/	DPL	F R L T T	L <sub>(COOH)</sub>
CL22/	ARARCHRGRGEGSSSVRKAATLPQDGT	L C L H T	C <sub>(COOH)</sub>
CL51/	GIN	L F L Y T	C <sub>(COOH)</sub>
CL25/	FAYLFKNKNTQNKFK	L Y I Y T	V <sub>(COOH)</sub>
CL43/	ARSWT	L K L Q T	V <sub>(COOH)</sub>
CL46/	RBM6 $\Delta$ 6(aa 274–514)	L V L Q T	M <sub>(COOH)</sub>
<b>Consensus sequence</b>		<b>L X L X T <math>\Phi</math></b>	<b>N</b>

	<b>Cleavage site</b>	<b>P<sub>6</sub></b>	<b>P<sub>5</sub></b>	<b>P<sub>4</sub></b>	<b>P<sub>3</sub></b>	<b>P<sub>2</sub></b>	<b>P<sub>1</sub>/P<sub>1</sub>'</b>
HRV-2 polyprotein		R	I	I	T	T	A/GPS
HRV-62 polyprotein		Q	N	L	Q	T	A/GPS
PABP		T	S	T	Q	T	M/GPR

**FIG 1** Amino acid sequences of the HRV-2 2A<sup>Pro</sup>-binding peptides identified by the yeast two-hybrid system. Peptides are arranged to illustrate the consensus sequence found, where X is any amino acid and  $\Phi$  is a hydrophobic amino acid. Alignments of the carboxy termini of 2A<sup>Pro</sup>-binding peptides with natural cleavage sites of 2A<sup>Pro</sup> are also shown.

HRV 2A<sup>Pro</sup>, a plasmid expressing a LexA–HRV-2 2A<sup>Pro</sup> fusion protein was used to screen a human placenta cDNA library using Y187 (*mata*) and L40 $\alpha$ Gal4 (*mata*) yeast strains. Fifty million clones were screened, and 51 His<sup>+</sup> colonies were further isolated and characterized by DNA sequencing and sequence alignment analysis. Among these clones, nine encoded out-of-frame short polypeptides and one encoded the C-terminal part (amino acids 274 to 520) of the functionally uncharacterized RBM6 $\Delta$ 6 protein (GenBank accession number FLJ56542) (31). As depicted in Fig. 1, all exhibited related sequences that shared the same peptide consensus motif LXLX(T/N) $\Phi$ , where X represents any amino acid and  $\Phi$  represents a hydrophobic residue. Interestingly, this sequence partially mimics the consensus sequence <sub>P4</sub>LX(T/N)<sub>X</sub><sub>P1</sub> found in 2A<sup>Pro</sup> substrates where threonine (or asparagine) and leucine are required in positions P2 and P4, respectively, for 2A<sup>Pro</sup> cleavage (16). In addition, the tripeptide motifs <sub>P3</sub>QTM<sub>P1</sub> and <sub>P4</sub>LQT<sub>P2</sub> found in the RBM6 $\Delta$ 6 sequence are identical to those found at the corresponding positions within the 2A<sup>Pro</sup> substrates PABP1 and VP1-2A<sup>Pro</sup> junction of the HRV-62 polyprotein, respectively (16). Finally, the presence of methionine at the P1 position represents a favorable determinant for 2A<sup>Pro</sup> binding (28). Remarkably, the presence of a conserved leucine (or an equivalent hydrophobic residue) at the P6 position in all selected peptides suggests that this amino acid may represent an important parameter in the specificity of recognition by 2A<sup>Pro</sup>. Thus, these results strongly suggested that the LXLX(T/N) $\Phi$  motif peptides isolated in the double-hybrid screening are partners of HRV-2 2A<sup>Pro</sup>.

**The LXLX(T/N) $\Phi$  motif behaves as a pseudosubstrate of HRV-2 2A<sup>Pro</sup>.** To investigate whether the previously characterized peptides were pseudosubstrates of HRV-2 2A<sup>Pro</sup>, different hybrid peptides were built by fusing the six terminal amino acid residues of the 10 polypeptides identified by yeast two-hybrid screening with the GPSDM sequence found at the P1' and P5' positions of the authentic *cis*-cleavage site of the HRV-2 polyprotein (Fig. 1). The 11-mer peptides obtained were then inserted in frame into a genetically engineered firefly luciferase which was synthesized in a cell-free protein expression system in the presence of [<sup>35</sup>S]methionine and used as a protease substrate (Fig. 2A). In this assay, cleav-

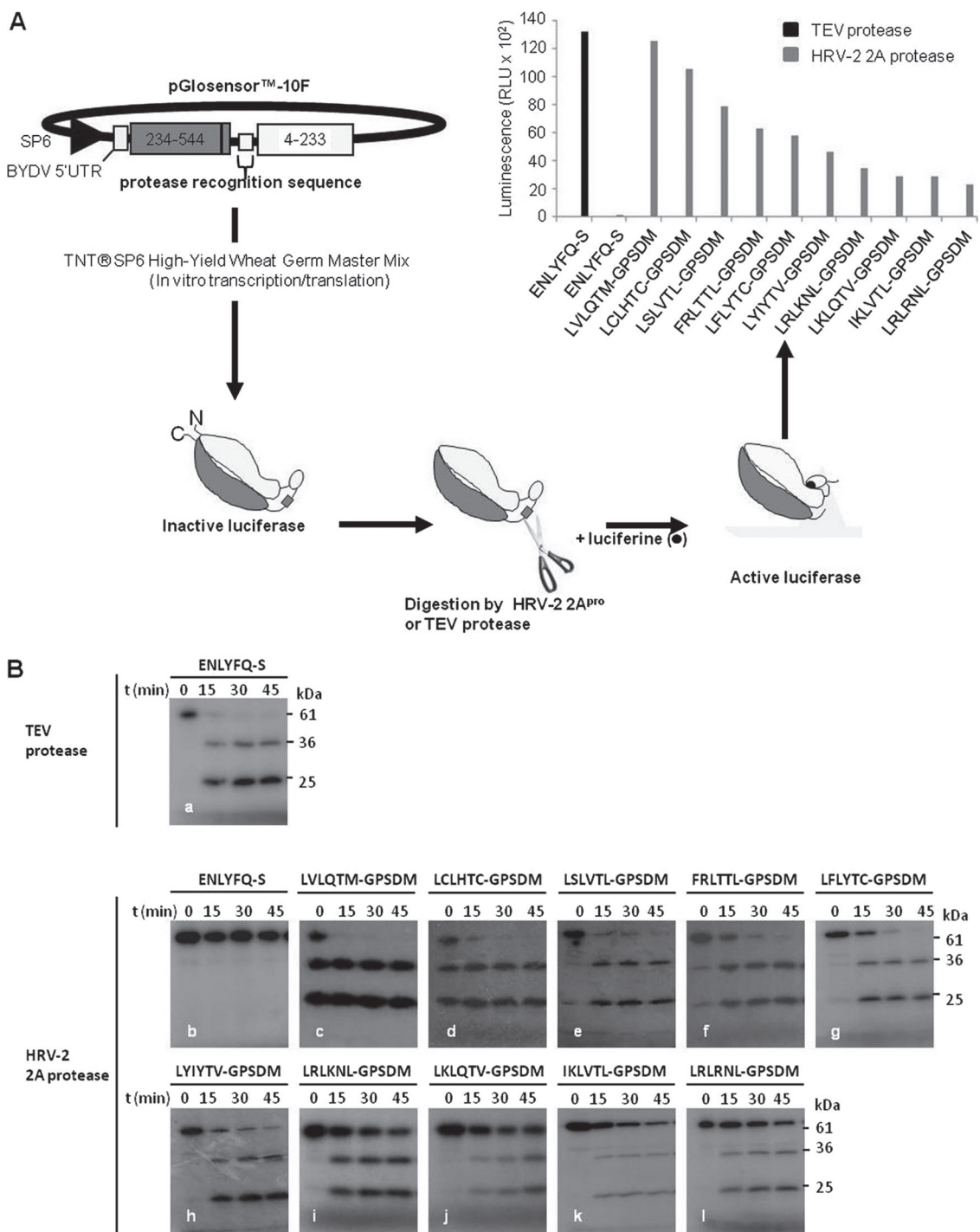


**FIG 2** HRV-2 2A<sup>pro</sup>-binding peptides identified by the yeast two-hybrid system are pseudosubstrates of the protease. (A) <sup>35</sup>S-labeled GloSensor protease site luciferase activation by HRV-2 2A<sup>pro</sup> digestion of hybrid sites generated from sequences depicted in Fig. 1. To generate the GloSensor protein, new N and C termini were created at amino acids 234 and 233, respectively. The protein-coding region of this circularly permuted firefly luciferase was carried on the pGloSensor-10F linear vector. Insertion of a protease recognition sequence between these native N and C termini and cleavage of the sequence by the cognate protease activate the luciferase enzyme. Plasmid DNAs encoding the protease recognition sequences indicated on the graph were transcribed and translated *in vitro* and incubated with purified HRV-2 2A<sup>pro</sup> or TEV protease for 45 min. Luminescent signal was measured by mixing an aliquot of each TNT reaction mixture with Bright-Glo assay reagent in triplicate and incubating for 5 min at room temperature. Luminescence was measured using a luminometer. A plasmid DNA encoding the <sup>35</sup>S-labeled GloSensor ENLYFQ-S protein, where ENLYFQ-S is a cleavage site of the TEV protease, was used as a control. RLU, relative light units. (B) The different <sup>35</sup>S-labeled GloSensor proteins containing the protease sites to be tested were synthesized *in vitro* as described above and then incubated with 2 μg of TEV protease or HRV-2 2A<sup>pro</sup> for 45 min, followed by SDS-PAGE and fluorography. Gel patterns corresponding to enzymatic digestion performed with TEV protease (a) and HRV-2 2A<sup>pro</sup> (b to l) are shown. The 0-h time point shows proteins that were harvested right after addition of the proteases in the incubation mixtures.

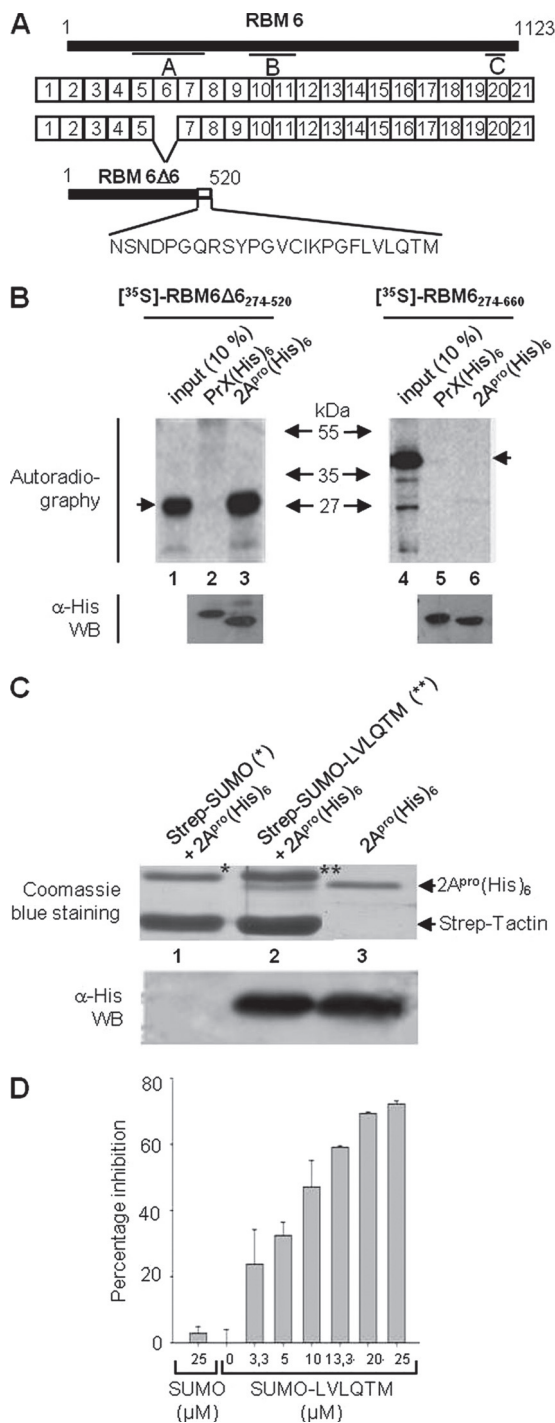


**FIG 3** The last six residues of RBM6Δ6 are necessary and sufficient for the interaction with HRV-2 2A<sup>pro</sup>. (A) Schematic representation of the exon structure of the RBM6 gene and the protein products derived from two splice variants (data are from references 14 and 31). Boxes represent exons and are not drawn to scale. The bars below RBM6 indicate different protein motifs, as follows: A and B, RNA binding motif RNP1 and RNP2; C, G patch. In the truncated RBM6Δ6 protein, the amino acid residues represented by the white part differ from those in the longer protein product RBM6 due to a frame shift caused by the splicing. (B) Results of a His pull-down assay with HRV-2 2A<sup>pro</sup> and RBM6Δ6. HRV-2 2A<sup>pro</sup>-(His)<sub>6</sub> was immobilized on affinity resin and incubated with *in vitro*-translated <sup>35</sup>S-labeled RBM6Δ6<sub>274-520</sub> or RBM6<sub>274-660</sub> protein. Bound proteins were resolved by SDS-PAGE and visualized by autoradiography. Lanes 1 and 4, 10% of total proteins from the initial incubation

age of the recombinant luciferase at the protease recognition sequence led to the activation of the luciferase enzyme, resulting in an increase in luminescence when a firefly luciferase substrate was added to the reaction mixture. Thus, if a peptide acted as a pseudosubstrate for 2A<sup>pro</sup>, an increase in luciferase activity would be observed. As shown in Fig. 2A, significant luciferase activity was detected for all constructs tested, and the best score was measured for the <sup>35</sup>S-labeled GloSensor LVLQTM-GPSDM protein, the protease site of which was derived from the C terminus of the RBM6Δ6 protein. Luminescence was hardly detectable when using the negative control, <sup>35</sup>S-labeled GloSensor-10F ENLYFQ-S protein, which was recognized by the tobacco etch virus protease but not by HRV-2 2A<sup>pro</sup>. In contrast and as expected, the <sup>35</sup>S-labeled GloSensor-10FENLYFQ-S protein was cleaved by the TEV protease, resulting in increased luminescence. Thus, our results confirmed that all peptides isolated by yeast two-hybrid screening behaved as potent substrate analogues of HRV-2 2A<sup>pro</sup>.

Cleavage of the <sup>35</sup>S-labeled GloSensor-10F-identified peptide-GPSDM luciferases (61 kDa) by HRV-2 2A<sup>pro</sup> was also visualized after separation of digested products by SDS-PAGE and autoradiography (Fig. 2B, panels c to l). Total inactivation of the proteases was effective only by boiling the sample for 5 min in SDS loading buffer, which may explain the partial substrate degradation at the initial time in panels c and d and reflected a higher affinity of HRV-2 2A<sup>pro</sup> for LVLQTM-GPSDM and LCLHTC-GPSDM sequences than for the other substrates. Moreover, all <sup>35</sup>S-labeled GloSensor-10F-identified peptide-GPSDM luciferases were hydrolyzed by HRV-2 2A<sup>pro</sup> into two predictive fragments of 36 and 25 kDa, confirming that all identified peptides were substrate analogues of 2A<sup>pro</sup>. As expected, the <sup>35</sup>S-labeled GloSensor-10F ENLYFQ-S protein was cleaved by the TEV protease but not by the 2A protease of HRV-2 (Fig. 2B, compare panels a and b). In addition, the kinetics of digestion were peptide dependent, with the highest rate being for the LVLQTM peptide. Thus, these results confirmed that the identified peptides acted as pseudosubstrates for HRV-2 2A<sup>pro</sup>.

**The LVLQTM peptide specifically interacts with HRV-2 2A<sup>pro</sup>.** Since the LVLQTM peptide displayed the highest affinity for the 2A protease, the interaction between these two binding

reaction; lanes 2 and 3, incubation of <sup>35</sup>S-labeled RBM6Δ6<sub>274-520</sub> with a control His-tagged protein and HRV-2 2A<sup>pro</sup>-(His)<sub>6</sub>, respectively; lanes 5 and 6, the corresponding assays conducted in the presence of RBM6<sub>274-660</sub>. Binding of His-tagged proteins on the affinity resin was checked by Western blotting (WB) using an antihistidine antibody. (C) Results of a Strep-Tag pull-down assay with HRV-2 2A<sup>pro</sup> and the RBM6Δ6-derived LVLQTM sequence. Bacterially expressed Strep-Tag-SUMO or Strep-Tag-SUMO-LVLQTM was incubated with HRV-2 2A<sup>pro</sup>-(His)<sub>6</sub> and Strep-Tactin-coated magnetic beads. A Coomassie blue-stained gel of proteins bound on the affinity resin is presented: lane 1, Strep-Tag-SUMO and HRV-2 2A<sup>pro</sup>-(His)<sub>6</sub>; lane 2, Strep-Tag-SUMO-LVLQTM and HRV-2 2A<sup>pro</sup>-(His)<sub>6</sub>; lane 3, purified HRV-2 2A<sup>pro</sup>-(His)<sub>6</sub>. Symbols: \*, Strep-Tag-SUMO; \*\*, Strep-Tag-SUMO-LVLQTM. The presence of HRV-2 2A<sup>pro</sup>-(His)<sub>6</sub> was confirmed by Western blot analysis using an antihistidine antibody. (D) Effect of the RBM6Δ6-derived peptide LVLQTM on cleavage of TRPIITTA-*p*-nitroanilide (TRPIITTA-*p*NA) by HRV-2 2A<sup>pro</sup>. Various concentrations of the purified SUMO-LVLQTM protein (0 to 25 μM) were added to the TRPIITTA-*p*NA peptide, and their inhibitory effect on HRV-2 2A<sup>pro</sup> catalysis was measured by collecting absorbance at 405 nm for 10 min at 25°C. The percentage of cleavage activity was calculated relative to the value obtained with no inhibitor. Data are expressed as means of three independent experiments, and standard deviations are indicated. SUMO protein was used as a control.

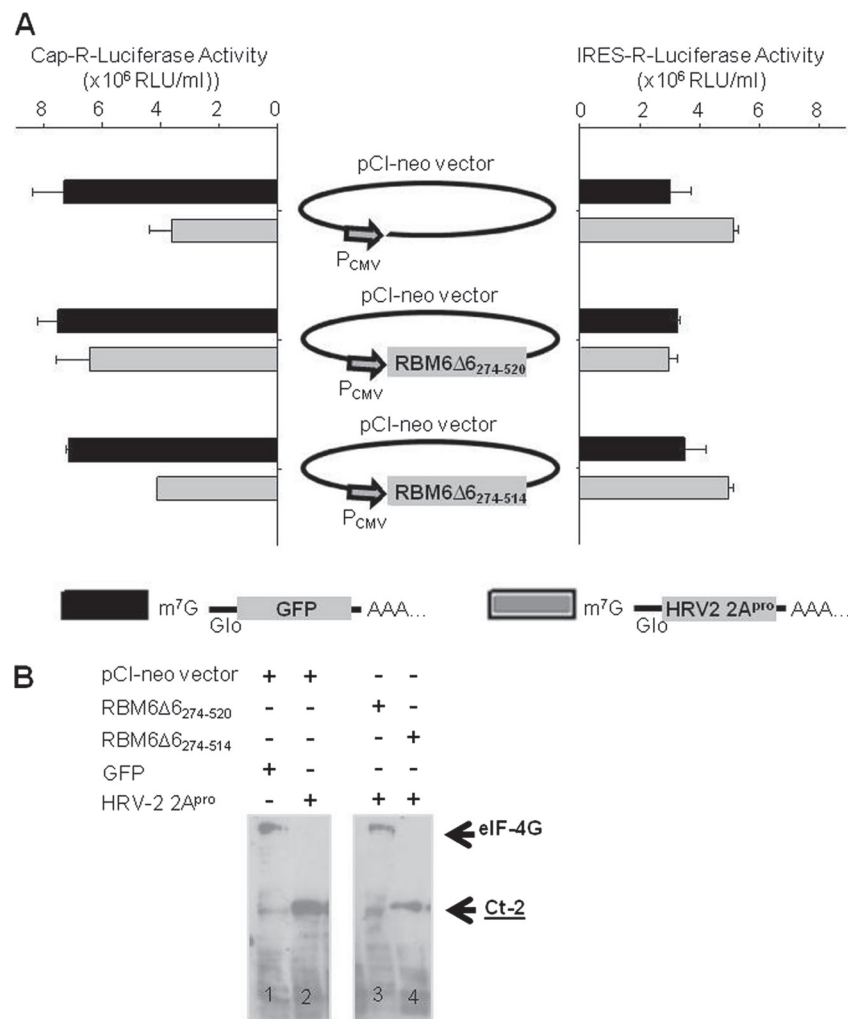


**FIG 4** RBM6Δ6<sub>274-520</sub> inhibits eIF4G cleavage activity of HRV-2 2A<sup>Pro</sup> in A549 cells. (A) A549 cells were transfected for 24 h with a pCI-neo plasmid harboring either the RBM6Δ6<sub>274-520</sub> or the RBM6Δ6<sub>274-514</sub> gene under the control of the cytomegalovirus (CMV) promoter and were subsequently transfected with an mRNA coding for HRV-2 2A<sup>Pro</sup> or GFP for 2 h. The effect of the 2A protease on eIF4G cleavage and thus on the translation of capped mRNA was measured using a capped mRNA or an IRES-containing mRNA, both coding for the *Renilla* luciferase. The first contained the 5' UTR of the  $\beta$ -globin gene, which directed cap-dependent translation. The second contained the 5' UTR of the encephalomyocarditis virus (EMCV) RNA, which ensured an IRES-dependent translation. After 3 h of transfection of the luciferase RNAs, cells were lysed and luciferase activity was measured by luminometry. Error bars denote the standard deviation from the mean of three independent experiments. (B) Inhibition of the eIF4G cleavage activity of HRV-2 2A<sup>Pro</sup>. A549 cells transiently expressing 2 $\times$  Strep•Tag-RBM6Δ6<sub>274-520</sub> protein or 2 $\times$  Strep•Tag-RBM6Δ6<sub>274-514</sub> for 24 h were subsequently transfected with an mRNA coding for HRV-2 2A<sup>Pro</sup> or the GFP for 5 h. Total protein extracts (60  $\mu$ g) were prepared from transfected cells, separated by 6% SDS-PAGE, and blotted with an antibody directed against the C-terminal part of the eIF4G protein. The main cleavage product (at about 100 kDa) which resulted from the proteolytic activity of 2A<sup>Pro</sup> is indicated Ct-2. The pCI-neo vector was used as a control for plasmid transfection. Of note, cells were lysed in the absence of protease inhibitor cocktail, possibly explaining the partial eIF4G hydrolysis observed in lanes 1 and 3.

partners was analyzed by two complementary pulldown assays. First, *in vitro*-translated [<sup>35</sup>S]methionine-labeled RBM6Δ6<sub>274-520</sub> (truncated protein detected by yeast two-hybrid screening, 28 kDa) or its alternative splicing isoform, RBM6<sub>274-660</sub> (44 kDa, Fig. 3A), was incubated with purified recombinant HRV-2 2A<sup>Pro</sup>-(His)<sub>6</sub> or with a His-tagged control protein bound to Ni-NTA magnetic agarose beads. As measured by densitometric analysis, about 15% of total RBM6Δ6<sub>274-520</sub> input bound to immobilized HRV-2 2A<sup>Pro</sup> (Fig. 3B; compare lanes 1 and 3) but not to the control His-tagged protein (lane 2). In contrast, RBM6<sub>274-660</sub> failed to bind either protein (lanes 5 and 6). These results demonstrated that RBM6Δ6<sub>274-520</sub> specifically interacted with HRV-2 2A<sup>Pro</sup>. Since RBM6Δ6<sub>274-520</sub> differed from RBM6<sub>274-660</sub> by its last

25 residues (Fig. 3A) and this region contained the particular LV LQTM sequence that was previously identified in the yeast two-hybrid system, these results suggested that LVLQTM was directly involved in the interaction with 2A<sup>Pro</sup>.

A Strep•Tag pulldown assay was then used to investigate whether LVLQTM-derived peptide was sufficient for 2A<sup>Pro</sup> binding (Fig. 3C). To this end, LVLQTM was first expressed in bacteria in fusion to the C terminus of a Strep•Tag-SUMO protein that allowed high specific binding on a Strep-Tactin affinity resin. Bacterial cell lysates containing either the Strep•Tag-SUMO-LV LQTM or the control Strep•Tag-SUMO recombinant protein were then mixed with a crude bacterial extract enriched with the recombinant HRV-2 2A<sup>Pro</sup>-(His)<sub>6</sub> protein. After 1 h of incubation

with the Strep-Tactin resin, protein complexes were subjected to SDS-PAGE separation and Coomassie blue staining or Western blotting using an antihistidine antibody (Fig. 3C). Results revealed that HRV-2 2A<sup>Pro</sup>-(His)<sub>6</sub> proteins coeluted with Strep•Tag-SUMO-LVLQTM protein (lane 2) but not with Strep•Tag-SUMO protein (lane 1). Therefore, the LVLQTM peptide was necessary and sufficient for the interaction with 2A<sup>Pro</sup>. Altogether, these results identified LVLQTM as a binding partner of HRV-2 2A<sup>Pro</sup>.

**HRV 2A<sup>Pro</sup> activity is inhibited by LVLQTM in a strain-independent manner.** We next investigated whether LVLQTM binding to HRV-2 2A<sup>Pro</sup> inhibited its activity. To this end, the 2A<sup>Pro</sup> activity was measured *in vitro* by a specific cleavage assay using the chromogenic substrate TRPIITTA-*p*-nitroanilide, which mimics the native HRV-2 2A<sup>Pro</sup> substrate sequence at the VP1-2A junction. As shown in Fig. 3D, addition of increasing concentrations of the Strep•Tag-SUMO-LVLQTM protein inhibited the activity of 2A<sup>Pro</sup> in a dose-dependent manner. The residual enzyme activity was about 30% at a saturating concentration of inhibitor (25  $\mu$ M). Control experiments showed that at the same concentration, the Strep•Tag-SUMO protein did not display any inhibitory effect on protease activity. Thus, LVLQTM inhibited the activity of the viral enzyme *in vitro*.

To investigate whether inhibition of 2A<sup>Pro</sup> by LVLQTM was relevant *in cellulo*, a three-step procedure for quantifying the inhibitory effect of LVLQTM on the cleavage of eIF4G by HRV-2 2A<sup>Pro</sup> was designed. In this protocol, A549 cells were transfected (i) for 24 h with a plasmid expressing either the RBM6 $\Delta$ 6<sub>274-520</sub> fragment or the RBM6 $\Delta$ 6<sub>274-514</sub> fragment which was deleted from the LVLQTM motif, then (ii) for 2 h with a capped and polyadenylated mRNA coding for the HRV-2 2A<sup>Pro</sup> or the GFP protein as a control, and finally (iii) for 3 h with a reporter *Renilla* luciferase (R-Luc) mRNA containing either the 5' untranslated (UTR) of the  $\beta$ -globin gene (capped mRNA) or the encephalomyocarditis virus (EMCV) internal ribosome entry site (IRES) sequence (uncapped mRNA). This assay relied on the fact that in eukaryotic cells, the distribution of mRNAs between capped and uncapped is largely in favor of capped mRNAs, for which translation initiation depends on intact initiation complex factors eIF4G/eIF4E. In contrast, translation of IRES-containing RNAs can occur in the presence of proteolyzed eIF4G, as the latter requires only the carboxy-terminal part of the eIF4G molecule. Thus, the presence of intact eIF4G allows the translation of capped mRNAs and its hydrolysis indirectly benefits the translation of uncapped mRNA. As depicted in Fig. 4, in the presence of the pCI-neo vector (empty vector) and the GFP-coding RNA, eIF4G was not cleaved (Fig. 4B, lane 1) and translation of capped mRNA, as measured by reporter Cap-R-Luc, activity was favored compared to IRES-driven translation, which explained the low level of IRES-R-Luc activity (Fig. 4A). In contrast, expression of HRV-2 2A<sup>Pro</sup> in the presence of the pCI-neo empty vector led to eIF4G cleavage (Fig. 4B, lane 2), which inhibited capped mRNA translation and indirectly increased IRES-driven translation, as measured by the decrease in Cap-R-Luc activity and the increase in IRES-R-Luc reporter activity (Fig. 4A). In cells overproducing the authentic C terminus of the RBM6 $\Delta$ 6 protein (RBM6 $\Delta$ 6<sub>274-520</sub>), the eIF4G cleavage activity of 2A<sup>Pro</sup> was notably reduced (Fig. 4B, lane 3) and the level of Cap-dependent luciferase translation was mildly affected (Fig. 4A). Expression of the C terminus of the RBM6 $\Delta$ 6 protein deleted from the LVLQTM sequence (RBM6 $\Delta$ 6<sub>274-514</sub>) did not affect

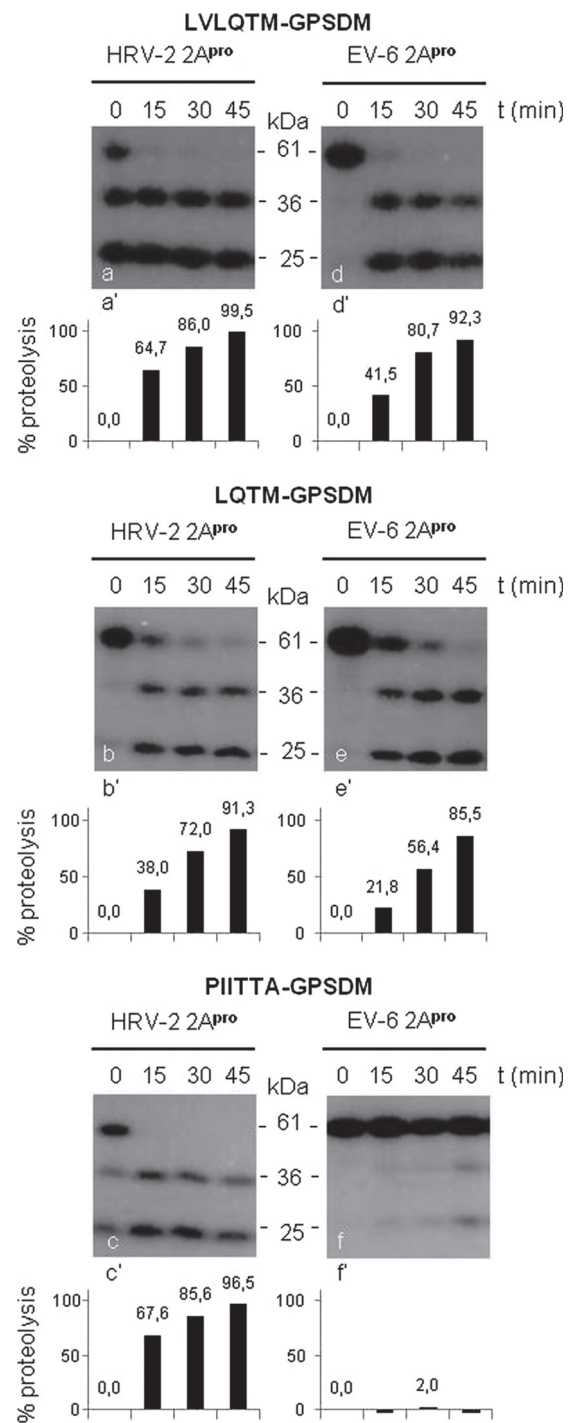


**FIG 5** The RBM6 $\Delta$ 6-derived LVLQTM peptide is a pseudosubstrate of HRV-2 and EV-6 2A<sup>Pro</sup>. Three different <sup>35</sup>S-labeled GloSensor proteins containing the protease sites to be tested were synthesized *in vitro* under the same conditions described in the legend of Fig. 2 and then incubated with 2  $\mu$ g of HRV-2 2A<sup>Pro</sup> or EV-6 2A<sup>Pro</sup> for 45 min in cleavage buffer, followed by SDS-PAGE and fluorography. Gel patterns corresponding to enzymatic digestion performed with HRV-2 2A<sup>Pro</sup> (a to c) or EV-6 2A<sup>Pro</sup> (d to f) are shown. The percent hydrolysis of the <sup>35</sup>S-labeled GloSensor luciferases was determined by densitometric analysis of the 61-kDa band and calculated relative to its initial (0-min) intensity (a' to f'). The 0-h time point shows proteins that were harvested right after addition of the proteases in the incubation mixtures.

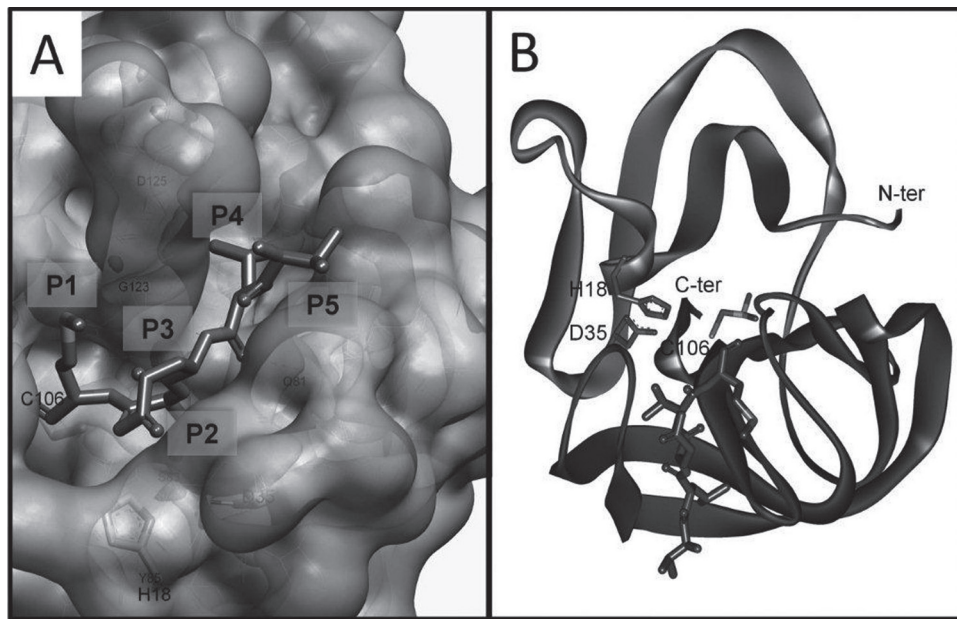


**FIG 6** Model of the interaction between VLQTM peptide and substrate-binding pocket residues of HRV-2 2A<sup>pro</sup>. (A) Close-up view of the binding of the P5 to P1 residues from the LVLQTM inhibitor. The protease backbone is depicted as a line covered by a semitransparent Van der Waals surface, except for catalytic residues with large labels, depicted as sticks; protease-interacting residues have small labels. (B) Ribbon diagram of the overall structure of HRV-2 2A<sup>pro</sup> in complex with the peptidic inhibitor. Catalytic triad residues are labeled. C-ter, C terminus; N-ter, N terminus.

HRV-2 2A<sup>pro</sup> activity, showing that the RBM6Δ6<sub>274-520</sub> fragment specifically inhibited HRV-2 2A<sup>pro</sup> activity through its LVLQTM motif.

We further investigated whether LVLQTM binding to 2A<sup>pro</sup> was strain specific. To this end, susceptibility of the <sup>35</sup>S-labeled GloSensor LVLQTM-GPSDM protein to degradation by the HRV-2 2A protease was compared to that by the echovirus 6 (EV-6) 2A<sup>pro</sup> by the protease-Glo assay described above. Briefly, after *in vitro* translation with [<sup>35</sup>S]methionine, the recombinant luciferase was incubated with purified HRV-2 2A<sup>pro</sup> or EV-6 2A<sup>pro</sup>, and the resulting digestion products were then separated by SDS-PAGE and visualized by autoradiography after treatment of gels with a fluorography solution. As shown in Fig. 5a, cleavage of full-length luciferase into its 36-kDa and 25-kDa predicted fragments was almost complete when HRV-2 2A<sup>pro</sup> was added to the reaction mix (0 h). Interestingly, a sequence lacking the LV residues (LQTM-GPSDM; Fig. 5b) had a significantly reduced hydrolysis rate (38%; Fig. 5b') after a 15-min incubation with the HRV-2 2A protease, showing that deletion of P5 and P6 residues in the LVLQTM-GPSDM sequence was detrimental to the recognition by HRV-2 2A<sup>pro</sup>. A control luciferase containing the authentic cleavage site found in the HRV-2 polyprotein (PIITTA-GPSDM; Fig. 5c and c') was cut by HRV-2 2A<sup>pro</sup> to the same extent as the LVLQTM-GPSDM hybrid site (Fig. 5a and a'). Similar results were obtained when reactions were carried out in the presence of purified 2A<sup>pro</sup> enzyme from EV-6, another member of the enterovirus genus (compare Fig. 5a to d and b to e, respectively). In contrast, a marked difference was observed for the HRV-2 control site, PIITTA-GPSDM, which, while cut by HRV-2 2A<sup>pro</sup>, was hardly recognized by the EV-6 2A<sup>pro</sup> (compare Fig. 5c and f), thus reflecting differences in substrate specificity between the two proteases, which share a relatively low level (40%) of amino acid sequence identity. Finally, the LVLQTM sequence in

RBM6Δ6 seemed to bind to the substrate-binding pocket of both HRV-2 and EV-6 2A<sup>pro</sup>, thus suggesting that this peptide may be effectively recognized by and thereby inhibit a wide range of 2A proteases.

**Virtual docking of LVLQTM peptide into HRV-2 2A<sup>pro</sup> catalytic site.** To get further insights into the interaction between the protease and its peptidic inhibitor, we decided to explore the orientations of the peptide by virtual docking in the substrate-binding pocket of HRV-2 2A<sup>pro</sup>. In conjunction, an extensive investigation of the impact of sequence variation in the peptide on the rate of cleavage was performed.

In the model depicted in Fig. 6B, the peptide largely bound within a deep surface groove that was diagonally oriented and intersected the cleft at the active site. Consequently, residues P5 to P1 mainly contacted the C-terminal β barrel, and the length of the groove was sufficient to accommodate residues P4 to P1 of the peptide. P5 Val at the N terminus of the peptide was largely solvent exposed (Fig. 6A), making a unique H bond through its N terminus, while its side chain was surrounded by polar side chains of Gln81 and Asp125. This lack of specific contact might suggest only a modest effect on substrate cleavage upon substitution at this position. On the other hand, P4 Leu was accommodated in an apolar depression defining the beginning of the peptide-binding groove, which consisted of side chains of Tyr78, Ile80, Ile96, and Ala129 (Fig. 6A). The side chain of P3 Gln pointed toward the solvent, which explained why, in common with other similar proteases, there was no strong preference for a particular residue at this position. Indeed, as shown by the protease-Glo assay approach, peptides displaying relatively different residues (Q, H, or V) at the P3 position were digested to about the same extent by 2A<sup>pro</sup> (Fig. 2A and B). The P2 Thr side chain inserted into the cleft between the β barrel and the N-terminal β sheet of the protease (Fig.

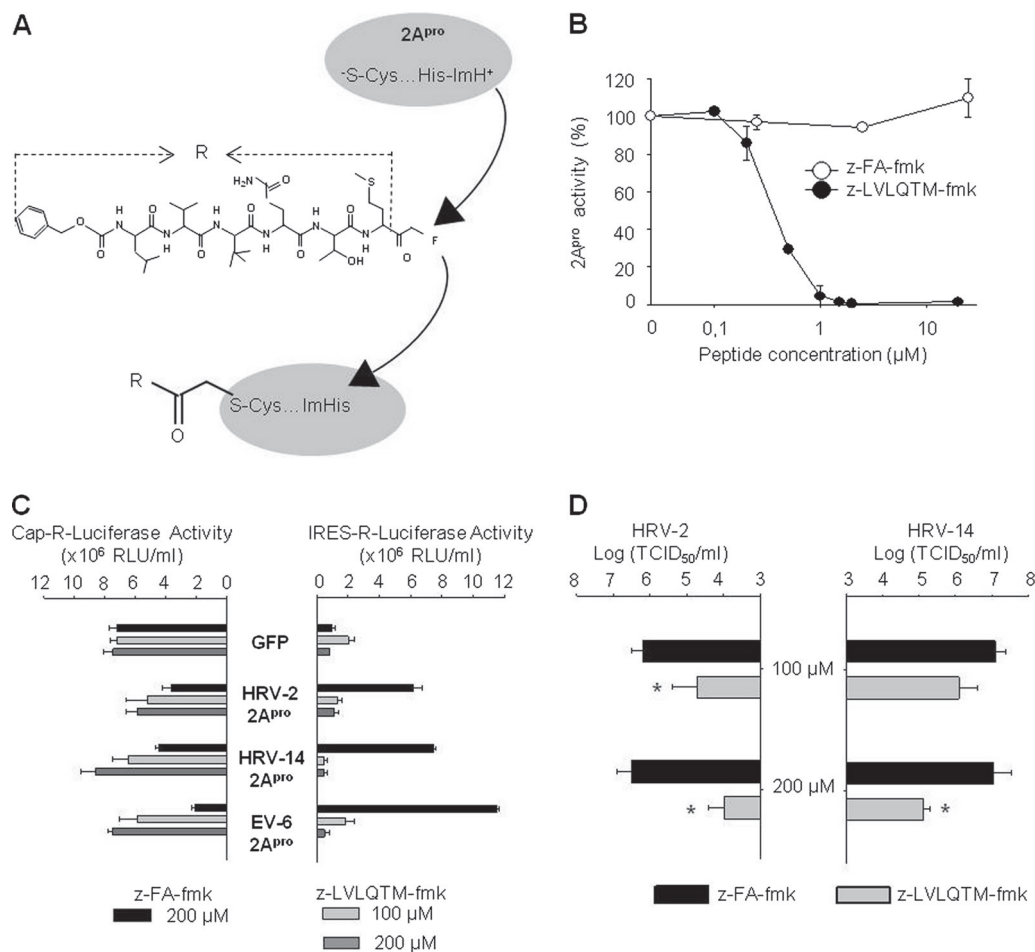


**FIG 7** The z-LVLQTM-fmk peptide inhibits 2A<sup>Pro</sup> activity and HRV replication in A549 cells. (A) The LVLQTM peptide was synthesized and modified (MP Biomedicals Company) by adding a benzyloxycarbonyl (z) at its N terminus and a fluoromethylketone (fmk) group at its C terminus to form z-LVLQTM-fmk. The latter is known to form a covalent link with the catalytic cysteine of the 2A<sup>Pro</sup> (20). (B) Effect of z-LVLQTM-fmk on cleavage *in vitro* of TRPIITTA-*p*-nitroanilide by the HRV-2 2A<sup>Pro</sup>. Various concentrations (0 to 25  $\mu$ M) of z-LVLQTM-fmk or z-FA-fmk (RnD Systems) were added to the TRPIITTA-pNA peptide, and their effects on HRV-2 2A<sup>Pro</sup> catalysis was measured by collecting the absorbance at 405 nm for 10 min at 25°C. The percentage of cleavage activity was calculated relative to the value obtained with no inhibitor. Data are expressed as means of three independent experiments, and standard deviations are indicated. (C) A549 cells were treated with 100  $\mu$ M or 200  $\mu$ M z-LVLQTM-fmk or z-FA-fmk for 1 h and were subsequently transfected with an mRNA coding for HRV-2 2A<sup>Pro</sup>, HRV-14 2A<sup>Pro</sup>, EV-6 2A<sup>Pro</sup>, or GFP for 2 h. Cells were then transfected for 3 h with a capped mRNA or an IRES-containing mRNA, both coding for the *Renilla* luciferase. The first contained the 5' UTR of the  $\beta$ -globin gene, and the second contained the 5' UTR of the encephalomyocarditis virus (EMCV) RNA. Cells were subsequently lysed, and luciferase activity was measured by luminometry. Error bars denote the standard deviations from the mean values obtained from three independent experiments. (D) A549 cells were treated with different concentrations of z-LVLQTM-fmk or z-FA-fmk and infected with HRV-2 or HRV-14 at a multiplicity of infection of 1 for 12 h. The TCID<sub>50</sub> in the supernatant of infected cells was determined as described in Materials and Methods.

6A), where it made two hydrogen bonds with residues Ser83 and Tyr85, both belonging to the same side of the pocket. In our model and contrary to the one discussed by Petersen et al. (24), binding of P2 Thr did not require a prior rotation of Tyr85.

Finally, the P1 Met side chain made three hydrogen bonds with the substrate-binding pocket: two between its carbonyl group and both the carbonyl and side chain of Cys106 (3.1 Å for both H bonds) and one between its N atom and the hydroxyl group of Tyr85 (2.9 Å) (Fig. 6A). The flat and narrow pocket displayed very good chemical complementarities to the P1 Met side chain.

In the light of this structural model, we showed that the double mutation S83A/D125A resulted in an approximately 20-fold decrease in the initial rate of TRPIITTA-pNA hydrolysis by 2A<sup>Pro</sup>

(data not shown), confirming that these two residues played a major role in the interaction with the LVLQTM peptide.

#### The z-LVLQTM-fmk peptide inhibits the replication of HRV-2 in A549 cells.

As LVLQTM was found to inhibit 2A<sup>Pro</sup> activity, we then investigated whether it also inhibited HRV replication *ex vivo*. As pseudosubstrates are more potent inhibitors when covalently bound to their target proteases, we synthesized a modified LVLQTM peptide containing a fluoromethylketone group at its C terminus which forms a persistent, nonlabile covalent bond with the catalytic cysteine (Fig. 7A). Moreover, a benzyloxycarbonyl group was added at its N terminus to increase its cell permeation. As expected, the z-LVLQTM-fmk molecule gave a sharp decrease in HRV-2 2A<sup>Pro</sup> activity in the TRPIITTA-pNA substrate cleavage assay with a 50% inhibitory con-

centration value of 0.3  $\mu\text{M}$  (Fig. 7B). In contrast, no inhibitory effect on 2A<sup>pro</sup> activity was observed when this assay was conducted in the presence of the control peptide z-FA-fmk, which shared the same chemical changes as z-LVLQTM-fmk. Furthermore, inhibition of capped mRNA translation by HRV-2 2A<sup>pro</sup> was significantly reduced by the z-LVLQTM-fmk peptide used at 100  $\mu\text{M}$  and 200  $\mu\text{M}$  (Fig. 7C) compared to the z-FA-fmk control peptide. These concentrations showed no cytotoxic effect on A549 cells (data not shown). The same inhibitory effect was observed using the same test with HRV-14 2A<sup>pro</sup> (belonging to the rhinovirus species B) and EV-6 2A<sup>pro</sup>, which again reinforced the idea that z-LVLQTM-fmk was not strain specific (Fig. 7C). Thus, the z-LVLQTM-fmk-modified peptide strongly and specifically inhibited several 2A<sup>pro</sup> enzymes.

We next investigated the effect of LVLQTM on virus replication in A549 cells. For this purpose, cells were infected with HRV-2 or HRV-14 at a multiplicity of infection (MOI) of 1 in the presence of z-LVLQTM-fmk (100  $\mu\text{M}$  or 200  $\mu\text{M}$ ) or the unrelated control peptide z-FA-fmk. At 12 h postinfection, the 50% tissue culture infective dose (TCID<sub>50</sub>) value in the supernatants of infected cells was determined. Results depicted in Fig. 7D indicated that the z-LVLQTM-fmk peptide inhibited HRV-2 and HRV-14 replication in a dose-dependent manner compared to the unrelated control peptide. Altogether, our data demonstrated that the observed decrease in virus production correlated directly with 2A<sup>pro</sup>-mediated inhibition by the z-LVLQTM-fmk peptide.

**The z-LVLQTM-fmk peptide protects against rhinovirus infection *in vivo*.** To assess the role of z-LVLQTM-fmk *in vivo*, we investigated whether z-LVLQTM-fmk could inhibit HRV replication in mice. For this purpose, mice were inoculated with HRV-2 (10<sup>5</sup> PFU/mouse) and, at the same time, treated or not with various concentrations of z-LVLQTM-fmk. Lungs of infected mice were then harvested at different time points postinfection, and infectious particles were evaluated by determining the TCID<sub>50</sub>. As shown in Fig. 8A, compared to DMSO-treated mice, z-LVLQTM-fmk-treated mice had significantly fewer infectious viruses in their lungs. Without peptide treatment (DMSO) and at 24, 48, and 120 h postinfection, infectious virus titers reached 10<sup>6</sup>, 10<sup>6.75</sup>, and 10<sup>6.82</sup> TCID<sub>50</sub>/ml, respectively. In contrast, after treatment of mice with 20, 200, or 500  $\mu\text{M}$  z-LVLQTM-fmk, virus titers dropped to 10<sup>4.2</sup> to 10<sup>5</sup> TCID<sub>50</sub>/ml for all the conditions tested. To confirm replication, an additional experiment was performed where mice were infected and lungs were harvested either immediately or at 48 h postinfection and then subjected to viral titrations (Fig. 8B). Results showed that the inoculum was totally recovered in the lungs of infected mice at day 0 postinoculation. When lungs were harvested at 48 h postinfection, the viral titer significantly increased, thus showing that viral replication indeed occurred after infection of the mice. In addition, the z-LVLQTM-fmk-mediated inhibition was specific since this peptide also impaired virus replication compared to the unrelated control peptide z-FA-fmk at 48 h postinfection (Fig. 8B). More importantly, when administration of the peptide was performed at 12 h postinfection, inhibition of viral replication was also readily detectable (Fig. 8C). The viral titers from control-treated animals reached 10<sup>6.53</sup> TCID<sub>50</sub>/ml, while the viral titer of z-LVLQTM-fmk-treated animals was 10<sup>4.08</sup> TCID<sub>50</sub>/ml at 48 h postinfection. Altogether, these results suggested that LVLQTM inhibited virus replication *in vivo* and could be of particular interest for anti-HRV therapies.

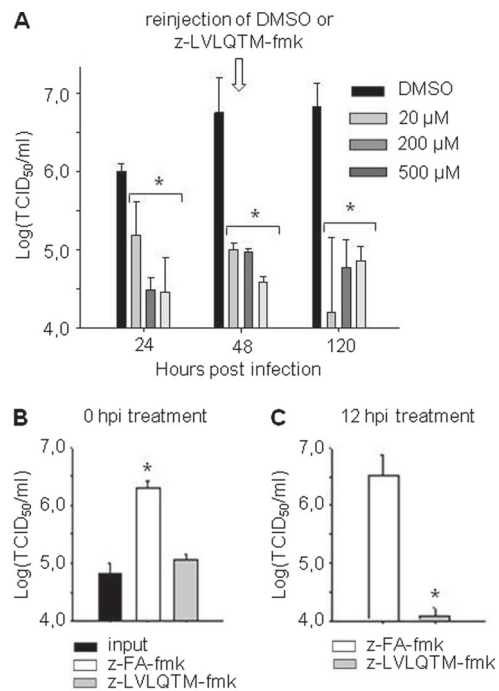


**FIG 8** z-LVLQTM-fmk specifically inhibits HRV replication *in vivo*. (A) Mice were inoculated intranasally with 100,000 PFU HRV-2 per mouse (in a 25- $\mu\text{l}$  volume) and treated with additional 25  $\mu\text{l}$  of a solution containing the indicated concentrations of peptide or 1% DMSO. Lungs of infected mice were harvested at 24, 48, and 120 h postinfection, and virus titers were determined. (B) Mice were infected with HRV-2 as described above and treated with 20  $\mu\text{M}$  z-LVLQTM-fmk or z-FA-fmk (control peptide). Lungs of infected mice were harvested immediately (input) or at 48 h postinfection (hpi). Virus titers were determined as described in Materials and Methods. (C) Mice were infected with HRV-2 (100,000 PFU) and treated with 20  $\mu\text{M}$  z-LVLQTM-fmk or z-FA-fmk at 12 h postinfection. Lungs of infected mice were harvested at 48 h postinfection and virus titers were measured. \*,  $P < 0.05$ .

## DISCUSSION

Rhinoviruses are responsible for a large number of respiratory tract infections which range from the common cold to more serious complications, such as pneumonia, bronchitis, or bronchiolitis in children as well as in adults. These infections constitute a major public health problem and have a significant socioeconomic impact due to the fact that there is currently no effective drug to fight against HRV. In the search for an effective treatment against rhinovirus, we identified a peptide inhibitor of the viral 2A<sup>pro</sup> by a yeast two-hybrid screening. This high-throughput screening allowed us to successfully identify 10 different peptides that were nonhydrolyzable by the 2A protease. Based on their sequence analysis, we postulated that these peptides could bind to the protease in a substrate-like manner (lock-and-key model). Direct evidence of peptide binding to the protease was provided by the protease-Glo assay, which elected the sequence motif LVLQTM derived from the very C terminus of the RBM6 $\Delta$ 6 protein to be the best candidate for subsequent development as an irreversible inhibitor of 2A<sup>pro</sup>. This peptide had the following main features: (i) it specifically bound *in vitro* to the HRV-2 2A<sup>pro</sup>, as demonstrated by pulldown assays. (ii) Its strong similarity to the amino-terminal half of natural cleavage sites of the protease meant that this motif behaved *in vitro* as a perfect pseudosubstrate not only of HRV-2 2A<sup>pro</sup> but also

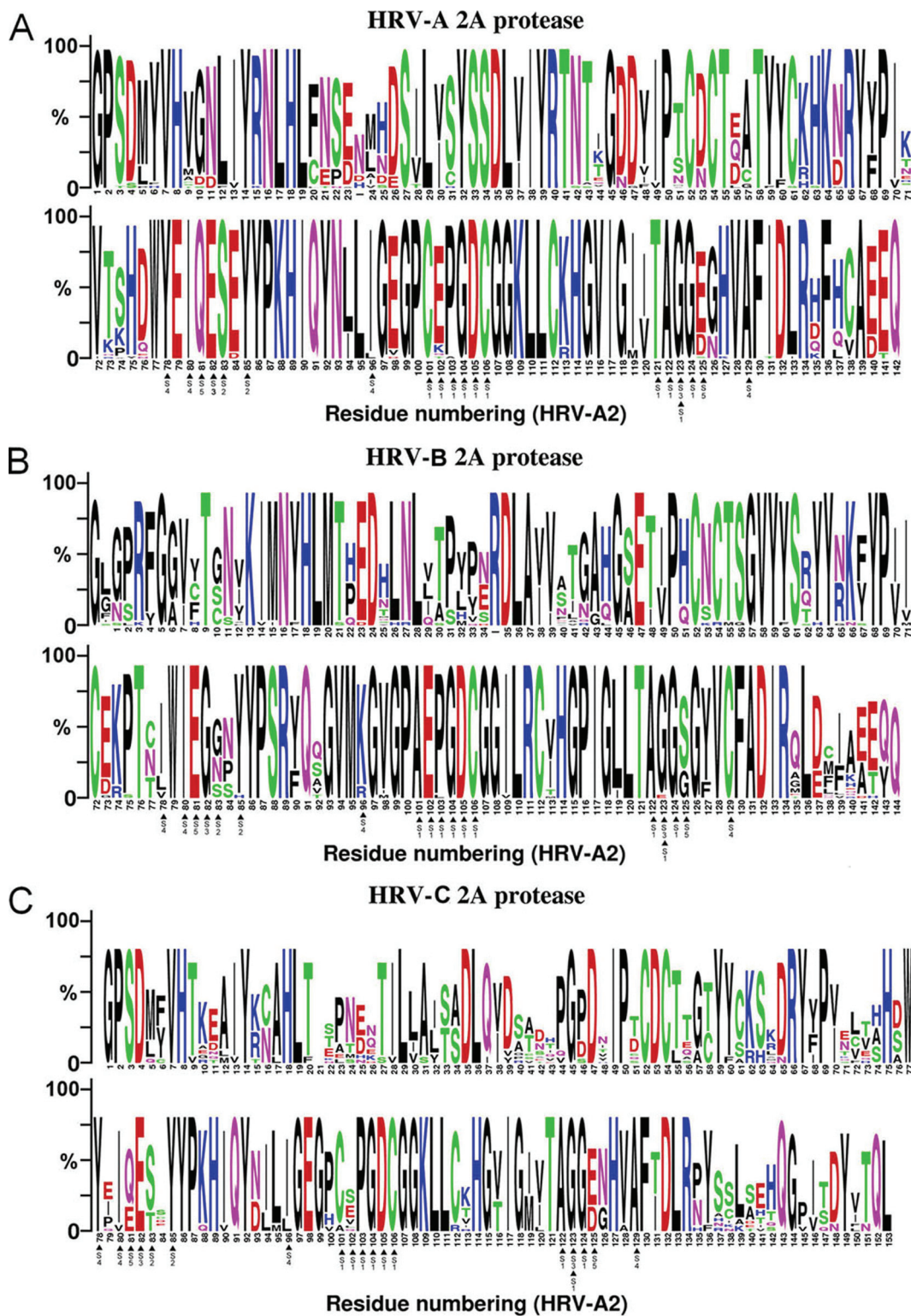


FIG 9 WebLogo sequence based on alignments of HRV type A, B, and C 2A proteases. These WebLogo sequences were generated using the WebLogo sequence generator (4) at <http://weblogo.berkeley.edu/logo.cgi> and were created using an alignment of 40 HRV-A sequences (A1, A2, A7, A9, A10, A11, A12, A13, A15, A16, A23, A24, A28, A29, A30, A34, A36, A38, A39, A41, A44, A46, A49, A53, A55, A56, A59, A64, A73, A74, A75, A76, A78, A82, A88, A89, A94, A101, A102, and A103) (A), 25 HRV-B sequences (B3, B4, B5, B6, B14, B17, B26, B27, B35, B37, B42, B48, B52, B69, B70, B72, B79, B83, B84, B86, B89, B91, B92, B93, B97, and B99) (B), and 12 HRV-C sequences (C1 to C11 and C15) (C). The letter size is proportional to the degree of amino acid conservation, and arrows indicate residues involved in the binding of the LVLQTM peptide at subsites S5 to S1.

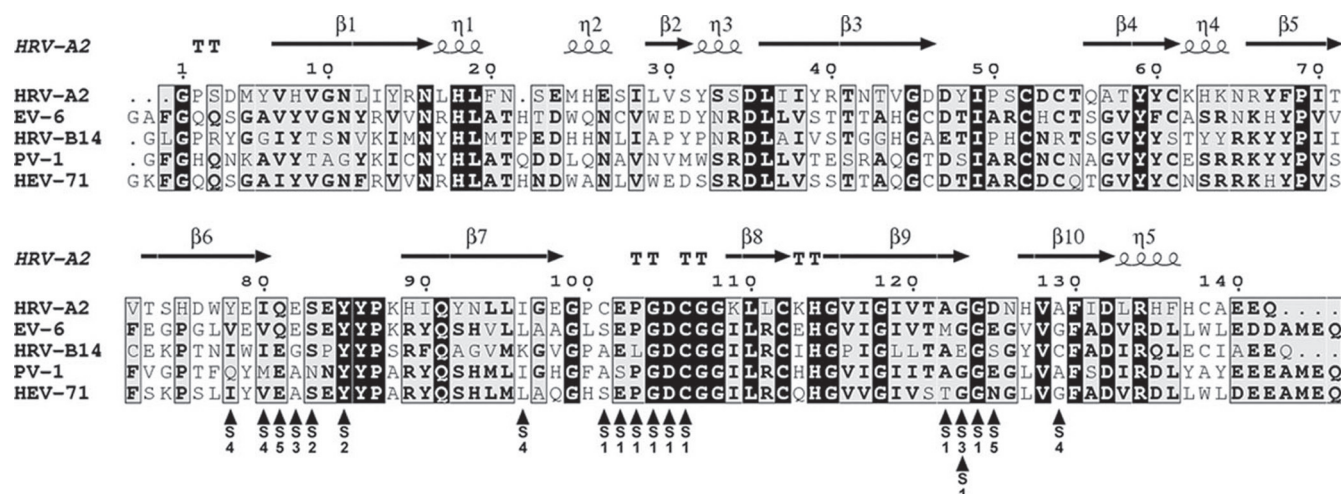


FIG 10 Multiple-sequence alignments of enterovirus 2A<sup>pro</sup>. Sequence alignment was performed using the ClustalW program and plotted with the ESPrnt program (8). Similar residues are highlighted in gray; identical residues are in black. Secondary structure elements of HRV-2 A<sup>pro</sup> are shown above the sequences, while arrows indicate residues involved in the binding of the VLQTM peptide at subsites S5 to S1.

of EV-6 2A<sup>pro</sup>, another enteroviral 2A protease. These enzymes share a relatively low level of amino acid sequence identity (40%), leading to substantially different surface characteristics, and thus represent two extremes in the primary sequence diversity of the 2A<sup>pro</sup> family. (iii) It contained a P1 Met which was demonstrated to enhance significantly the binding affinity of the peptide for the enzyme (4, 28).

Therefore, our results support a molecular model whereby the C terminus of RBM6Δ6, acting as a competitive inhibitor of 2A<sup>pro</sup>, docks into the substrate-binding pocket of the enzyme. Notably, in their screening of a HeLa cell cDNA expression library by the yeast two-hybrid procedure, Ventoso et al. (1999) (33) had previously characterized several four-amino-acid-binding peptides that interfered *in vitro* with PV-1 2A<sup>pro</sup> activity. However, our data indicate that compared to its shorter version, LQTM, the LVLQTM sequence confers higher binding affinity to RBM6Δ6 for 2A<sup>pro</sup>. These results thus highlighted the benefit which may be gained by using 6-mer-based peptides instead of 4-mer-based compounds directed against HRV 2A<sup>pro</sup>.

To achieve a more potent inhibition of the 2A<sup>pro</sup>, the LV LQTM peptide was modified so that it contained an electrophilic group (fmk) to enable the formation of a covalent bond with the active-site thiol and a benzyloxycarbonyl group (z) to increase its cell permeation. So modified, the z-LVLQTM-fmk compound was an effective inhibitor of purified HRV-2 2A<sup>pro</sup> activity with a *K<sub>i</sub>* value of 0.3 μM, which is about 20 times lower than that of the CBV 2A<sup>pro</sup> inhibitor z-IETD-fmk (*K<sub>i</sub>* = 7.7 μM) (1) and the caspase inhibitor z-VAD-fmk, which is also active against HRV 2A<sup>pro</sup> (*K<sub>i</sub>* = 5.6 μM) (5). Then we showed that z-LVLQTM-fmk specifically inhibited HRV-2 replication *in vitro* in A549 cells but also *in vivo* in BALB/c mice. The mouse model has features very similar to those observed in rhinovirus infection in humans, including augmentation of allergic airway inflammation (2), and to our knowledge, our study is the first one to validate *in vivo* in mice an antiviral drug directed against HRV. Mouse infection by HRV-2 was made possible by the fact that this virus strain, which belongs to the minor HRV group, uses a member of the low-

density-lipoprotein receptor family and can bind the mouse counterpart. Moreover, direct injection of the peptide by the intranasal route in mice several hours after infection prefigures the outline for administration of a drug that could be used in humans for efficient anti-HRV therapy.

On the basis of HRV-2 2A<sup>pro</sup> crystallographic data, a virtual docking model was then proposed to predict the inhibitor binding mode into the ligand binding pocket of the enzyme. Sequence comparison between different 2A<sup>pro</sup> enzymes from HRV-A, -B, and -C species revealed that amino acid residues involved in the interaction with the inhibitor in our model are relatively well conserved.

The alignment of 40 HRV-A 2A<sup>pro</sup> sequences (Fig. 9A) shows that for eight serotypes analyzed, Ile96 is replaced by a Leu, which displays the same physicochemical properties and so likely mediates the same hydrophobic interactions with P4 Leu. Interestingly, Asp125 found in 10 serotype sequences is replaced by a Glu, whose longer side chain may enhance a major interaction with P5 Val. Concerning the 25 HRV-B 2A proteins analyzed (Fig. 9B), hydrophobic interactions with P4 Leu are conserved through hydrophobic residues Ile, Leu, and Val at position 78. Ser83, which appears to be crucial for interaction with P3 Gln, is poorly conserved in type B sequences, as a Gly and an Asn are found at 50% and 35%, respectively. The second highlighted interaction through Asp125 also seems to be weakened in type B, as a serine is generally found at this position. Basic residues Arg and Lys are found at position 96, probably changing interaction modalities with the hydrophobic P4 Leu; nevertheless, the peptide LVLQTM seems to well accommodate in the catalytic cleft, even though a Lys is found at position 96 in HRV-B14. On the other hand, the Cys at position 129 (A129 in HRV-A2 2A<sup>pro</sup>) found in all type B sequences may reinforce the hydrophobic interaction with P4 Leu. Finally, I80V, S83T, I96L, C101A, and D125E mutations occurring in only a few type C sequences (Fig. 9C) should have no detrimental effects on the interaction between the enzyme and its inhibitor, as they represent conservative mutations from a physicochemical point of view.

If our peptide inhibitor may be of general use against all HRV serotypes, its use for therapeutic purposes could be extended to other enterovirus-associated diseases since it is also active against poliovirus 1 (PV-1; GenBank accession number [VO1149](#)) and human enterovirus 71 (HEV-71; GenBank accession number [AEF32490](#)) 2A proteases (data not shown). Comparison of the sequences of these proteases with those of other proteases tested in this study for their interaction with LVLQTM reveals only minor differences (Fig. 10). In particular, S5 Gln81 is present in EV-6, while a similar glutamate is found in the other viruses. Asp125 properties are conserved through the glutamate or the asparagine in EV-6 and PV-1 or HEV-71, respectively. The serine at the same position in HRV-B14 with a side chain shorter than Asp and obviously shorter than Glu may reflect some flexibility of the substrate at P5, where it is largely solvent exposed (Fig. 5A). The apolar depression defining S4 is conserved, as all residues at positions 78, 80, 96, and 129, even though they are not similar, are hydrophobic, except for PV-1 at Gln78 and HRV-B14 at Lys96. Glu82 and Gly123 at S3 are not well conserved, but peptide interactions occur through their backbone; this would not have any consequences on affinity. Tyr85 and Ser83 are strictly conserved at S2, except PV-1 displays a glutamine at position 83. Finally, the flat and narrow pocket displaying very good chemical complementarities to the P1 Met side chain is well conserved among the different viruses, as residues 101 to 106 and 122 to 124 as well as Tyr85 are homologous. Therefore, this model allows accurate prediction of the interaction of the peptide inhibitor with a large spectrum of 2A proteases. This model also suggests affinity differences between enteroviral 2A proteases for the LVLQTM peptide. In particular, the longer side chain of S4 I80 and S4 I96 in the HRV-2 2A protease compared to S4 V80 and S4 L96 in EV-6 2A<sup>Pro</sup> (Fig. 10) might reinforce the Van der Waals interactions with the P4 L in the peptide inhibitor. Moreover, the presence of a hydrophobic cysteine 101 at position S1 in HRV-2 2A<sup>Pro</sup> instead of a polar serine in EV-6 2A<sup>Pro</sup> likely strengthens the interaction with the P1 methionine in the peptide inhibitor. Such predictions could thus account for the better affinity of HRV-2 2A<sup>Pro</sup> for the LVLQTM peptide compared to the EV-6 2A<sup>Pro</sup>, as confirmed by our experimental data (compare Fig. 5a and d).

From a more fundamental point of view, this study also highlights several clues concerning the exact role, if any, played by the RBM6Δ6 protein in the context of virus-infected cells. One possibility is that RBM6Δ6 is an antidote molecule which is expressed by the cell in response to viral infection and which specifically neutralizes protein poison 2A<sup>Pro</sup>. Conversely, and more likely, binding of the protease on RBM6Δ6 could have a more or less profound impact on normal function of this protein in favor of viral infection. Experiments are under way to try to resolve this new and very exciting enigma.

#### ACKNOWLEDGMENTS

We thank Monique Ballandras for technical assistance as well as Leslie C. Sutherland and Sophie Bonnal for providing a plasmid encoding the full-length RBM6 protein.

This project was supported by the National Reference Center of Enteroviruses, the Institut de Veille Sanitaire, and the Agence Nationale de la Recherche (ANR; to Béatrice Riteau).

The funders had no role in study design, data collection and analysis, decision to publish, or preparation of the manuscript.

We declare no competing financial interests.

#### REFERENCES

- Badorff C, et al. 2000. Enteroviral protease 2A directly cleaves dystrophin and is inhibited by a dystrophin-based substrate analogue. *J. Biol. Chem.* 275:11191–11197.
- Bartlett NW, et al. 2008. Mouse models of rhinovirus-induced disease and exacerbation of allergic airway inflammation. *Nat. Med.* 14:199–204.
- Belov GA, et al. 2000. Early alteration of nucleocytoplasmic traffic induced by some RNA viruses. *Virology* 275:244–248.
- Deszcz L, Cencic R, Sousa C, Kuechler E, Skern T. 2006. An antiviral peptide inhibitor that is active against picornavirus 2A proteinases but not cellular caspases. *J. Virol.* 80:9619–9627.
- Deszcz L, Seipelt J, Vassilieva E, Roetzer A, Kuechler E. 2004. Antiviral activity of caspase inhibitors: effect on picornaviral 2A proteinase. *FEBS Lett.* 560:51–55.
- Fromont-Racine M, Rain JC, Legrain P. 1997. Toward a functional analysis of the yeast genome through exhaustive two-hybrid screens. *Nat. Genet.* 16:277–282.
- Garcia-Calvo M, et al. 1998. Inhibition of human caspases by peptide-based and macromolecular inhibitors. *J. Biol. Chem.* 273:32608–32613.
- Gouet P, Robert X, Courcelle E. 2003. ESPript/ENDscript: extracting and rendering sequence and 3D information from atomic structures of proteins. *Nucleic Acids Res.* 31:3320–3323.
- Gustin KE, Sarnow P. 2002. Inhibition of nuclear import and alteration of nuclear pore complex composition by rhinovirus. *J. Virol.* 76:8787–8796.
- Joachims M, Van Breugel PC, Lloyd RE. 1999. Cleavage of poly(A)-binding protein by enterovirus proteases concurrent with inhibition of translation in vitro. *J. Virol.* 73:718–727.
- Jurgens CK, et al. 2006. 2Apro is a multifunctional protein that regulates the stability, translation and replication of poliovirus RNA. *Virology* 345:346–357.
- Kempf BJ, Barton DJ. 2008. Poliovirus 2A(Pro) increases viral mRNA and polysome stability coordinately in time with cleavage of eIF4G. *J. Virol.* 82:5847–5859.
- Khoulache K, et al. 2009. Protective role for protease-activated receptor-2 against influenza virus pathogenesis via an IFN-gamma-dependent pathway. *J. Immunol.* 182:7795–7802.
- Kistler A, et al. 2007. Pan-viral screening of respiratory tract infections in adults with and without asthma reveals unexpected human coronavirus and human rhinovirus diversity. *J. Infect. Dis.* 196:817–825.
- Konig H, Rosenwirth B. 1988. Purification and partial characterization of poliovirus protease 2A by means of a functional assay. *J. Virol.* 62:1243–1250.
- Laine P, Savolainen C, Blomqvist S, Hovi T. 2005. Phylogenetic analysis of human rhinovirus capsid protein VP1 and 2A protease coding sequences confirms shared genus-like relationships with human enteroviruses. *J. Gen. Virol.* 86:697–706.
- Lamphear BJ, et al. 1993. Mapping the cleavage site in protein synthesis initiation factor eIF-4 gamma of the 2A proteases from human coxsackievirus and rhinovirus. *J. Biol. Chem.* 268:19200–19203.
- Molla A, Hellen CU, Wimmer E. 1993. Inhibition of proteolytic activity of poliovirus and rhinovirus 2A proteinases by elastase-specific inhibitors. *J. Virol.* 67:4688–4695.
- Ohlmann T, Rau M, Pain VM, Morley SJ. 1996. The C-terminal domain of eukaryotic protein synthesis initiation factor (eIF) 4G is sufficient to support cap-independent translation in the absence of eIF4E. *EMBO J.* 15:1371–1382.
- Otto HH, Schirmeister T. 1997. Cysteine proteases and their inhibitors. *Chem. Rev.* 97:133–172.
- Palmenberg AC, et al. 2009. Sequencing and analyses of all known human rhinovirus genomes reveal structure and evolution. *Science* 324:55–59.
- Papi A, et al. 2006. Infections and airway inflammation in chronic obstructive pulmonary disease severe exacerbations. *Am. J. Respir. Crit. Care Med.* 173:1114–1121.
- Park N, Katikaneni P, Skern T, Gustin KE. 2008. Differential targeting of nuclear pore complex proteins in poliovirus-infected cells. *J. Virol.* 82:1647–1655.
- Petersen JF, et al. 1999. The structure of the 2A proteinase from a common cold virus: a proteinase responsible for the shut-off of host-cell protein synthesis. *EMBO J.* 18:5463–5475.

25. Prevot D, et al. 2003. Characterization of a novel RNA-binding region of eIF4GI critical for ribosomal scanning. *EMBO J.* 22:1909–1921.
26. Reed LJ, Muench H. 1938. A simple method of estimating 50 per cent endpoints. *Am. J. Hyg.* 27:493–497.
27. Sommergruber W, et al. 1994. 2A proteinases of coxsackie- and rhinovirus cleave peptides derived from eIF-4 gamma via a common recognition motif. *Virology* 198:741–745.
28. Sommergruber W, et al. 1992. Cleavage specificity on synthetic peptide substrates of human rhinovirus 2 proteinase 2A. *J. Biol. Chem.* 267: 22639–22644.
29. Soto Rifo R, Ricci EP, Decimo D, Moncorge O, Ohlmann T. 2007. Back to basics: the untreated rabbit reticulocyte lysate as a competitive system to recapitulate cap/poly(A) synergy and the selective advantage of IRES-driven translation. *Nucleic Acids Res.* 35:e121.
30. Studier FW. 2005. Protein production by auto-induction in high density shaking cultures. *Protein Expr. Purif.* 41:207–234.
31. Timmer T, et al. 1999. A comparison of genomic structures and expression patterns of two closely related flanking genes in a critical lung cancer region at 3p21.3. *Eur. J. Hum. Genet.* 7:478–486.
32. van Gunsteren WF. 1996. Biomolecular simulation: the GROMOS96 manual and user guide. vdf, Zürich, Switzerland.
33. Ventoso I, Barco A, Carrasco L. 1999. Genetic selection of poliovirus 2Apro-binding peptides. *J. Virol.* 73:814–818.
34. Vojtek AB, Hollenberg SM. 1995. Ras-Raf interaction: two-hybrid analysis. *Methods Enzymol.* 255:331–342.
35. Zunszain PA, et al. 2010. Insights into cleavage specificity from the crystal structure of foot-and-mouth disease virus 3C protease complexed with a peptide substrate. *J. Mol. Biol.* 395:375–389.

## REFERENCES

## Références

- (WHO) WHO. 2014. Influenza (Seasonal) Fact sheet N°211. <http://www.who.int/mediacentre/factsheets/fs211/en/>
- Abdul-Careem MF, Firoz Mian M, Gillgrass AE, Chenoweth MJ, Barra NG, et al. 2011. FimH, a TLR4 ligand, induces innate antiviral responses in the lung leading to protection against lethal influenza infection in mice. *Antiviral research* 92: 346-55
- Aerts L, Hamelin ME, Rheume C, Lavigne S, Couture C, et al. 2013. Modulation of protease activated receptor 1 influences human metapneumovirus disease severity in a mouse model. *PLoS One* 8: e72529
- Alexopoulou L, Holt AC, Medzhitov R, Flavell RA. 2001. Recognition of double-stranded RNA and activation of NF-kappaB by Toll-like receptor 3. *Nature* 413: 732-8
- Andronicos NM, Chen EI, Baik N, Bai H, Parmer CM, et al. 2010. Proteomics-based discovery of a novel, structurally unique, and developmentally regulated plasminogen receptor, Plg-RKT, a major regulator of cell surface plasminogen activation. *Blood* 115: 1319-30
- Anhlan D, Grundmann N, Makalowski W, Ludwig S, Scholtissek C. 2011. Origin of the 1918 pandemic H1N1 influenza A virus as studied by codon usage patterns and phylogenetic analysis. *Rna* 17: 64-73
- Antoniak S, Owens AP, 3rd, Baunacke M, Williams JC, Lee RD, et al. 2013. PAR-1 contributes to the innate immune response during viral infection. *J Clin Invest* 123: 1310-22
- Armstrong SM, Wang C, Tigdi J, Si X, Dumpit C, et al. 2012. Influenza infects lung microvascular endothelium leading to microvascular leak: role of apoptosis and claudin-5. *PloS one* 7: e47323
- Arora P, Ricks TK, Trejo J. 2007. Protease-activated receptor signalling, endocytic sorting and dysregulation in cancer. *Journal of cell science* 120: 921-8
- Asokanathan N, Graham PT, Fink J, Knight DA, Bakker AJ, et al. 2002. Activation of protease-activated receptor (PAR)-1, PAR-2, and PAR-4 stimulates IL-6, IL-8, and prostaglandin E2 release from human respiratory epithelial cells. *Journal of immunology* 168: 3577-85
- Bachli EB, Pech CM, Johnson KM, Johnson DJ, Tuddenham EG, McVey JH. 2003. Factor Xa and thrombin, but not factor VIIa, elicit specific cellular responses in dermal fibroblasts. *J Thromb Haemost* 1: 1935-44
- Boilard E PG, Rousseau M, Cloutier N, Dubuc I, Lévesque T, Borgeat P, Flamand L. 2014. Influenza virus H1N1 activates platelets through FcγRIIA signaling and thrombin generation.
- Bouvier NM, Palese P. 2008. The biology of influenza viruses. *Vaccine* 26 Suppl 4: D49-53
- Busso N, Chobaz-Peclat V, Hamilton J, Spee P, Wagtmann N, So A. 2008. Essential role of platelet activation via protease activated receptor 4 in tissue factor-initiated inflammation. *Arthritis research & therapy* 10: R42
- Cady SD, Luo W, Hu F, Hong M. 2009. Structure and function of the influenza A M2 proton channel. *Biochemistry* 48: 7356-64
- Cheung CY, Poon LL, Lau AS, Luk W, Lau YL, et al. 2002. Induction of proinflammatory cytokines in human macrophages by influenza A (H5N1) viruses: a mechanism for the unusual severity of human disease? *Lancet* 360: 1831-7
- Choe WH, Cho YU, Chae JD, Kim SH. 2013. Pseudothrombocytopenia or platelet clumping as a possible cause of low platelet count in patients with viral infection: a case series

- from single institution focusing on hepatitis A virus infection. *Int J Lab Hematol* 35: 70-6
- Cirino G, Vergnolle N. 2006. Proteinase-activated receptors (PARs): crossroads between innate immunity and coagulation. *Current opinion in pharmacology* 6: 428-34
- Collen D. 1980. On the regulation and control of fibrinolysis. Edward Kowalski Memorial Lecture. *Thrombosis and haemostasis* 43: 77-89
- Coughlin SR. 1999. How the protease thrombin talks to cells. *Proceedings of the National Academy of Sciences of the United States of America* 96: 11023-7
- Coughlin SR. 2000. Thrombin signaling and protease-activated receptors. *Nature*
- Coughlin SR. 2005. Protease-activated receptors in hemostasis, thrombosis and vascular biology. *J Thromb Haemost* 3: 1800-14
- Cunha BA. 2013. In hospitalized adults the combined presence of leukocytosis, relative lymphopenia, and thrombocytopenia is predictive of swine influenza (H1N1). *The Journal of infection* 67: 489-90
- Darbousset R, Thomas GM, Mezouar S, Frere C, Bonier R, et al. 2012. Tissue factor-positive neutrophils bind to injured endothelial wall and initiate thrombus formation. *Blood* 120: 2133-43
- Davey RT, Jr., Lynfield R, Dwyer DE, Losso MH, Cozzi-Lepri A, et al. 2013. The association between serum biomarkers and disease outcome in influenza A(H1N1)pdm09 virus infection: results of two international observational cohort studies. *PLoS One* 8: e57121
- Dawood FS, Iuliano AD, Reed C, Meltzer MI, Shay DK, et al. 2012. Estimated global mortality associated with the first 12 months of 2009 pandemic influenza A H1N1 virus circulation: a modelling study. *The Lancet. Infectious diseases* 12: 687-95
- de Jong MD, Simmons CP, Thanh TT, Hien VM, Smith GJ, et al. 2006. Fatal outcome of human influenza A (H5N1) is associated with high viral load and hypercytokinemia. *Nat Med* 12: 1203-7
- Degen JL, Bugge TH, Goguen JD. 2007. Fibrin and fibrinolysis in infection and host defense. *J Thromb Haemost* 5 Suppl 1: 24-31
- Dellinger RP. 2003. Inflammation and coagulation: implications for the septic patient. *Clinical infectious diseases : an official publication of the Infectious Diseases Society of America* 36: 1259-65
- Engelmann B, Massberg S. 2013. Thrombosis as an intravascular effector of innate immunity. *Nature reviews. Immunology* 13: 34-45
- Escuret V, Frobert E, Bouscambert-Duchamp M, Sabatier M, Grog I, et al. 2008. Detection of human influenza A (H1N1) and B strains with reduced sensitivity to neuraminidase inhibitors. *Journal of clinical virology : the official publication of the Pan American Society for Clinical Virology* 41: 25-8
- Feistritzer C RM. 2005. Endothelial barrier protection by activated protein C through PAR1-dependent sphingosine 1-phosphate receptor-1 crossactivation. *Blood*
- Feldmann A, Schafer MK, Garten W, Klenk HD. 2000. Targeted infection of endothelial cells by avian influenza virus A/FPV/Rostock/34 (H7N1) in chicken embryos. *Journal of virology* 74: 8018-27
- Fiers W, De Filette M, Birkett A, Neiryck S, Min Jou W. 2004. A "universal" human influenza A vaccine. *Virus research* 103: 173-6
- Forsgren M, Raden B, Israelsson M, Larsson K, Heden LO. 1987. Molecular cloning and characterization of a full-length cDNA clone for human plasminogen. *FEBS letters* 213: 254-60

- Gando S, Nanzaki S, Kemmotsu O. 1999. Disseminated intravascular coagulation and sustained systemic inflammatory response syndrome predict organ dysfunctions after trauma: application of clinical decision analysis. *Annals of surgery* 229: 121-7
- Gao HN, Lu HZ, Cao B, Du B, Shang H, et al. 2013. Clinical findings in 111 cases of influenza A (H7N9) virus infection. *The New England journal of medicine* 368: 2277-85
- Garcia-Sastre A. 2012. The neuraminidase of bat influenza viruses is not a neuraminidase. *Proceedings of the National Academy of Sciences of the United States of America* 109: 18635-6
- Garcia CC, Russo RC, Guabiraba R, Fagundes CT, Polidoro RB, et al. 2010. Platelet-activating factor receptor plays a role in lung injury and death caused by Influenza A in mice. *PLoS pathogens* 6: e1001171
- Garten RJ, Davis CT, Russell CA, Shu B, Lindstrom S, et al. 2009. Antigenic and genetic characteristics of swine-origin 2009 A(H1N1) influenza viruses circulating in humans. *Science* 325: 197-201
- Gawaz M, Langer H, May AE. 2005. Platelets in inflammation and atherogenesis. *J Clin Invest* 115: 3378-84
- Goeijenbier M, van Gorp EC, Van den Brand JM, Stittelaar K, Bakhtiari K, et al. 2014. Activation of coagulation and tissue fibrin deposition in experimental influenza in ferrets. *BMC microbiology* 14: 134
- Gong Y, Hart E, Shchurin A, Hoover-Plow J. 2008. Inflammatory macrophage migration requires MMP-9 activation by plasminogen in mice. *J Clin Invest* 118: 3012-24
- Guanfang Shi CNM. 2011. Platelets as initiators and mediators of inflammation at the vessel wall. *Thrombosis research*
- Hawrylowicz CM, Howells GL, Feldmann M. 1991. Platelet-derived interleukin 1 induces human endothelial adhesion molecule expression and cytokine production. *The Journal of experimental medicine* 174: 785-90
- Heil F, Hemmi H, Hochrein H, Ampenberger F, Kirschning C, et al. 2004. Species-specific recognition of single-stranded RNA via toll-like receptor 7 and 8. *Science* 303: 1526-9
- Herfst S SE, Linster M, Chutinimitkul S, de Wit E, Munster VJ, Sorrell EM, Bestebroer TM, Burke DF, Smith DJ, Rimmelzwaan GF, Osterhaus AD, Fouchier RA. 2012. Airborne transmission of influenza A/H5N1 virus between ferrets. *Science* 336(6088):1534-41
- Hollenberg MD. 2003. Proteinase-mediated signaling: proteinase-activated receptors (PARs) and much more. *Life sciences* 74: 237-46
- Honda K, Ohba Y, Yanai H, Negishi H, Mizutani T, et al. 2005. Spatiotemporal regulation of MyD88-IRF-7 signalling for robust type-I interferon induction. *Nature* 434: 1035-40
- Ichinohe T, Pang IK, Iwasaki A. 2010. Influenza virus activates inflammasomes via its intracellular M2 ion channel. *Nature immunology* 11: 404-10
- Jagger BW, Wise HM, Kash JC, Walters KA, Wills NM, et al. 2012. An overlapping protein-coding region in influenza A virus segment 3 modulates the host response. *Science* 337: 199-204
- Jenkins RG, Su X, Su G, Scotton CJ, Camerer E, et al. 2006. Ligation of protease-activated receptor 1 enhances alpha(v)beta6 integrin-dependent TGF-beta activation and promotes acute lung injury. *J Clin Invest* 116: 1606-14
- Jennwein C, Tran N, Paulus P, Ellinghaus P, Eble JA, Zacharowski K. 2011. Novel aspects of fibrin(ogen) fragments during inflammation. *Molecular medicine* 17: 568-73
- Jensen T, Kierulf P, Sandset PM, Klingenberg O, Joo GB, et al. 2007. Fibrinogen and fibrin induce synthesis of proinflammatory cytokines from isolated peripheral blood mononuclear cells. *Thrombosis and haemostasis* 97: 822-9

- Johnson NP, Mueller J. 2002. Updating the accounts: global mortality of the 1918-1920 "Spanish" influenza pandemic. *Bulletin of the history of medicine* 76: 105-15
- Jones CI, Barrett NE, Moraes LA, Gibbins JM, Jackson DE. 2012. Endogenous inhibitory mechanisms and the regulation of platelet function. *Methods in molecular biology* 788: 341-66
- Kadl A, Leitinger N. 2005. The role of endothelial cells in the resolution of acute inflammation. *Antioxidants & redox signaling* 7: 1744-54
- Kaplanski G, Fabrigoule M, Boulay V, Dinarello CA, Bongrand P, et al. 1997. Thrombin induces endothelial type II activation in vitro: IL-1 and TNF-alpha-independent IL-8 secretion and E-selectin expression. *Journal of immunology* 158: 5435-41
- Kaplanski G, Marin V, Fabrigoule M, Boulay V, Benoliel AM, et al. 1998. Thrombin-activated human endothelial cells support monocyte adhesion in vitro following expression of intercellular adhesion molecule-1 (ICAM-1; CD54) and vascular cell adhesion molecule-1 (VCAM-1; CD106). *Blood* 92: 1259-67
- Kato H, Sato S, Yoneyama M, Yamamoto M, Uematsu S, et al. 2005. Cell type-specific involvement of RIG-I in antiviral response. *Immunity* 23: 19-28
- Keller TT, K. F. van der Sluijs, M. D. de Kruif, V. E. Gerdes, J. C. Meijers, S. Florquin, T. van der Poll, E. C. van Gorp, D. P. Brandjes, H. R. Buller, and M. Levi. 2006. Effects on coagulation and fibrinolysis induced by influenza in mice with a reduced capacity to generate activated protein C and a deficiency in plasminogen activator inhibitor type 1. *Circ Res*
- Krummel-McCracken K. 2011. Stroke as a complication of H1N1 influenza infection: a case study. *Critical care nurse* 31: e1-8
- Kuiken T, Riteau B, Fouchier RA, Rimmelzwaan GF. 2012. Pathogenesis of influenza virus infections: the good, the bad and the ugly. *Current opinion in virology* 2: 276-86
- Kunisaki KM, Janoff EN. 2009. Influenza in immunosuppressed populations: a review of infection frequency, morbidity, mortality, and vaccine responses. *The Lancet. Infectious diseases* 9: 493-504
- La Gruta NL, Kedzierska K, Stambas J, Doherty PC. 2007. A question of self-preservation: immunopathology in influenza virus infection. *Immunology and cell biology* 85: 85-92
- Lan RS, Stewart GA, Goldie RG, Henry PJ. 2004. Altered expression and in vivo lung function of protease-activated receptors during influenza A virus infection in mice. *American journal of physiology. Lung cellular and molecular physiology* 286: L388-98
- LaRosa SP. 2010. Activated protein C for H1N1 influenza? More work to do! *Critical care* 14: 156
- Le Goffic R, Balloy V, Lagranderie M, Alexopoulou L, Escriou N, et al. 2006. Detrimental contribution of the Toll-like receptor (TLR)3 to influenza A virus-induced acute pneumonia. *PLoS pathogens* 2: e53
- Le Goffic R, Pothlichet J, Vitour D, Fujita T, Meurs E, et al. 2007. Cutting Edge: Influenza A virus activates TLR3-dependent inflammatory and RIG-I-dependent antiviral responses in human lung epithelial cells. *Journal of immunology* 178: 3368-72
- Leavell KJ, Peterson MW, Gross TJ. 1996. The role of fibrin degradation products in neutrophil recruitment to the lung. *American journal of respiratory cell and molecular biology* 14: 53-60
- LeBouder F, Morello E, Rimmelzwaan GF, Bosse F, Pechoux C, et al. 2008. Annexin II incorporated into influenza virus particles supports virus replication by converting plasminogen into plasmin. *Journal of virology* 82: 6820-8

- Leung YH, Nicholls JM, Ho CK, Sia SF, Mok CK, et al. 2014. Highly pathogenic avian influenza A H5N1 and pandemic H1N1 virus infections have different phenotypes in Toll-like receptor 3 knockout mice. *The Journal of general virology* 95: 1870-9
- Lin CH, Cheng HW, Hsu MJ, Chen MC, Lin CC, Chen BC. 2006. c-Src mediates thrombin-induced NF-kappaB activation and IL-8/CXCL8 expression in lung epithelial cells. *Journal of immunology* 177: 3427-38
- Lu PP, Liu JT, Liu N, Guo F, Ji YY, Pang X. 2011. Pro-inflammatory effect of fibrinogen and FDP on vascular smooth muscle cells by IL-6, TNF-alpha and iNOS. *Life sciences* 88: 839-45
- Luo D DS, Vela A, Kohlway A, Lindenbach BD, Pyle AM. 2011. Structural insights into RNA recognition by RIG-I. *Cell* 14;147(2):409-22.
- Masaki Imai TW, Masato Hatta, Subash C. Das, Makoto Ozawa, Kyoko Shinya, Gongxun Zhong, Anthony Hanson, Hiroaki Katsura, Shinji Watanabe, Chengjun Li, Eiryu Kawakami, Shinya Yamada, Maki Kiso, Yasuo Suzuki, Eileen A. Maher, Gabriele Neumann & Yoshihiro Kawaoka. 2012. Experimental adaptation of an influenza H5 HA confers respiratory droplet transmission to a reassortant H5 HA/H1N1 virus in ferrets. *Nature* 486, 420–428 (21 June 2012)
- Matrosovich MN, Matrosovich TY, Gray T, Roberts NA, Klenk HD. 2004. Human and avian influenza viruses target different cell types in cultures of human airway epithelium. *Proceedings of the National Academy of Sciences of the United States of America* 101: 4620-4
- McCracken JM, Allen LA. 2014. Regulation of human neutrophil apoptosis and lifespan in health and disease. *Journal of cell death* 7: 15-23
- Medzhitov R. 2001. Toll-like receptors and innate immunity. *Nature reviews. Immunology* 1: 135-45
- Mercer PF, Deng X, Chambers RC. 2007. Signaling pathways involved in proteinase-activated receptor1-induced proinflammatory and profibrotic mediator release following lung injury. *Ann N Y Acad Sci* 1096: 86-8
- Mercer PF, Williams AE, Scotton CJ, Jose RJ, Sulikowski M, et al. 2014. Proteinase-activated receptor-1, CCL2, and CCL7 regulate acute neutrophilic lung inflammation. *Am J Respir Cell Mol Biol* 50: 144-57
- Mitsuhashi M, Tanaka A, Fujisawa C, Kawamoto K, Itakura A, et al. 2001. Necessity of thromboxane A2 for initiation of platelet-mediated contact sensitivity: dual activation of platelets and vascular endothelial cells. *Journal of immunology* 166: 617-23
- Mohammed Selman SKD, Nicole E Forbes, Jian-Jun Jia and Earl G Brown. 2012. Adaptive mutation in influenza A virus non-structural gene is linked to host switching and induces a novel protein by alternative splicing. *Emerging Microbes & Infections* 1, e42
- Moons L, Shi C, Ploplis V, Plow E, Haber E, et al. 1998. Reduced transplant arteriosclerosis in plasminogen-deficient mice. *J Clin Invest* 102: 1788-97
- Morens DM, Fauci AS. 2007. The 1918 influenza pandemic: insights for the 21st century. *The Journal of infectious diseases* 195: 1018-28
- Morrell CN, Aggrey AA, Chapman LM, Modjeski KL. 2014. Emerging roles for platelets as immune and inflammatory cells. *Blood* 123: 2759-67
- Muramoto Y, Noda T, Kawakami E, Akkina R, Kawaoka Y. 2013. Identification of novel influenza A virus proteins translated from PA mRNA. *Journal of virology* 87: 2455-62
- Narasaraju T, Yang E, Samy RP, Ng HH, Poh WP, et al. 2011. Excessive neutrophils and neutrophil extracellular traps contribute to acute lung injury of influenza pneumonitis. *The American journal of pathology* 179: 199-210

- Nayak DP, Hui EK, Barman S. 2004. Assembly and budding of influenza virus. *Virus research* 106: 147-65
- Netea MG, Simon A, van de Veerdonk F, Kullberg BJ, Van der Meer JW, Joosten LA. 2010. IL-1beta processing in host defense: beyond the inflammasomes. *PLoS pathogens* 6: e1000661
- Neumann G, Castrucci MR, Kawaoka Y. 1997. Nuclear import and export of influenza virus nucleoprotein. *Journal of virology* 71: 9690-700
- Nguyen T, Kyle UG, Jaimon N, Tchamtschi MH, Coss-Bu JA, et al. 2012. Coinfection with *Staphylococcus aureus* increases risk of severe coagulopathy in critically ill children with influenza A (H1N1) virus infection. *Crit Care Med* 40: 3246-50
- Niessen F, Furlan-Freguia C, Fernandez JA, Mosnier LO, Castellino FJ, et al. 2009. Endogenous EPCR/aPC-PAR1 signaling prevents inflammation-induced vascular leakage and lethality. *Blood* 113: 2859-66
- Niessen F, Schaffner F, Furlan-Freguia C, Pawlinski R, Bhattacharjee G, et al. 2008. Dendritic cell PAR1-S1P3 signalling couples coagulation and inflammation. *Nature* 452: 654-8
- Noda T, Sagara H, Yen A, Takada A, Kida H, et al. 2006. Architecture of ribonucleoprotein complexes in influenza A virus particles. *Nature* 439: 490-2
- O'Connell PA, Surette AP, Liwski RS, Svenningsson P, Waisman DM. 2010. S100A10 regulates plasminogen-dependent macrophage invasion. *Blood* 116: 1136-46
- O'Neill RE, Talon J, Palese P. 1998. The influenza virus NEP (NS2 protein) mediates the nuclear export of viral ribonucleoproteins. *The EMBO journal* 17: 288-96
- Ohrui T, Takahashi H, Ebihara S, Matsui T, Nakayama K, Sasaki H. 2000. Influenza A virus infection and pulmonary microthromboembolism. *The Tohoku journal of experimental medicine* 192: 81-6
- Opitz B RA, Dauber B, Eckhard J, Vinzing M, Schmeck B, Hippenstiel S, Suttorp N, Wolff T. 2007. IFNbeta induction by influenza A virus is mediated by RIG-I which is regulated by the viral NS1 protein. *Cell Microbiol*
- Palese PaS, ML. 2001. Orthomyxoviridae: The Viruses and Their Replication. *Fields Virology, 5th edition D.M. Knipe and P.M. Howley, Editors. 2006, Lippencott Williams and Wilkins: Philadelphia ISBN-10: 0-7817-6060-7: 1647-89*
- Pang IK IA. 2011. Inflammasomes as mediators of immunity against influenza virus. *Trends Immunol.*
- Pichlmair A, Schulz O, Tan CP, Naslund TI, Liljestrom P, et al. 2006. RIG-I-mediated antiviral responses to single-stranded RNA bearing 5'-phosphates. *Science* 314: 997-1001
- Ploplis VA, French EL, Carmeliet P, Collen D, Plow EF. 1998. Plasminogen deficiency differentially affects recruitment of inflammatory cell populations in mice. *Blood* 91: 2005-9
- Qi J, Kreutzer DL, Piela-Smith TH. 1997. Fibrin induction of ICAM-1 expression in human vascular endothelial cells. *Journal of immunology* 158: 1880-6
- Rehwinkel J, Tan CP, Goubau D, Schulz O, Pichlmair A, et al. 2010. RIG-I detects viral genomic RNA during negative-strand RNA virus infection. *Cell* 140: 397-408
- Reid AH, Taubenberger JK, Fanning TG. 2004. Evidence of an absence: the genetic origins of the 1918 pandemic influenza virus. *Nature reviews. Microbiology* 2: 909-14
- Reperant LA, van de Bildt MW, van Amerongen G, Leijten LM, Watson S, et al. 2012. Marked endotheliotropism of highly pathogenic avian influenza virus H5N1 following intestinal inoculation in cats. *Journal of virology* 86: 1158-65

- Rondina MT, Brewster B, Grissom CK, Zimmerman GA, Kastendieck DH, et al. 2012. In vivo platelet activation in critically ill patients with primary 2009 influenza A(H1N1). *Chest* 141: 1490-5
- Rupa-Matysek J, Gil L, Wojtasinska E, Zajdel K, Ciepluch K, Komarnicki M. 2014. Coagulation profile in patients with H1N1 influenza A infection undergoing treatment for haematological malignancies. *Blood Coagul Fibrinolysis*
- Ruuskanen O, Lahti E, Jennings LC, Murdoch DR. 2011. Viral pneumonia. *Lancet* 377: 1264-75
- Sasai M, Linehan MM, Iwasaki A. 2010. Bifurcation of Toll-like receptor 9 signaling by adaptor protein 3. *Science* 329: 1530-4
- Schouten M, de Boer JD, van der Sluijs KF, Roelofs JJ, van't Veer C, et al. 2011. Impact of endogenous protein C on pulmonary coagulation and injury during lethal H1N1 influenza in mice. *American journal of respiratory cell and molecular biology* 45: 789-94
- Schouten M, Sluijs KF, Gerlitz B, Grinnell BW, Roelofs JJ, et al. 2010. Activated protein C ameliorates coagulopathy but does not influence outcome in lethal H1N1 influenza: a controlled laboratory study. *Critical care* 14: R65
- Schouten M, van't Veer C, Roelofs JJ, Levi M, van der Poll T. 2012. Protease-activated receptor-1 impairs host defense in murine pneumococcal pneumonia: a controlled laboratory study. *Crit Care* 16: R238
- Schulz O, Diebold SS, Chen M, Naslund TI, Nolte MA, et al. 2005. Toll-like receptor 3 promotes cross-priming to virus-infected cells. *Nature* 433: 887-92
- sfh SFdh. 2011. Hématologie. *Elsevier MASSON*
- Shaw ML, Stone KL, Colangelo CM, Gulcicek EE, Palese P. 2008. Cellular proteins in influenza virus particles. *PLoS pathogens* 4: e1000085
- Shimizu T, Takizawa N, Watanabe K, Nagata K, Kobayashi N. 2011. Crucial role of the influenza virus NS2 (NEP) C-terminal domain in M1 binding and nuclear export of vRNP. *FEBS letters* 585: 41-6
- Shirey KA, Lai W, Scott AJ, Lipsky M, Mistry P, et al. 2013. The TLR4 antagonist Eritoran protects mice from lethal influenza infection. *Nature* 497: 498-502
- Short KR, Kroeze EJ, Fouchier RA, Kuiken T. 2014. Pathogenesis of influenza-induced acute respiratory distress syndrome. *The Lancet. Infectious diseases* 14: 57-69
- Shuman MA, Botney M, Fenton JW, 2nd. 1979. Thrombin-induced platelet secretion. Further evidence for a specific pathway. *J Clin Invest* 63: 1211-8
- Skehel JJ, Wiley DC. 2000. Receptor binding and membrane fusion in virus entry: the influenza hemagglutinin. *Annual review of biochemistry* 69: 531-69
- Soepandi PZ, Burhan E, Mangunegoro H, Nawas A, Aditama TY, et al. 2010. Clinical course of avian influenza A(H5N1) in patients at the Persahabatan Hospital, Jakarta, Indonesia, 2005-2008. *Chest* 138: 665-73
- Sugama Y, Tiruppathi C, offakidevi K, Andersen TT, Fenton JW, 2nd, Malik AB. 1992. Thrombin-induced expression of endothelial P-selectin and intercellular adhesion molecule-1: a mechanism for stabilizing neutrophil adhesion. *The Journal of cell biology* 119: 935-44
- Syrovets T, Lunov O, Simmet T. 2012. Plasmin as a proinflammatory cell activator. *Journal of leukocyte biology* 92: 509-19
- Syrovets T, Tippler B, Rieks M, Simmet T. 1997. Plasmin is a potent and specific chemoattractant for human peripheral monocytes acting via a cyclic guanosine monophosphate-dependent pathway. *Blood* 89: 4574-83

- Teijaro JR, Walsh KB, Cahalan S, Fremgen DM, Roberts E, et al. 2011. Endothelial cells are central orchestrators of cytokine amplification during influenza virus infection. *Cell* 146: 980-91
- To KK, Hung IF, Li IW, Lee KL, Koo CK, et al. 2010. Delayed clearance of viral load and marked cytokine activation in severe cases of pandemic H1N1 2009 influenza virus infection. *Clinical infectious diseases : an official publication of the Infectious Diseases Society of America* 50: 850-9
- Tong S, Zhu X, Li Y, Shi M, Zhang J, et al. 2013. New world bats harbor diverse influenza A viruses. *PLoS pathogens* 9: e1003657
- Tran TH, Nguyen TL, Nguyen TD, Luong TS, Pham PM, et al. 2004. Avian influenza A (H5N1) in 10 patients in Vietnam. *N Engl J Med* 350: 1179-88
- Tressel SL, Kaneider NC, Kasuda S, Foley C, Koukos G, et al. 2011. A matrix metalloprotease-PAR1 system regulates vascular integrity, systemic inflammation and death in sepsis. *EMBO molecular medicine* 3: 370-84
- Tsai SY, Segovia JA, Chang TH, Morris IR, Berton MT, et al. 2014. DAMP molecule S100A9 acts as a molecular pattern to enhance inflammation during influenza A virus infection: role of DDX21-TRIF-TLR4-MyD88 pathway. *PLoS pathogens* 10: e1003848
- Tscherne DM, Garcia-Sastre A. 2011. Virulence determinants of pandemic influenza viruses. *J Clin Invest* 121: 6-13
- Urso R, Bevilacqua N, Gentile M, Biagioli D, Lauria FN. 2011. Pandemic 2009 H1N1 virus infection associated with purpuric skin lesions: a case report. *Journal of medical case reports* 5: 132
- van Biesen T, Hawes BE, Luttrell DK, Krueger KM, Touhara K, et al. 1995. Receptor-tyrosine-kinase- and G beta gamma-mediated MAP kinase activation by a common signalling pathway. *Nature* 376: 781-4
- Visseren FL, Bouwman JJ, Bouter KP, Diepersloot RJ, de Groot PH, Erkelens DW. 2000. Procoagulant activity of endothelial cells after infection with respiratory viruses. *Thrombosis and haemostasis* 84: 319-24
- Vu TK, Hung DT, Wheaton VI, Coughlin SR. 1991. Molecular cloning of a functional thrombin receptor reveals a novel proteolytic mechanism of receptor activation. *Cell* 64: 1057-68
- Wang JP, Bowen GN, Padden C, Cerny A, Finberg RW, et al. 2008. Toll-like receptor-mediated activation of neutrophils by influenza A virus. *Blood* 112: 2028-34
- Wang ZF, Su F, Lin XJ, Dai B, Kong LF, et al. 2011. Serum D-dimer changes and prognostic implication in 2009 novel influenza A(H1N1). *Thromb Res* 127: 198-201
- Warren-Gash C, Hayward AC, Hemingway H, Denaxas S, Thomas SL, et al. 2012. Influenza Infection and Risk of Acute Myocardial Infarction in England and Wales: A CALIBER Self-Controlled Case Series Study. *J Infect Dis* 206: 1652-9
- Warren-Gash C, Smeeth L, Hayward AC. 2009. Influenza as a trigger for acute myocardial infarction or death from cardiovascular disease: a systematic review. *Lancet Infect Dis* 9: 601-10
- Webster RG, Hulse DJ. 2004. Microbial adaptation and change: avian influenza. *Revue scientifique et technique* 23: 453-65
- Webster RG, Peiris M, Chen H, Guan Y. 2006. H5N1 outbreaks and enzootic influenza. *Emerging infectious diseases* 12: 3-8
- Weiler H. 2010. Regulation of inflammation by the protein C system. *Critical care medicine* 38: S18-25

- Wise HM, Foeglein A, Sun J, Dalton RM, Patel S, et al. 2009. A complicated message: Identification of a novel PB1-related protein translated from influenza A virus segment 2 mRNA. *Journal of virology* 83: 8021-31
- Wise HM, Hutchinson EC, Jagger BW, Stuart AD, Kang ZH, et al. 2012. Identification of a novel splice variant form of the influenza A virus M2 ion channel with an antigenically distinct ectodomain. *PLoS pathogens* 8: e1002998
- Wu S, Metcalf JP, Wu W. 2011. Innate immune response to influenza virus. *Current opinion in infectious diseases* 24: 235-40
- Wygrecka M, Marsh LM, Morty RE, Henneke I, Guenther A, et al. 2009. Enolase-1 promotes plasminogen-mediated recruitment of monocytes to the acutely inflamed lung. *Blood* 113: 5588-98
- Yang H, Ko HJ, Yang JY, Kim JJ, Seo SU, et al. 2013. Interleukin-1 promotes coagulation, which is necessary for protective immunity in the lung against *Streptococcus pneumoniae* infection. *J Infect Dis* 207: 50-60
- Yewdell J, Garcia-Sastre A. 2002. Influenza virus still surprises. *Current opinion in microbiology* 5: 414-8
- Zarbock A, Polanowska-Grabowska RK, Ley K. 2007. Platelet-neutrophil-interactions: linking hemostasis and inflammation. *Blood reviews* 21: 99-111
- Zeng H, Pappas C, Belser JA, Houser KV, Zhong W, et al. 2012. Human pulmonary microvascular endothelial cells support productive replication of highly pathogenic avian influenza viruses: possible involvement in the pathogenesis of human H5N1 virus infection. *Journal of virology* 86: 667-78

## **Abstract**

Influenza is an acute respiratory disease caused by infection with influenza virus and is a major public health problem. A better understanding of the interaction between influenza virus and host allow us to better understand the pathophysiology of influenza infection, and thus, ultimately, to better protect themselves against the disease. Morbidity and mortality caused by severe influenza infections are associated with dysregulation of the immune response in the lung. This deleterious inflammation is the cause of lung collateral damage, causing a decrease in the patient's breathing capacity. Although the mechanisms involved are not fully understood, recent studies point to a central role of endothelial cells in the deregulation of the host response to influenza infection. During endothelium aggression, the physiological process of hemostasis (platelet activation, coagulation and fibrinolysis) is activated in order to allow wound healing and to maintain the integrity of blood vessels. In many inflammatory diseases, the only dysregulation of hemostasis is directly linked to a deleterious inflammatory response. During my thesis, we hypothesized that hemostasis could be the cause of the inflammatory dysregulation during influenza infections. Our data show the role of two factors strongly involved in hemostasis: the thrombin activated receptor, PAR-1 (protease activated receptor 1) and plasminogen, in the deleterious lung inflammation and in the pathogenicity of influenza virus. Besides the role of hemostasis, we have also been able to show that the influenza virus incorporates cellular proteins in the viral envelope, allowing it to evade the immune system, which could also contribute to the deregulation of the host response. All the results obtained allowed to better understand the mechanisms involved in immune response dysregulation during influenza infection and suggest new therapeutic targets to fight against the disease.